uOttawa

L'Université canadienne
Canada's university

FACULTÉ DES ÉTUDES SUPÉRIEURES ET POSTOCTORALES

uOttawa

L'Université canadienne
Canada's university

FACULTY OF GRADUATE AND POSDOCTORAL STUDIES

Fuad Ababneh
AUTEUR DE LA THÈSE / AUTHOR OF THESIS

Ph.D. (Chemistry)
GRADE / DEGREE

Department of Chemistry
FACULTÉ, ÉCOLE, DÉPARTEMENT / FACULTY, SCHOOL, DEPARTMENT

Application of chemical kinetics to mercury cycling in the aquatic environment: Photoreduction of Hg(II) and binding of Hg(II) and $MeHg^{+}$ to natural ligands.

TITRE DE LA THÈSE / TITLE OF THESIS

David Lean
DIRECTEUR (DIRECTRICE) DE LA THÈSE / THESIS SUPERVISOR

CO-DIRECTEUR (CO-DIRECTRICE) DE LA THÈSE / THESIS CO-SUPERVISOR

EXAMINATEURS (EXAMINATRICES) DE LA THÈSE / THESIS EXAMINERS

Nimal De Silva

Javier Giorgi

Jerome Nriagu

Tito Scaiano

Gary W. Slater
LE DOYEN DE LA FACULTÉ DES ÉTUDES SUPÉRIEURES ET POSTDOCTORALES /
DEAN OF THE FACULTY OF GRADUATE AND POSTDOCORAL STUDIES

# Application of chemical kinetics to mercury cycling in the aquatic environment: Photoreduction of Hg(II) and binding of Hg(II) and $MeHg^+$ to natural ligands.

**Fuad A. Ababneh**

Thesis submitted to the

School of Graduate Studies and Research

University of Ottawa

In partial fulfillment of the requirements for the

Ph.D degree in

Chemistry

Department of Chemistry

University of Ottawa

Ottawa-Ontario

Canada

*Your file Votre référence*
*ISBN: 0-494-10938-6*
*Our file Notre référence*
*ISBN: 0-494-10938-6*

**List of Abbreviations**

**CLEM**: Competitive ligand exchange method

**CLE-SPE**: Competitive ligand exchange followed by solid phase extraction

**CV-AAS**: Cold vapor – Atomic absorption spectrophotometer.

**D.I.W**: Deionized water

**DOC**: Dissolved organic carbon

**DOM**: Dissolved organic materials

**EDLE**: Equilibrium dialysis ligand exchange

**FA**: Fulvic acid

**$Fe(ox)_n$**: Ferric oxalate complexes

**GFC**: Gel filtration chromatography

**HA**: Humic acid

**HMW**: High molecular weight

**HS**: Humic substances

**ICP-MS**: Inductively coupled plasma –Mass spectrometer.

**kD**: kilo Dalton

**LMW**: Low molecular weight

**MeHg**: Methylmercury.

**MWCO**: Molecular weight cut off

**TFUF**: Tangential flow ultrafiltration

**TOC**: Total organic carbon

**UVA**: Ultraviolet A-radiation(320-400 nm)

**Abstract**

The thesis comprises four main chapters on chemical reactions and kinetics of some of the processes involved in the global mercury cycle. In the first chapter, the UVA irradiation of aqueous acidic mercuric chloride in the presence of large excess of Fe(III) organic diacid complexes results in partial reduction of the mercuric ion to elemental mercury. The pseudo-first-order rate constant (k) for photoreduction reaction is pH-dependent. Similar results were obtained using visible irradiation although the rates were ca. 10 times slower.

The mechanism of photoreduction is inferred to involve reaction of Hg(II) with a secondary photoproduct, the strongly reducing radical anion $CO_2^{-\bullet}$. No other previous reports have suggested the involvement of this radical in mercury reduction. In the presence of dissolved oxygen, competition for $CO_2^{-\bullet}$ between Hg(II) and $O_2$ reduces the rate and efficiency of mercuric ion reduction. The $O_2^{-\bullet}/HO_2$ products do not reduce Hg(II). On the contrary, their disproportionation leads to the formation of $H_2O_2$ which causes a slow reoxidation of Hg(0).

In the second chapter, the reaction rate of UVA photoreduction of Hg(II) ions by fulvic and humic acids was found to have higher values in the pH range of 5 to 6 which is relevant to most aquatic environments, within this pH range, speciation calculations show that most of Hg(II) will bind to DOC. The effects of environmentally relevant parameters such as Hg(II)/ HS ratio, and chloride concentration were investigated and the likely mechanism identified.

The interaction of DOC with Hg species is not only limited to photoreactions but also the complexation reaction affects the bioavailability and speciation of Hg. This was the topic of the last two chapters. The kinetic stability of Hg-HS and MeHg-HS complexes was characterized by different combined techniques; the competitive ligand exchange method (CLEM) combined with inductively coupled plasma-mass spectrometer (CLEM-ICP-MS) and the tangential flow ultrafiltration (TFUF) combined to CLEM-ICP-MS. The Hg-HS complexes can be described by at least two kinetically distinguished components; the more inert (slow) with a dissociation rate constant in the order of $10^{-5}$ $s^{-1}$, and a labile component with a dissociation rate constant in the order of

$10^{-3}$ $s^{-1}$, protons ($H^+$) was found to compete with $Hg^{2+}$ for the strong binding sites, Hg/HS concentration ratio also was an important parameter, when [$Hg^{2+}$] was high then the strong binding sites was saturated and the excess Hg bound to the weak sites. For the MeHg-HS species, our work demonstrates that this complex contains more than two kinetically distinguished components but the more inert ones have similar kinetic dissociation and it was difficult to separate them. Even though we spiked our model solutions with high initial concentration of Hg species ($\geq$ 1μg/L), our final results show that only 240-440 ng/L were found in the kinetically more inert components.

The distributional speciation shows that more than 50% of Hg-HS and MeHg-HS complexes were found in the colloidal phase of the size fractions > 30 kD. Detailed kinetic analysis show that the kinetically inert species were predominantly found in the size fractions of < 5kD. This support the observation that for the low levels of Hg and MeHg in nature, most is associated with low molecular weight DOC.

**Résumé**

La thèse se comporte de quatre chapitres principaux sur les réactions chimiques et la cinétique de certains processus impliqués dans le cycle global du mercure.

Dans le premier chapitre, l'irradiation UVA du chlorure d'acide de mercure aqueux en présence d'un grand excès de complexes organiques du diacide de Fer(III) a comme conséquence la réduction partielle de l'ion mercurique au mercure élémentaire. La constante du taux de pseudo-premier-ordre (k) pour la réaction de photoreduction est dépendante du pH. Des résultats semblables ont été obtenus en utilisant l'irradiation visible bien que les taux ait été approximativement 10 fois plus lentes. Le mécanisme de la photoreduction implique la réaction de Hg(II) avec un photoproduit secondaire, l'anion radicalaire réducteur fort $CO_2^{-\cdot}$. Aucun rapport ultérieur n'a suggéré la participation de ce radical dans la réduction de mercure. En présence de l'oxygène dissous, la compétition pour le $CO_2^{-\cdot}$ entre Hg(II) et $O_2$ réduit le taux et l'efficacité de la réduction de l'ion de mercure. Les produits $O_2^{-\cdot}/HO_2$ ne réduisent pas le Hg(II). Au contraire, leur disproportionement à la formation de $H_2O_2$ qui cause une réoxidation lente de Hg(0).

Dans le deuxième chapitre, le taux de réaction de photoreduction AUV des ions de Hg(II) par les acides fulvic et humiques s'est avéré avoir des valeurs plus élevées dans l'intervalle de pH 5 à 6 ce qui est appropriée à la plupart des environnements aquatique, dans cette marge de pH, les calculs de spéciation montre que la majeure partie de Hg(II) se coordonne avec le COD. Les effets des paramètres environnementaux appropriés tels que le rapport de Hg(II)/HS, et la concentration en chlorure ont été étudiés ainsi que l'identification d'un mécanisme probable a ce phénomène.

Dans le troisième et le quatrième chapitre nous avons étudié l'interaction du COD avec des espèces de mercure, qui ne se limite pas seulement a la photoreaction mais également a leur complexation ce qui affecte la disponibilité biologique et la spéciation du mercure. La stabilité cinétique des complexes Hg-HS et MeHg-HS a été caractérisé par la combinaison de différentes techniques; la méthode d'échange de ligand compétitive (CLEM) combiné avec la spectrométrie de plasma-masse inductivement couplé (CLEM-ICP-MS) et l'ultrafiltration de flux (TFUF) a combiné avec CLEM- ICP-MS. Cinétiquement les complexes de Hg-HS peuvent être décrits par au moins deux

composants distingués; un composant plus inerte (lent) avec une constante du taux de dissociation de l'ordre de $10^{-5}s^{-1}$ et un autre composant labile avec une constante du taux de dissociation de l'ordre de $10^{-3}$ $s^{-1}$, On a trouve qu'il y a une compétition entre les protons ($H^+$) et les ions $Hg^{2+}$ pour la coordination avec les accepteurs forts, le taux de concentration de Hg/HS était un paramètre important dans le processus, quand [$Hg^{2+}$] étaient hauts alors les accepteurs forts ont été saturés et l'excès Hg bondissent aux emplacements faibles. Pour les espèces de MeHg-HS, notre travail montre que ce complexe contient plus de deux composants cinétiquement distingués mais les plus inertes ont une dissociation cinétique semblable et il était difficile de les séparer. Quoique nous marquions nos solutions modèles avec la concentration initiale élevée des espèces d'hectogramme ($\geq$ 1μg/L) mais nos résultats finaux montrent que seulement 240-440 ng/L ont été trouvés dans les composants cinétiquement plus inertes.

La distribution de spéciation que plus de 50% de complexes Hg-HS et de MeHg-HS a été trouvé dans la phase colloïdale du kD des fractions de taille >30kD. L'analyse cinétique détaillée montre que les espèces cinétiquement inertes ont été principalement trouvées dans les fractions de taille de <5kD. Ce qui confirme l'observation pour les bas nivaux de Hg et MeHg dans la nature, la plus part étant associe avec des molécules de faible poids COD.

**ACKNOWLEDGEMENT**

First, I would like to thank my supervisors Dr. David lean and Dr. Susannah Scott for their advice, guidance and scientific support through the completion of this thesis. I would like also to extend my thanks to Dr. Conrad Grégoire, the head of the analytical chemistry lab at the Natural Resource Canada, for enabling me to carry out parts of the research using the ICP-MS at his lab and for the valuable scientific discussion.

I feel a deep sense of gratitude for my parents, brothers and sisters in Jordan for their long-suffering patience and for their understanding and moral support. I am very grateful for my wife Hanan, for her patience and assistance during my research and the completion of this thesis. The best experiences that we lived through in this period were the birth of our son Mohammad and daughters Noor and Doha; they added a joyful dimension to our life mission.

I would also like to thank the examiners (committee members) of my PhD thesis who took effort in reading and providing me with valuable comments and corrections on earlier version of this thesis. Dr. Jerome Nriagu, Dr. Nimal De Silva, Dr. Javier Giorgi and Dr. Tito Scaiano. I also would like to thank the people working in the graduate study office especially Lise Maisonneuve and Marc Landreville from (Admission and theses) office, they were very helpful and doing an excellent job. Last but not least, many thanks go to my friends, for their encouraging words and trust, John Murimboh (Acadia University), Hassan Al-Reasi, Ziyad Taha, Ghazar Aharonian, Abdulrahman Al-Hazmi, Rachid Touzani, Nabil Benabbou, Sadok Lataeif, Raed Abu-Reziq...and the list goes on.

**Table of contents**



## CHAPTER 1

**General Introduction**

## CHAPTER 2

### Experimental

## CHAPTER 3

**Photochemical reduction of aqueous mercuric chloride and reoxidation in the presence of ferrioxalate and air**



## CHAPTER 4

**Photoreduction of Hg (II) under UVA irradiations of humic and fulvic acids**

## CHAPTER 5

**Kinetic studies on the speciation of Hg(II) and MeHg(I) complexes with natural ligands in aquatic systems**



## CHAPTER 6

**Size fractionation and kinetic studies of Hg(II) and MeHg(I) complexes with natural ligands in aquatic systems**

**List of Figures**

## CHAPTER 1



## CHAPTER 2

## CHAPTER 3

## CHAPTER 4

## CHAPTER 5

## CHAPTER 6

**List of Tables**

## CHAPTER 1



## CHAPTER 2



## CHAPTER 4

## CHAPTER 5



## CHAPTER 6

# Chapter 1

# General introduction

## 1.1 Thesis rationale

In this first section we provide an overview with details in following sections. Mercury as $Hg^0$ is known to have a relatively high volatility compared to other trace metals; even Hg(II) associated with chloride, sulfide and oxide has some volatility. Because of the low solubility of $Hg^0$ in water and favorable Henry's law constant, evasion of Hg from soil and water into atmosphere has been recorded. The atmosphere represents a large reservoir of Hg with a long residence time (1-2 years). Indeed, $Hg^0$ is subject to long-range atmospheric transfer.

From the atmosphere, dry and wet deposition takes place onto land and water surfaces. Most of Hg in the atmosphere found in the elemental form ($Hg^0$). The high water and snow contents of Hg create the impression that Hg must be oxidized to the more soluble form Hg(II) before deposition. In one part of this work, we investigate the kinetics of oxidation of Hg(0) by HOCl and $OCl^-$, which are important species in aerosol droplets especially in the marine environment.

After deposition onto the surface of water, different processes occur that affect the speciation of Hg in aquatic systems. The evasion of Hg back to the atmosphere is significant at midday in the summer. Investigations refer to photochemical reduction of the Hg(II) to Hg(0). Various candidates are hypothesized to play the role of photoreducing

agent. Iron species are commonly present in freshwaters, and Fe(III) complexes with organic carboxylates are photosensitive compounds. When exposed to radiation of suitable wavelength, they undergo ligand-to-metal charge transfer, resulting in an excited state which decomposes with formation of Fe(II) and highly reducing organic radicals. These radicals play an important role in the reduction of Hg(II). The aim of one part of the research is to study the photoreduction of Hg species by UVA irradiation of aqueous solutions contain Fe(III) oxalate complexes and Hg(II). Knowing that the carboxylate group is one of the major functional groups in humic materials, ferrioxalate is therefore a model for the role of iron-humic complexes in the photoreduction of mercuric ion. However, humic substances (HS) also play an indirect role in the photoreduction of Hg(II) species. Upon irradiation, different reactive oxygen species and the hydrated electron are produced. In this research, we investigate the role of HS in photoreduction of Hg(II), along with the effects of environmentally relevant parameters such as pH , Hg(II)/HS ratio, and chloride concentration.

In addition to the photochemical role of DOC, complexation reaction with both Hg(II) and $MeHg^+$ are very important in the aquatic environment and play a key role in the speciation of Hg(II), and this, in turn, affects the bioavailability and mobility of different Hg species. The majority of the research work on the complexation of Hg species with DOC concentrates on thermodynamic properties. The kinetics of dissociations of Hg-DOC and MeHg-DOC complexes have received little attention. The purpose of our work in this area is to fill the gap in the knowledge about the kinetics of Hg-DOC species and try to relate these results to the observed thermodynamic constants.

The size distribution of Hg-DOC and MeHg-DOC complexes is a factor that affects the bioavailability of Hg species. The high molecular weight fractions (HMW) of DOC are more bioavailable and they are utilized by bacteria more rapidly than the low molecular weight fractions (LMW). The distribution of some functional groups like hydroxylates is also affected by the size fraction, and this in turn results in a range of complexation strengths of DOC toward metal ions. In this research area, we investigate the kinetics of Hg-DOC and MeHg-DOC binding in different size fractions with some emphasis on the effects of pH and concentration ratio of Hg to DOC.

The mercury cycle in the environment is very complex and different transformations occur simultaneously under the same conditions. Examples include the methylation of Hg and demethylation of MeHg, photooxidation and photoreduction, evasion and deposition. As a result, different mechanisms are involved in this cycle. The general purpose of this work is to provide some information and knowledge about these processes and the environmental parameters that affect these reactions.

## 1.2 Chemistry of mercury

Mercury (Hg) is a naturally-occurring metal in the environment. Usually it is found in the earth's crust in the form of cinnabar (HgS), either in a red or amorphous black form. Major deposits of HgS are significant in Spain, Slovenia and Italy.[1] The element constitutes only 0.5 ppm (average value) of the earth's crust and it is 62$^{nd}$ in order of abundance.[2] The preparation of mercury from cinnabar (HgS) ore is very simple. The ore is ground up and heated to high temperature (~600 °C) in the presence of oxygen. Mercury vapour escapes

from the ore and is trapped by condensation. After treatment with acid and using vacuum distillation, the product appears as a shiny, silvery metallic liquid at room temperature.

*1.2.1 Some physical and chemical properties*

Mercury belongs to group IIB of the periodic table with an atomic number of 80 and an average atomic weight of 200.59 g/mol. It has seven stable isotopes: $^{196}Hg$, $^{198}Hg$, $^{199}Hg$, $^{200}Hg$, $^{201}Hg$, $^{202}Hg$, and $^{204}Hg$. The most abundant one is $^{202}Hg$ (29.86%), while $^{196}Hg$ represents only 0.15 % of all stable Hg isotopes.[1]

As a liquid, metallic mercury has a high specific gravity, weighing 13.6 times as much as an equal volume of water.[1] Mercury freezes at a temperature of -38.89 °C, which makes it the only liquid metal at room temperature. It has a boiling point of 356.58 °C, and a high vapour pressure of $1.2 \times 10^{-3}$ mmHg at 20 °C.[2] Because of its high volatility, and low solubility in water ($\sim 3.3 \times 10^{-7}$ mol/L),[3,4] mercury is subject to long range atmospheric transfer processes.

The three ionization potentials for the mercury are 10.43, 18.65 and 34.3 eV.[5] The third value is very high; this indicates that mercury forms complexes mainly in the oxidation states (I) and (II) . Hg(III) is not yet well-characterized.[5]

*1.2.2 Uses*

Mercury and its compounds have many applications in the industrial and pharmaceutical industries as well as other fields. As a liquid metal, mercury is used in electrical switches in thermostats and alarm clocks. Because of its high thermal expansion coefficient, it is extensively used in thermometers. Another application is the use of mercury as an electrode in the production of chlorine gas and caustic soda.

Amalgam, which is an alloy formed from the reaction of metallic mercury with other metals like silver, tin or gold, is used in dental fillings. Also, the gold mining operation may use mercury to extract gold from ores. Mercury vapor is used in UV and fluorescent lamps.

Mercury salts, such as the oxide, chloride, and sulphide, as well as different organic forms, have many applications. For instance, mercuric chloride ($HgCl_2$ was used as an insecticide, bactericide and disinfectant. Mercuric sulphide (HgS), in one of its forms, is used as a pigment (red coloring agent). Mercuric oxide (HgO) has been used in skin ointment as an antifungal agent. It has been reported that the skin-lightening creams contain high levels of mercuric compounds.[6] Mercurous chloride ($Hg_2Cl_2$) is widely used in electrochemistry as the calomel electrode. Mercury and some of its compounds are used as a catalyst in organic synthesis, polymerization and manufacturing.

Even though considered to be the most toxic forms of Hg species, organomercury compounds have some applications and uses in our daily life. Merbromin (known as Mercurochrome) and Thimerosal (Figure 1.1) are used as an antiseptic[7] and vaccine preservative,[7,8] respectively. Organic mercury compounds were employed in antisyphilitic drugs and laxatives.[9] Methoxyethyl- and phenylmercuric bromide or acetate were used as pesticides, and as fungicides in seed dressings and paints. Methylmercury was also used as a fungicide.

It is worth mentioning that some applications and uses of mercury and its compounds have been canceled or banned due to their high toxicity.

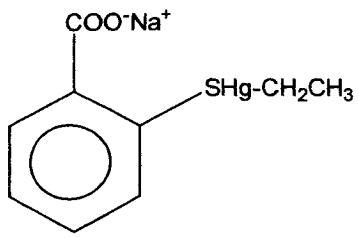


Thimerosal

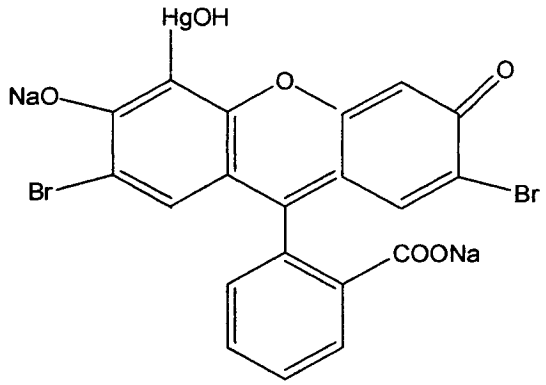


Mercurochrome

**Figure 1.1** Molecular structures of the organo-mercury compounds Merbromin (Mercurochrome) and Thimerosal.

*1.2.3 Mercury compounds*

Mercury has two common oxidized forms: mercurous ($Hg^{1+}$) and mercuric ($Hg^{2+}$). The mercurous form exists as a dimer ($Hg_2^{2+}$) with a metal-metal bond. It can be prepared by mixing Hg(II) with Hg(0), or by the reduction of Hg(II). The dimer ($Hg_2^{2+}$) disproportionates to Hg(0) and Hg(II) according to equation 1.1 .

$$Hg_2^{2+} \rightleftarrows Hg^0 + Hg^{2+} \qquad (1.1)$$

Mercurous halides have been shown to have almost a linear structure (X-Hg-Hg-X).[10] The stability order of these compounds depends on the electronegativity and size of the ligands, as shown below:[10]

$Hg_2F_2 > Hg_2Cl_2 > Hg_2Br_2 > Hg_2I_2$.

Solid mercurous iodide ($Hg_2I_2$) is the least stable. It undergoes dissociative vaporization (equation 1.2).[11]

$$Hg_2I_{2(s)} \rightleftarrows HgI_{2(s)} + Hg^0_{(g)} \qquad (1.2)$$

$$\downarrow$$

$$HgI_{2(g)}$$

Oxoanions form complexes with $Hg^{1+}$ like $Hg_2(BrO_3)_2$ and $Hg_2(ClO_3)_2$.[12] The azide complex $Hg_2(N_3)_2$ is also known.[13]

The mercuric ion ($Hg^{2+}$) has an ionic radius of 116 pm (assuming hexaaqua complex), which is close to that of $Ca^{2+}$ (114 pm), and both are doubly charged. However, $Hg^{2+}$ is considerably more polarizing and so its compounds have more covalent bond character. In mercuric chloride ($HgCl_2$), the Hg-Cl bond has only 23% ionic character.[14] This implies that when mercuric chloride is dissolved in water it remains largely undissociated. As a soft acid, the mercuric ion ($Hg^{2+}$) tends to bind to soft ligands with sulfur donor atoms. But it also forms complexes with stable Hg-C bonds known as organomercury compounds. Preparation of this category of compounds has been reported in the literature.[2,15,16] As an example, methylmercury chloride (MeHgCl) is a linear molecule, with an Hg-C bond length of 2.06-2.12 Å, [17,18] In general, the Hg-C bond is very stable in many different chemical environments,[18] but it can be ruptured with mineral acids according to equations 1.3 - 1.4

$$CH_3HgCH_3 + HX \rightarrow CH_4 + CH_3HgX \qquad (1.3)$$

$$CH_3HgX + HX \rightarrow CH_4 + HgX_2 \qquad (1.4)$$

where X= halide. The acid cleavage of aryl-Hg bonds is much easier than that of alkyl-Hg bonds.[19]

Mercury clusters are also known. Examples include $Hg_3^{4+}$ with a triangular ($D_{3h}$) structure,[20] $Hg_3^{2+}$ with a liner ($D_{\infty h}$) structure,[21,22] and $Hg_4^{2+}$ with a nearly linear structure.[23] These clusters are prepared as a result of the disproportionation reactions of $Hg_2Cl_2$ or $Hg_2F_2$ in the presence of elemental mercury and a suitable ligand.

## 1.3 Mercury in the environment

Mercury is widely distributed in the environment. The total amount of mercury present in the troposphere and in natural water bodies has been estimated to be $6.0 \times 10^6$ and $1.1 \times 10^7$ kg respectively.[24] Both natural and anthropogenic sources contribute to the total input of mercury into the environment. In 1983 the estimated anthropogenic emission of Hg to the atmosphere was ~ $3.6 \times 10^6$ kg/yr while natural emissions were $2.5 \times 10^6$ kg/yr.[25] Natural sources include volcanic activity, degassing and erosion of soil and emission from ocean and other water bodies. The main anthropogenic sources are coal burning,[26] mining activities, especially gold mining,[27] ore roasting and processing, waste incineration and some industrial activities.[26]

*1.3.1 Mercury in the atmosphere*

In the atmosphere, mercury is mainly found in the elemental form, Hg(0)[28], whose residence time in the atmosphere is estimated to be about 1 year.[29,30] This long lifetimes has led to long–range atmospheric transport and global mercury pollution.

The ocean receives 90% of its mercury through wet and dry deposition from the atmosphere.[31] It is hypothesized that Hg(0) in the atmosphere is first oxidized to the more soluble form $Hg^{2+}$ before deposition. Ozone ($O_3$) is reported to have the ability to oxidize Hg(0) in the atmospheric aqueous phase (fog and cloud droplets) [32] and in the gas phase[33] (equations 1.5 -1.6 ).

$$Hg^0_{(aq)} + O_{3\,(aq)} \rightarrow HgO_{(aq)} + O_{2\,(aq)} \quad k = 4.7 \times 10^{7}\, M^{-1}s^{-1} \qquad (1.5)$$

$$Hg^0_{(g)} + O_{3\,(g)} \rightarrow HgO_{(g)} + O_{2\,(g)} \quad k = 3 \times 10^{-20}\, cm^3 molecule^{-1}\, s^{-1} \qquad (1.6)$$

Chlorine species such as $OCl^-$ and HOCl were reported to oxidize Hg(0).[34] This may implicate the sea salt aerosol in Hg(0) oxidation. The ·OH radical is produced photochemically in the atmosphere and is reported to be a daytime oxidant for Hg(0) in both gas and condensed phases[35-37] (equations 1.7 - 1.8).

$$\cdot OH + Hg^0 \rightarrow \cdot HgOH \qquad (1.7)$$

$$\cdot HgOH + H_2O + O_2 \rightarrow Hg(OH)_2 + H^+ + O_2^- \qquad (1.8)$$

Because it is rapidly photolyzed by solar irradiation, the nitrate ($NO3^-$) is known as a nighttime oxidant,[24] The kinetics of its oxidation of Hg(0) has been investigated.[38] The chemical reaction is shown in eq. 1.9.

$$Hg^0 + NO_{3\,(g)} \rightarrow HgO_{\,(g)} + NO_{2\,(g)} \qquad (1.9)$$

After the oxidation of Hg(0), the Hg(II) produced in cloud and water droplets may undergo reduction. Sulfite ($SO_3^{2-}$) was found to reduce Hg(II) through the formation of the $HgSO_3$ complex.[39]

*1.3.2 Mercury in the aquatic environment*

The chemical form of Hg in the aquatic environment is strongly influenced by the pH, concentration of organic and inorganic complexing ligands as well as their complexation stability constants toward Hg, and the temperature, which is an important factor in the methylation of Hg.[40-42]

In oceanic water, 10-30 % of the dissolved Hg is found in gaseous form and mainly as Hg(0).[43,44] This indicates an oversaturation of the water relative to the atmosphere, and leads to evasion of Hg(0), which is an important part of mercury cycling. Hg(0) in aquatic systems may be produced by either biotic[45,46] or abiotic[47-50] reduction of Hg(II), but the exact mechanisms of such processes are still unclear.

The most abundant forms of Hg in the aquatic environment are Hg(II) species, Hg(II) is either truly dissolved or adsorbed to particulates species. Distribution coefficients depend on pH, ionic strength, and the concentration of DOC. For example, the

concentration of dissolved mercury in the Mediterranean Sea represents on average 70% of the total Hg (0.8 pM),[51] while in lakes, the particulate Hg concentration ranges from 0.09-1.7 μg $g^{-1}$ and the dissolved Hg from 0.16-3.6 $ngL^{-1}$.[52] These latter implies that the particulate phase plays an important role in the speciation and transportation of Hg in aquatic systems,[53-55] especially in fresh and coastal water systems. [53]

The speciation of dissolved Hg(II) in aquatic systems is regulated by chloride ($Cl^-$), hydroxide ($OH^-$), sulphide and bisulphide ($S^{2-}$ & $HS^-$) and DOC. In sea water, chloride complexes with the formula $[HgCl_n]^{2-n}$ were found to be the predominant Hg(II) species,[55] while in freshwater, dissolved Hg(II) was mainly found associated with DOC.[56-58]

Organomercury compounds are also found in aquatic environments. The fraction of total Hg that is MeHg is very low in marine water compared to freshwater.[53,59] Methyl- and dimethylmercury are thought to occur naturally in water due to biotic[60,61] and abiotic[62,63] methylation of Hg(II). The literature contains many reviews on the methylation process of Hg(II) in aquatic system.[64-66] However, human activities are also involved in the total input of MeHg .

## 1.4 Photochemistry of mercury

Photochemical reactions are important in the mercury cycle and can be classified as either direct or indirect. In direct photoreactions, the species of interest absorbs the radiation. This causes an activation of the molecule followed by bond cleavage, fragmentation or charge transfer. In contrast, target molecules are inert toward irradiation (no absorption) in indirect photoreactions. Irradiation causes excitation of another species, the sensitizer, which in turn

initiates chemical reactions of the target molecules in the same environmental compartment.

*1.4.1 Basics of photochemical processes* [67,68]

Electromagnetic radiation is a type of energy that is transmitted through either space or vacuum with no a requirement for a supporting medium. It is defined as a stream of discrete particles or wave packets of energy known as photons. The energy of each photon is proportional to the frequency of the radiation, according to equation 1.10.

$$E = h\nu; \quad \nu = c/\lambda \tag{1.10}$$

where $E$ is the energy, $h$ is Planck's constant, $c$ is the velocity of light, $\nu$ is the frequency and $\lambda$ is the wavelength. The electromagnetic spectrum covers a broad range of wavelengths. At one end, it is highly energetic with very short wavelengths ($\lambda \sim 10^{-11}$ cm for gamma radiation). At the other end, it is low in energy with long wavelengths ($\lambda \sim 10^{3}$ cm for radio frequency). Different chemical processes can be induced by absorption from different electromagnetic regions. For example, absorption in the infrared region causes vibrational excitation of molecules, while absorption in the UV-VIS region results in electronic transitions. In organic molecules, electrons in bonding ($\pi$, $\sigma$) and non-bonding (**n**) molecular orbitals are involved in these transitions. The most common are $\mathbf{n}\rightarrow\pi^*$ and $\pi\rightarrow\pi^*$, while $\mathbf{n}\rightarrow\sigma^*$ and $\sigma\rightarrow\sigma^*$ transitions are more energetic, the **d-d** and **f-f** electronic transitions and charge transfers are common in transition metal and lanthanide complexes.

When a beam of radiation in the UV-visible range passes through a sample containing molecules represented by (A), the following actions are possible:

1) If the energy of the incident radiation is less than the energy required for an electronic transition of the molecule (A), then the light is transmitted without any absorption. As an example, water molecules in the vapor phase do not absorb above ~ 180 nm, which implies that, any radiation with $\lambda > 200$ nm can pass through water vapor if other possibilities like refraction, reflection or scattering are eliminated.

2) If the energy of the incident radiation is sufficient to cause an excitation of the molecule, then excited state $A^*$ is produced. This state has a very short life time $10^{-8}$ - $10^{-9}$ s. The energy gained is degraded into heat or re-emitted as radiation; the latter phenomenon can be either fluorescence or phosphorescence (equations 1.11 - 1.13)

$$A \xrightarrow{h\nu_1} A^* \qquad (1.11)$$

$$A^* \rightarrow A + \text{heat} \qquad (1.12)$$

$$A^* \rightarrow A + h\nu_2 \text{ (fluorescence or phosphorescence with } h\nu_2 \leq h\nu_1) \qquad (1.13)$$

3) If excitation of the molecule leads to its decomposition into smaller molecules or produces radicals, or it causes some chemical changes, then this is known as a direct photochemical reaction (equation 1.14). The excited molecule also can lose the extra energy by collisions with another molecule, and this may lead to excitation of that molecule (equation 1.15). Chemical changes that occur in molecule D which did not absorb radiation (equation 1.16) represent the indirect photochemical reaction of D.

$$A^* \rightarrow B + C \quad \text{(radicals, bond cleavage, chemical changes)} \qquad (1.14)$$

$$A^* + D \rightarrow A + D^* \quad \text{(collision with another molecule)} \qquad (1.15)$$

$$\downarrow$$

$$B \text{ or } C + D \rightarrow \text{chemical changes in D} \qquad (1.16)$$

Thus, availability of light with sufficient energy is necessary but not sufficient for a photochemical reaction to occur, since the absorption of light can lead to other processes.

### *1.4.2 Direct photochemical reactions of Hg species in the aquatic environment*

#### *1.4.2.1 Elemental form Hg(0)*

In the gas phase, elemental mercury Hg(0) is found in the atomic form. It has an intense absorption line at 254 nm,[69] and it also emits at the same wavelength.[69] This means that upon irradiation of Hg(0) in the gas phase, absorption and fluorescence emission occur without any net photochemical reaction.( equation 1.17)

$$Hg^0 + h\nu\ (\lambda{=}254\text{ nm}) \xrightarrow{\text{Excitation}} (Hg^0)^* \xrightarrow{\text{Emission}} Hg^0 + h\nu\ (\lambda = 254\text{ nm}) \qquad (1.17)$$

In the liquid phase, the absorption line of Hg(0) is broadened. This phenomenon may be due to collisions of mercury atoms with surrounding solvent molecules.[70] The absorption peak of Hg(0) in aqueous solution was observed at 255 nm.[70]

At ambient temperature, the metal atoms in solution tend to bind to each other to form clusters, colloid particles or even precipitates. Such processes cause serious interference in atomic absorption and emission. Combined with the low solubility of Hg in water in the range of 58-63 μg/L,[3,4] the details of Hg(0) photolysis in water are not easily interpreted .

In aquatic systems, solar irradiation has a wavelength of $\lambda > 290$ nm. Since Hg(0) does not absorb in that region, direct photooxidation of Hg(0) is not possible.

*1.4.2.2 Mercurous form Hg(I)*

In aqueous solutions, the mercurous ion is found as a dimer, $Hg_2^{2+}$, and is stable only in acidic medium. It disproportionates to $Hg^{2+}$ and $Hg^0$ in the presence of σ-donor ligands such as $Cl^-$, $CN^-$ or $OH^-$. The diaqua complex $Hg_2(H_2O)_2^{2+}$ has an intense absorption maximum at 237 nm,[71,72] and other two absorption bands at 214 nm and 204 nm.[71] The absorption of $Hg_2(H_2O)_2^{2+}$ is due to an electronic transition from the **σ** bonding to **σ*** anti-bonding molecular orbital of the Hg- Hg bond. Absorption therefore leads to dissociation of the $Hg_2^{2+}$ molecule (equation 1.18)[71]

$$Hg_2^{2+}{}_{(aq)} \xrightarrow{237\ nm} 2\ Hg^{+}{}_{(aq)} \qquad (1.18)$$

Because $Hg_2^{2+}$ is found in equilibrium with its disproportionation products (equation 1.19),[73] the $Hg^+$ formed from equation 1.18 reacts with $Hg^0$ to produce another short lived intermediate (equation 1.20):

$$Hg_2^{2+} \rightleftarrows Hg^0 + Hg^{2+} \qquad (1.19)$$

$$Hg^+ + Hg^0 \rightarrow Hg_2^+ \qquad (1.20)$$

Both intermediates ($Hg^+$ and $Hg_2^+$) react with dissolved oxygen in aqueous solution to produce $O_2^-$ (equations 1.21 - 1.22).[74] which leads to the formation of $H_2O_2$.

$$Hg^{+} + O_2 \rightarrow Hg^{2+} + O_2^{-} \quad (1.21)$$

$$Hg_2^{+} + O_2 \rightarrow Hg_2^{2+} + O_2^{-} \quad (1.22)$$

The result of the direct photolysis of $Hg_2^{2+}$ is the production of Hg(II) and Hg(0). However in the presence of Hg(II), self-regeneration of $Hg_2^{+2}$ is observed upon irradiation.[75] Those reactions may not be very significant in the aquatic environment because they occur outside the wavelength range of the solar irradiation that reaches the earth's surface.

*1.4.2.3 Mercuric form Hg(II)*

With a filled $d^{10}$ electronic configuration, Hg(II) is not expected to show a **d-d** electronic transitions. Hg(II) forms complexes with linear, trigonal planar and tetrahedral structures and coordination number of 2, 3 and 4 respectively.[76] Mercuric halide complexes with the general formula $[HgX_n]^{-(n-2)}$ are well- known, where X = $Cl^-$, $Br^-$ or $I^-$ and n = 2, 3 or 4. Solutions of these complexes absorb significantly in the region 200-250 nm (Table 1.1). In aqueous solution, the absorption maxima of these complexes may deviate by several nanometers from those reported in organic solvents. Irradiation of mercuric halide complexes with light of an appropriate wavelength results in reduction of Hg(II) and formation of $X_2^-$ radical anions.[77] The mechanism involves ligand–to–metal charge transfer (LMCT). Halide complexes of Hg(II) are important in sea water.

**Table 1.1** Absorption maxima of some mercuric complexes and their extinction coefficients.

| Mercuric species | Absorption maxima ($\lambda$, nm) | $\varepsilon \times 10^{-3}$ $M^{-1} cm^{-1}$ |
|---|---|---|
| $HgCl_2$ [80] | ~200 | 2.1[a] |
| $HgCl_3^-$ [80] | 240 | 21.2[a] |
| $HgCl_4^{2-}$ [80] | 234 | 41.8[a] |
| $HgBr_2$ [81] | ~200 | 9.0[b] |
| | 232 | 4.5[b] |
| $HgBr_3^-$ [81] | 260 | 18.0[b] |
| $HgBr_4^{2-}$ [81] | 250 | 37.0[b] |
| $HgI_2$ [82] | 211 | 19.0[a] |
| | 266 | 5.2[a] |
| $HgI_3^-$ [82] | 217 | 35.0[a] |
| . | 256 | 22.8[a] |
| | 301 | 16.1[a] |
| $HgI_4^{2-}$ [82] | 273 | 37.9[a] |
| | 329 | 22.4[a] |
| $HgS_2^{2-}$ [78] | < 330 [c] | --- |
| $Hg(OH)_2$ [78] | < 350 [c] | --- |

a In acetonitrile, b In methanol, c In water

Other Hg(II) compounds, such as $Hg(OH)_2$ and HgS, are also photosensitive. UV-irradiation of aqueous solutions of $Hg(OH)_2$ and HgS results in the formation of Hg(0).[78] The mechanism of $Hg(OH)_2$ reduction was suggested by Nriagu, [79] and is shown below (equations 1.23 - 1.24) :

$$Hg(OH)_2 \xrightarrow{h\nu} [Hg(OH)_2]^* \longrightarrow {}^{\cdot}Hg(OH)_{aq}(\textit{unstable}) + {}^{\cdot}OH \qquad (1.23)$$

$$2\ Hg(OH) \longrightarrow Hg^0 + Hg(OH)_2 \quad \text{(disproportionation)} \qquad (1.24)$$

*1.4.2.4 Organomercury species (methyl and dimethylmercury)*

Methylmercury chloride ($CH_3HgCl$) absorbs from the electromagnetic radiation below 310 nm.[83] It has been reported that direct UV irradiation of aqueous solutions of 10-100 μg/L MeHgCl results in the formation of elemental mercury ($Hg^0$) and $Hg_2Cl_2$ with $C_2H_6$ as the major organic product.[84] The proposed mechanism involves a cleavage of the Hg-C bond and formation of a C-C bond (equations 1.25 -1.27)[84]:

$$CH_3HgCl + h\nu \longrightarrow {}^{\cdot}CH_3 + HgCl \qquad (1.25)$$

$$2\ {}^{\cdot}CH_3 \longrightarrow C_2H_6 \qquad (1.26)$$

$$2\ {}^{\cdot}HgCl \longrightarrow Hg_2Cl_2 \qquad (1.27)$$

Based on a theoretical justification, Tossel[17]also proposed that the first step in the photodecomposition of methylmercury is cleavage of Hg-C bond, but with ultimate production of Hg(II) and Hg(0).

It has been shown that solar irradiation of lake water leads to photodecomposition of methylmercury.[85] The rate was found to be first order in the concentration of $MeHg^+$, but the end products were not identified.[85] For the photodecomposition of dimethylmercury, a mechanism was proposed by Nriagu.[79] Cleavage of the Hg-C bond and the formation of $C_2H_6$ via the production of methyl radical ($^{\cdot}CH_3$) was involved.

*1.4.3 Indirect photochemical reactions of Hg species in aquatic environment*

Other than $MeHg^+$, most Hg species in the aquatic environment does not absorb solar irradiation efficiently. This implies that their photoreactions are most probably of the indirect type. Species like DOC, nitrate ($NO_3^-$) and inorganic metal oxides ($M_xO$) have been suggested as candidates to initiate indirect photoreactions of Hg species.

*1.4.3.1 The role of DOC*

UV-irradiation of DOC results in changes in chemical structure of the humic and fulvic acids that are the major constituents of DOC, producing transient species in the aquatic environment. Ejection of an electron from DOC to produce a hydrated electron was proposed by Fisher and co-workers.[86] In support of this hypothesis, it was reported that photolysis of some organic compounds with carboxylic and polyhydroxy aromatic moieties (which are common in DOC) led to formation of hydrated electrons.[87,88] As a reducing agent, the hydrated electron is able to convert $Hg^{2+}$ to $Hg^{1+}$ and further to the elemental

form, $Hg^0$. A recent study utilized the hydrated electron mechanism to explain their findings of photoreduction of the $Hg^{2+}$ in lake water.[89]

In aqueous solution, the hydrated electron with a lifetime of 1.5 μs [89] reacts with dissolved oxygen to produce superoxide ($O_2^-$) which in turn produces hydrogen peroxide ($H_2O_2$). By exposing surface and ground water to sunlight, $H_2O_2$ was photochemically generated and its concentration was found to be related to the total organic carbon (TOC) concentration. [90]

In surface water, various transient oxidant species are produced by the photolysis of DOC. These include the hydroxyl radical (·OH),[91] singlet oxygen $^1O_2$,[92] and hydrogen peroxide($H_2O_2$).[93] Hydroxyl radical (·OH) is one of the most reactive photochemical products in the aquatic environment. It is produced by the photolysis of nitrate ($NO_3^-$) and DOC,[91] and can be scavenged by DOC.[94,95] It plays an important role in the oxidation of $Hg^0$ in water.[96-98] Gårdfeldt *et al.*[97] proposed a mechanism for $Hg^0$ oxidation by hydroxyl radical ·OH in aqueous solution (equations 1.28-1.29)

$$Hg^0 + {\cdot}OH \longrightarrow {\cdot}HgOH \qquad (1.28)$$

$$HgOH + {\cdot}OH \longrightarrow Hg(OH)_2 \qquad (1.29)$$

Another possible path is shown in equation 1.30:

$$2\ {\cdot}HgOH \longrightarrow Hg_2(OH)_2 \longrightarrow Hg^0 + Hg(OH)_2 \qquad (1.30)$$

·HgOH may also react with dissolved oxygen (equation 1.31):

$$^{\cdot}HgOH + O_2 + H_2O \longrightarrow Hg(OH)_2 + H^+ + O_2^- \quad (1.31)$$

Homolytic cleavage of the O-O bond in hydrogen peroxide ($H_2O_2$) leads to the formation of hydroxyl radical $^{\cdot}OH$ (equation 1.32). Due to the fact that the absorption coefficient of $H_2O_2$ in the range 200-300nm is low, either a high concentration of $H_2O_2$ or highly energetic UV below 200nm is needed to efficiently form $^{\cdot}OH$. However thermal oxidation or reduction of Hg species by $H_2O_2$ is possible (equations 1.33-1.34).[99]

$$H_2O_2 + h\nu\ (\lambda < 350\ nm) \longrightarrow 2\ ^{\cdot}OH \quad (1.32)$$

$$H_2O_2 + 2\ H^+ + Hg^0 \longrightarrow Hg^{2+} + 2\ H_2O \quad (1.33)$$

$$H_2O_2 + 2\ OH^- + Hg^{2+} \longrightarrow Hg^0 + 2\ H_2O + O_2 \quad (1.34)$$

Olefinic moieties in DOC also can play a role in the photochemistry of Hg. It has been reported that, in aqueous solution, $Hg^{2+}$ can readily add to the C=C group of cyclohexene (equation 1.35). [100]

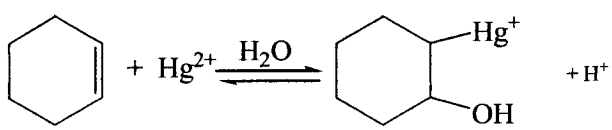


(1.35)

The equilibrium in the above reaction is disrupted by UV-irradiation at 230 nm, leading to the formation of $Hg_2^{2+}$ (equation 1.36). Prolonged irradiation led to the formation of metallic mercury. [100]

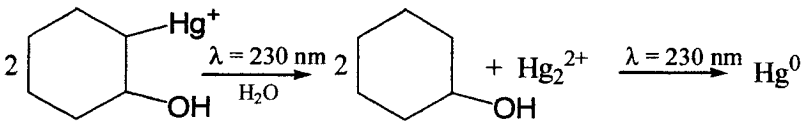

(1.36)

DOC containing conjugated olefin can form a complex by addition of $Hg2^{+}$ that will absorb from electromagnetic radiation at longer wavelength (red-shift). It may then absorb solar radiation such that $Hg^{2+}$ can be reduced. This represents another route for the photoreduction of $Hg^{2+}$ in the aquatic environment.

*1.4.3.2 The role of nitrate*

Nitrate occurs naturally in soil and water. It is the primary source of nitrogen for plants. Surface water may contain elevated concentrations of nitrate due to the extensive use of nitrogen fertilizers in agricultural areas. Nitrate absorbs at 200 nm with a high molar extinction coefficient ($\varepsilon = 9900\ M^{-1}\ cm^{-1}$),[101] while it absorbs weakly at 310 nm ($\varepsilon = 7.4\ M^{-1}\ cm^{-1}$). At the latter wavelength, nitrate absorption of solar radiation leads to the formation of hydroxyl radical ·OH (eq. 1.37),[102,103] which is a known oxidant for $Hg^{0}$.[96-98]

$$NO_3^- \xrightarrow{h\nu} [NO_3^-]^* \longrightarrow NO_2\cdot + O^{\cdot -} \xrightarrow{H_2O} NO_2\cdot + \cdot OH + OH^- \quad (1.37)$$

*1.4.3.3 The role of inorganic metal oxides as photocatalysts*

Mercury in the water column is found either in the form of a truly dissolved species or associated with colloidal or particulate materials. In fresh water systems, a considerable

fraction of Hg species is found in the particulate phase.[104] Silica, clay, sediment and calcite are constituents of the particulate phase.[105,106] Insoluble metal oxides and sulfides like ZnO, $Fe_2O_3$, $TiO_2$, HgO, $Al_2O_3$, ZnS and $MnO_2$ also contribute to the particulate phase.[105] Some of these oxides and sulfides have semiconducting properties, and work as photocatalysts.[107-109] For example, when $TiO_2$ is excited by radiation with energy higher than its band gap (3.2 eV), an electronic transition occurs to the conduction band, leaving behind a positive hole in the valence band (equation 1.38 ).[110,111]

$$TiO_2 + h\nu \longrightarrow TiO_2 (\mathbf{h}^+ + \mathbf{e}^-) \qquad (1.38)$$

In natural water, a significant fraction of heavy metal ions is adsorbed on the surface of particulate materials.[112] Some of the adsorbed metal ions can be reduced by capturing the electrons released from the metal oxide surface. For example, Fe(III), Hg(II), Cr(VI) and Cu(II) are reported to be reduced upon irradiation in the presence of a $TiO_2$ suspension.[113-115] The positive hole ($\mathbf{h}^+$) oxidizes a water molecule ( equation 1.39) or other available organic compounds.[110,111,115]

$$H_2O + \mathbf{h}^+ \longrightarrow {}^{\cdot}OH + H^+ \qquad (1.39)$$

In the presence of organic compounds, It has been reported that the photoreduction of metal ions is enhanced.[116] This implies that, in natural water, DOC plays an important role in the photocatalytic reduction of adsorbed Hg(II). DOC forms a layer that covers the surface of metal oxide particulates. The oxidation of such organics leads to suppression of electron-hole recombination in the photocatalyst. This process makes the released electron

more efficient for metal ion reduction. Dissolved oxygen in the water competes efficiently for the electron released from the photocatalyst. Its reaction produces superoxide and hydrogen peroxide (equations 1.40 - 1.42).[117]

$$O_2 + e^- \longrightarrow O_2^{\cdot -} \qquad (1.40)$$

$$O_2^{\cdot -} + H^+ \rightleftarrows HO_2^{\cdot} \qquad (1.41)$$

$$2\, HO_2^{\cdot} \longrightarrow H_2O_2 + O_2 \qquad (1.42)$$

Various applications have been documented in the literature for the purification and removal of Hg(II) from water using $TiO_2$ as a photocatalyst.[118,119] In natural water, other oxides such as $Fe_2O_3$, ZnO, $SiO_2$ and $MnO_2$ individually or as mixtures maybe involved in the photocatalytic reduction of Hg(II). This research area is poorly studied or documented.

## 1.5 Humic substances in the aquatic environment

### *1.5.1 Formation of humic substances*

Humic substances are formed as organic products by the decomposition of plant materials and the decay of animal and microbial remains.[120,121] The incomplete mineralization of the dead biomass "plant and animal tissues" results in accumulation of microbial refractory components which become a source material for a process called humification, in which humic substances are produced through multiple steps of oxidative degradation along with biological and enzymatic processes.

Various pathways have been suggested for the transformation of the source materials into humic substances (HS). One is the partial biodegradation of lignin (an important part of plant structural material). Oxidative degradation leads to the formation of humic acid (HA). Further oxidative degradation results in the formation of fulvic acid (FA). Another possible route is the reaction of modified lignin with amino compounds or proteins to form HS. This pathway is known as the lignin theory.[122] The polyphenol theory suggests condensation or polymerization reactions. Biodegradation of lignin could produce polyphenol, which is oxidized by enzymatic catalysis to quinine. The latter polymerizes with amines or amino acids to produce HS.[120, 123]

While the plants play an important role as the source material for the formation of HS in terrestrial and freshwater systems, microorganisms like phytoplankton also contribute to marine DOC. It was proposed that the release of unsaturated lipids by algae, and the free radical cross-linking of those lipids are partially responsible for the formation of marine humic materials.[124]

It is evident that the HS formation mechanism is affected by conditions such as the climatic, geography, physical and biological circumstances. The role of lignin is very important as a starting material for HS production.[125] A recent study showed that the structure of HS reflects its origin from lignin.[126]

### *1.5.2 Molecular structure*

It is very difficult to specify a definite structure for the HS because of its heterogeneity and molecular irregularity. This originates from the complexity of the starting (mixed) materials that enter the humification process to produce HS.

Various analytical methods have been used to identify HS. Partial success was achieved by identifying chemical fractions or units, as well as some functional groups. The pyrolysis products of HS identified by gas chromatography (GC) include simple aromatic compounds like benzene and toluene, substituted phenols, thiophene, $C_2$-$C_3$ carboxylic acids, pyrrole and $C_{11}$-$C_{15}$ saturated and unsaturated hydrocarbons.[127] The degradation of the carboxylic functional group of HS during pyrolysis was the driving force to develop, modify, and use non-degradative spectroscopic techniques like IR and combinations of solid state $^{13}C$ and $^{1}H$ NMR.[126] As a result, various species were identified in HS including amino acids,[128] glucosamine,[129] carbohydrates[130] and long chain fatty acids.[131] Thus HS contains a variety of functional groups classified as acidic, basic or neutral. Carboxylic and phenolic functional groups represent the most abundant acidic groups, while amine and amide groups are the main basic groups.[132] Ketones, aldehydes, ethers and esters groups represent the neutral components. All of these functional groups are distributed in both the aliphatic and aromatic moieties of humic substances.

Several HS structures have been suggested in consistent with some of the elemental analysis, parts of NMR data, the titration analysis and the acidity of carboxylic groups. Model structures for humic[133] and fulvic acids[134] are shown in Figures 1.2 and 1.3.respectively.

It is worth noting that sulfur and phosphorus are not represented in these structures, even though sulfur has been quantified in different humic substances, and reduced sulfur groups play an important role in the binding and chemistry of soft metal ions in the aquatic environment, especially mercury. Phosphorus (P) is also expected to contribute to the HS mass.

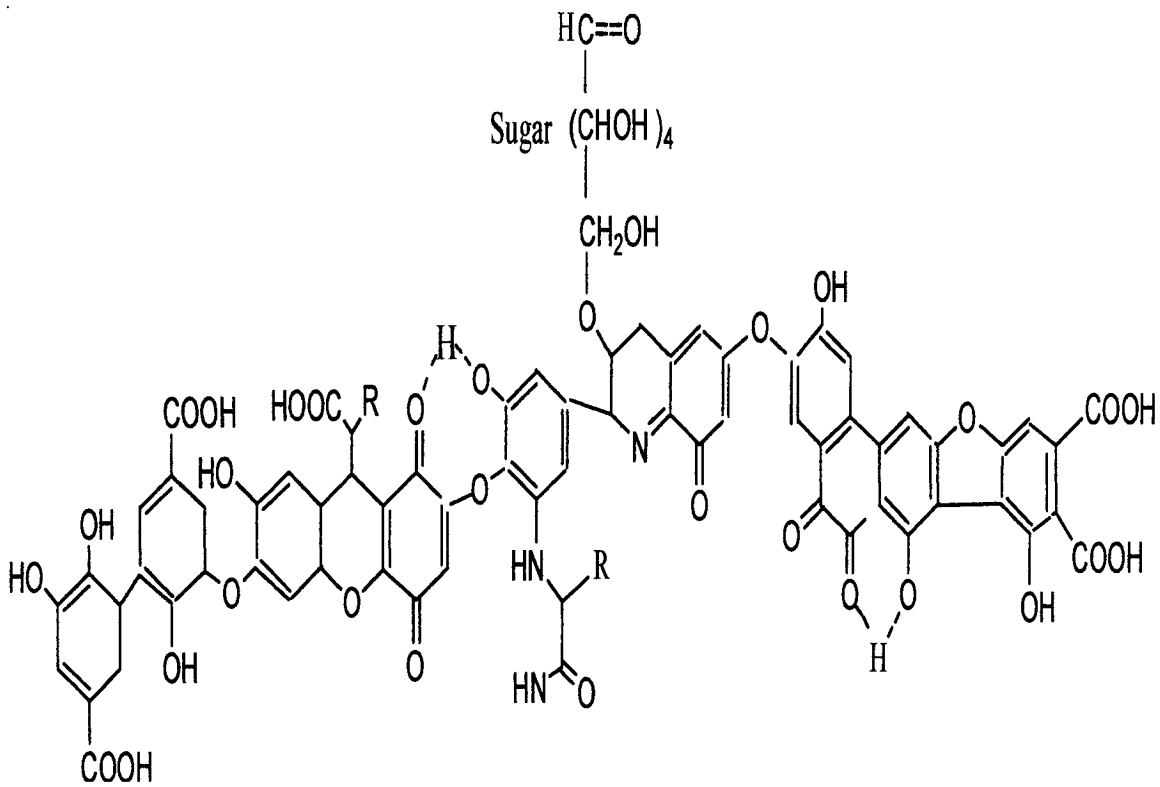


**Figure 1.2** Structural model for humic acid (adapted from reference 133.)

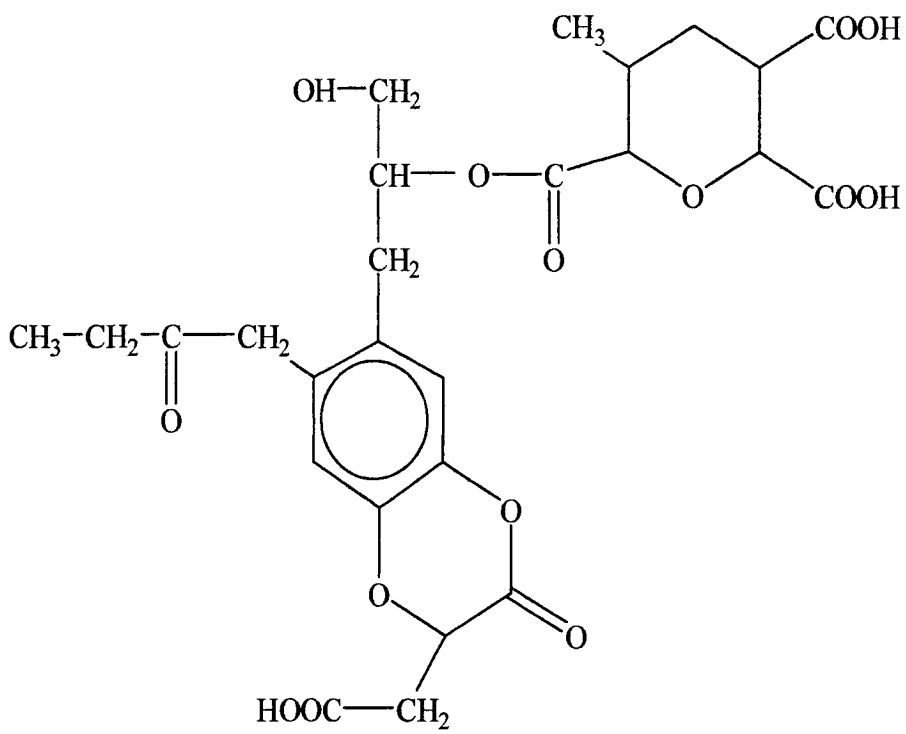


**Figure 1.3** Structural model for Suwannee River fulvic acid (adapted from reference 134).

*1.5.3 Chemical properties*

In the aquatic environment, humic substances constitute a major part of DOC. They are heterogeneous mixtures of organic compounds, and their chemical composition and molecular structure vary depending on their source and location. In general, it has been reported that the carbon content of humic substances contributes more than 50% of their total mass, while nitrogen contributes only 0.8- 6 % and sulfur 0.1- 4% of the total mass. [135]

Solid state $^{13}$C-NMR has been used to determine the distribution of carbon functional groups in HS. For Suwannee River fulvic acid, the aromatic and aliphatic carbon contents are 23.3% and 33.6%, respectively.[136] The aromatic moieties are the locations of the $\pi$ electrons and are responsible for the UV-absorption. Quinone, as a part of the aromatic system, is believed to be responsible for the redox properties of HS.[137]

Aliphatic structure, which mainly includes carbohydrates, sugar acids and amino acids, is the main part of HS that is biodegradable. [138] It was reported that the carbohydrate of the aliphatic structure are involved in metal ion complexation.[139] However, acidic functional groups, which mainly consist of carboxylic and phenolic groups, are the most abundant complexing sites for metal ions. The acid-base properties are essential factors that influence the complexing ability of HS toward trace metal ions.[140-142] The high content of the humic material in both carboxylic and phenolic groups leads to two acid dissociation constants, $K_{a1}$ and $K_{a2}$. For Suwannee River fulvic acid, $pK_{a1}$ covers a range from 3.7-5.0, [143] which means that at pH > 5 the carboxylic groups will be fully deprotonated. The value of $pK_{a2}$ is reported to be > 9.5,[143] implying that only at pH > 9.5 will the phenol groups be fully deprotonated.

**References**


(1) Schroeder, W. H.; Munthe, J. *Atmos. Environ.* **1998**, *32*, 809-822.

(2) Bailar, J. C., Jr; Emeleus, H. J; Nyholm, S. R; Trotman-Dickenson, A. F. Comprehensive Inorganic Chemistry, Pergamon Press: Elmsford,N.Y., 1973. Vol.3

(3) Onat, E. *J. Inorg. Nucl. Chem.* **1974**, *36*, 2029-2032.

(4) Clever, H. L.; Johnson, S. A.; Derrick, M. E. *J. Phys. Chem. Ref. Data* **1985**, *14*, 632- 680.

(5) Cotton, F. A.; Wilkinson, G. Advanced inorganic chemistry: a comprehensive text; Wiley: New York, 1980.

(6) Al-Saleh, I.; Al-Doush, I. *J. Toxicol. Environ. Health*, **1997**, *51*,123–130.

(7) Audicana, M. T.; Muñoz, D.; Dolores del Pozo, M.; Fernández, E.; Gastminza, G.; Fernández de Corres, L. *American Journal of Contact Dermatitis*, **2002**, *13*, 3-9.

(8) Geier, M. R.; Geier, D. A. *J. Am. Phys. Surg.* **2003**, *8*, 6-11.

(9) Wands, J. R.; Weiss, S. W.; Yardley, J. H.; Maddrey, W. C. *American Journal of Medicine*, **1974**, *57*, 92–101.

(10) Liao, M-S.; Zhang, Q-E. *J. Mol. Structure (Theochem).* **1995**, *358*, 195-203.

(11) Piechotka, M.; Kaldis, E. *J. Less-Common Metals*, **1986**, *115*, 315-324.

(12) Göbbels, D.; Meyer, G. *Z. Anorg. Allg. Chem.* **2003**, *629*, 2446-2447.

(13) Nockemann, P.; Cremer, U.; Ruschewitz, U.; Meyer, G. *Z. Anorg. Allg. Chem.* **2003**, *629*, 2079-2082.

(14) Eland, J. H. D. *Int. J. Mass. Spectrom. Ion. Phys.* **1970**, *4*, 37-49.

(15) Barbaro, P.; Cecconi, F.; Ghilardi, C. A.; Midollini, S.; Orlandini, A.; Vacca, A. *Inorg. Chem*, **1994**, *33*, 6163-6170.

(16) Larock, R. C.; Organomercuric compounds in organic synthesis; Springler-Verlag: New York, 1985.

(17) Tossell, J. A. *J. Phys. Chem.* A **1998**, *102*, 3587-3591.

(18) Barone, V.; Bencini, A.; Totti, F.; Uytterhoeven, M. G. *J. Phys. Chem.* **1995**, *99*, 12743-12750.

(19) Barone, V.; Bencini, A.; Totti, F.; Uytterhoeven, M. G. *Organometallics* **1996**, *15*, 1465-1469.

(20) Hämmerle, B.; Müller, E. P.; Wilkinson, D. L.; Müller, G.; Peringer, P. *J. Chem. Soc., Chem. Commun.* **1989**, *20*,1527-1528

(21) Ellisom, R. D.; Levy, H. A.; Fung, K. W. *Inorg. Chem.* **1972**, *11*, 833-836.

(22) Cutforth, B. D.; Davies, C. G.; Dean, P. A. W.; Gillespie, R. J.; Ireland,P. R.; Ummat, P. K. *Inorg. Chem.* **1973**, *12*, 1343-1347.

(23) Cutforth, B. D.; Gillespie, R. J.; Ireland, P.; Sawyer, J. F.; Ummat, P. K. *Inorg. Chem.* **1983**, *22*, 1344-1347.

(24) Lin, C.-J.; Pehkonen, S. O. *Atmos. Environ.* 1999, *33*, 2067-2077.

(25) Nriagu, J. O. *Science* **1989**, *338*, 47-49.

(26) Hylander, L. D. *Water Air Soil Pollut.* **2001**, *125*, 331-334.

(27) Wong, H. K. T. ; Gauthier, A. ; Nriagu, J. O. *Sci. Total Environ.* **1999**, *228*, 35-47.

(28) Nriagu, J. O. *Nature* **1993,** *363*, 589.

(29) Shia, R. -L.; Seigneur, C.; Pai, P.; Ko, M.; Sze, N. D. *J. Geophys. Res. D.* **1999**, *104*, 23747-23760.

(30) Lindqvist, O.; Johansson, K.; Aastrup, M.; Andersson, A.; Bringmark, L.; Hovenius, G.; Hakånsson, L.; Iverfeldt, Å.; Meili, M.; Timm, B. *Water Air Soil Pollut.* **1991**, *55*, 1-261.

(31) Mason, R. P.; Fitzgerald, W. F.; Morel, F. M.; *Geochim. Cosochim. Acta.* **1994**, *58*, 3191-3198.

(32) Munthe, J. *Atmos. Environ.* **1992**, *A26*, 1461-1468.

(33) Hall, B. *Water Air Soil Pollut.* **1995**, *80*, 301-315.

(34) Lin, C.-J.; Pehkonen, S. O. *Chemosphere* **1999**, *38*, 1253-1263.

(35) Lin, C.-J.; Pehkonen, S. O. *Atmos. Environ.* **1997**, *31*, 4125-4137.

(36) Sommar, J.; Gärdfeldt, K.; Strömberg, D.; Feng, X. *Atmos. Environ.* **2001**, *35*, 3049-3054.

(37) Gärdfeldt, K; Sommar, J.; Strömberg, D.; Feng, X. *Atmos. Environ.* **2001**, *35*, 3039-3047.

(38) Sommer, J.; Hallquist, M.; Ljunstrom, E.; Linqvist, O. *J. Atmos. Chem.* **1997**, *27*, 233-247.

(39) Munthe, J.; Xiao, Z. F.; Lindquist, O. *Water Air Soil Pollut.* **1991**, *56*, 621-630.

(40) Mauro, J. B. N. *Appl. Organomet. Chem.* **1999**, *13*, 631-636.

(41) Guimarães, J. R. D.; Meili, M.; Malm, O.; Brito, E. M. S. *Sci. Total Environ.* **1998**, *213*, 165-175

(42) Ullrich, S. M.; Tanton, T. W.; Abdrashitova, S. A. *Crit. Rev. Environ. Sci. Tec.* **2001**, *31*, 241-293.

(43) Kim, J.; Fitzgerald, W. *Geophys. Res. Lett.* **1988**, *15*, 40-43.

(44) Mason, R. P.; Fitzgerald, W. F. *Deep-Sea Res. PT II. (Topical Studies in Oceanography)* **1993**, *40*, 1897-1924.

(45) Mason, R. P.; Morel, F. M. M.; Hemond, H. F. *Water Air Soil Pollut.* **1995**, *80*, 775-787.

(46) Siciliano, S. D.; O' Driscoll, N.; Lean, D. *Environ. Sci. Technol.* **2002**, *36*, 3064-3068.

(47) Allard, B.; Arsenie, I. *Water Air Soil Pollut.* **1991**, *56*, 457-464

(48) Amyot, M.; Mierle, G.; Lean, D. McQueen, D. J. *Geochim. Cosmochim. Acta.* **1997**, *61*, 975-988.

(49) Rocha, J. C.; Jr-Sargentini, E. ; Zara, L. F. ; Rosa, A. H. ; dos Santos, A. ; Burba, P. *Talanta* **2003**, *61*, 699-707.

(50) Amyot, M.; Lean, D.; Mierle, G. *Environ. Toxicol. Chem.* **1997**, *16*, 2054-2063.

(51) Horvat, M.; Kotnik, J.; Logar, M.; Fajon, V.; Zvonarić, T.; Pirrone, N. *Atmos. Environ.* **2003**, *37*, Supplement 1: S93-S108.

(52) Watras, C. J.; Morrison, K. A.; Bloom, N. S. *Water Air Soil Pollut.* **1995**, *84*, 253-267.

(53) Coquery, M.; Cossa, D.; Sanjuan, J. *Mar. Chem.* **1997**, *58*, 213-227.

(54) Maurice-Bourgoin, L.; Quiroga, I.; Chincheros, J.; Courau, P. *Sci. Total Environ.* **2000**, *260*, 73- 86.

(55) Hahne, H. C. H. ; Kroontje, W. *J. Environ. Qual.* **1973**, *2*, 444-450.

(56) Mantoura, R. F. C. ; Dickson, A. ; Riley, J. P. *Estuarine Coastal Mar. Sci.* **1978**, *6*, 387- 408.

(57) Driscoll, C. T.; Blette, V.; Yan, C.; Schofield, C. L.; Munson, R.; Holsapple, J. *Water Air Soil Pollut.* **1995**, *80*, 499-508.

(58) Kolka, R. K., Grigal, D. F.; Verry, E. S.; Nater, E. A. *J. Environ. Qual.***1999**, *28*, 766-775.

(59) Kudo, A.; Nagase, H.; Ose, Y. *Water Res.* **1982**, *16*, 1011-1015.

(60) Siciliano, S. D.; Lean, D. R. S. *Environ. Toxicol. Chem.* **2002**, *22*, 1184-1190.

(61) Benoit, J. M.; Gilmour, C. C.; Mason, R. P. *Environ. Sci. Technol.* **2001**, *35*, 127-132.

(62) Beijer, K.; Jernelov, A. In: The biogeochemistry of mercury in aquatic environment. Nriagu, J. O., Eds.; Elsevier: North-Holland Biomedical press. 1979, pp 203-210.

(63) Siciliano, S. D.; O' Driscoll, N. J.; Tordon, R.; Hill, J.; Beauchamp, S.; Lean, D. R. S. *Environ. Sci. Technol.* **2005**, *39*, 1071-1077.

(64) Weber, J. H.; *Chemosphere* **1993**, *26*, 2063-2077.

(65) Winfrey, M. R.; Rudd, J. W. M. *Environ. Toxicol Chem.* **1990**, *9*, 853-869.

(66) Ullrich, S. M.; Tanton, T. W. ; Abdrashitova, S. A. *Crit. Rev. Environ. Sci. Techno.* **2001**, *31*, 241-293.

(67) Wayne, R. P. Principles and applications of photochemistry; Oxford University Press: Oxford (England), 1988.

(68) Gilbert, A.; Baggott, J. Essentials of molecular photochemistry, CRC Press: Boca Raton, 1991.

(69) Callear, A. B. *Chem. Rev.*, **1987**, *87*, 335-355.

(70) Tao, S.; Gong, S.; Xu, L.; Fanguy, J. C. *Analyst*, **2004**, *129*, 342-346.

(71) Mason, W. R. *Inorg. Chem.* **1983**, *22*, 147-150.

(72) Vogler, A.; Hunkely, H. *Inorg. Chim. Acta.***1989**, *162*, 169-170.

(73) Baltisberger, R. J.; Hilderbrand, D. A.; Grieble, D.; Ballintine, T. A. *Anal. Chim. Acta* **1979**, *111*, 111-112.

(74) Horváth, O.; Mikó, I. *J. Photochem. Photobiol. A* **1999**, *128*, 33-38.

(75) Horváth, O.; Ford, P. C.; Vogler, A. *Inorg. Chem.* **1993**, *32*, 2614-2615.

(76) Dean, P. A. W. *Prog. Inorg. Chem.* **1978**, *24*, 109-178.

(77) Langmuir, M. E.; Hayon, E. *J. Phys. Chem.* **1967**, *71*, 3808- 3814.

(78) Xiao, Z. F.; Munyhe, J.; Stromberg, D.; Lindqvist, O. In: Mercury pollution: integration and synthesis. Watras, C. J.; Huckabee, J. W., Eds.; Lewis Publishers, Boca Raton, 1994, pp 581-595.

(79) Nriagu, J. O. *Sci. Total Environ.* **1994**, *154*, 1-8.

(80) Horváth, O.; Vogler, A. *Inorg. Chem.* **1993**, *32*, 5485-5489

(81) Griffiths, T. R.; Anderson, R. A. *Can. J. Chem.* **1990**, *69*, 451-457.

(82) Horváth, O.; Vogler, A. *Inorg. Chim. Acta* **1994**, *221*, 79-84.

(83) Leiva-Presa, À.; Capdevila, M.; Cols, N.; Atrian. S.; González-Duarte, P *Eur. J. Biochem.* **2004**, *271*, 1323-1328.

(84) Inoko, M. *Environ. Pollut. B*, **1981**, *2*, 3-10.

(85) Sellers, P.; Kelly, C. A.; Rudd, J. W. M; Machutchon, A. R. *Nature*, **1996**, *380*, 694-697.

(86) Fisher, A.; Kliger, D.; Winterle, J.; Mill, T. *Chemosphere* **1985**, *14*, 1299-1306

(87) Joschek, H.; Grossweiner, L. I. *J. Am. Chem. Soc.* **1966**, *88*, 3261-3268.

(88) Köhler, G.; Solar, S.; Getoff, N.; Holzwarth, A. R.; Schaffner, K. *J. Photochem.* **1985**, *28*, 383-391.

(89) Zepp, R. J.; Braun, A. M.; Hoigné, J.; Leenheer, J. A. *Environ. Sci. Technol.* **1987**, *21*, 485-490.

(90) Cooper, W.; Zika, R. G. *Science* **1983**, *220*, 711-712.

(91) Vaughan, P. P.; Blough, N. V.; *Environ. Sci. Technol.***1998**, *32*, 2947-2953.

(92) Haag, W. R. ; Hoigne, J. *Environ. Sci. Technol.***1986**, *20*, 341-348.

(93) Cooper, W. J.; Lean, D. R. S. *Environ. Sci. Technol.* **1989**, *23*, 1425-1428.

(94) Zepp, R. G.; Hoigne, J.; Bader, H. *Environ. Sci. Technol.* **1987**, *21*, 443-450.

(95) Goldstone, J. V.; Pullin, M. J.; Bertilsson, S.; Voelker, B. M. *Environ. Sci. Technol.* **2002**, *36*, 364-372.

(96) Lin, C. -J.; Pehkonen, S. O. *Atmos. Environ.* **1997**, *31*, 4125-4137.

(97) Gårdfeldt, K.; Sommar, J.; Strömberg, D.; Feng, X. *Atmos. Environ.* **2001**, *35*, 3039- 3047.

(98) Lalonde, J. D.; Amyot, M.; Orvoine, J.; Morel, F. M. M.; Auclair, J.; Ariya, P. A. *Environ. Sci. Technol.* **2004**, *38*, 508-514.

(99) Schroeder, W. H.; Yarwood, G.; Niki, H. *Water Air Soil Pollut.* **1991**, *56*, 653-666.

(100) Horváth, O.; Vogler, A. *Inorg. Chem. Comm.* **1998**, 270-272.

(101) Maria, H. J.; McDonald, J. R.; McGlynn, S. P. *J. Am. Chem. Soc.* **1973**, *95*, 1050-1056

(102) Warneck, P.; Wurzinger, C.; *J. Phys. Chem.* **1988**, *92*, 6278-6283.

(103) Zepp, R. G.; Hoigne, J.; Bader, H. *Environ. Sci. Technol.***1987**, *21*, 443-450.

(104) Rolfhus, K. R.; Sakamoto, H. E.; Cleckner, L. B; Stoor, R. W.; Babiarz, C. L.; Back, R. C.; Manolopoulos, H; Hurley, J. P. *Environ. Sci. Tecnol.* **2003**, *37*, 865-872.

(105) Turner, A.; Millward, G. E. *Estuar. Coast. Shelf Sci.***2002**, *55*, 857-883.

(106) Buffle, J.; Leppard, G. G. *Environ. Sci. Technol.* **1995**, *29*, 2196-2175.

(107) Wang, J.; Uma, S.; Klabunde, K. J. *Appl. Catal. B-Environ.* **2004**, *48*, 151-154.

(108) Cun, W. ; Jincai, Z. ; Xinming, W. ; Bixian, M. ; Guoying, S.; Ping'an, P.; Jiamo, F. *Appl. Catal. B-Environ.* **2002**, *39*, 269-279.

(109) Pal, B.; Hata, T.; Goto, K.; Nogami, G. *J. Mol. Catal: A. Chem.* **2001**, *169*, 147-155.

(110) Hoffmann, M. R.; Martin, S. T.; Choi, W.; Bahnemann, D. W. *Chem. Rev.* **1995**, *95*, 69-96.

(111) Hsien, V. –H.; Chang, C. –F. ; Chen, Y. H. ; Cheng, S. *Appl. Catal. B-Environ.* **2001**, *31*, 241- 249

(112) Nagano, T.; Yanase, N.; Tsuduki, K.; Nagao, S. *Environ. Int.* **2003**, *28*, 649-658.

(113) Kanki, T. ; Yoneda, H. ; Sano, N.; Toyoda, A.; Nagai, C. *Chem. Eng. J.* **2004**, *97*, 77-81.

(114) Chen, D. ; Ray, A. K. *Chem. Eng. Sci.* **2001**, *56*, 1561-1570.

(115) Herrmann, J. M. *Catal. Today* **1999**, *53*, 115-129.

(116) Wang, Y. -Y.; Wan, C. –C. *J. Photochem. Photobio. A Chem.* **1994**, *84*, 195-202.

(117) Wang, K.; Hsieh, Y.; Chen, L.; *J. Hazard. Mater.* **1998**, *59*, 251-260.

(118) Zhang, F. –S.; Nriagu, J. O.; Itoh, H. *Water Res.* **2005**, *39*, 389-395.

(119) Khalil, L. B.; Rophael, M. W.; Mourad, W. E. *Appl. Catal. B-Environ.* **2002**, *36*, 125-130.

(120) Stevenson, F. J. Humus Chemistry; Wiley: New York, 1994.

(121) Huang, P. M. *Advances in Agronomy* **2004**, *82*, 391-472.

(122) Tipping, E. Cation binding by humic substances; Cambridge University Press: Cambridge UK, 2002.

(123) Huang, P. M. In Handbook of soil science. Sumner, M.E., Ed. CRC press: Boca Raton, FL, 2000, pp B303-334.

(124) Harvey, G. R.; Boran, D. A.; Piotrowicz, S. R.; Weisel, C. P. *Nature* **1984**, 309, 244-246.

(125) Wershaw, R. L.; Pinckney, D. L.; Llaaguno, E. C.; Vincentte-Bekett, V. *Anal. Chim. Acta* **1990**, 232, 31-42.

(126) Mao, J. –D.; Xing. B.; Schmidt-Rohr. K. *Environ. Sci. Technol.* **2001**, *35*, 1928-1934.

(127) Gaffney, J. S.; Marley, N. A.; Clark, S. B. In: Humic and fulvic acids: Isolation, structure, and environmental role. Gaffney, J. S., Marley, N. A., Clark, S. B., Eds.; American Chemical Society: Chicago, Illinois, USA, 1996.pp1-16.

(128) Jahnel, J. B.; Frimmel, F. H. *Acta. Hydrochim. Hydrobiol.* **1995**, *23*, 31-35.

(129) Jahnel, J. B.; Frimmel, F. H. *Fres. J. Anal. Chem.* **1996**, *354*, 886-888.

(130) Haiber, S.; Herzog, H.; Burba, P.; Gosciniak, B.; Labert, J. *Fres. J. Anal. Chem.* **2001**, *369*, 457-460.

(131) Jandl, G.; Sculten, H. R.; Leinweber, P. *J. Plant Nutr. Soil Sci.* **2002**, *165*, 133-139.

(132) Thurman, E. M. Organic geochemistry of natural waters; Martinus Nijhof/Dr. W. junk publishers: Dordrecht, Boston, 1985.

(133) Stevenson, F. J. Humus Chemistry; Wiley: New York, 1982

(134) Leenheer, J. A.; Wershaw, R.L.; Reddy, M. M. *Environ. Sci. Technol.***1995**, 29, 399-405.

(135) Perdue, E. M. In Aquatic humic substances: ecology and biogeochemistry. Hessen, D. O, Tranvik, L. J. Eds.; Springer, New York 1998, pp 41-61.

(136) Brown, G. K.; MacCarthy, P.; Leenheer, J. A. *Anal. Chim. Acta.* **1999**, *402*, 169-181.

(137) Scott, D. T.; McKnight, D. M.; Blunt-Harris, E. L.; Kolesar, S. E.; Lovley, D. R. *Environ. Sci. Technol.* **1998**, *32,* 2984-2989.

(138) Sun, L.; Perdue, E. M.; Meyer, J. L.; Weis, J. *Limnol. Oceanogr.* **1997**, 42, 714-721.

(139) Quigly, M. S.; Santtschi, P. H.; Hung, C. C.; Guo, L.; Honeyman, B. D. *Limnol. Oceanogr.* **2002**, *47*, 367-377.

(140) Christensen, J. B.; Christensen, T. H. *Water Res.* **2000**, *34*, 3743-3754.

(141) Lu, Y.; Allen, H. E. *Water Res.* **2002**, *36*, 5083-5101.

(142) Ramos, M. A.; Fiol, S.; Lopez, R.; Antelo, J. M.; Arce, F. *Environ. Sci. Technol.* **2002**, *36*, 3109-311

(143) Ritchie, J. D.; Perdue, E. M. *Geochim. Cosmochim. Acta* **2003**, *67*, 85-96.

# Chapter 2

# Experimental procedures

## 2.1 Preparation of reagents and solutions

Milli-Q deionised water (18.2 MΩ-cm) was used in the preparation of standards and working solutions. All glassware and Teflon bottles were soaked with 10% $HNO_3$ and rinsed thoroughly with deionised water prior to use.

### *2.1.1 Hg(II) solutions*

A known weight of red HgO (Aldrich, 99.99%) was dissolved in concentrated $HClO_4$ (Analar, 70%). Diluted stock solution was prepared in 0.2 M $HClO_4$ and titrated with 0.05 M KSCN (Baker ACS reagent) to the ferric alum endpoint, [1] which was determined by the appearance of the light red-brown color of $Fe(SCN)^{2+}$, (equations 2.1-2.3).

$$Hg^{2+} + SCN^- \rightleftarrows Hg(SCN)^+ \quad (2.1)$$

$$Hg(SCN)^+ + SCN^- \rightleftarrows Hg(SCN)_2 \quad (2.2)$$

$$Fe^{3+} + SCN^- \rightarrow Fe(SCN)^{2+} \quad (2.3)$$

The stock solution of Hg(II) is stable for a couple of months, however, diluted working solutions were prepared on a daily basis.

In one set of experiments (Chapter 3), $HgCl_2$ (EMD Chemicals, 99.5%) was prepared in diluted $H_2SO_4$. Its concentration was checked against a certified 100 ppm atomic absorption standard (VWR) in nitric acid.

### *2.1.2 Elemental $Hg^0$ in aqueous solution*

An aqueous solution was bubbled with argon for 30 min to remove dissolved oxygen. A chromous tower was used to remove oxygen from the argon. A drop of metallic mercury (Aldrich, 99.99%) was washed 3-4 times with 0.1 M $HClO_4$, followed by deionized water, placed in the argon-saturated solution and stirred overnight.[2]

The concentration of $Hg^0_{(aq)}$ was determined colorimetrically with dithizone (Sigma), according to a standard method.[3] To 50 ml of the $Hg^0$ solution, 1 ml of 1% $KMnO_4$ and 1ml concentrated $H_2SO_4$ were added, then the solution was boiled for ~20 min to ensure complete oxidation of $Hg^0$, 1ml of 2% $K_2S_2O_8$ was added. After cooling, the pink color was discharged by few drops of hydroxylamine hydrochloride ($NH_2OH.HCl$), then the pH of the solution was adjusted to 7 by phosphate/carbonate buffer. In a separatory funnel, the solution was extracted with chloroform solution containing 6 μg/L of dithizone. The orange Hg-dithizone complex was collected and the multiple extracts were combined. The absorbance of the complex at 495 nm was measured and the concentration of $Hg^{2+}$ was calculated from a calibration curve (Figure 2.1) obtained by spiking aqueous solutions with known amounts of $Hg^{2+}$ which were treated by the same procedure. The concentration of $Hg^0_{(aq)}$ measured in this way, $(2.0 \pm 0.2) \times 10^{-7}$ M, agrees well with its reported solubility.[4]

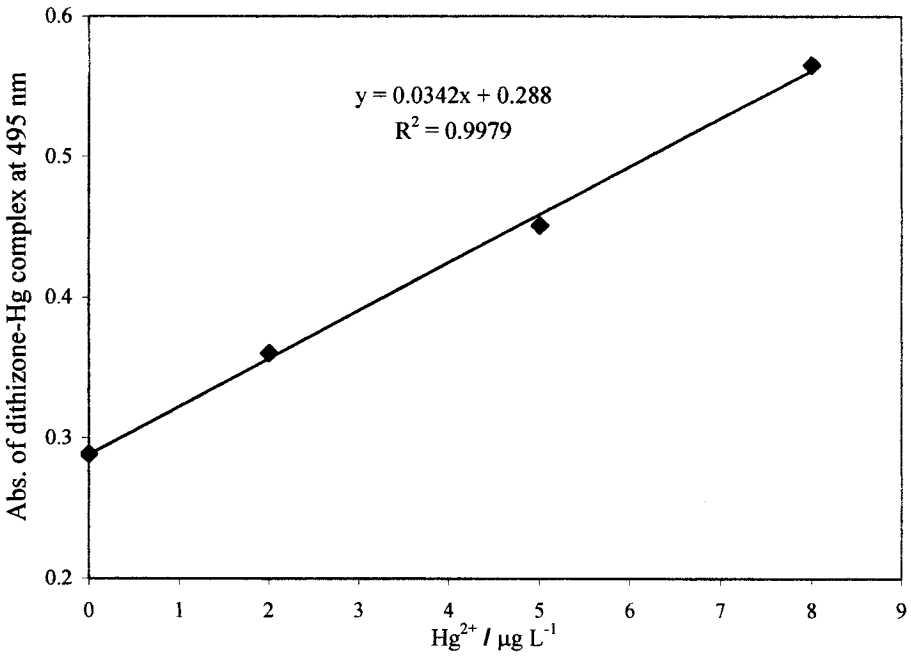


**Figure 2.1** Calibration curve for $Hg^{2+}$ using dithizone as a complexing colorimetric reagent.

### *2.1.3 Methylmercury "MeHg"*

Solid methyl mercury chloride (Aldrich) was used as a starting material to prepare stock solutions. The Hg-Cl bond in $CH_3Hg$-Cl has 62% ionic character,[5] thus an aqueous solution of $CH_3HgCl$ will contain an appreciable concentration of $CH_3Hg^+$. In addition, the reaction to form methyl mercury hydroxide at 25 °C is exothermic and spontaneous from thermodynamic considerations (equations 2.4-2.5).[6]

| | $-\Delta H$ (kJ $mol^{-1}$) | $\Delta S$ ($J.mol^{-1}K^{-1}$) | |
|---|---|---|---|
| $CH_3Hg^+ + OH^- \rightarrow CH_3HgOH$ | 35.8 | 55.7 | (2.4) |
| $CH_3Hg^+ + CH_3HgOH \rightarrow (CH_3Hg)_2\ OH^+$ | 16.1 | -9 | (2.5) |

We prepared our stock solution in aqueous alkaline solution (0.5N of NaOH). Under thes conditions $CH_3HgOH$ and $(CH_3Hg)_2OH^+$ are present. of. The concentration of the working solution was checked against a standard solution by using an ICP-MS.

**Safety considerations**: Methylmercury is a very toxic compound; it causes kidney damage, and causes neurological damage. Direct contact with skin could cause death. This material must be handled with extreme caution, using appropriate clothing and gloves in well-ventilated fume hood.

### *2.1.4 Humic substances "HS"*

Suwannee River fulvic acid standard (1S101F) and Leonardite humic acid standard (1S104H-5) were obtained from the International Humic Substances Society (IHSS). A stock solution of fulvic acid (FA) was prepared in deionized water by dissolving a precisely weighed amount. The stock solution of humic acid was prepared in 0.1 M of NaOH that was itself prepared by diluting a standard solution (VWR). Stock solutions of HS were kept in dark bottles in the refrigerator. Working solutions were prepared by proper dilution from stock solutions.

#### *2.1.4.1 Chemical properties of HS*

The results of elemental analysis, in %(w/w) of a dry, ash-free sample, as well as % $H_2O$ and ash content as % (w/w) inorganic residue, are shown in Table 2-1 .

**Table 2.1** Elemental compositions* of Leonardite humic and Suwannee River fulvic acids.

| Sample | %$H_2O$ | %Ash | %C | %H | %O | %N | %S |
|---|---|---|---|---|---|---|---|
| Leonardite HA | 7.2 | 2.58 | 63.81 | 3.7 | 31.27 | 1.23 | 0.76 |
| Suwannee River FA | 8.8 | 0.46 | 52.44 | 4.31 | 42.20 | 0.72 | 0.44 |

* Elemental analysis by Huffman Laboratories, Wheat Ridge, CO, USA.

The $^{13}C$ NMR of the HS shows the distribution of carbon atoms in various functional groups. The % integrated peak areas along with the chemical shift of each group are shown in Table 2.2.[7]

**Table 2.2** Integrated peak area in $^{13}C$ NMR for fulvic and humic acid solutions.

| Functional group | Carbonyl | Carboxyl | Aromatic | Acetal | Heteroaliphatic | Aliphatic |
|---|---|---|---|---|---|---|
| Chemical shift, ppm | 220-190 | 190-165 | 165-110 | 110-90 | 90-60 | 60-0 |
| Sample | % integrated peak area | | | | | |
| Leonardite HA | 8 | 15 | 58 | 4 | 1 | 14 |
| Suwannee River FA | 7 | 20 | 24 | 5 | 11 | 33 |

The acidic content of humic substances arises mainly from carboxylic and phenolic functional groups. Their amounts are presented in Table 2.3.[8] The logarithmic values of the acid dissociation constants are also presented. [8]

**Table 2.3** Carboxylic and phenolic group contents of HS and their acid dissociation constants.

| Sample | Carboxylic mol $kg^{-1}$ C | Phenolic mol $kg^{-1}$C | $pK_{a1}$ | $pK_{a2}$ |
|---|---|---|---|---|
| Leonardite HA | 7.46 | 2.31 | 4.59 | 9.72 |
| Suwannee River FA | 11.44 | 2.91 | 3.80 | 9.52 |

### *2.1.5 Other chemicals*

Potassium iron oxalate trihydrate (Alfa Aesar) and ferric ammonium citrate (Sigma-Aldrich) were used to prepare ferrioxalate and ferric citrate solutions, respectively. Both solutions were freshly prepared (as needed) in the dark and stored in dark brown bottles wrapped in aluminum foil.

Sodium hypochlorite solutions were made by diluting a commercial aqueous solution containing about 4% active chlorine (Aldrich), and were standardized by titration with $Na_2S_2O_3$ (Sigma, 99%) in the presence of potassium iodide (Aldrich, 99%). The chemical equations which describe this titration are shown below (equations 2.6-2.7).

$$OCl^- + H_2O + 2\ I^- \rightarrow Cl^- + 2\ OH^- + I_2 \qquad (2.6)$$

$$I_2 + 2\ S_2O_3^{2-} \rightarrow 2\ I^- + S_4O_6^{2-} \qquad (2.7)$$

For the quantification of metal ions in water samples, certified standards were used: Zn(II), Pb(II), Cd(II), and Cu(II) (AA standards, Certipur $^{TM}$).

Duolite GT-73 resin (16-50 mesh, protonated form, Sigma) was soaked in Milli-Q deionised water for 24 hours before use. Chelex100 (100-200 mesh, Na form, Bio-Rad) was washed with deionised water prior to use.

## 2.2 Instruments and equipments

### *2.2.1 Photoreactor*

A Luzchem LZC-4V photoreactor was used in photolysis experiments. The machine is equipped with a carousel capable of holding 16 samples (10 mm diameter

quartz test tubes). The irradiation chamber is approximately (30 x 30 x 22 cm). Several switches allow the choice of specific lamps. The side irradiation was performed with an array of either 4 UV-A lamps (average irradiance 1.41 ± 0.08 $mW/cm^2$) or 6 visible lamps (average illuminance 868 ± 30 foot candles). Radiation intensity was measured with a power meter at the carousel position. An airflow cooler controls the temperature inside the chamber to within 3-4 °C above room temperature.

### *2.2.2 Cold Vapor Atomic Absorption Spectroscopy (CV-AAS)*

A Varian M-6000A CETAC Technologies CV-AAS instrument was used for quantitative measurements of inorganic mercury ($Hg^{2+}$) in aqueous solutions. A 5 % $SnCl_2$ solution (Sigma) in 15% HCl was used as the reducing agent. Solutions of $Hg^{2+}$ and $SnCl_2$ were mixed by a peristaltic pump, $Hg^{2+}$ was reduced to $Hg^0$ according to equations 2.8-2.9:

$$2Hg^{2+} + Sn^{2+} \rightarrow Hg_2^{2+} + Sn^{4+} \quad (2.8)$$

$$Hg_2^{2+} + Sn^{2+} \rightarrow Hg^0 + Sn^{4+} \quad (2.9)$$

The $Hg^0$ produced was separated from the liquid in a gas liquid separator. The mercury vapor was swept in to the sample cell using high purity nitrogen as the carrier gas. Its absorbance was measured at 254 nm.

For the determination of $Hg^{2+}$ in aqueous solution, a calibration curve from 1 to 15 ppb (Figure 2.2) was prepared using an Hg(II) standard solution (VWR). The detection limit was around 0.20 ppb.

### *2.2.3 Ultrafiltrator*

The Tangential Flow Ultrafiltration Technique (TFUT) was used for partitioning water samples into different molecular weight (MW) size fractions. A PALL Tangential Flow Centramate$^{TM}$ Ultrafiltrator was attached to a peristaltic pump (Masterflex L/S standard drive model No. 7520-00), which was operated at low pressure (< 10 psi) and directs the flow of the solution parallel to the membrane cassettes (OMEGA). Membranes have a surface area of ~ 0.09 $m^2$ and are made of polyethersulfone.

Membranes with molecular weight cut-offs (MWCO) of 500-kilo Dalton (kD), 300 kD, 30 kD, 5 kD and 1 kD were used sequentially. Molecules with sizes smaller than the (MWCO) penetrate the membrane, and are called the filtrate. After each filter change, deionized water was passed through the entire filtration system for cleaning. Membranes were stored in 0.1 M NaOH solution, and soaked in D.I. water, for at least 12 hours before use.

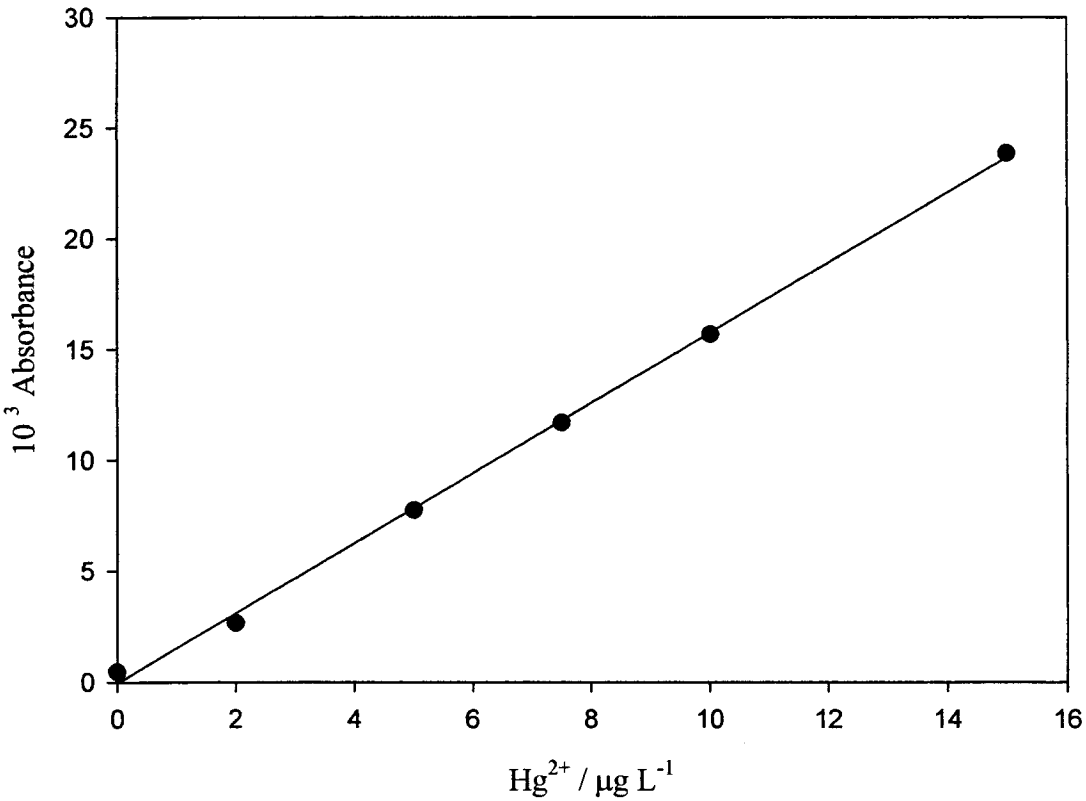


| Equation **y = m x** | |
|---|---|
| Parameter | Value |
| m | 1582 |
| R | 0.999 |

**Figure 2.2**. Calibration curve for Hg(II) using CV-AAS.

### *2.2.4 ICP-MS & CLEM Reactor*

Inductively coupled plasma–mass spectrometery (ICP-MS) was used for quantitative determinations and the kinetic dissociations of trace metal ions (Cu(II), Zn(II), Pb(II), Cd(II), Hg(II) and $MeHg^+$ ) in water samples. The ICP-MS machine used was ELAN6100DRC (PERKIN-ELMER). Argon was used as the ICP gas. It has high ionization energy (15.76 eV) and is chemically inert. An external radio frequency is fed into a tightly wound coil, where it generates an intense alternating magnetic field. When an electrical spark is passed momentarily through the argon gas, some of the argon atoms are ionized and the resultant cations and electrons are accelerated toward the magnetic field of the RF coil. Stable high temperature plasma (6000 K in the analytical zone and 10000 K in the atomization zone) is generated. Aqueous sample solutions are introduced to the plasma as a fine aerosol by a nebulizer, which undergoes instantaneous evaporation, atomization and ionization. Some of the formed ions will pass through the skimmer cone orifice at the plasma-MS interface and accelerated by a high voltage potential gradient. They pass through a series of focusing lenses into the mass analyzer, operated at high vacuum. The quadrupole mass analyzer is able to separate and identify ions according to their m/z values. The operational parameters of the ICP-MS are shown in Table 2.4.

For quantification of metal ions in aqueous solution, calibration curves were obtained directly using ICP-MS (Figures 2.3-2.8). For the kinetic dissociation experiments, a Teflon reactor (Figure 2.9) was used. The solution from the reactor was pumped to the nebulizer by means of a peristaltic pump.

A 5 ppm gold standard was passed through the system for washing and cleaning after analysis of Hg-containing samples.[9]

**Table 2.4** Operational parameters for ICP-MS and data acquisition (instrument settings)

| Parameter | Value |
|---|---|
| Nebulizer gas flow | 1 L/min |
| Auxiliary gas flow | 1.3 L/min |
| Plasma gas flow | 15 L/min |
| Pulse stage voltage | 1100 V |
| Lens voltage | 5.7 V |
| ICP-RF power | 1200 W |
| CeO/ Ce | < 0.03 |
| Detector working mode | Pulse and analogue |
| Scan mode | Peak hop |
| Dwell time | 50 ms |
| Detected signal | Counts/ s |

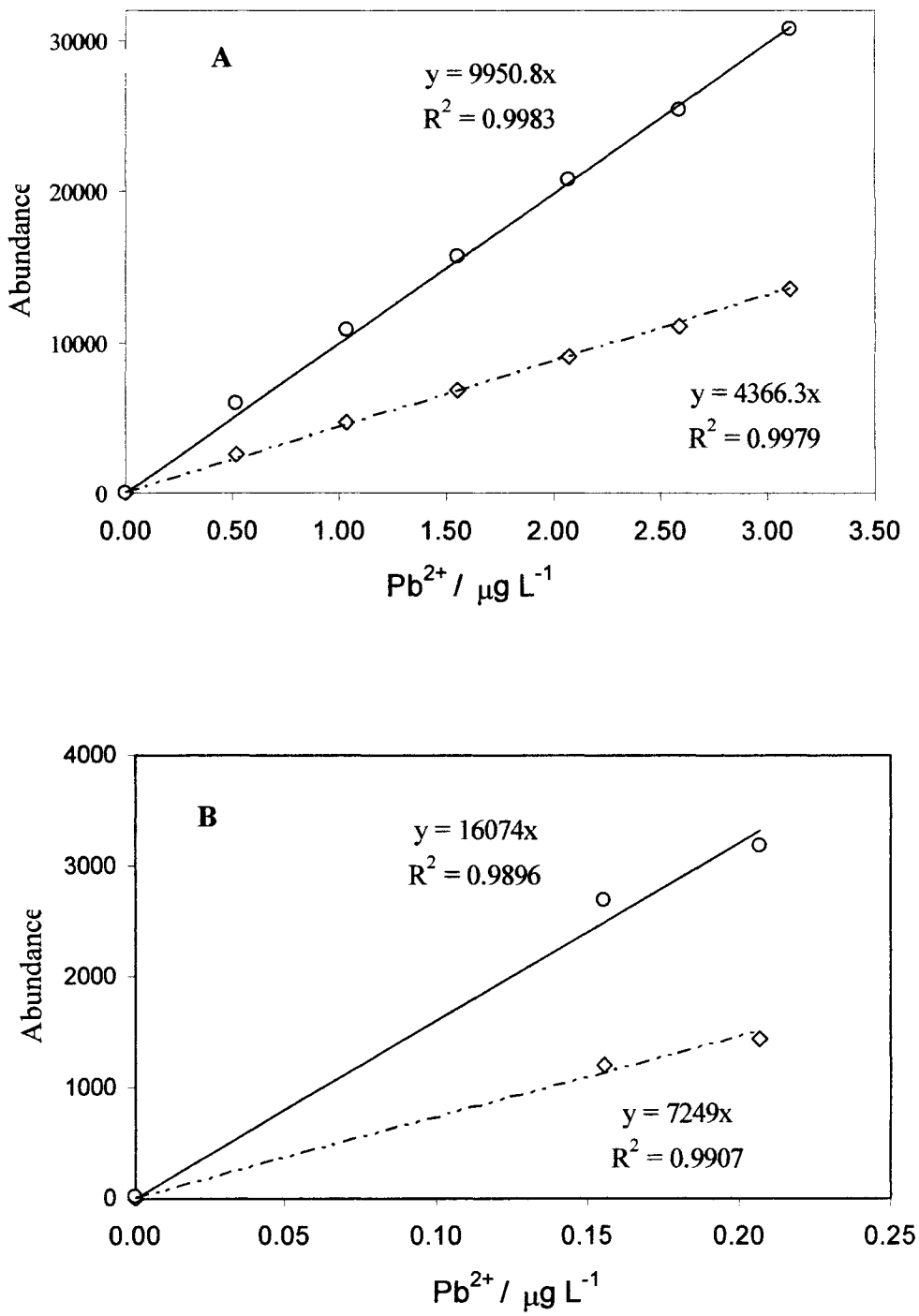


**Figure 2.3** Calibration curves for $Pb^{2+}_{(aq)}$ for high (A) and low (B) concentrations using ICP-MS: ○ $^{208}Pb$, ◊ $^{206}Pb$.

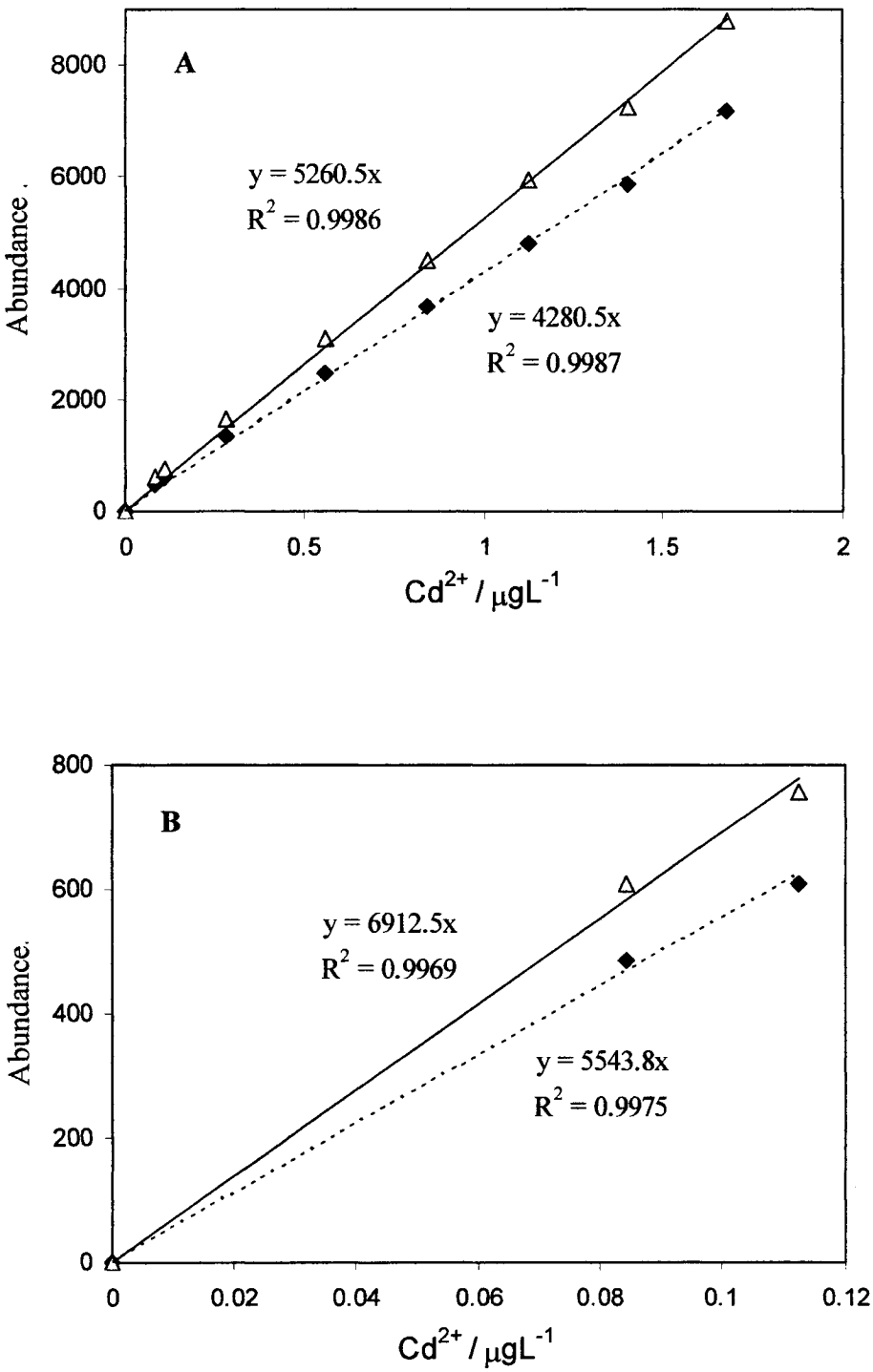


**Figure 2.4** Calibration curves for $Cd^{2+}_{(aq)}$ for high (A) and low (B) concentrations using ICP-MS: △ $^{114}Cd$ , ◆ $^{112}Cd$.

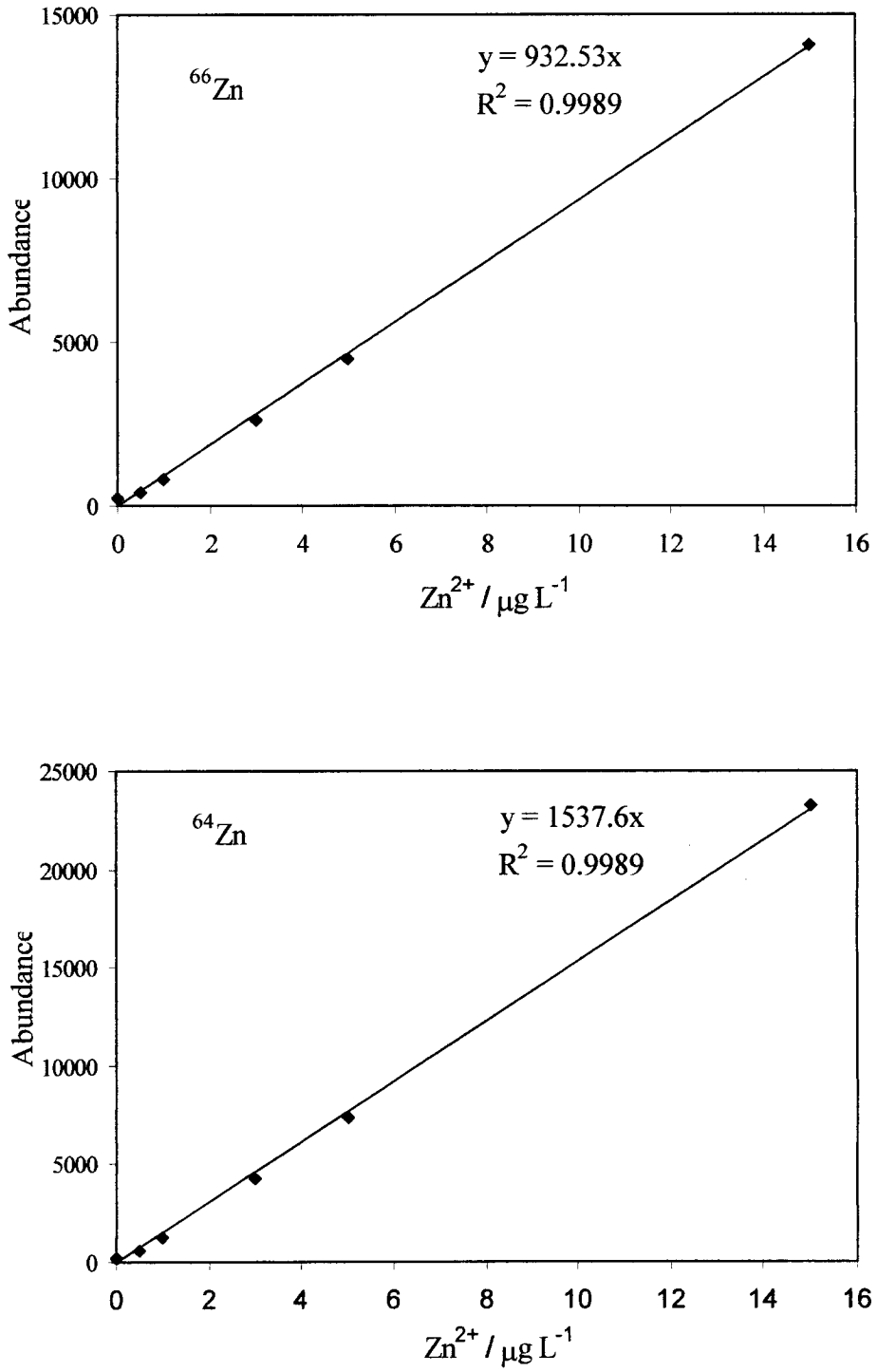


**Figure 2.5** Calibration curves for $Zn^{2+}_{(aq)}$ for two isotopes ($^{66}$Zn and $^{64}$Zn) using ICP-MS.

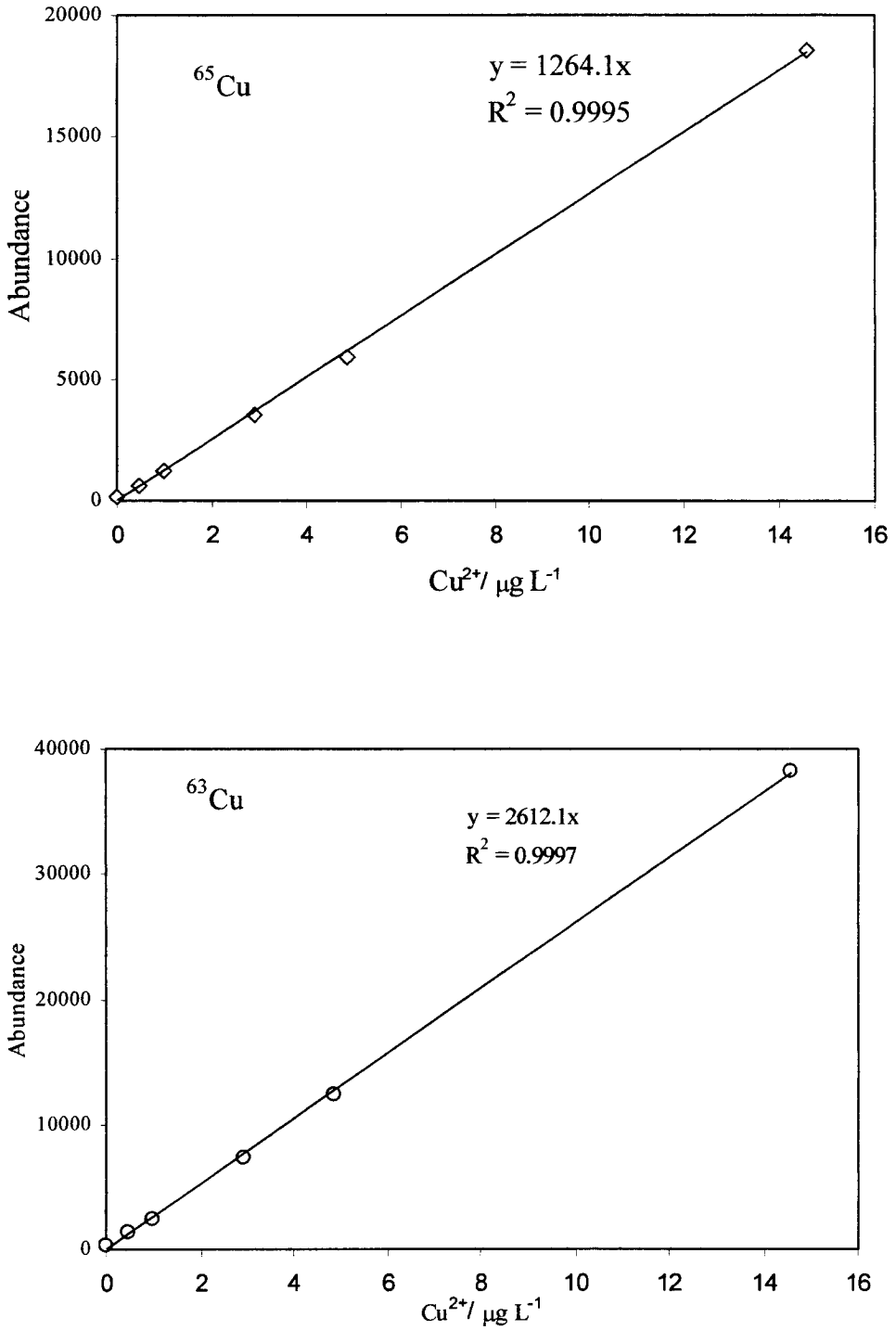


**Figure 2.6** Calibration curves for $Cu^{2+}_{(aq)}$ for two isotopes ($^{65}Cu$ and $^{63}Cu$) using ICP-MS.

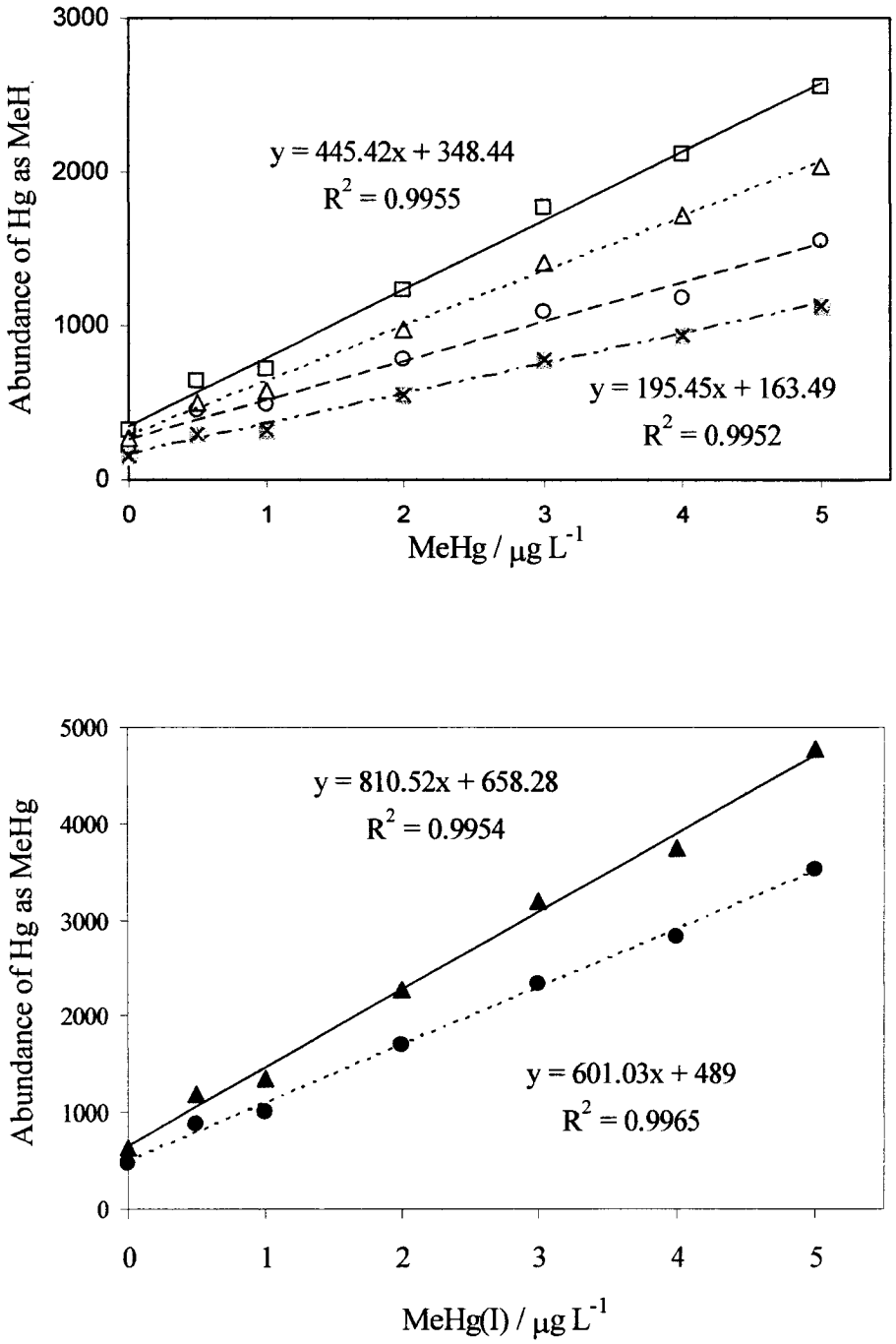


**Figure 2.7** ICP-MS calibration curves for $MeHg^{+}_{(aq)}$: □ $^{199}Hg$, △ $^{201}Hg$, ○ $^{198}Hg$, ⊠ $^{204}Hg$, ▲ $^{202}Hg$, ● $^{200}Hg$.

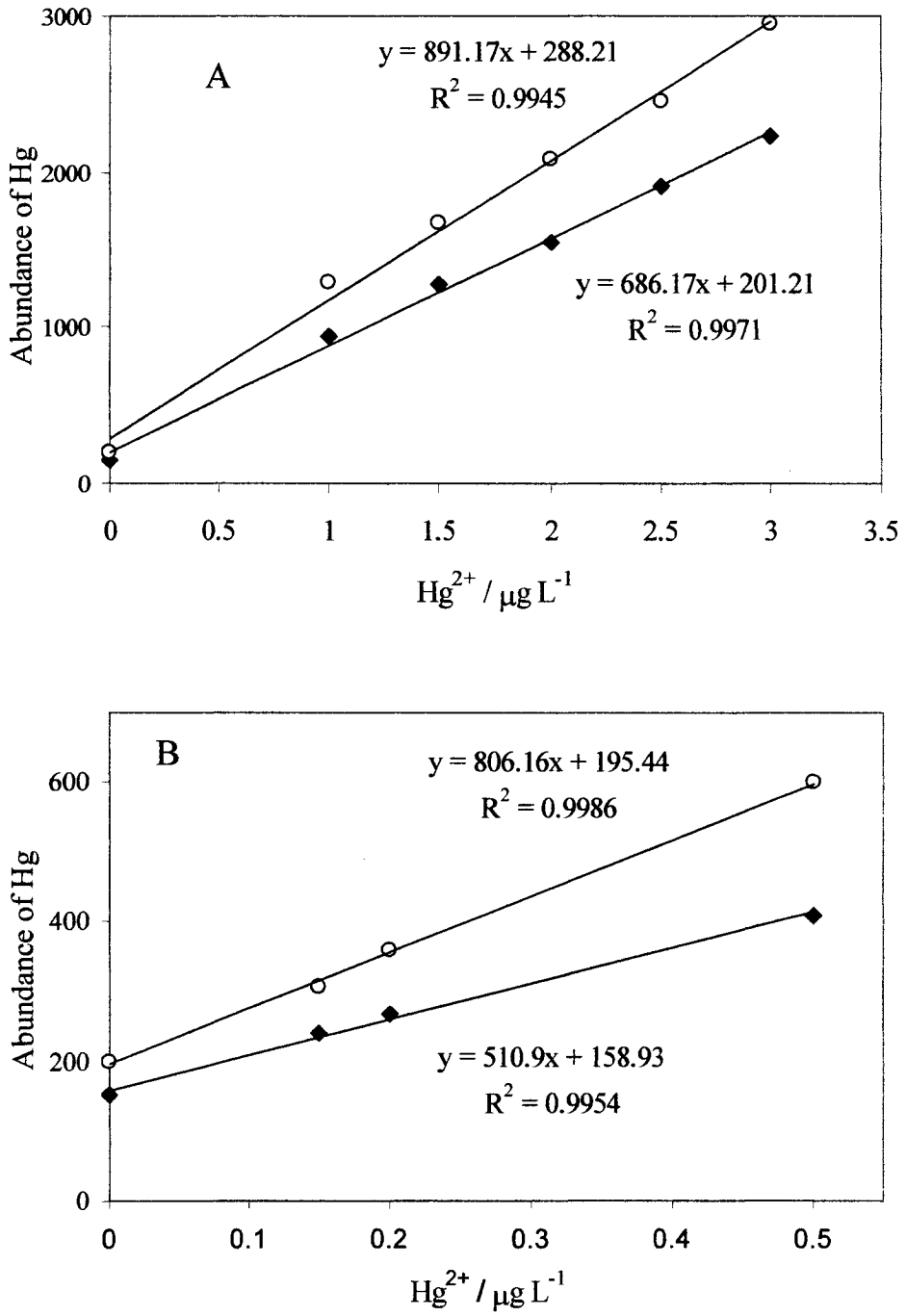


**Figure 2.8** Calibration curves for $Hg^{2+}_{(aq)}$ at high (A) and low (B) concentrations using ICP-MS. ○ $^{202}Hg$, ◆ $^{200}Hg$ .

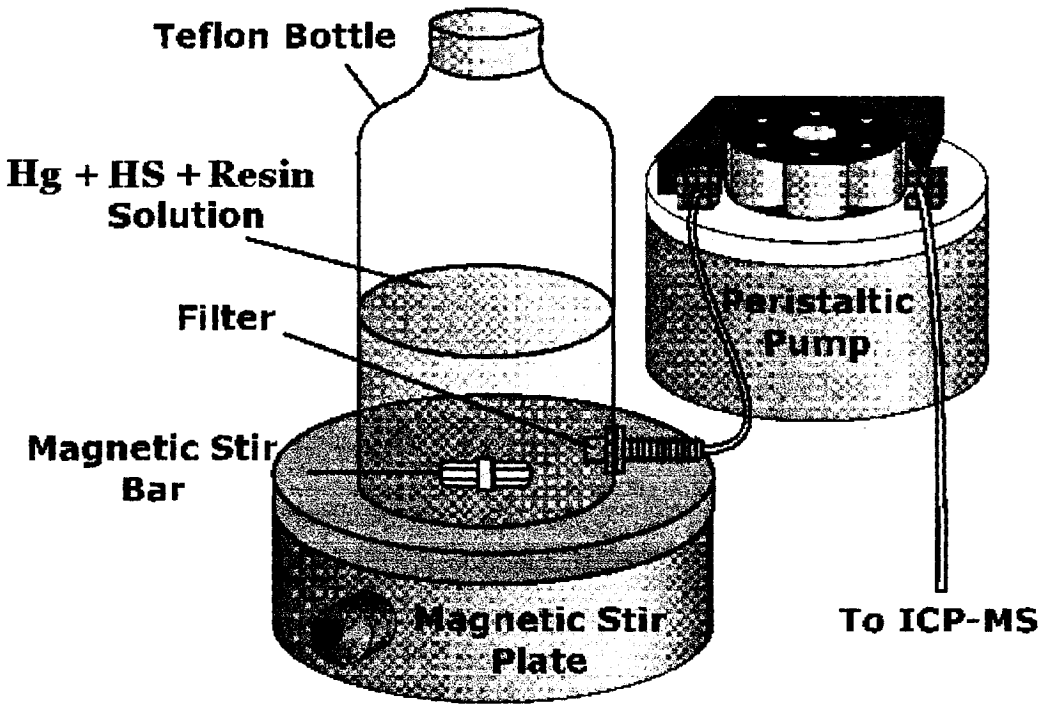


**Figure 2.9** Teflon reactor used in CLEM experiments. (Adapted from ref.10)

#### *2.2.2.5 Other equipment and software*

A UV-visible spectrophotometer (Cary 300) was used to record electronic spectra in 1 cm square quartz cuvettes, with a resolution of 1 nm and a scan speed of 100 nm/min.

A pH meter (Thermo Orion model 525A) was used for pH measurement and adjustment; it was equipped with a combined Thermo Orion glass electrode and a (Ag/AgCl/0.1 M KCl) reference electrode. The pH meter was calibrated using two standard buffers at pH 4 and pH 9 to establish a linear response in these pH regions.

Sigma plot 8 (Systat Software Inc) and Kaleidagraph 3.5 (Synergic software) were used for non-linear curve fitting of kinetic data.

## 2.3 Procedures

### *2.3.1 Photolysis experiments*

Working solutions of ferrioxalate, ferric citrate or humic substance were prepared daily in the dark and stored in dark brown bottles wrapped in aluminum foil. Addition of mercuric ion to these solutions was accomplished in flasks wrapped in Al foil, and the pH was adjusted as necessary with dilute aqueous solutions of $H_2SO_4$ or NaOH. Solutions were then transferred to 10 mm diameter quartz test-tubes, capped with white rubber septa (Aldrich). They were placed in a carousel and irradiated with either UVA or visible radiation (Luzchem LZC-4V photoreactor). During each photochemical experiment, the quartz tubes were removed from the photoreactor at timed intervals and stirred with a Teflon-coated magnetic stirbar. 200 μL aliquots were removed (Eppendorf pipettes) and diluted to 10 mL with acidified Milli-Q water ($H_2SO_4$, pH 3). The diluted samples were

sparged with nitrogen or argon for at least 20 minutes to remove volatile Hg(0) formed during irradiation. (Longer sparging times gave similar results.) The remaining Hg(II) was determined with a Varian M-6000A mercury analyzer.

In order to quantify the elemental mercury formed during irradiation, some samples were not sparged with an inert gas. Instead, they were analyzed directly from plastic Falcon tubes, omitting the addition of $SnCl_2$ and using a new gas-liquid separator never exposed to $SnCl_2$. The blank reading, obtained with a 20 ppb standard solution of $HgCl_2$, was always at least an order of magnitude lower than that of the 2 ppb Hg(0) standard, prepared in a Teflon bottle under argon.

### *2.3.2 CLEM experiments*

The Hg-HS and MeHg-HS model solutions were prepared so that the initial concentrations of Hg(II) or $MeHg^+$ ranged from 1-10 μg/L and HS (either Suwannee River fulvic acid or Leonardite humic acid) concentrations ranged from 1-20 mg/L, at pH 5 and pH 9. Samples were 4-6 L in volume and prepared in Teflon bottles (2L capacity). After equilibration for 4-6 hours, samples were fractionated using a sequential ultrafiltration procedure (PALL Tangential Flow Centramate™ Ultrafiltrator).

From each size fraction an aliquot of 250 ml was kept in a Teflon bottle in the refrigerator for the CLEM kinetics experiment. Another aliquot of 40 mL was acidified with $HNO_3$, preserved by the addition of gold standard,[9] and used for the distributional speciation.

In CLEM experiments, 250 ml of specified size fraction was transferred to the Teflon reactor. The solution was pumped to the ICP-MS by means of peristaltic pump.

The abundances of six Hg isotopes were monitored until a maximum and stable response was achieved. 2.5 g of solid, spherical beads (particles) of resin (Duolite GT-73) was added to the solution in Teflon reactor. This resin is known to adsorb Hg species very efficiently. Since its particulates cannot pass through the filter (0.45 μm) only complexed mercury (Hg-HS) in the solution is detected by ICP-MS.

### *2.3.3 Oxidation of $Hg^0$ in aqueous solution*

Addition of methylene blue to a freshly-prepared solution containing 0.080 μM Cl(I) resulted in partial bleaching of the blue color of the indicator, the extent of which corresponds to the concentration of Cl(I) present. Likewise, addition of methylene blue immediately after mixing 0.080 μM Cl(I) with 0.22 μM Hg(0) resulted in the same amount of bleaching of the methylene blue color by Cl(I). However, when methylene blue was added some time after the onset of reaction between Hg(0) and Cl(I), less bleaching resulted. The intensity of the methylene blue spectrum therefore depends on the time elapsed between mixing and quenching. Since the reaction between methylene blue and Cl(I) is fast (complete upon mixing) compared to the reaction of Hg(0) with Cl(I), this technique allows us to probe the kinetics of the rate-determining oxidation of Hg(0).

Temperature control was established by immersing reagents and reaction mixtures in a constant temperature recirculating water bath (VWR Scientific). Air-free solutions of Cl(I) were mixed with saturated aqueous solutions of Hg(0), such that $Hg(0)_{(aq)}$ was in excess. Aliquots withdrawn at measured time intervals were quenched by the addition of

1.3 μM methylene blue. The visible spectrum of the unbleached methylene blue was recorded immediately.

**References**


(1) Kolthoff, M.; Sandell, E. B.; *Textbook of Quantitative Inorganic Analysis*; Macmillan: New York , 1952.

(2) Lin, C.-J.; Pehkonen, S. O.; *J. Geophys. Res.* **1998**, *103*, 28093-28102.

(3) Eaton, A. D.; Clesceri, L. S.; Greenberg, A. E. *Standard Methods for the Examination of Water and Wastewater;* American Public Health Assn: Washington, DC,19th Edition-1995.

(4) Clever, H.; Johnson, S. A.; Derrick, M. E. *J. Phys. Chem. Ref. Data* **1985**, *14*, 631-680.

(5) Gordy, W.; Sheridan, J. *J. Chem. Phys.* **1954**, *22*, 92-95.

(6) Alderighi, L.; Gans, P.; Midollini, S.; Vacca, A. *Inorg. Chim. Acta* **2003**, *356*, 8-18.

(7) Thorn, K. A.; Folan, D. W.; MacCarthy, P. U.S. Geological Survey, Water- Resources, Investigations Report 89-4196, Denver, CO, 1989, pp.93.

(8) Ritchie, J. D.; Perdue, E. M. *Geochim. Cosmochim. Acta* **2003**, *67*, 85-96.

(9) Allibone, J.; Fatemian, E.; Walker, P. J. *J. Ana. Atom. Spectr.* **1999**, *14*, 235-239.

(10) Guthrie, J. W. Ph.D. Thesis, Carleton University, Ottawa-Canada, 2004.

# Chapter 3

## Photochemical reduction of aqueous mercuric chloride and reoxidation in the presence of ferrioxalate and air

### 3.1 Introduction

Widespread low-level mercury contamination now exists because of its release into the air through human activities such as mining and coal burning[1]. Mercury contamination of pristine areas results from long range atmospheric transport as well as natural geological weathering of mercury-containing minerals in the soil and sediments. Some of the mercury deposited by precipitation into lakes or waterways is converted to methylmercury.[2-4] An alternate transformation of mercury which can occur after deposition is reduction to volatile Hg(0), which then reenters the atmosphere due to its low water solubility.[5] The removal of Hg through photoreduction reduces the quantity available for methylation and, as a consequence, bioaccumulation. For this reason, it is important to understand the dynamic chemical behavior of mercury in atmospheric and surface waters.

Various biotic and abiotic processes have been proposed to be responsible for mercury reduction.[6] Recent evidence points to the importance of photoreduction, since DGM (dissolved gaseous mercury) formation correlates with diel cycles of solar irradiation, and Hg(0) is the principal form of DGM.[7] Various biotic and abiotic processes could be responsible for this reduction, including photosensitized DOC,[8-11] or

other coordinated organic acids,[12,13] sulfide complexes,[14,15] and photobiological and bacterial activity.[6,16]

Zhang and Lindberg reported that Fe(III) spikes induced photochemical production of DGM, approaching a plateau with increasing exposure time.[17] Complexes of Fe(III) with chelating ligands such as oxalate, citrate, and malonate are photosensitive in aqueous solution. Upon absorption of a suitable photon, they undergo ligand-to-metal charge transfer, resulting in an excited state which decomposes with formation of Fe(II) and highly reducing organic radicals. Fe(II) is then reoxidized slowly by dissolved $O_2$. The iron cycle in natural bodies of water can produce different reactive oxygen species such as $^{\cdot}OH$, $HO_2/O_2^{-\cdot}$ and $H_2O_2$.[18-23] Iron photoreactivity plays an important role in cycles of other metals, including the reduction of heavy metals.[24]

Chelating ligands such as oxalate and citrate have been detected in atmospheric water droplets.[25,26] Their sources include incomplete combustion and photooxidation of hydrocarbons in the gas phase and in atmospheric water droplets. A recent study showed that hydroxyl radical attack on ethylene or acetylene in the gas phase produces glyoxal and gloxalaldehyde, respectively. After hydration in cloud water, further hydroxyl radical attack leads to the formation of gloxylic acid, which is oxidized to oxalic acid.[27] Typical oxalate concentrations in atmospheric water range from 1.5 to 13.8 μM,[28] but higher concentration levels to $5 \times 10^{-4}$ M have been reported.[22] In western Pacific rain, the range of concentration of the various diacids is 36 to 959 μg/L and represents 3% of the TOC.[29] Furthermore, 40% of the DOC of North Carolina rain comes from various organic acids, including acetic, formic, oxalic, lactic, malonic, maleic and succinic acid.[30] Fe(III) in surface water is readily complexed with these acids, especially the diacids.

Ferrioxalate may well play a direct role in the photoreduction of mercury. The carboxylate group is a known functional group in humic materials, which themselves have a strong influence on mercury bioavailability and the mercury cycle. Since iron is commonly present in freshwaters, ferrioxalate is therefore a model for the role of iron-humic complexes in the photoreduction of mercuric ion.

The rate and mechanism of photoreduction of Hg(II) in aqueous solution were investigated in the presence of UVA and visible light using ferrioxalate as a photosensitive source of reducing radicals. In addition, the influence of dissolved oxygen and chloride concentration was also investigated.

### 3.2 Photolysis of ferrioxalate

The photochemistry of $Fe(C_2O_4)_3^{3-}$ is well-known, and is the basis for a chemical actinometer. Light absorption results in the formation of Fe(II) and the oxalyl radical anion $C_2O_4^{-\bullet}$, equation 3.1.

$$Fe(C_2O_4)_3^{3-} + h\nu \rightarrow Fe(II) + C_2O_4^{-\bullet} + 2\,C_2O_4^{2-} \qquad (3.1)$$

The affinity of Fe(II) for oxalate is much less than the affinity of Fe(III), resulting in the rapid release of oxalate into solution. Fe(II) is detected as the strongly absorbing complex $Fe(phen)_3^{2+}$ at 510 nm by addition of 1,10-phenanthroline, providing a convenient method of monitoring the progress of the photochemical reaction. The oxalyl

radical anion $C_2O_4^{-\bullet}$ undergoes rapid decarboxylation to $CO_2^{-\bullet}$, according to equation 3.2.[31]

$$C_2O_4^{-\bullet} \rightarrow CO_2 + CO_2^{-\bullet} \qquad k_2 = 2 \times 10^6\ s^{-1} \tag{3.2}$$

The latter is a strong reducing agent, $E^\circ(CO_2/CO_2^{-\bullet}) = -2.0$ V. In the presence of air, it reacts with dissolved $O_2$ to form superoxide and, ultimately $H_2O_2$, equations 3.3-3.5.

$$CO_2^{-\bullet} + O_2 \rightarrow CO_2 + O_2^{-\bullet} \qquad k_3 = 2.4 \times 10^9\ M^{-1}\ s^{-1} \tag{3.3}$$

$$CO_2^{-\bullet} + 1/2\ O_2 + H^+ \rightarrow CO_2 + HO^{\cdot} \qquad k_4 = 1 \times 10^9\ M^{-1}s^{-1} \tag{3.4}$$

$$O_2^{-\bullet} + H^+ \leftrightarrows HO_2 \rightarrow 1/2\ O_2 + 1/2\ H_2O_2 \tag{3.5}$$

In the absence of $O_2$, the $CO_2^{-\bullet}$ radical anion reduces $Fe(C_2O_4)_3^{3-}$, generating a second equiv. of Fe(II), equation 3.6.

$$CO_2^{-\bullet} + Fe(C_2O_4)_3^{3-} \rightarrow CO_2 + Fe(II) + 3\ C_2O_4^{2-} \tag{3.6}$$

The efficiency of Fe(II) formation is strongly wavelength-dependent, as expected. A 4.0 mM aqueous solution of ferrioxalate at pH 4.0 was completely photolyzed in 5 minutes of UVA irradiation in the Luzchem photoreactor, Figure 3.1. In contrast, visible irradiation required 60 minutes to completely convert 4.0 mM ferrioxalate to Fe(II).

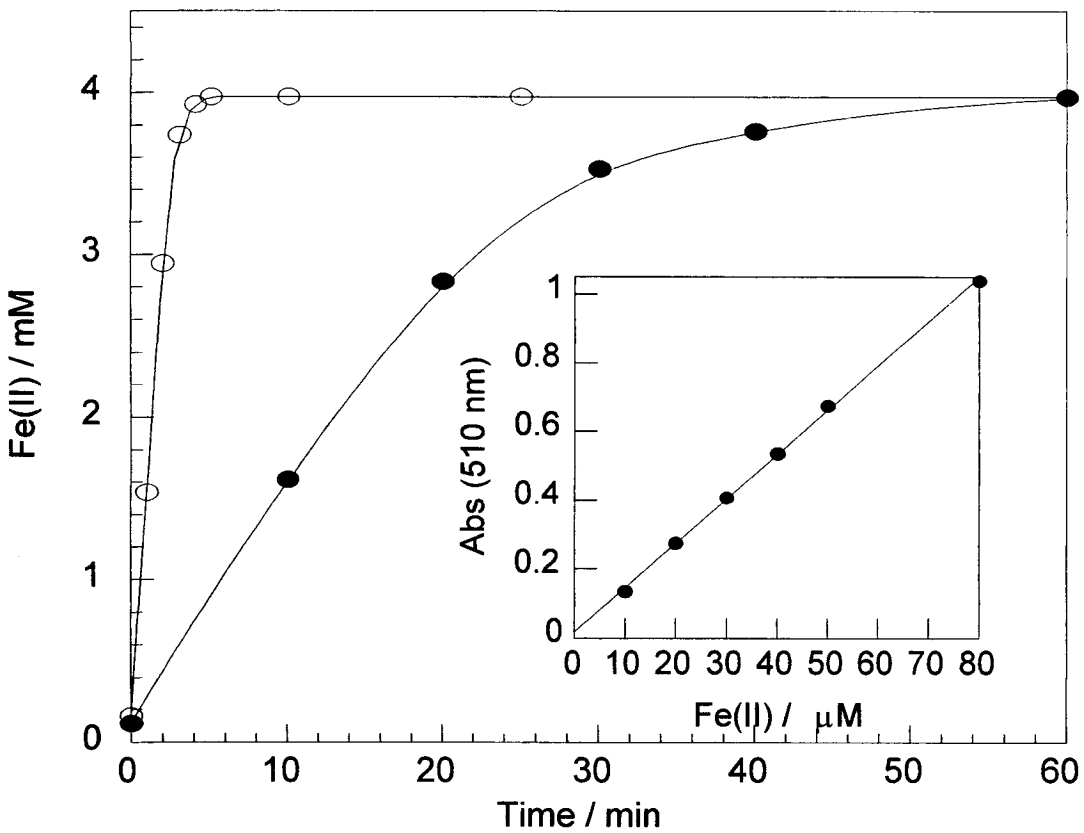


**Figure 3.1.** Formation of Fe(II) during irradiation of an air-saturated 4.0 mM $Fe(C_2O_4)_3^{2-}$ solution at pH 4 ($H_2SO_4$) by UVA light (open circles) and visible light (filled circles). The inset shows the calibration plot at 510 nm due to $Fe(phen)_3^{2+}$ used to calculate the photochemical yield of Fe(II).

### 3.3 Rate law for photoreduction of Hg(II)

If we represent the ferrioxalate reactant by R and the products by P, then for the photochemical reaction (equation 3.6), the quantum yield ($\Phi_\lambda$) at any wavelength λ is defined by equation 3.8.

$$R + h\nu \rightarrow P \tag{3.7}$$

$$\phi_\lambda = \frac{Moles.of.product."P."}{Moles.of.photons.absorbed} \tag{3.8}$$

The rate of this photochemical reaction is given by equation 3.9: [32]

$$\frac{-d[R]}{dt} = \sum_\lambda \phi_\lambda I_\lambda \tag{3.9}$$

Where $I_\lambda$ is the average rate of light absorption by R which is related to incident light intensity $I_o$ by equation 3.10:

$$I_\lambda = I_o (1 - 10^{-\varepsilon_\lambda [R] b}) D \tag{3.10}$$

where $D$ is the surface area of the cell that the light passes through ($cm^2$) divided by the volume of the irradiated solution ($cm^3$), ε is the molar absorptivity of the reactant at the specific wavelength (λ), $I_o$ is measured at the same wavelength (λ) in einsteins.$cm^{-2}$.$s^{-1}$, and b is the light path length (cm) which is equal to 1 under our experimental conditions.

By substitution of equation 9 into equation 8 then we get equation 3.11.

$$\frac{-d[R]}{dt} = \sum_{\lambda} \phi_{\lambda} I_o (1 - 10^{-\varepsilon_{\lambda}[R]}) D = \sum_{\lambda} k_o (1 - 10^{-\varepsilon_{\lambda}[R]}) \qquad (3.11)$$

where $k_o$ represent the product of the constants in the equation ($k_o = \Phi_{\lambda} I_o D$). At high initial reactant concentration [R] (optically dense solution, ε [R] b >2),[32] then the rate of the photoreaction is a function of $k_0$ only, this refers to zero order reaction. However for an optically thin solution (ε [R] b <0.05),[32] equation 3.11 converts to equation 3. 12

$$\frac{-d[R]}{dt} = \sum_{\lambda} \phi_{\lambda} I_o (1 - 10^{-\varepsilon_{\lambda}[R]}) D \sim 2.303 \sum_{\lambda} k_o . \varepsilon_{\lambda} [R] \qquad (3.12)$$

$$\sim \sum_{\lambda} k_1 [R]$$

where $k_1$ represents the product of the constants in the equation. The rate of the photoreaction is now a function of [R], this situation corresponds to first order reaction.

Under our experimental conditions the $Fe(C_2O_4)_3^{3-}$ concentration ranges from 400 to 500 μM, and the value of the product ε [R] extends from < 0.05 to > 2. This wide range of

ε [R] values is due to the large variation in the molar absorptivity (ε) of $Fe(C_2O_4)_3^{3-}$ over the UVA and visible region. As a result, our data may obey either zero- or first-order kinetics. Figure 3.1 shows that for the first 3 data points in the visible irradiation experiments, the reaction rate has zero-order character (straight line), while if we consider all the data sets, the photolysis rate is better fitted to first-order reaction kinetics. The same behavior was observed for the UVA experiments.

If we assume that the radicals produced from the photolysis of ferrioxalate are responsible for the reduction of Hg(II), then this reaction is controlled by the diffusion rates. This implies that the observed rate of photoreduction of Hg(II) could be either first- or zero-order. We fitted all of our experimental data to first-order rates equation.

### 3.4 UVA photoreduction of Hg(II).

UVA irradiation of an air-saturated aqueous solution containing 4.98 μM mercuric chloride at pH 3.0 for 20 minutes resulted in a negligible change in the concentration of Hg(II). Addition of 100 μM ferrioxalate also produced insignificant reduction of Hg(II) under UVA irradiation for 20 minutes. However, when the concentration of ferrioxalate was increased to (500) μM, a rapid decrease in the concentration of Hg(II) was observed, Figure 3.2. Loss of Hg(II) may be due to its reaction with the primary photoproducts Fe(II) and $C_2O_4^{-\bullet}$, or with the secondary photoproducts $CO_2^{-\bullet}$ and $O_2^{-\bullet}/HO_2$. Fe(II) is a very slow reductant towards Hg(II)[33], and is unlikely to react on this timescale. A bimolecular reaction of the oxalyl radical anion ($C_2O_4^{-\bullet}$) with Hg(II) cannot compete kinetically with its rapid unimolecular decomposition. Therefore we attribute the reduction of Hg(II) to a

secondary photoproduct. The $CO_2^{-\bullet}$ radical anion is a strong reducing agent, $E^\circ(CO_2/CO_2^{-\bullet})$ = -2.0 V , equations 3.13-3.14 .

$$Hg(II) + CO_2^{-\bullet} \rightarrow Hg(I) + CO_2 \quad (3.13)$$

$$2\,Hg(I) \leftrightarrows Hg(0) + Hg(II) \quad (3.14)$$

In contrast, $O_2^{-\bullet}/HO_2$ is thought to be unable to reduce Hg(II)(*vide infra*).[34]

The rate of photoreduction is strongly pH-dependent, Figure 3.3. At pH 1.0, the reaction is complete after 20 mins irradiation. At pH 2.0, only 10 mins irradiation is required to attain a stable value of [Hg(II)]. At pH 3.0 and 4.0, the photoreaction is complete in 5 mins, consistent with the time required for complete photolysis of the ferrioxalate at this pH (*vide supra*). The pseudo-first-order rate constants $k_{obs}$ for UVA photoreduction are (0.65 ± 0.04) $min^{-1}$ at pH 3.0 and (0.59 ± 0.03) $min^{-1}$ at pH 4.0. In contrast, $k_{obs}$ = (0.25 ± 0.02) $min^{-1}$ at pH 2.0.

The dependence of the rate of photoreduction on pH can be explained by acid-base equilibria. At pH <3, oxalate is protonated (oxalic acid, pKa = ) and no longer binds to Fe(III). The formation of species less photoreactive than $Fe(C_2O_4)_3^{3-}$ is therefore more significant at low pH (Figure 3.4). In light of this effect, and given their relevance to environmental conditions, all subsequent experiments were performed at pH ≥ 3.

Photoreduction of the mercuric ion does not proceed to completion, even after complete photolysis of a 100-fold excess of ferrioxalate. The amount of residual Hg(II) is slightly pH-dependent, Figure 3.3, with twice as much remaining at pH 1-2 (0.8 μM) than at pH 3-4 (0.4 μM).

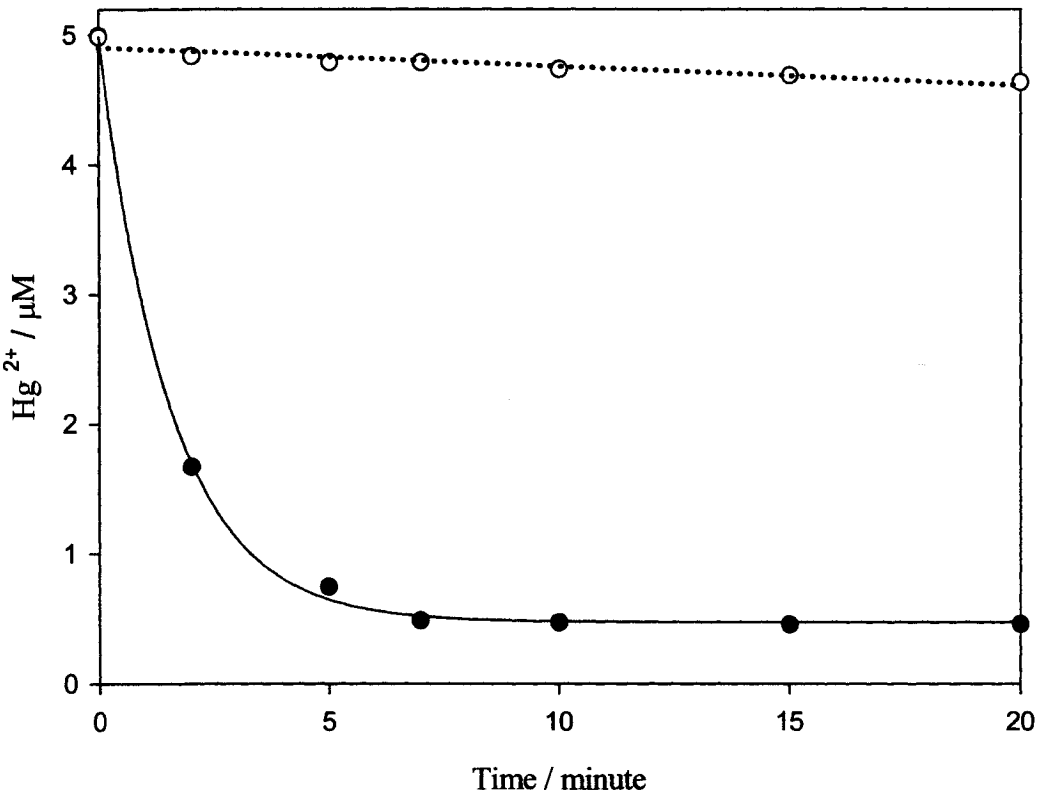


**Figure 3.2.** Reduction of air-saturated Hg(II) at pH 3 ($H_2SO_4$) under UVA irradiation in the presence of 100 μM $Fe(C_2O_4)_3^{3-}$ (open circles) and 500 μM $Fe(C_2O_4)_3^{3-}$ (filled circles).

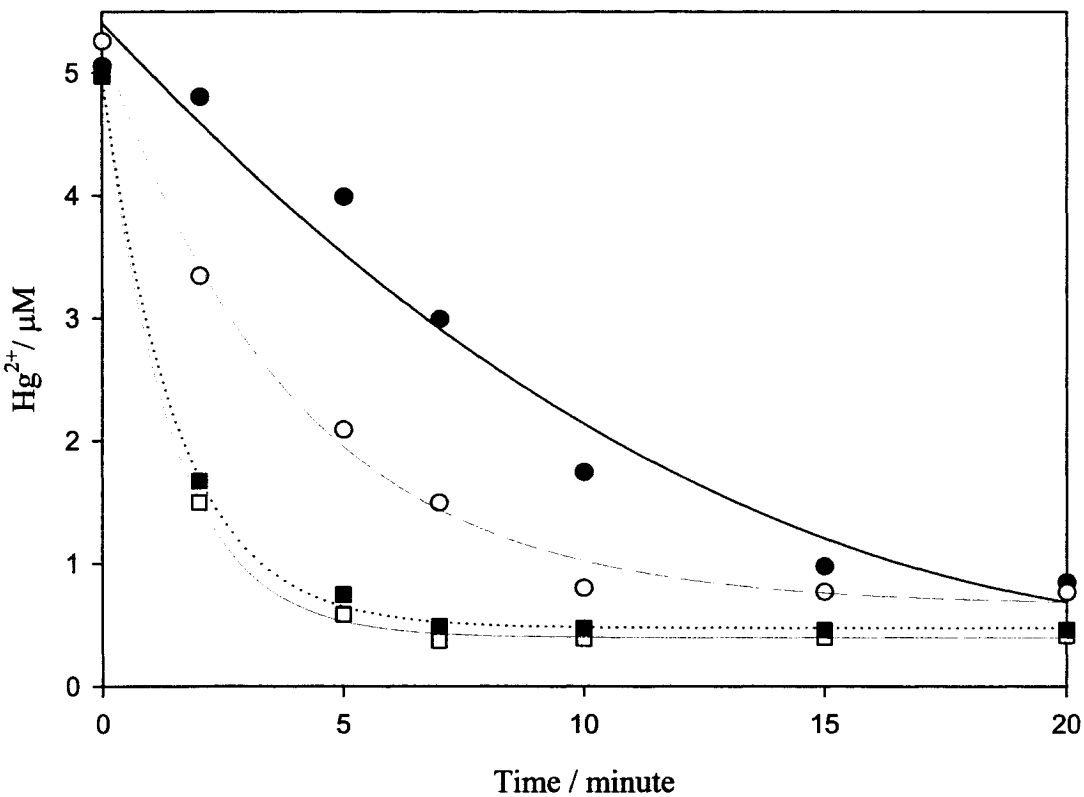


**Figure 3.3** Reduction of air-saturated Hg(II) under UVA irradiation in the presence of 500 μM $Fe(C_2O_4)_3^{3-}$ at pH 1.0 (filled circles), 2.0 (open circles), 3.0 (open squares) and 4.0 (filled squares).

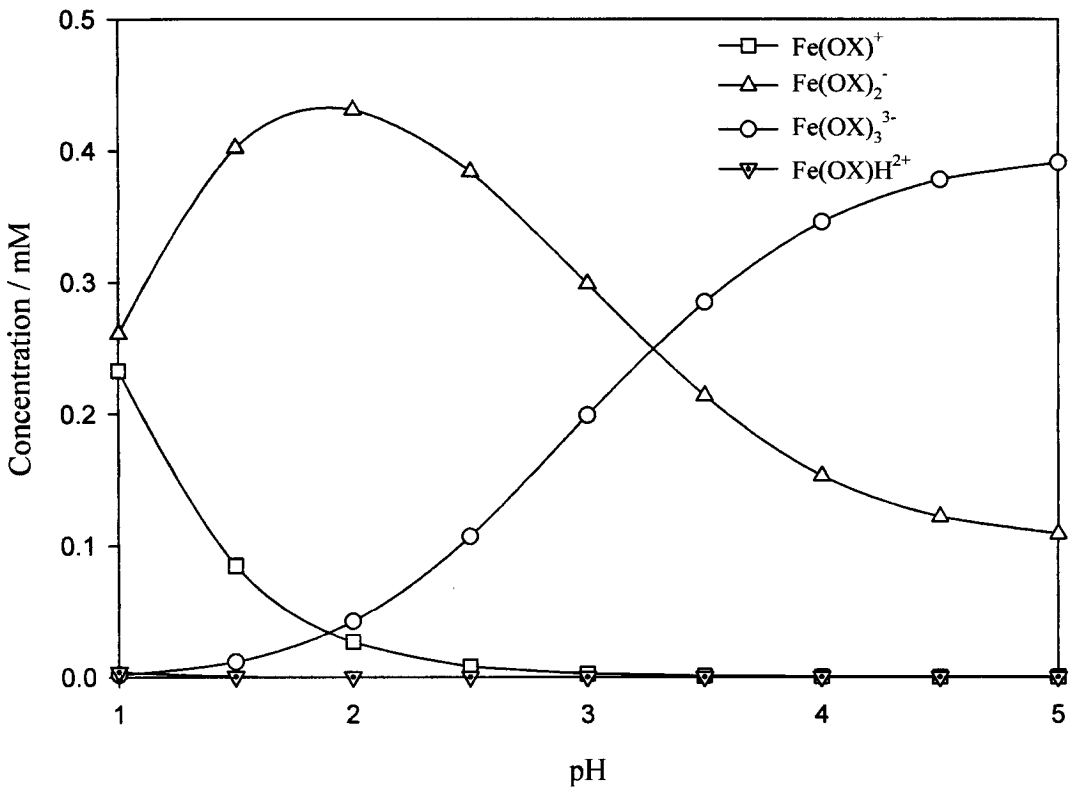


**Figure 3.4** Speciation of 0.5 mM Fe(III) in the presence of 1.5 mM oxalate as a function of pH.

### 3.5 Formation of Hg(0)

Photoreduction of Hg(II) was confirmed by monitoring the production of Hg(0) at pH 3.0 during UV-A irradiation of a 5.0 μM solution of Hg(II) in the presence of 500 μM ferrioxalate, Figure 3.5. The expected yield of Hg(0) is 4.6 μM, based on the measurement of 0.4 μM residual Hg(II) (*vide supra*). After 5 mins irradiation, 3.6 μM Hg(0) was detected. The measured yield of Hg(0) is therefore ca. 80%. However, at this concentration the solubility of Hg(0) is exceeded by about one order of magnitude,[35] therefore most is present not in solution but in colloidal form. Incomplete recovery of Hg(0) may be due to its adsorption on the walls of the quartz tubes, or evasion into the headspace of the reaction solution due to its high volatility and low solubility. The formation of other reduced forms of Hg such as the insoluble $Hg_2Cl_2$, is also possible.

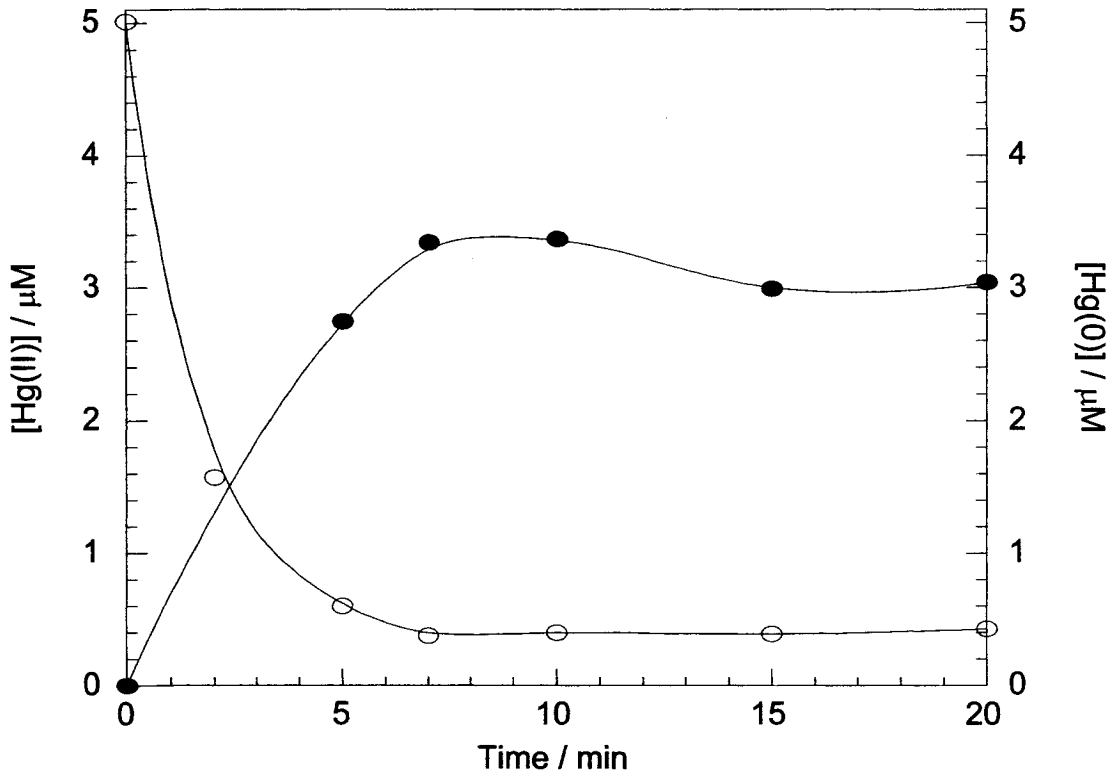


**Figure 3.5.** Comparison of Hg(II) loss (○) and Hg(0) formation (●)during UVA irradiation of an air-saturated solution containing 5.0 μM Hg(II) and 500 μM $Fe(C_2O_4)_3^{3-}$ at pH 3.0 ($H_2SO_4$).

### 3.6 Visible photoreduction of Hg(II)

Photoreduction can also be achieved with visible irradiation. The absorption of ferrioxalate extends into the visible region of the spectrum as far as 550 nm.[36] The rate of visible photoreduction is ca. 10 times slower than the rate of UVA photoreduction and is weakly pH-dependent in the range $3.0 \leq pH \leq 5.0$ , Figure 3.6. The difference in ability of UVA and visible irradiation to induce reduction of Hg(II) is evident from a comparison of Figures 3.2 and 3.5. This effect is expected based on the differing rates of photolysis of ferrioxalate under these conditions, Figure 3.1. A substantial amount of Hg(II) is not reduced at pH 5 (2.0 μM), compared to pH 3-4 (0.8 μM).

### 3.7 The effect of dissolved oxygen

The level of dissolved oxygen is a very important parameter in water quality. The concentration of oxygen in air-saturated water at 25°C is 0.25 mM. [19] Under-saturation of oxygen in water bodies can be a consequence of the presence of chemical oxidizing agents or biological activity. Oxygen deficiency was observed to increase in colored water spiked with Fe(III) upon light irradiation,[37] presumably due to photolysis of iron complexed to DOC. In the presence of air, Hg(II) must compete with $O_2$ for $CO_2^{-\bullet}$. At high enough levels of dissolved oxygen, most $CO_2^{-\bullet}$ will be diverted to reaction (3.3). Under the acidic conditions used in this study ($pH \leq 5$), superoxide is protonated to form $HO_2$ ($pK_a$ 4.8). Since neither $O_2^{-\bullet}$ nor $HO_2$ are thought to be capable of reducing Hg(II),[38] the expected effects are to decrease the yield and the rate of Hg(0) formation.

In order to explore this hypothesis, we irradiated argon-saturated aqueous mixtures of ferrioxalate and mercuric ion in the absence of $O_2$. Efficient reduction of 5.0 μM Hg(II) was observed even with concentrations of ferrioxalate which were ineffective in the presence of air. Thus UVA irradiation of a 50 μM ferrioxalate solution caused 87% reduction of Hg(II) to Hg(0), while irradiation of a 5.0 μM ferrioxalate solution caused 72% reduction of Hg(II), Figure 3.7. The inability of an acidic 100 μM ferrioxalate solution to generate Hg(0) in the presence of air, Figure 3.2, conflicts with an earlier suggestion that $O_2^{-\bullet}/HO_2$ can reduce Hg(II).[17]

Hg(0) is not reoxidized in irradiated argon-saturated solutions. However, Hg(0) in (initially) air-saturated solutions which were irradiated for long periods of time (≥ 20 mins) suffered eventual reoxidation to Hg(II), Figure 3.8. Under conditions such that Hg(II) cannot compete with $O_2$ for $CO_2^{-\bullet}$, the fate of the $O_2^{-\bullet}/HO_2$ photoproduct is disproportionation to $H_2O_2$, equation 3.5 When both $H_2O_2$ and Hg(0) are formed, reoxidation of Hg(0) is a possibility,[39] equation 3.15.

$$Hg(0) + H_2O_2 + 2\,H^+ \rightarrow Hg(II) + 2\,H_2O \qquad (3.15)$$

Alternately, Hg(0) may be oxidized by hydroxyl radicals generated by the Fenton reaction,[34] equation 3.16

$$Fe(II) + H_2O_2 \rightarrow Fe(III) + OH^- + OH \qquad (3.16)$$

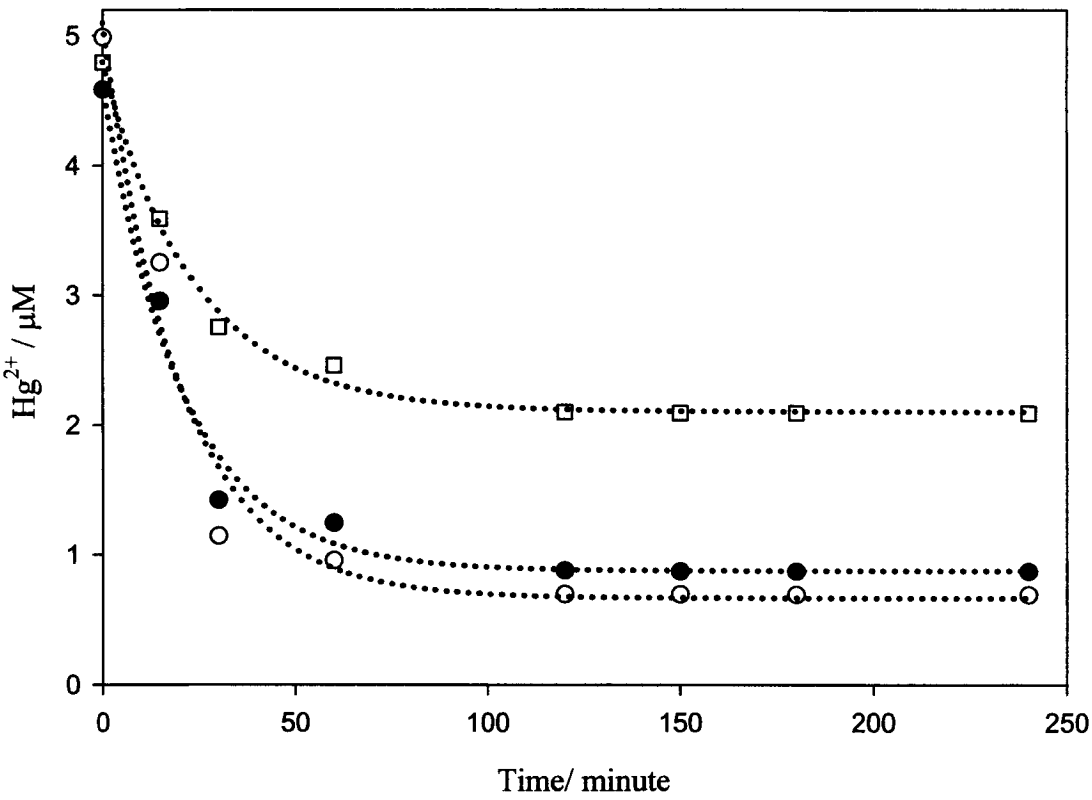


**Figure 3.6.** Evolution of air-saturated Hg(II) under visible irradiation in the presence of 500 μM $Fe(C_2O_4)_3^{3-}$ at pH 3.0 (open circles), 4.0 (filled circles) and 5.0 (open squares).

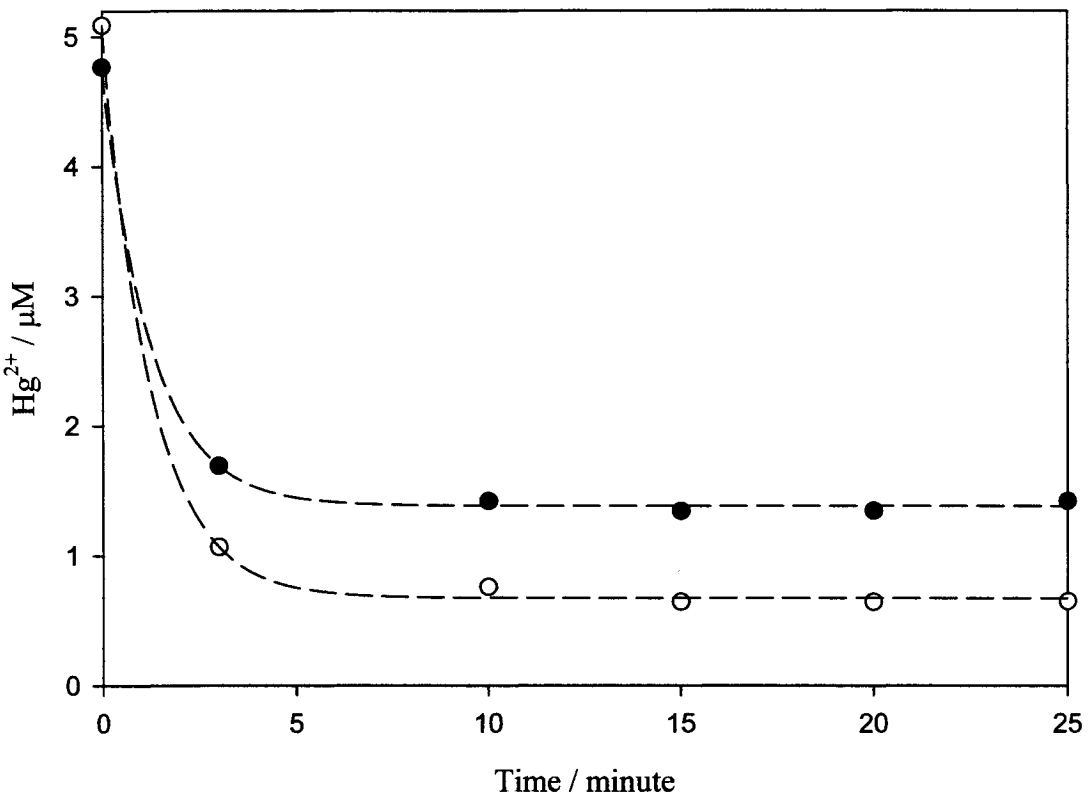


**Figure 3.7.** Evolution of Hg(II) in an argon-saturated solution at pH 3 ($H_2SO_4$) under UVA irradiation in the presence of 50 μM $Fe(C_2O_4)_3^{3-}$ (open circles) and 5.0 μM $Fe(C_2O_4)_3^{3-}$ (filled circles).

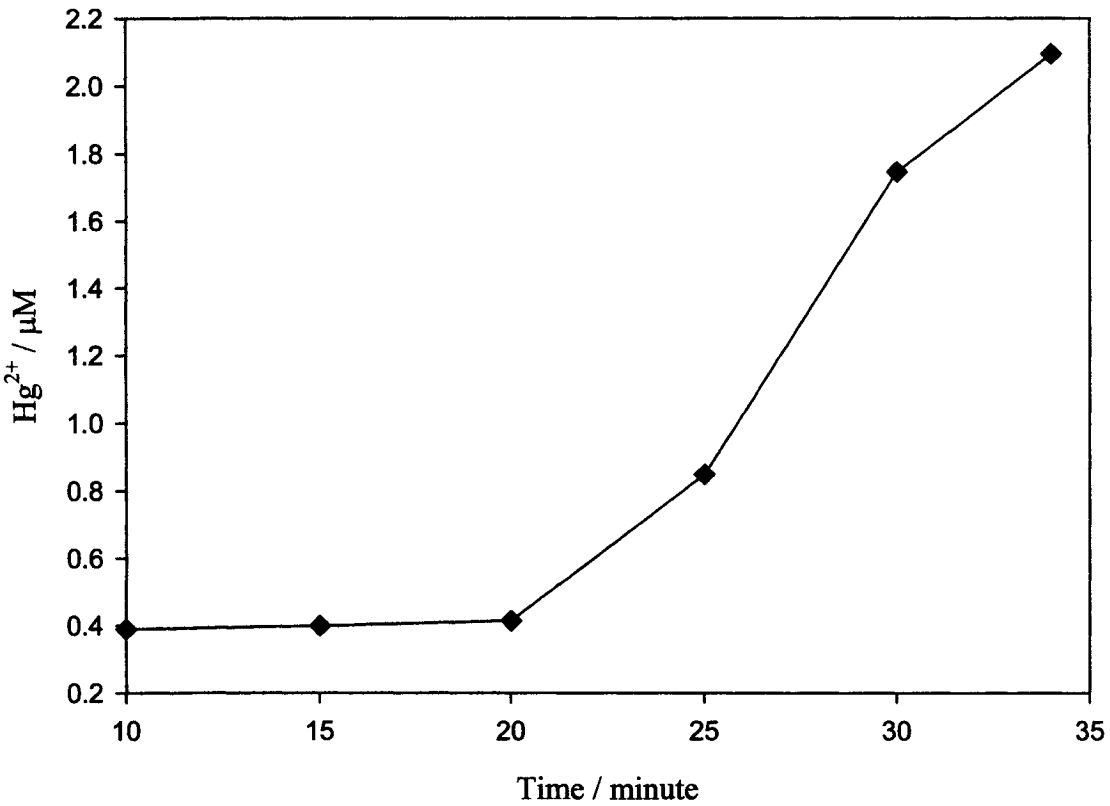


**Figure 3.8.** Evolution of air-saturated Hg(II) under UVA irradiation in the presence of 500 μM $Fe(C_2O_4)_3^{3-}$ at pH 3.0 ($H_2SO_4$).

### 3.8 Effect of oxalate

Since oxalate is liberated during photolysis of ferrioxalate (eq 3.1), the photochemistry of mercury-oxalate complexes must also be considered. UV irradiation ($\lambda > 290$ nm) of an aqueous solution of $HgC_2O_4$ was reported to result in formation of Hg(0),[38] equation 3.17.

$$HgC_2O_4 + h\nu \rightarrow Hg(0) + 2\,CO_2 \qquad (3.17)$$

However, continued irradiation of the ferrioxalate/Hg(II) mixture after the complete photolysis of ferrioxalate (i.e., longer than 10 mins) did not result in further reduction of Hg(II), as shown by the steady state regions in Figures 3.2, 3.3, 3.5, and 3.6.

In an additional control experiment, a mixture 1.5 mM $HC_2O_4^-$ and 5 μM Hg(II) at pH 3.0 was irradiated with UVA radiation. A slow loss of Hg(II) was observed, Figure 3.9, consistent with the results of a recent study.[38] However, the rate is much slower than in the presence of Fe(III) under similar pH conditions.

### 3.9 The effect of chloride

Concentrated aqueous solutions of $HgCl_2$ (0.02 M) are reported to undergo photoreduction of Hg(II) when irradiated with UV.[40] However, addition of 1 mM chloride ion to an air-saturated ferrioxalate/Hg(II) mixture at pH 1.7 resulted in a dramatic slowing of the rate of photoreduction, Figure 3.10. The effect increases slightly with increasing chloride concentration up to 0.1 M. Complexation of Hg(II) by chloride may raise the redox potential for the Hg(II)/Hg(0) couple.

The effect of chloride is less significant at higher pH values. For example, at pH 4 the addition of 1 mM chloride had no significant effect on the rate of photoreduction of 5 μM Hg(II). These observations suggest that the formation of $HgCl_3^-$ and $HgCl_4^{2-}$ under acidic condition may inhibit the photoreduction of $Hg^{2+}$. Compared to $HgCl_2$, both $HgCl_3^-$ and $HgCl_4^{2-}$ absorb efficiently at longer wavelengths (red shift), and this absorption leads to ligand- to-metal charge transfer as shown in equations 3.18-3.19:.

$$2HgCl_4^{2-} \xrightarrow{h\nu} 2[Hg^{+}Cl_4^{3-}] \rightarrow Cl^{\cdot} + HgCl_3^- \qquad (3.18)$$

$$Cl. + Cl^- \rightarrow Cl_2^{\cdot -} \qquad (3.19)$$

The radical anion ($Cl_2^{\cdot -}$) is reported to react with oxalate,[40] Production of this radical anion decreases the ability of the oxalate radical to generate the $CO_2^{\cdot -}$ which is necessary to reduce $Hg^{2+}$.

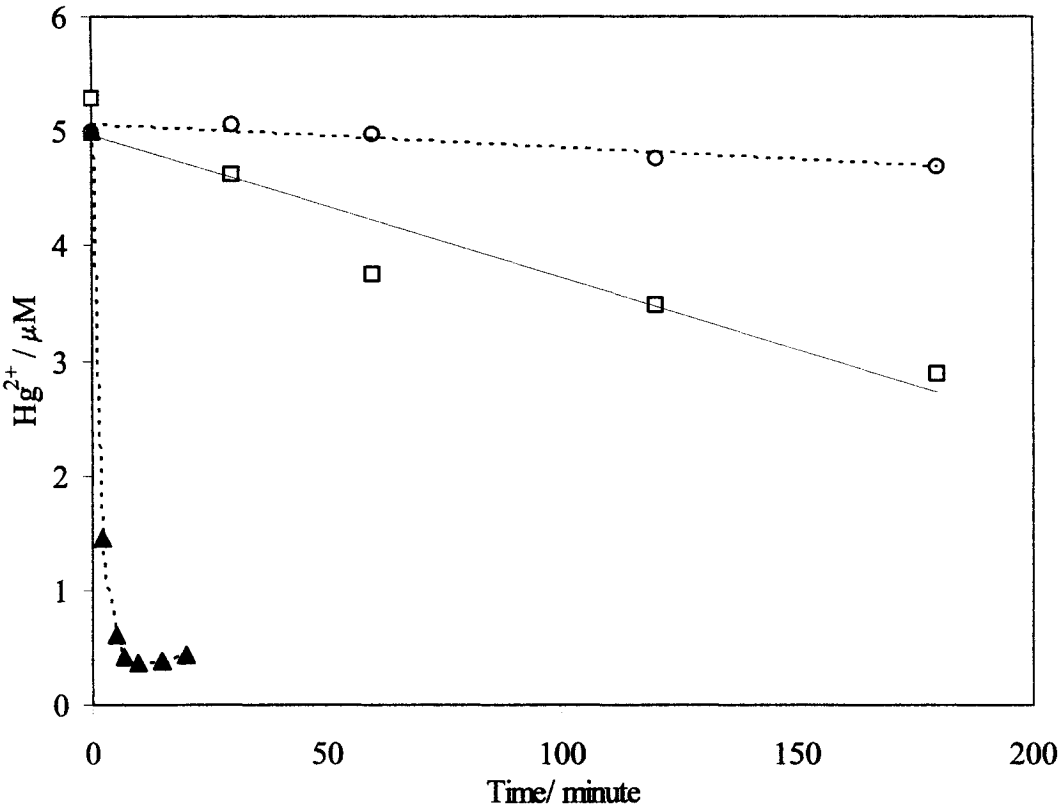


**Figure 3.9** Comparison of the rates of evolution of Hg(II) upon UVA irradiation of an air-saturated solution containing 5 μM $HgCl_2$ at pH 3.0 (open circles), and in the presence of 1.5 mM $HC_2O_4^-$ (open square), or 500 μM $Fe(C_2O_4)_3^{3-}$ (triangle).

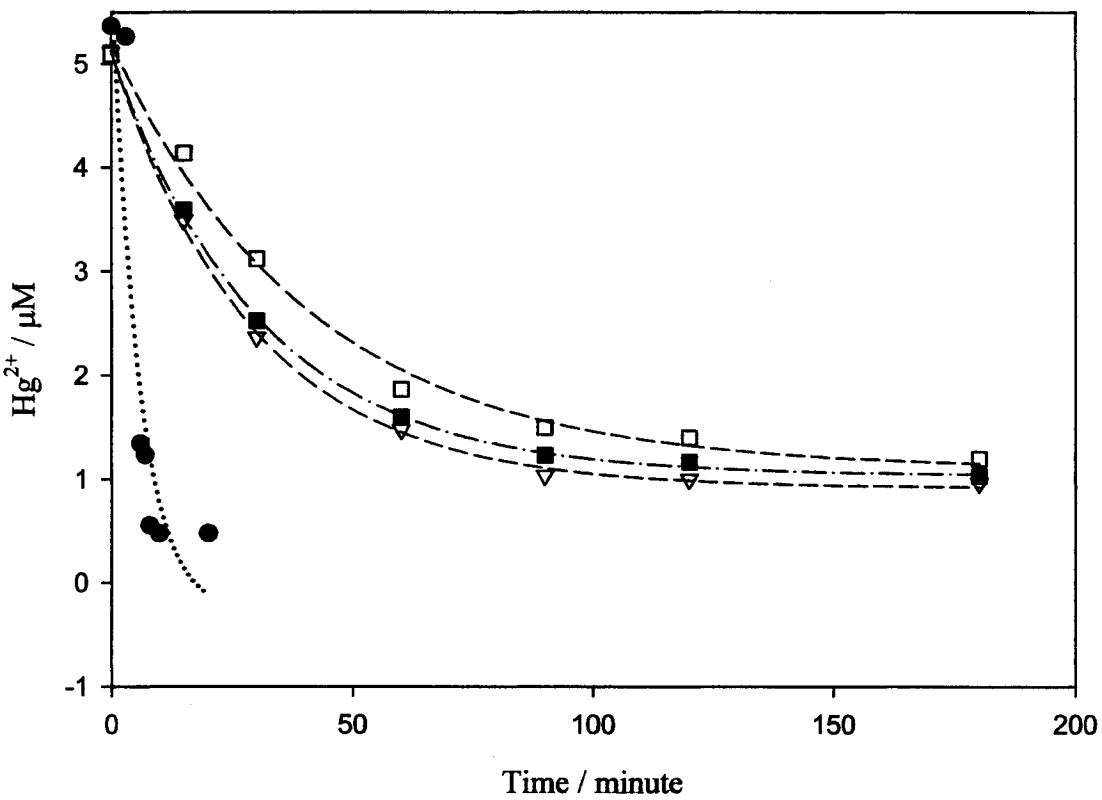


**Figure 3.10.** Evolution of air-saturated Hg(II) under UVA irradiation at pH 1.7 ($H_2SO_4$) in the presence of 500 μM $Fe(C_2O_4)_3^{3-}$ and 10 μM $Cl^-$ (filled circles), 5 mM $Cl^-$ (triangle), 10 mM $Cl^-$ (filled squares) and 100 mM $Cl^-$ (open squares).

### 3.10 Photoreduction of $Hg^{2+}$ using ferric citrate

Many iron(III) polyhydroxylate complexes are photosensitive. We hypothesized that compounds other than ferrioxalate would have the ability to reduce mercuric chloride compounds upon photolysis. To test this hypothesis, we used UVA to irradiate solutions of 0.7 mM ferric citrate containing 5 μM of $HgCl_2$ at pH 3-5. The Hg(II) concentration was reduced to a steady state within 5 minutes (Figure 3.11). This implies that such Fe(III) complexes may play a role in the reduction of mercuric chloride complexes. The proposed mechanism of ferric citrate photolysis is shown in Scheme 1.[41,19]

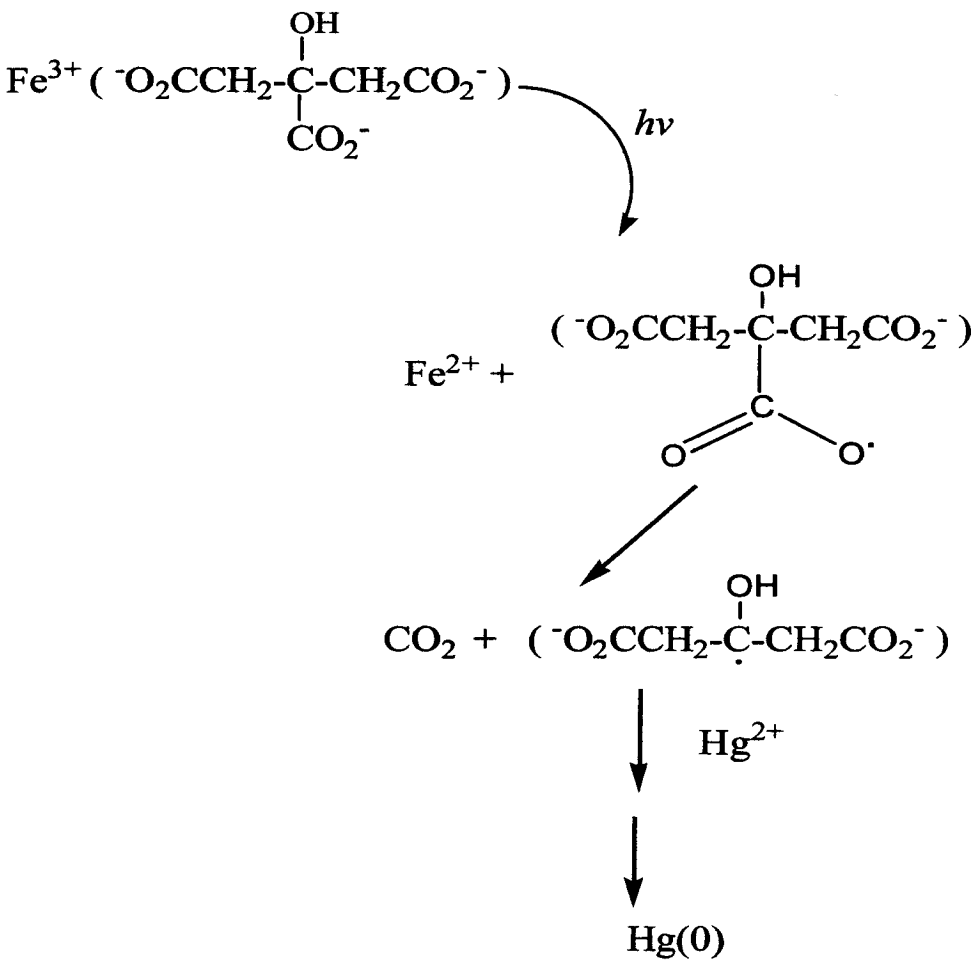


**Scheme 1.** Mechanism of Fe(III) citrate photolysis.

The results of photoreduction at pH 5 are complicated by the precipitation of $Fe(OH)_3$.

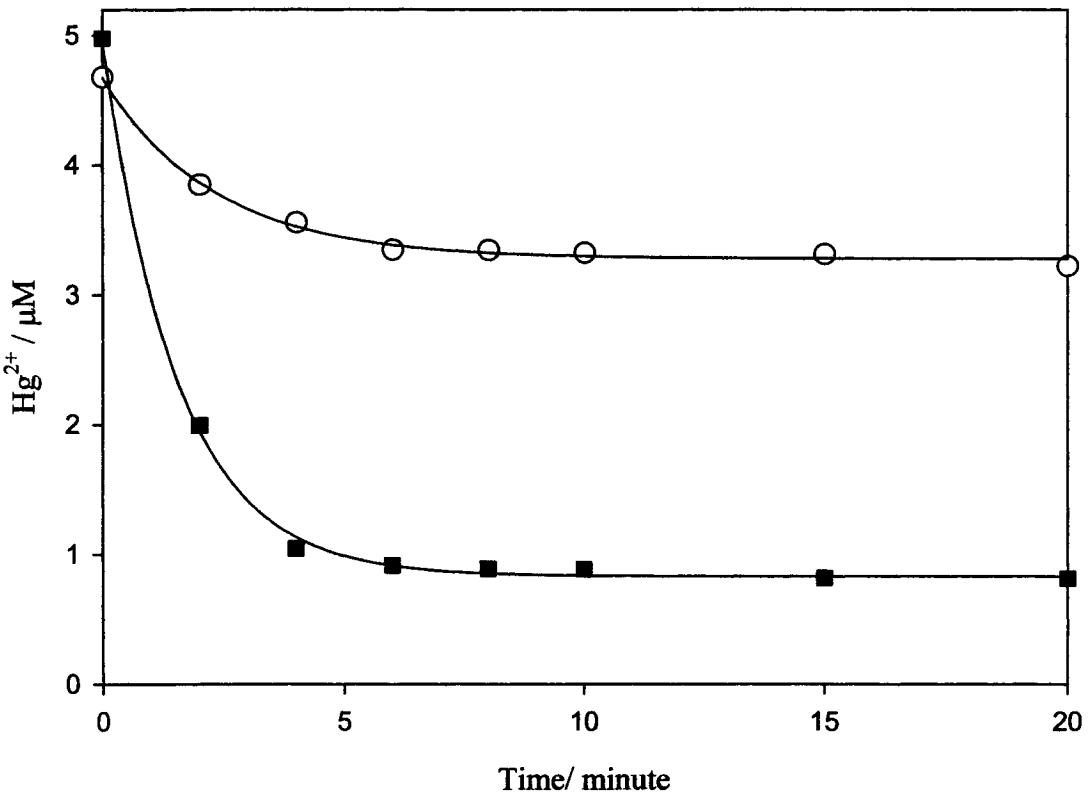


**Figure 3.11** Evolution of air-saturated Hg(II) under UVA irradiation in the presence of 500 μM Fe(III) citrate at pH 3.0 (filled squares), and pH 5.0 (open circles).

### 3.11 Conclusions

UVA irradiation of aqueous acidic mercuric chloride in the presence of a large excess of ferrioxalate results in partial reduction of the mercuric ion to elemental mercury. The pseudo-first-order rate constant k for photoreduction reaction is pH-dependent, as is the amount of residual Hg(II). Similar results were obtained using visible irradiation, although the rates are ca. 10 times slower. However, in the environment, intensity of visible radiation is 10 times greater it penetrates to much greater depths. Consequently, photoreduction by visible radiation may be more important. The mechanism of photoreduction is inferred to involve reaction of Hg(II) with a secondary photoproduct, the strongly reducing radical anion $CO_2^{-\bullet}$. In the presence of dissolved oxygen, competition for $CO_2^{-\bullet}$ between Hg(II) and $O_2$ reduces the rate and efficiency of mercuric ion reduction. The $O_2^{-\bullet}/HO_2$ products do not reduce Hg(II). On the contrary, their disproportionation leads to the formation of $H_2O_2$ which causes a slow reoxidation of Hg(0). Addition of chloride ion decreases the rate of the reduction of Hg(II), via the formation of anionic chloride complexes.

### References


(1) Pacyna, E. G.; Pacyna, J. M. *Water Air Soil Pollut.* **2002**, *137*, 149-165.

(2) Regnell, O.; Tunlid, A.; Ewald, G.; Sangfors, O. *Can. J. Fish Aquatic Sci.* **1996**, *53*, 1535-1545.

(3) Hintelmann, H.; Falter, R.; Ilgen, G.; Evans, R. D. *Fres. J. Anal. Chem.* **1997**, *358*, 363-70.

(4) Gilmour, C. G.; Henry, E. A.; Mitchell, R. *Environ. Sci. Technol.* **1992**, *26*, 2281-2287

(5) Fitzgerald, W. F.; Mason, R. P.; Vandal, G. M. *Water Air Soil Pollut.* **1991**, *65*, 745-767.

(6) Siciliano, S. D.; O' Driscoll, N.; Lean, D. *Environ. Sci. Technol.* **2002**, *36*, 3064-3068.

(7) Allard, B.; Arsenie, I. *Water Air Soil Pollut.* **1991**, *65*, 457-464.

(8) Nriagu, J. O. *Sci. Total Environ.* **1994**, *154*, 1-8.

(9) Pehkonen, S. O; Lin, C. J. *J. Air Waste Manag. Assoc.* **1998**, *48*, 144-150.

(10) Amyot, M.; Gill, G. A.; Morel, F. M. *Environ. Sci. Technol.* **1997**, *31*, 3606-3611.

(11) Alberts, J. J.; Schindler, J. E.; Miller, R. W. ; Jr- Nutter, D. E. *Science* **1974**, *184*, 895-897.

(12) Munthe, J.; McElroy, W. J. *Atmos. Environ.* **1992**, *26A*, 553-557.

(13) Xiao, Z. F.; Stromberg, D. *Water Air Soil Pollut.* **1995**, *80*, 789-798.

(14) Munthe, J.; Xiao, Z.; Lindqvist, O. *Water Air Soil Pollut.* **1991**, *56*, 621-630.

(15) Van Loon, L.; Mader, E.; Scott, S. L. *J. Phys. Chem. A* **2000**, *104*, 1621-1626.

(16) Mason, R. P.; Morel, F. M.; Hemond, H. F. *Water Air Soil Pollut.* **1995**, *80*, 775-787.

(17) Zhang, H. ; Lindberg, S. E. *Environ. Sci. Technol.* **2001**, *35*, 928-935.

(18) Zuo, Y.; Hoigené, J. *Environ. Sci. Technol.* **1992**, *26*, 1014-1022.

(19) Faust, B. C.; Zepp, R. G. *Environ. Sci. Technol.* **1993**, *27*, 2517-2522.

(20) King, D. W.; Lounsbury, H. A; Millero, F. J. *Environ. Sci. Technol.* **1995**, *29*, 818-824.

(21) Zepp, R. G.; Faust, B. C.; Hoigené, J. *Environ. Sci. Technol.* **1992**, *26*, 313-319.

(22) Sedlak, D. L.; Hoigené, J. *Atmos. Environ.* **1993**, *27A*, 2173-2185 .

(23) Voelker, B. M.; Sulzberger, B. *Environ. Sci. Technol.* **1996**, *30*, 1106-1114.

(24) Hug, S. J.; Laubscher, H. U.; James, B. R. *Environ. Sci. Technol.* **1997**, *31*, 160-170

(25) Joos, F.; Baltensperger, U. *Atmos. Environ.* **1991**, *25A*, 217-230.

(26) Steinberg, S.; Kawamura, K.; Kaplan, I. R. *Int. J. Environ. Anal. Chem.* **1987**, *19*, 251 260.

(27) Warneck, P. *Atmos. Environ.* **2003**, *37*, 2423-2427

(28) Erel, Y.; Pehkonen, S. O.; Hoffmann, M. R. *J. Geophys. Res. A* **1993**, *98*, 18423-18434.

(29) Sempéré, R.; Kawamura, K. *Atmos. Environ.* **1996**, 30, 1609-1619.

(30) Willey, J. D.; Keiber, R. J.; Eyman, M. S.; Avery, G. B. *Global Biogeochem. Cycl.* **2000**, 14, 139-148.

(31) Mulazzani, Q. G.; D'Angelantonio, M.; Venturi, M.; Hoffmann, M. Z.; Rodgers, M. A. J. *J. Phys. Chem.* **1986**, *90*, 5347-5352.

(32) Miller, W. L. In Aquatic humic substances: ecology and biogeochemistry. Hessen, D. O., Tranvik, L. J., Eds.; Springer-Germany, 1998; pp. 125-143.

(33) Raposo, R. R.; Enrique Meléndez-Hevia, E.; Spiro, M. *J. Mol. Catal. A: Chem,* **2000**, 164, 49-59.

(34) Gårdfeldt, K.; Jonsson, M. *J. Phys. Chem. A* **2003**, *107*, 4478-4482.

(35) Lin, C. –J.; Pehkonen, S.O. *J. Geophys. Res.* **1998**, 103, 28093-28102.

(36) Hislop, K. A.; Bolton, J. R. *Environ. Sci. Technol.* **1999**, 33, 3119-3126.

(37) Miles, C. J.; Brezonilk, P. L. *Environ. Sci. Technol.* **1981**, *15*, 1089-1095

(38) Gårdfeldt, K.; Sommar, J.; Strömberg, D.; Feng, X. *Atmos. Environ.* **2001**, *35*, 3039-3047.

(39) Brosset, C. *Water Air Soil Pollut.* **1987**, *34*, 145-166.

(40) Langmuir, M. E.; Hayon, E. *J. Phys. Chem.* **1967**, 71, 3808-3814.

(41) Dodge, C. J. ; Francis, A. J. *Environ. Sci. Technol.* **2002**, *36*, 2094-2100.

# Chapter 4

## Photoreduction of Hg(II) by UVA irradiation of humic and fulvic acids

### 4.1 Introduction

Humic substances (HS) are naturally occurring, heterogeneous, organic polyelectrolytes.[1] They constitute a major part of the total organic carbon (TOC) in the aquatic environment. The TOC consists of two operationally defined phases: particulate (POC) and dissolved (DOC). The latter is defined as the fraction that can pass through 0.45 μm filters, and consists of two fractions: non-humic and humic. The non-humic portion is composed of lipids, polysaccharides, and proteins, while the humic portion consists of fulvic (FA) and humic (HA) acids.[2] Detailed classification of the TOC is shown in Figure 4.1. Aquatic FA has molecular weight (MW) distributions that range from 500 to 2,000 Daltons.[3-6] It is soluble in aqueous solution at all pH values. On the other hand, aquatic HA has a higher MW distribution range of 2000 to more than 10,000 Daltons[5,7] and precipitates in aqueous solutions of $pH \leq 2$.

The concentration of DOC in natural freshwater samples of rivers and lakes is in the range of 0.1 to 100 mg C/L,[8] and is more commonly from 1 to 10 mg C/L.[9] Humic substances (HS) constitute 50-90% of the DOC,[8] and impart a yellowish-brown color to the water. Peat water or what is known as colored water contains high levels of DOC.

DOC plays an important role in the bioavailability, bioaccumulation, mobility, speciation and toxicity of contaminants ( metal ions and organic pollutants) as a result of its complexation ability toward metal ions,[10-12] and its interactions with organic

pollutants.[13,14] The interactions of DOC with metal ions are not only restricted to complexation; DOC also has the ability to reduce some ions, such as Fe(III),[15] Mn(IV),[16] V(V),[17] and Hg(II)[18,19] to lower oxidation states . Some of these reduction reactions are enhanced in the presence of solar radiation, as a result of HS photoactivation.

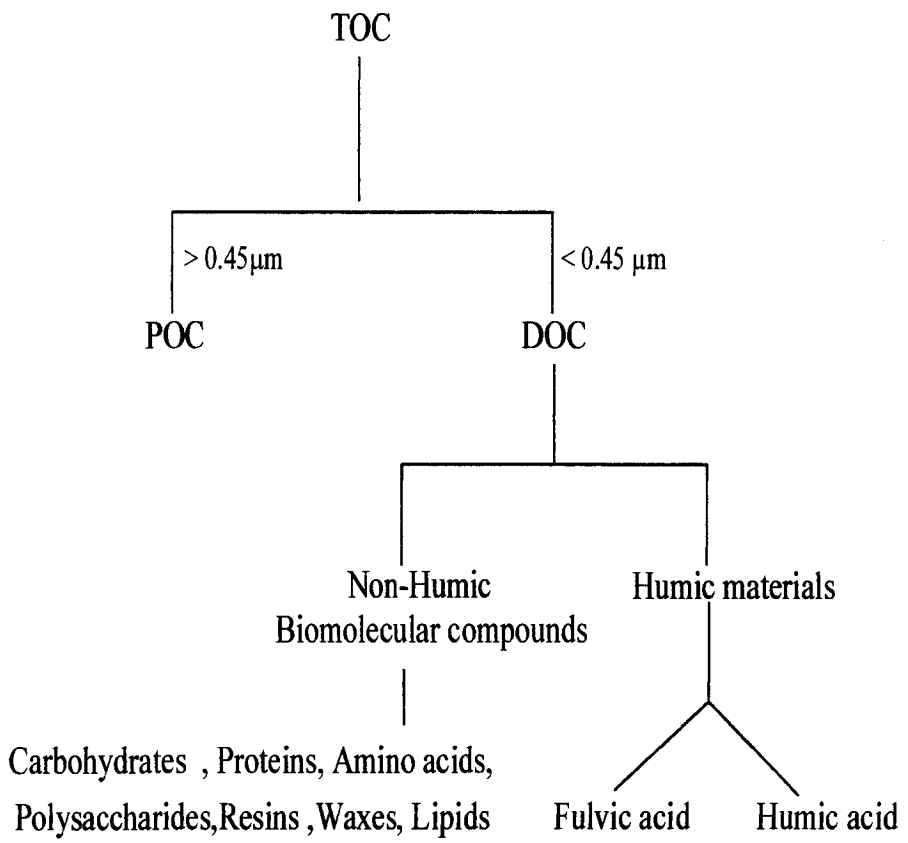


**Figure 4.1** Classification of TOC in water systems.

FA and HA are the major chromophores found in DOC. Exposure of DOC to UV or visible radiation can induce various photochemical reactions. For example, light-activated FA or HA in oxygen-saturated aqueous solutions can be deactivated to ground states by electron or energy transfer. In some cases, reactive oxygen species are produced.[20,21]These include peroxy radicals ROO·,[22] hydrogen peroxide $H_2O_2$,[23, 24] superoxide $O_2^{-}$,[25]singlet oxygen $^1O_2$,[26,27] and hydroxyl radical HO·.[28] It is reported that the hydrated electrons $e^-_{(aq)}$ are also produced.[29] UV-irradiation of DOC also results in changing the chemical structures of HA and FA, releasing of $CO_2$[30]and CO[31,32] produces smaller organic molecular weight (MW),[33] amino acids and ammonia [34] and short chain fatty acids such as oxalic, formic, acetic and malonic acids.[35,36] are examples of chemical structural changes of DOC.

Ozone ($O_3$) depletion from the stratosphere leads to an increase in the intensity of UV-radiation that reaches the earth's surface. DOC in water bodies works as a shield to reduce the penetration of UV-radiation by absorbing the incident light. Several studies have shown a positive correlation between the concentration of DOC and $Hg^{2+}$ in the aquatic environment.[37-41] Increasing intensity of UV–radiation that penetrates and strikes the water surface will thus significantly affect the speciation and availability of Hg and its compounds.

Methyl mercury is the most toxic form of Hg and the only form to accumulate in the food chain. It was found to be photodegraded in surface water.[42] The rate of photoreduction was highest in the top 10 cm and decreased with water depth.[42] Direct photoreduction of $MeHg^+$ species is possible. MeHgCl, for example, absorbs in the range of 200-315 nm,[43] and part of this absorption is located within the range of solar

irradiation that reaches the water surface (> 290 nm). However, DOC may induce the indirect photoreduction of MeHg. It was reported that the production of OH radicals as a result of DOC irradiation could be an important pathway for $MeHg^+$ photodegradation in surface water.[44]

In natural waters, the reduction of Hg(II) by HS can be photoinduced.[18, 45, 46] This leads to the formation of Hg(0), which has very low solubility in water[47, 48] and high volatility (equations 4.1-4.2). Both are determinant factors in the evasion of Hg(0) to the atmosphere. Flux rates of 1 to 20 pmol Hg(0) $m^{-2}$ $h^{-1}$ from lakes have been measured.[46,49,50] This evasion leads to long range atmospheric transport and global dispersal of elemental Hg(0).

$$Hg^0_{(l)} \rightleftarrows Hg^0_{(aq)} \qquad K = 3.3 \times 10^{-7}\ mol.L^{-1} \qquad (4.1)$$

$$Hg^0_{(g)} \rightleftarrows Hg^0_{(aq)} \qquad K = 2.56 \times 10^{-3}\ mol.L^{-1}.atm^{-1} \qquad (4.2)$$

The ability of HS to reduce Hg(II) in aqueous solution was the subject of several studies.[46,51,52] The evolution of elemental Hg was first characterized by Albert *et al.* [18] However, there are conflicting reports on the role of DOC in the photoreduction of Hg(II). Positive and negative relations between DOC and dissolved gaseous mercury have been reported in literature.[45,46,51,53] The origin of the inconsistencies may be the variable nature of DOC and other environmentally relevant parameters.[54]

The aim of the present study is to characterize the abiotic UVA photoreduction of Hg(II) ions in the presence of Suwannee River fulvic acid and Lonardite humic acid. A comparison between the UVA and dark reduction and the effects of environmentally relevant parameters such as pH, Hg(II)/HS ratio, and chloride concentration are investigated, as well as possible mechanism(s) involved.

## 4.2 Spectrophotometric characterization of humic substances

Aqueous solutions of humic and fulvic acids at ~ 5 to 10 mg/L have noticeable yellow to brown colors due to absorption in the visible region. Their absorbance in the UV-region is even more intense. Due to different contents of chromophoric groups, humic acid tends to have a higher absorbance than fulvic acid at the same mass concentration (Figure 4.2). The absorbance for both acids is slightly enhanced at higher pH values because of proton dissociation. The Beer-Lambert law is obeyed for DOC concentrations of 3-100 mg/ L in the range 220 – 450 nm.[55]

Irradiation of an HS solution results in spectral changes, as a result of the interaction of HS with UVA which leads to the activation of HS. Various photochemical processes are induced,[56] and as a consequence, alterations in the functional groups and intramolecular interactions of HS. Breaking of chemical bonds in HS structure may also be involved. In natural water bodies, the interaction of DOC with solar radiation leads to a reduction in water color, a phenomenon which is known as photobleaching. It is more significant during summer months.[57] Another phenomenon due to the interaction of solar radiation with HS is photomineralization, in which the DOC concentration decreases as a result of formation of "inorganic carbon", CO and $CO_2$.[58,30,32] Vähätalo *et al.* [59] reported

that UVA contributes to 68% photomineralization of DOC in a humic lake. The decrease in DOC content is slow. Dahelén *et al.* [60] reported a decrease of 0.83 mg/L out of 15.9 mg/L DOC after 89 hours of UVA irradiation (5.1 W $m^{-2}$).

Under our experimental conditions, UV spectral changes in HS upon UVA irradiation were also very slow. Absorbance changes in the UV region 200-400 nm, were more pronounced than in the visible. After 48 hours UVA irradiation, the absorbance of humic acid was reduced by 28% at 300 nm and by 32% at 400 nm. For fulvic acid, the absorbance was reduced by 32% at 300 nm and by 30 % at 400 nm. The absorbance ratio $E_2/E_3$ ($A_{250}$ / $A_{365}$) increased for both acids; this may imply a decrease in aromaticity and molecular size of HS. These data are presented in Table 4.1.

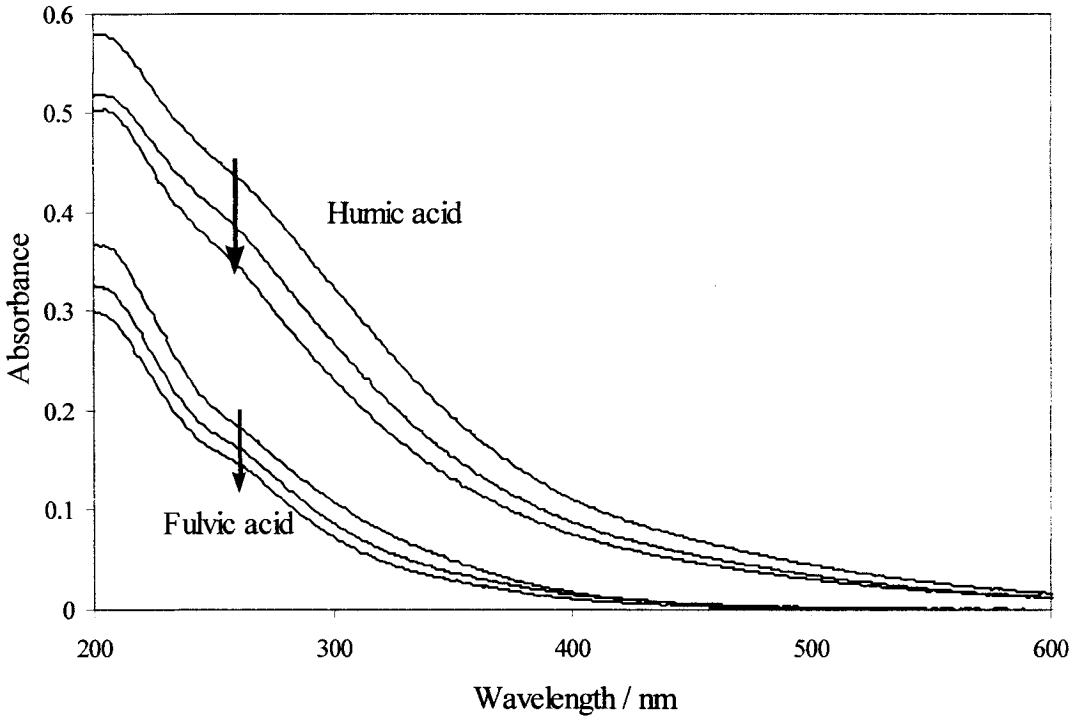


**Figure 4.2** UV-visible spectra of Suwannee River fulvic acid and Leonardite humic acid in aqueous solution at concentration level of 10 mg/ L and pH 5, after 0, 24 and 48 hours of UVA irradiation (I= 1.4 mW/ $cm^2$), respectively.

**Table 4.1** Some spectral changes for fulvic and humic acids at pH 5 during UVA irradiation.

| UVA Irradiation time / hours | Wavelength / nm | | | | | | Absorbance ratio $E_2/E_3$* |
|---|---|---|---|---|---|---|---|
| | 250 | | 300 | | 400 | | |
| | Abs. | Change% | Abs. | Change% | Abs. | Change% | |
| **A- fulvic acid 10 mg/L** | | | | | | | |
| Initial "0" | 0.202 | 0 | 0.108 | 0.00 | 0.018 | 0.00 | 5.47 |
| 24 | 0.177 | 12.58 | 0.086 | 20.001 | 0.015 | 12.05 | 6.16 |
| 48 | 0.160 | 20.75 | 0.073 | 32.55 | 0.013 | 30.59 | 7.14 |
| **B- humic acid 10 mg/L** | | | | | | | |
| Initial "0" | 0.455 | 0.0 | 0.324 | 0.0 | 0.111 | 0.0 | 2.78 |
| 24 | 0.404 | 11.3 | 0.267 | 17.5 | 0.088 | 21.0 | 3.12 |
| 48 | 0.368 | 19.1 | 0.232 | 28.8 | 0.075 | 31.9 | 3.33 |

* The absorbance ratio ($A_{250}$ / $A_{365}$)

### 4.3 Dark "electrochemical" reduction of Hg (II) by HS

An aqueous solution containing 5 x $10^{-6}$ M Hg (II) and 10 mg/L Leonardite humic acid or Suwannee River fulvic acid was kept in the dark at 23-25°C for 27 hours. The concentration of Hg (II) was continuously monitored during this time. A very slow reduction of Hg(II), presumably producing Hg(0), was observed at pH 8 (Figure 4.3). The experimental data were fitted to pseudo-first order kinetics (excess HS compared to Hg(II)). The rate constant (k) for the reduction of Hg(II) by humic acid ($k_{HA}$= 2.9 x $10^{-3}$ $min^{-1}$) is slightly higher than that for fulvic acid ( $k_{FA}$= 1.8 x $10^{-3}$ $min^{-1}$). The efficiency of this process after 27 hours is low. Of the initial 5 x $10^{-6}$ M Hg(II), only 25% was reduced by humic acid while 20 % was reduced by fulvic acid. Changing the pH of the solution from basic to an acidic (pH 8 to pH 5) under the same conditions (i.e;10 mg/ L of HS in dark) caused the rate of reduction and the efficiency ( % reduced Hg(II) relative to initial Hg(II) ) to increase. The rate constant was found to be $k_{HA}$= 4.1 x $10^{-3}$ $min^{-1}$ and the reduction efficiency reached 30% (Figure 4.4).

The reduction potential versus the neutral hydrogen electrode was estimated to be 0.7 V for humic acid,[61] whereas it was 0.5 V for fulvic acid.[62,63] Comparing these values with the standard potential reduction of Hg(II),0.85 V, demonstrates that spontaneous reduction of Hg(II) is possible. The half cell equations are shown in equations 4.3 to 4.5. In good agreements with our results, it was reported that the addition of 2.77 x $10^{-8}$ M of Hg(II) solution to a fulvic acid solution (10-25 mg/L) at pH < 5 led to the formation of brown precipitates in the presence of alumina.[64] This implies the formation of Hg(0) which is easily adsorbed by alumina.

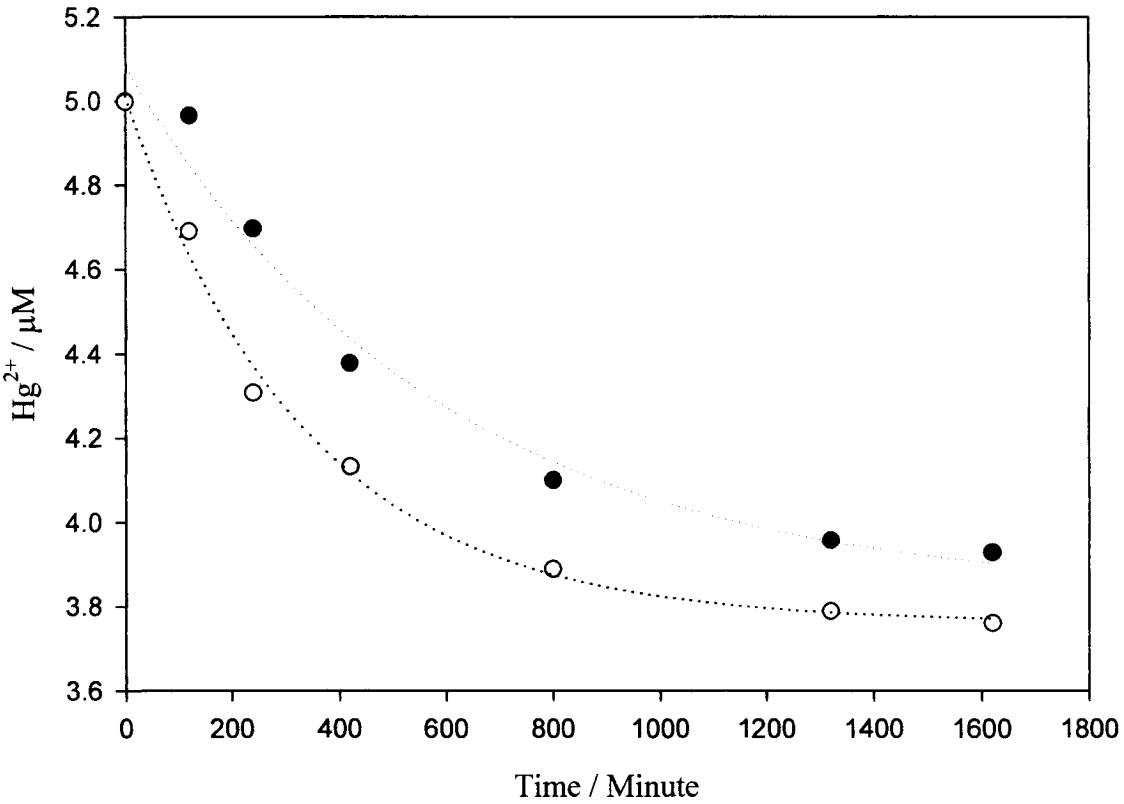


**Figure 4.3** Kinetic profiles for the dark reduction of $5x10^{-6}$ M Hg(II) by 10 mg/L each of humic (open circle) and fulvic (closed circle) acids at pH 8 and 23-25 °C.

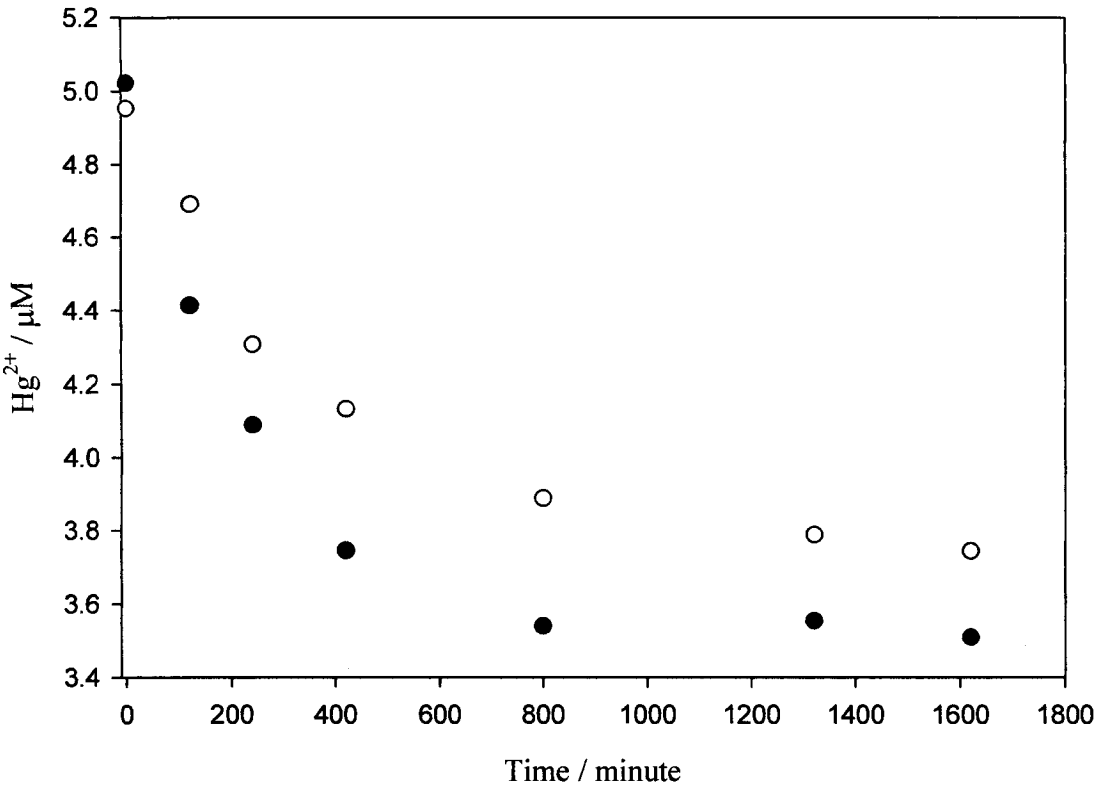


**Figure 4.4** Kinetic profiles for the dark reduction of $5x10^{-6}$ M Hg(II) by 10 mg/L humic acid at pH 5 (closed circles) and pH 8 (open circles), both at 23-25 °C.

$$FA(Red) \rightarrow FA(Oxd) + ne^- + mH^+ \qquad E^o = -0.5V \qquad (4.3)$$

$$HA(Red) \rightarrow HA(Oxd) + ne^- + mH^+ \qquad E^o = -0.7V \qquad (4.4)$$

$$Hg(II) + 2e^- \rightarrow Hg(0) \qquad E^o = +0.85V \qquad (4.5)$$

The extent of reduction depends on the reducing capacity of the humic and fulvic materials. Figure 4.5 compares dark of Hg (II) by 5 and 10 mg/L humic acid at pH 5. The rate constant (k) was 3.56 x $10^{-3}$ $min^{-1}$ with a reduction efficiency of ~ 20 % with 5mg/L humic acid, while (k) was 4.12 x $10^{-3}$ $min^{-1}$ and the efficiency was ~ 30 % when 10 mg/L humic was used.

Concentration levels of HS used in these experiments are relevant to those of natural waters. We found that the dark reduction is highly depend on Hg(II) concentration. At low Hg(II) concentrations (< 5 x $10^{-8}$ M) the reduction of Hg(II) was not readily detectable (Figure 4.6). As a consequence, dark or thermal reduction of Hg(II) in aquatic environment may be important only in highly contaminated areas such as in gold mining tailings or when accidental spills occur.

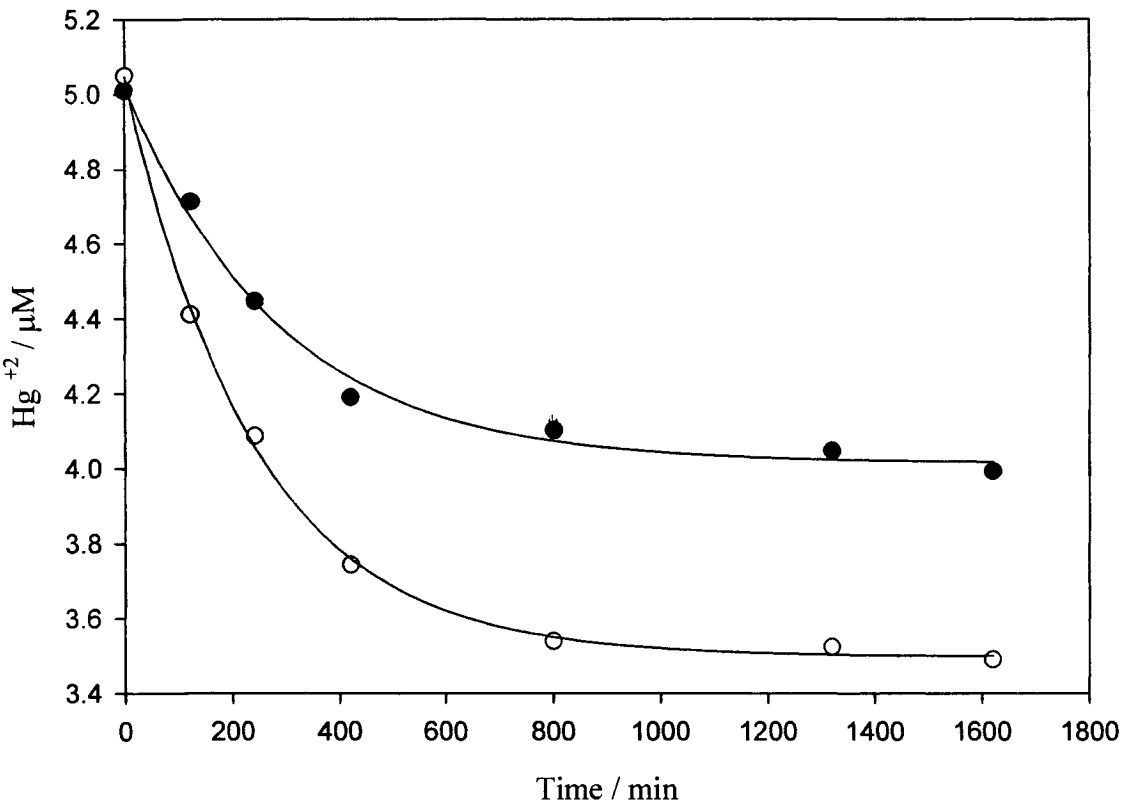


**Figure 4.5** Dependence of the extent of dark reduction of Hg(II) on HS capacity: 5 x $10^{-6}$ M Hg(II) reduced by 5 (closed circle) and 10 (open circle) mg/L humic acid at pH 5.

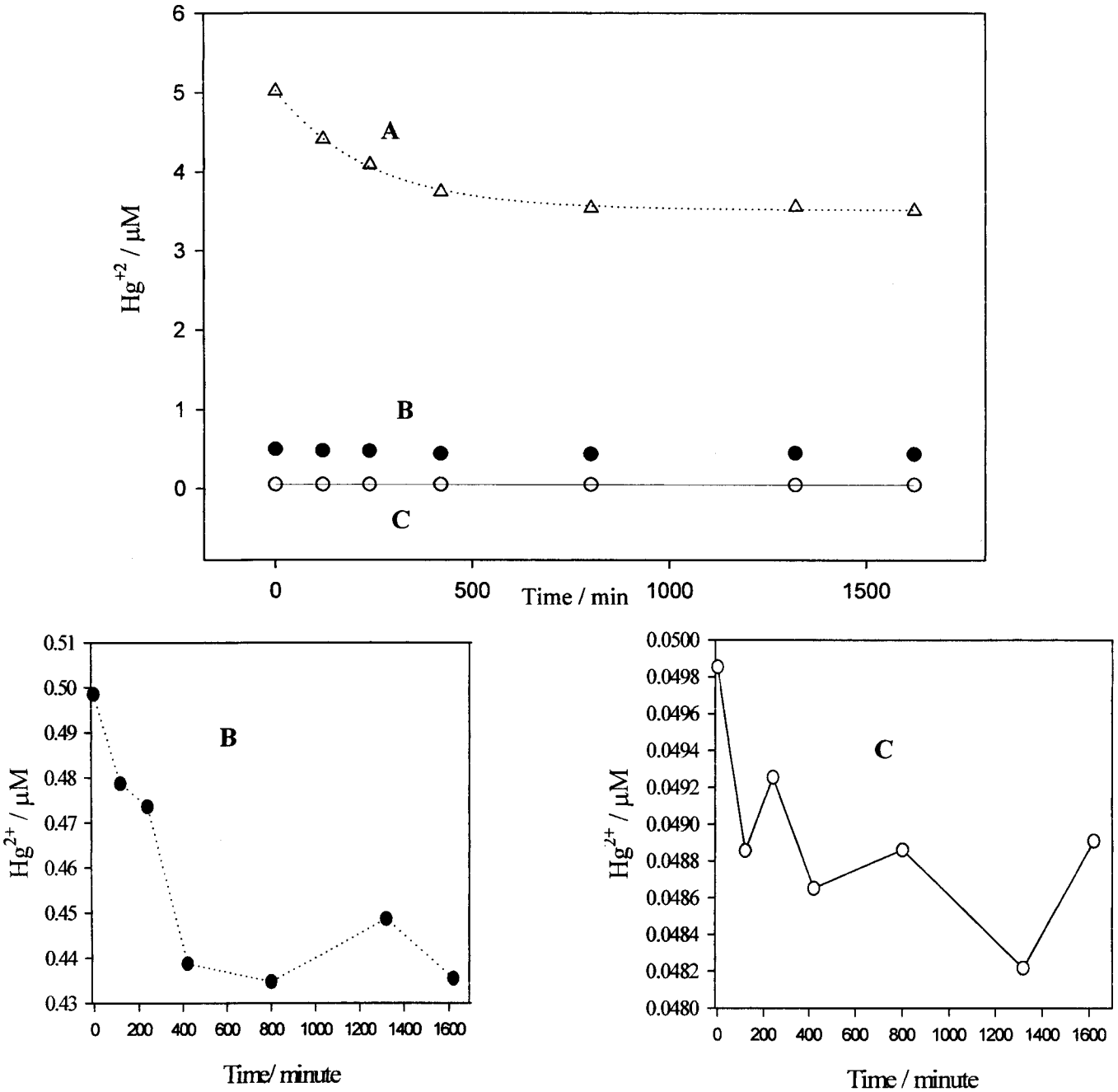


**Figure 4.6** Effect of initial Hg(II) concentrations on the dark reduction of Hg(II) at constant humic acid concentration of 10 mg/L and pH = 5. Initial [$Hg^{+2}$] is **A-** 5 x $10^{-6}$ M **B-** 5 x $10^{-7}$ M and **C-** 5 x $10^{-8}$ M.

### 4.4 Photoreduction of Hg(II) by humic substances

Aqueous solutions of $HgCl_2$ do not absorb in the UVA region: $HgCl_2$ has an absorption peak at 200 nm with an extinction coefficient (ε) of 2100 $M^{-1}cm^{-1}$ in acetonitrile.[65] This implies that the UVA can not produce any direct photochemical reaction of $HgCl_2$ in aqueous solution. However, in the presence of humic or fulvic acids, chemical reduction of Hg(II) was more efficient and faster than in the control dark reduction. As shown in Figure 4.7, after 27 hours of UVA irradiation of aqueous solution containing 5 x $10^{-7}$ M Hg(II) and 5 mg/L fulvic acid at pH 5, the initial Hg(II) concentration was reduced by 87%.

In order to determine the rate law of the reaction, we assumed that fulvic acid is the sole UVA absorber in the system. The relatively high initial fulvic acid concentration which remains essentially unchanged during the reaction, and under constant UVA irradiation intensity, causes the rate law to obey pseudo-first order kinetics. For an aqueous solution of 5 x $10^{-7}$ M Hg(II ) and 5 mg/L fulvic acid at pH 5, the pseudo-first order rate constant "$k_{obs}$" was found to be 1.12 x $10^{-2}$ $min^{-1}$ .

#### 4.4.1 Effect of pH

The rate and efficiency of the photoreduction of Hg(II) by HS was found to be pH dependent, Figure 4.8. At either extreme pH, the reaction is less efficient. At low pH values, some the negatively charged complexing sites of HS become protonated,

decreasing the charge on the HS. This leads to aggregation and colloidal formation, which could cause UV absorption to increase, and its penetration of the solution to decrease. This effect is more pronounced with humic acid of high molecular weight, since it starts to precipitate at pH $\leq 2$. At high pH, formation of $Hg(OH)_2$ may occur. It has low solubility in aqueous solution and it is photolytic(ally) unreactive.

The maximum reduction efficiency and highest reduction rate constants was found at pH 5 to 6 (see Figure 4.9).

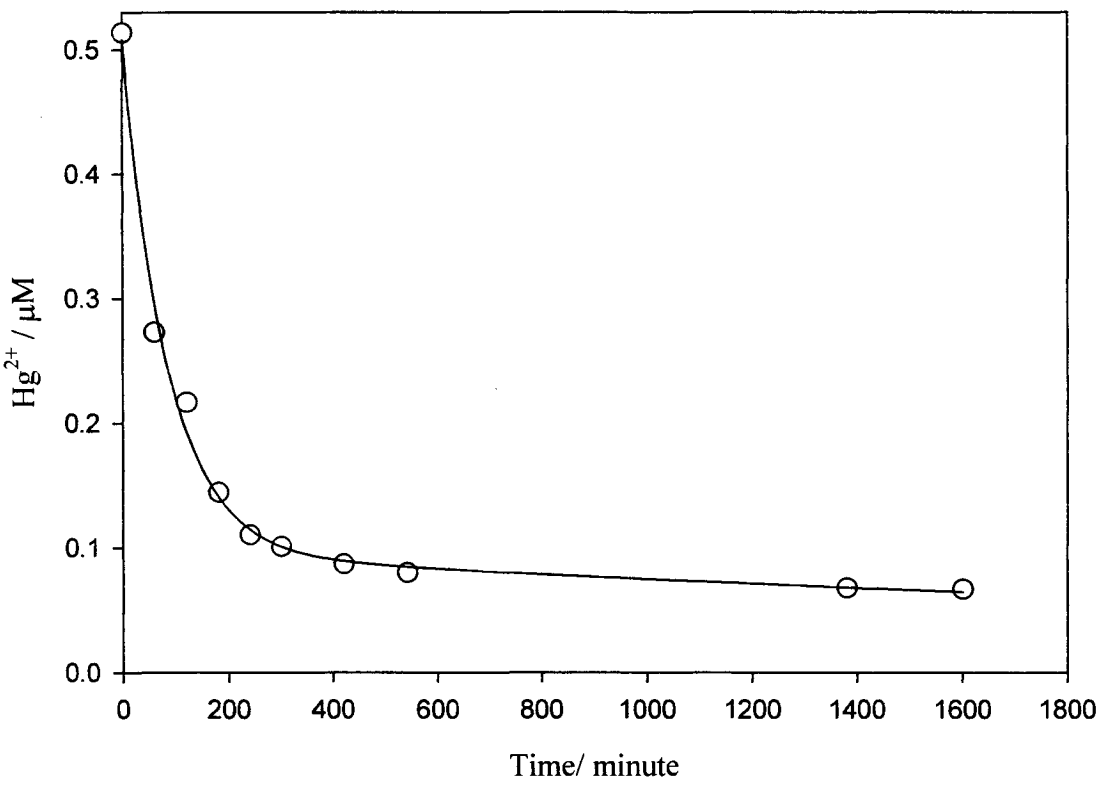


**Figure 4.7** Kinetic profile for the reduction of Hg(II) by 5 mg/ L fulvic acid at pH 5 under UV-A irradiation.

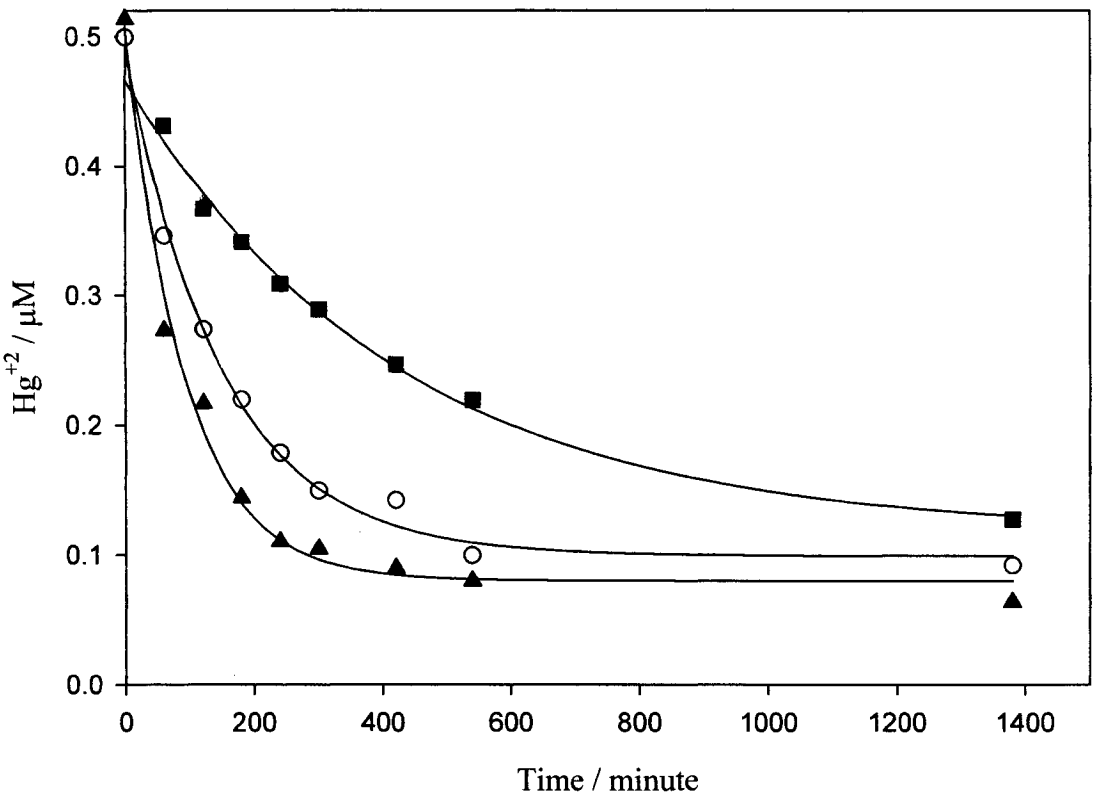


**Figure 4.8** Kinetic profile for the reduction of Hg (II) by 5 mg/ L fulvic acid at different pH values under UVA irradiation. ■ pH 3, ▲pH 5 and ○ pH 8.

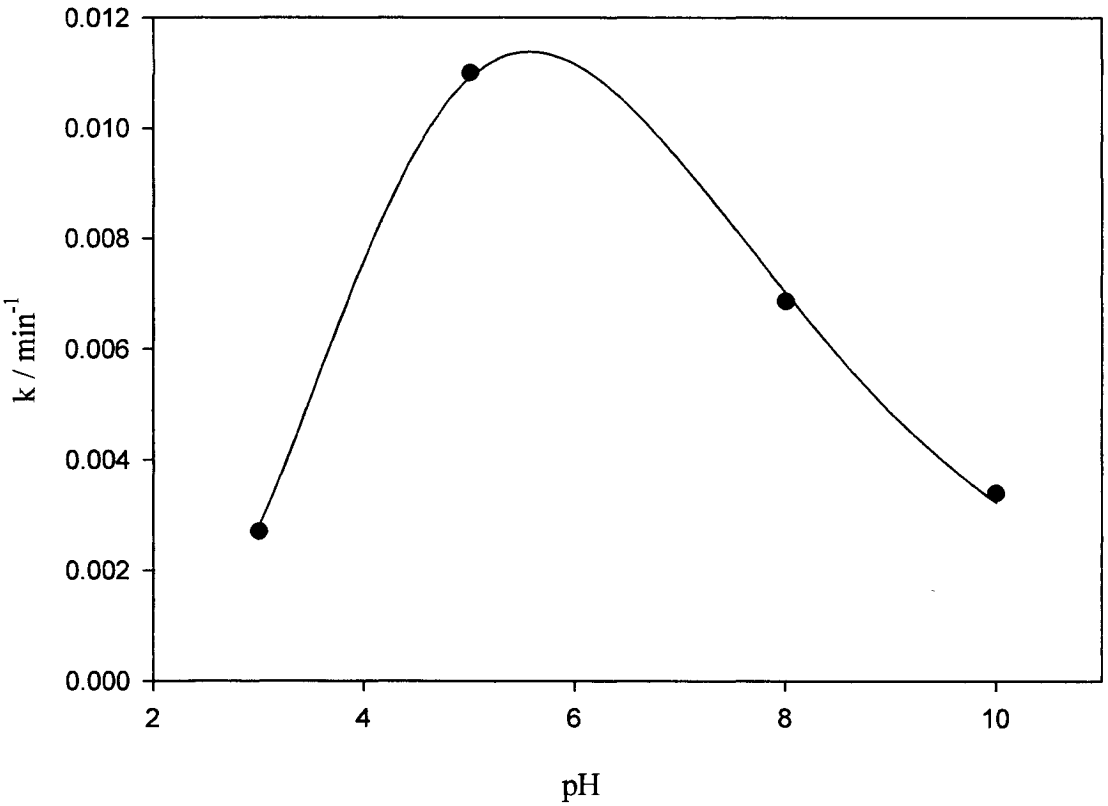


**Figure 4.9** Effect of pH on the pseudo-first-order rate constants for photoreduction of Hg(II) by 5 mg /L fulvic acid.

### 4.4.2 Effect of HS and Hg(II) concentrations

The rate and efficiency of photoreduction are affected by the fulvic acid concentration in the range1-10 mg/L. The photoreduction reaction kinetics is shown in Figure 4.10. The pseudo-first order rate constants are linearly proportional to the initial fulvic acid concentrations, Figure 4.11. The overall second-order-rate constant is calculated to be k= $2.0 \times 10^{-3}$ $min^{-1}.mg^{-1}.L$.

When the fulvic acid concentration exceeds 10 mg/L, values of $k_{obs}$ deviate slightly from linearity. For humic acid, linearity in the plot of $k_{obs}$ versus concentration was achieved only at lower concentrations below 5 mg/ L.

The dependence of the photolysis rate on the initial concentration of HS was also observed for the photodegradation of tetraphenylborate and diphenylboric acid.[66] However, the initial Hg(II) concentration may also be a factor in this process, especially at the very low levels. We examined the effectiveness of photoreduction at $1x10^{-8}$ M Hg(II) using ICP-MS (with operating conditions have been defined in Chapter 2). All forms of Hg species are atomized and detected. The result is shown in Figure 4.12. It implies that photoreduction occurs in the presence of HS even at very low Hg(II) levels.

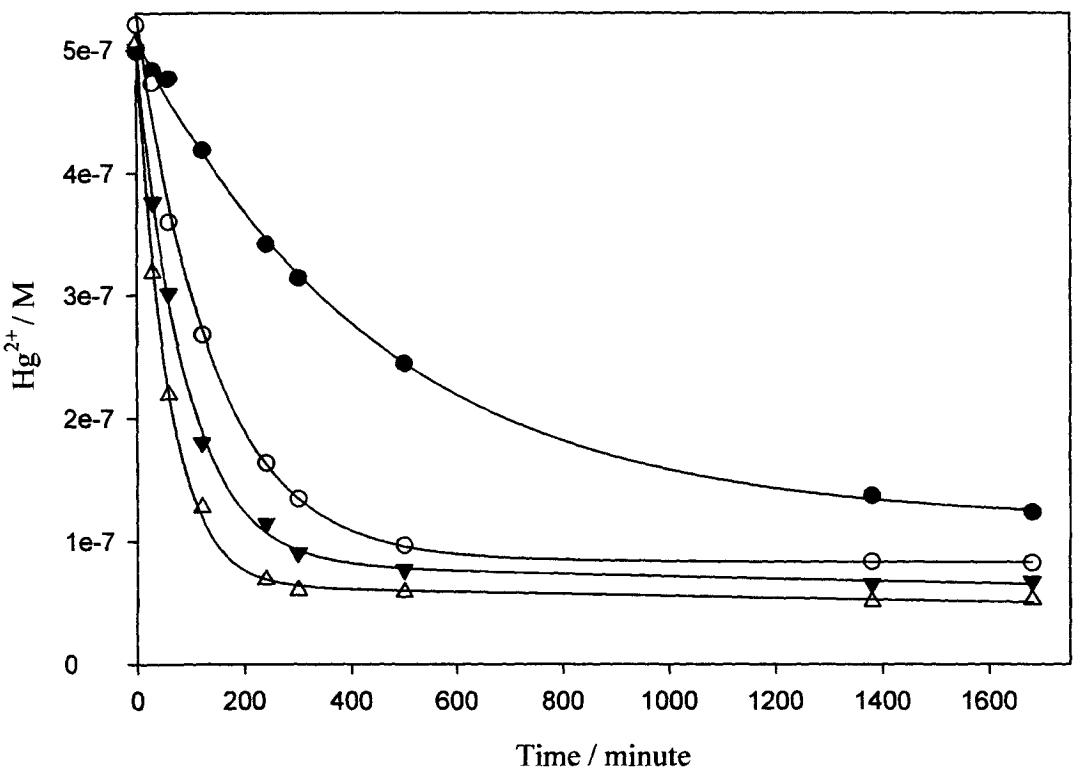


**Figure 4.10** Kinetic profiles for the UV-A photoreduction of Hg(II) by different initial fulvic acid concentrations: ● 1 ppm ○ 3 ppm ▼ 5 ppm and △ 10 ppm, all at pH 5.

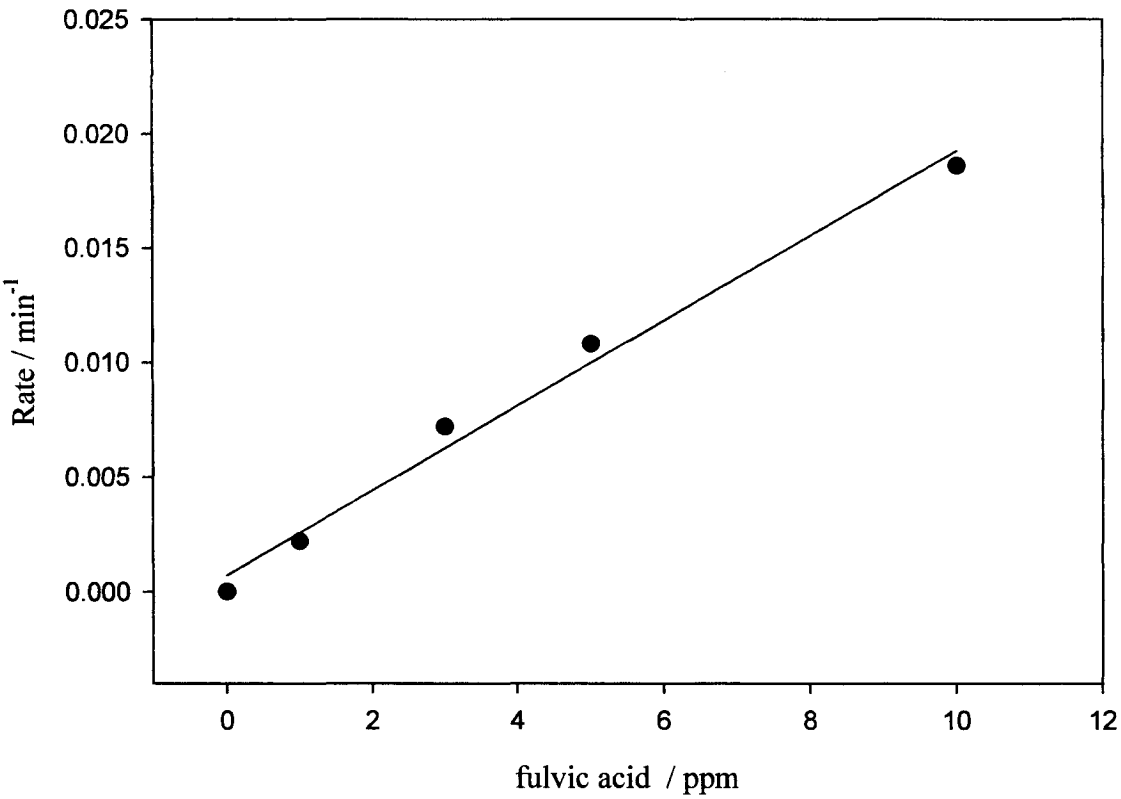


**Figure 4.11** Dependence of the pseudo-first order rate constants of the UVA photoreduction of Hg(II) on the initial concentration of fulvic acid at pH 5.

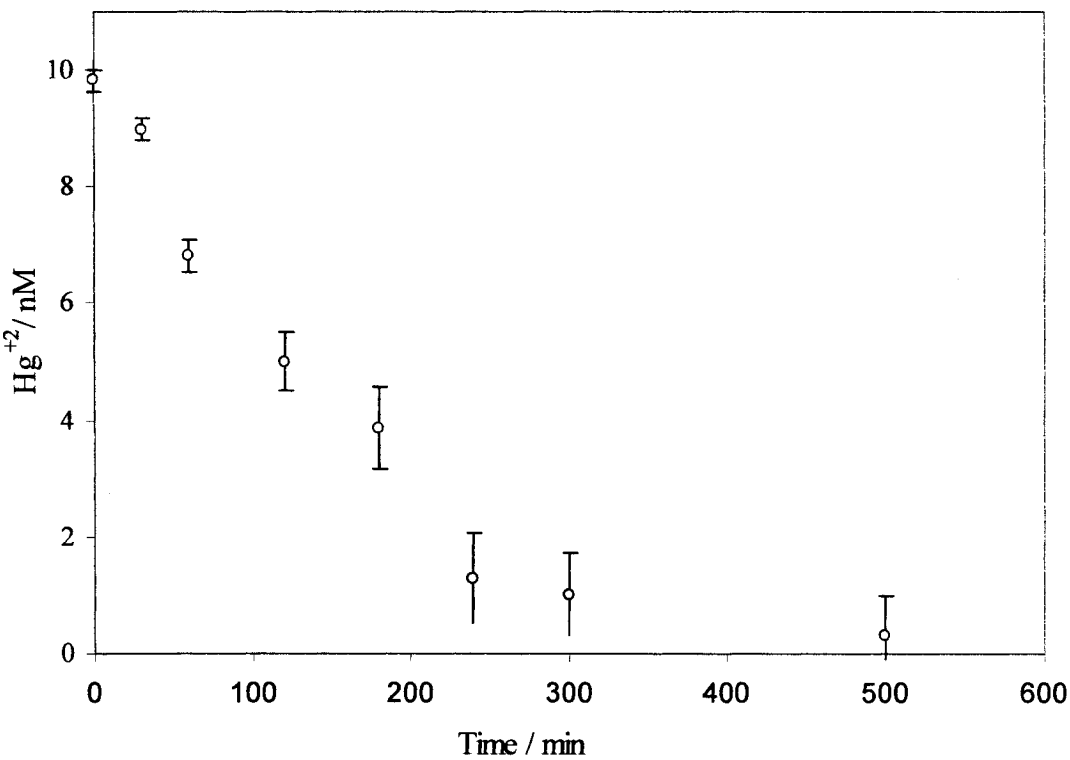


**Figure 4.12** Kinetic profiles for the UVA photoreduction of 9.8 nM Hg(II) by 5 mg/L of fulvic acid at pH 5, using ICP-MS for detection.

### 4.4.3 Effect of chloride

When chloride in the form of $KCl_{(aq)}$ was added to an aqueous solution of 0.5 μM Hg(II) and irradiated at pH 5 in the presence of 5mg/L fulvic acid, both the efficiency and the rate of reduction decreased. The pseudo-first-order rate constant for the photoreduction of 0.5 μM Hg(II) decreased from $1.08 \times 10^{-2}$ to $6.0 \times 10^{-3}$ $min^{-1}.mg^{-1}.L$ when 0.4 mM $Cl^-$ was added, and overall consumption of Hg(II) decreased from 87% to 70 %. This is represented in Figure 4.13. The effects of chloride in reducing photoreduction efficiencies and rates may be explained by the simultaneous photooxidation of Hg(0)[52] or the formation of chloro-mercury complexes.

For a set of experiments at variable initial concentrations of fulvic acid and fixed concentrations of 0.4mM, and 0.5 μM Hg(II), the second-order rate constant was decreased. The results of these experiments are shown in Figure 4.14.

The effect of chloride was more pronounced in acidic medium. Table 4.2 shows the effect at two different pH values. Since the formation of chloro-mercury complexes is not pH-dependent, the effect of chloride may be explained as the enhanced rate of oxidation of Hg(0) in the acidic medium.

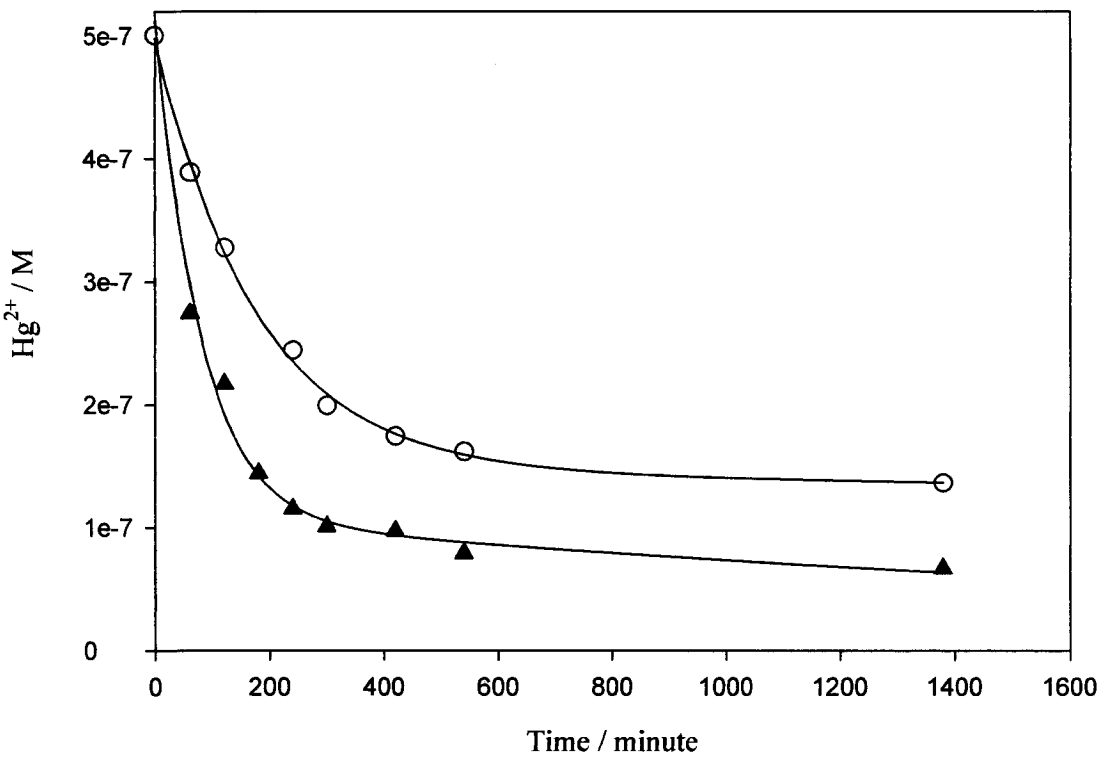


**Figure 4.13** Kinetic profiles for the UVA photoreduction of 0.5 μM Hg(II) in the presence of 5 mg/L of fulvic acid at pH 5 , with 0.4mM chloride(open circle) and without added chloride(triangle up).

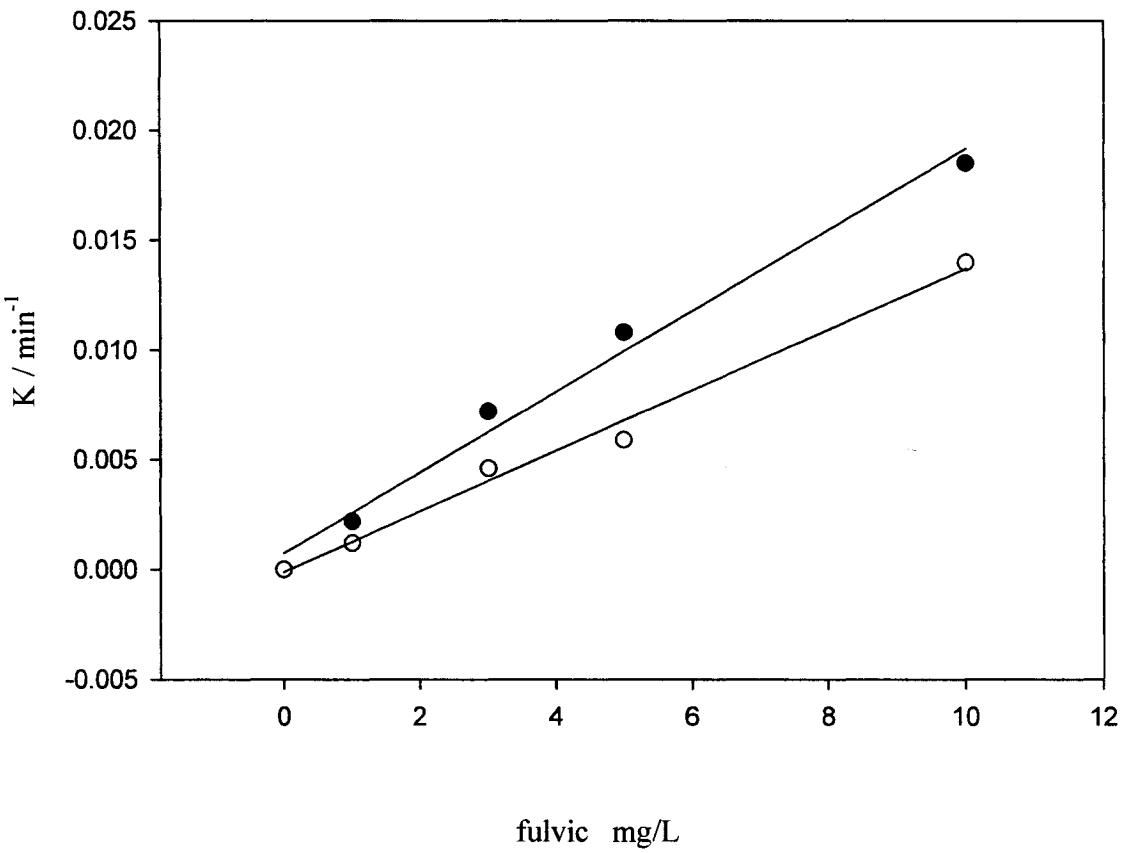


**Figure 4.14** Dependence of pseudo-first-order rate constants for UVA photoreduction of 0.5 μM Hg(II) at pH 5 on fulvic acid concentration, without added chloride (closed circles) and with 0.4 mM chloride (open circles).

**Table 4.2** Effect of 0.4 mM Cl- on the pseudo-first-order rate constants and second – order rate constants for the UVA photoreduction of 0.5 μM Hg(II) at pH 5 and 8.

| fulvic mg/L | $k_1 \times 10^3$ , $min^{-1}$ at pH 5 | | $k_1 \times 10^3$ in $min^{-1}$ at pH 8 | |
|---|---|---|---|---|
| | No chloride | 0.4mM $Cl^-$ | No chloride | 0.4mM $Cl^-$ |
| 1 | 2.2 | 1.2 | 1.2 | 1.05 |
| 3 | 7.2 | 4.6 | 3.7 | 3.04 |
| 5 | 10.8 | 5.9 | 6.7 | 5.85 |
| 10 | 18.5 | 14.0 | 10.3 | 9.56 |
| second -order rate constant $10^3$ k , $min^{-1}.mg^{-1}.L$ | 2.0 | 1.4 | 1.04 | 0.93 |

### 4.4.4 Effect of Oxygen

Patel-Sorrentino *et al.* [67] found that DOC photodegradation rate in natural water samples was greater in the presence of oxygen compared to samples in which oxygen was removed by nitrogen bubbling. We compared rates of Hg(II) photoreduction in an air-saturated solution and one bubbled with argon, both with 5 mg/L. Photoreduction efficiency was lower when the solution was air-saturated (Figure 4.15). After UVA irradiation for 1 hour, the efficiency of photoreduction 0.5 μM Hg(II) in air was 39%, while it was 48% under argon. This indicates that the oxygen may act as a quencher of the photoreduction either directly or via a reactive oxygen species produced during photolysis.

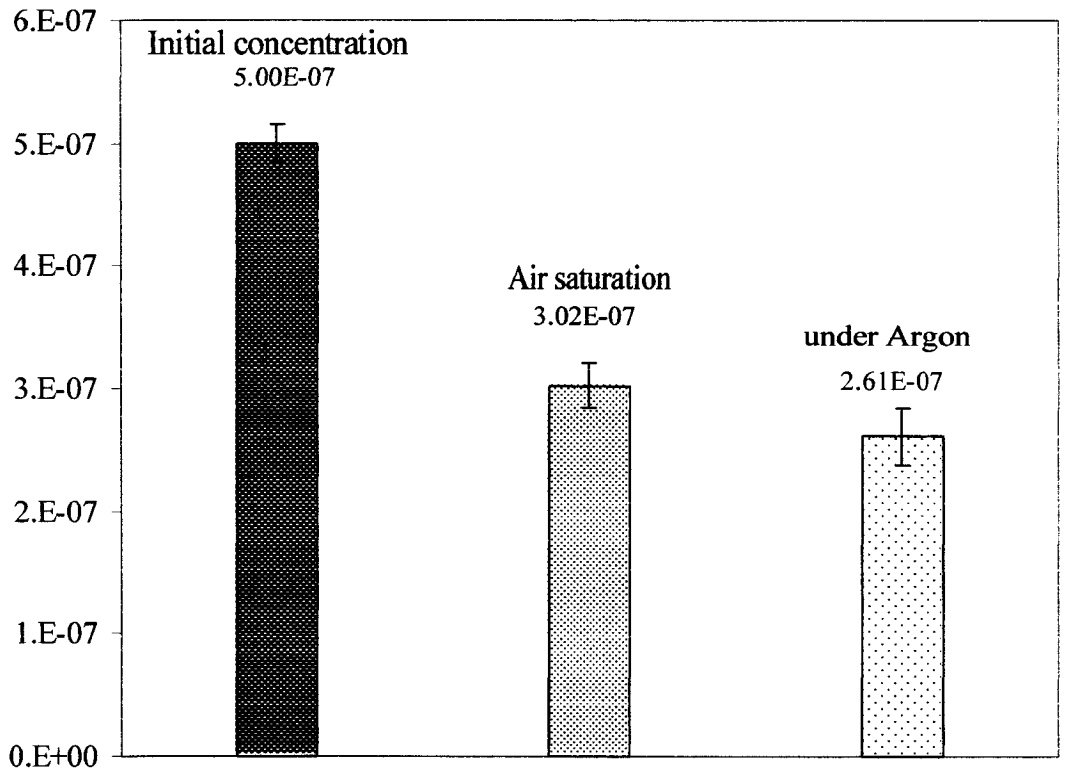


**Figure 4.15** Concentration Hg(II) after one hour of UVA irradiation of 5 μM Hg(II) and 5 mg/L fulvic acid at pH 5, under air and argon atmosphere.

### 4.5 Reaction of Hg(II) with dimercaptobenzene, an organic S-donor ligand

Thiophenolic and sulphidic groups in HS exhibit strong complexation ability towards Hg(II) ions. They play an important role in stabilization of Hg(II). Although the total sulfur content of HS is very low (<5%), and is the fraction of reduced sulfur, the low level of Hg(II) in the aquatic environment favors the complexation with these specific strong binding sites of HS. At high concentrations of Hg(II), O-donor sites of HS may also be involved.

Reaction of Hg(II) with thiolates gives complexes with the general formula $Hg(SR)_x$, in which R may be aliphatic or aromatic and x =2-4. When x =2, the oligomer formation is more likely. We examined the complex formation between Hg(II) and dimercaptobenzene using UV-Visible spectrophotometry. Hg(II) may interact strongly with both sulfur atoms to give complexes with various coordination numbers as shown below.

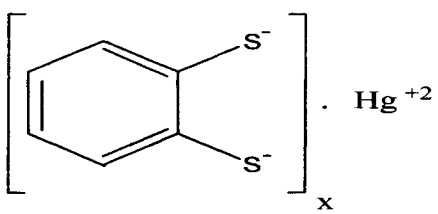


Under argon saturation and in acidic solution, dimercaptobenzene is stable. The UV-Visible spectrum of this compound is shown in Figure 4.16. Upon addition of aliquots of 0.53 mM Hg(II) to 0.03 mM dimercaptobenzene solution, the spectrum changed and a bathochromic shift was observed. The absorption at 227 nm decreased, while that at 355 nm increased. This change was maximized at metal: ligand ratio of 1:2.

This implies complex formation where x = 2, and a coordination number of 4 for Hg(II). The result of spectrophotometric titration is shown in Figure 4.17. The formation of a complex which absorbs at 355 nm makes it more susceptible to solar irradiation. We attempted to explore the effects of UVA irradiation on the complex. However, the solution becomes cloudy (milky). This may be due to the formation of polymer, or the oxidation of the dimercaptobenzene compound by trace amounts of oxygen.

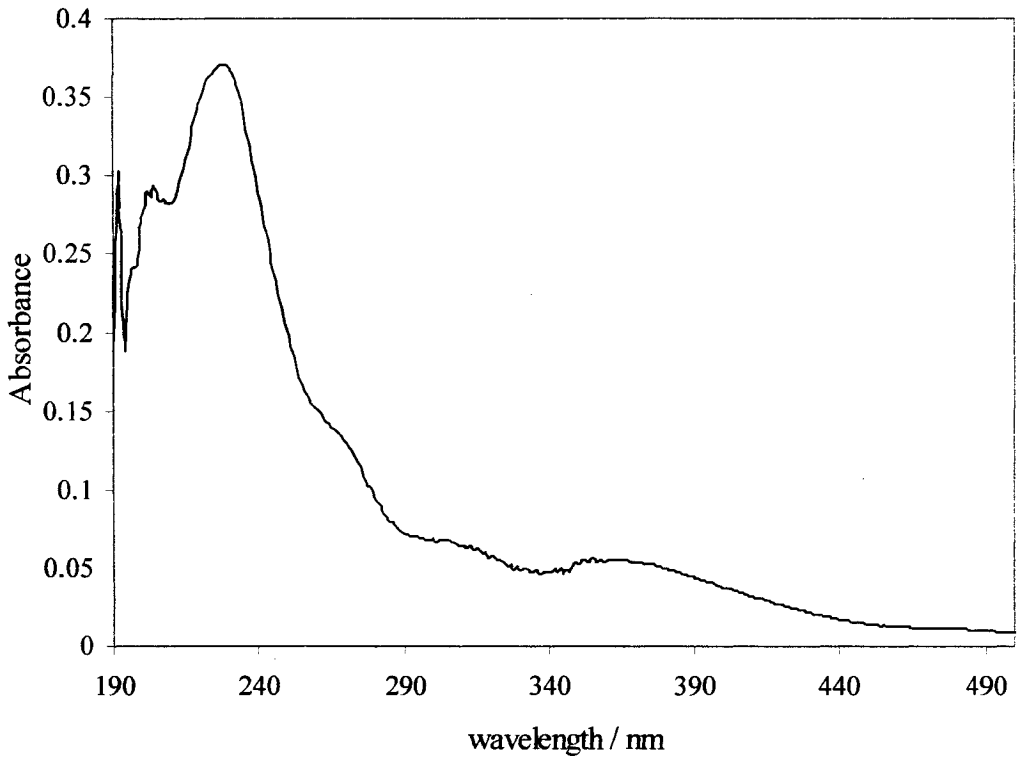


**Figure 4.16** UV-Visible spectrum of 0.031 mM dimercaptobenzene in aqueous solution at pH 5.

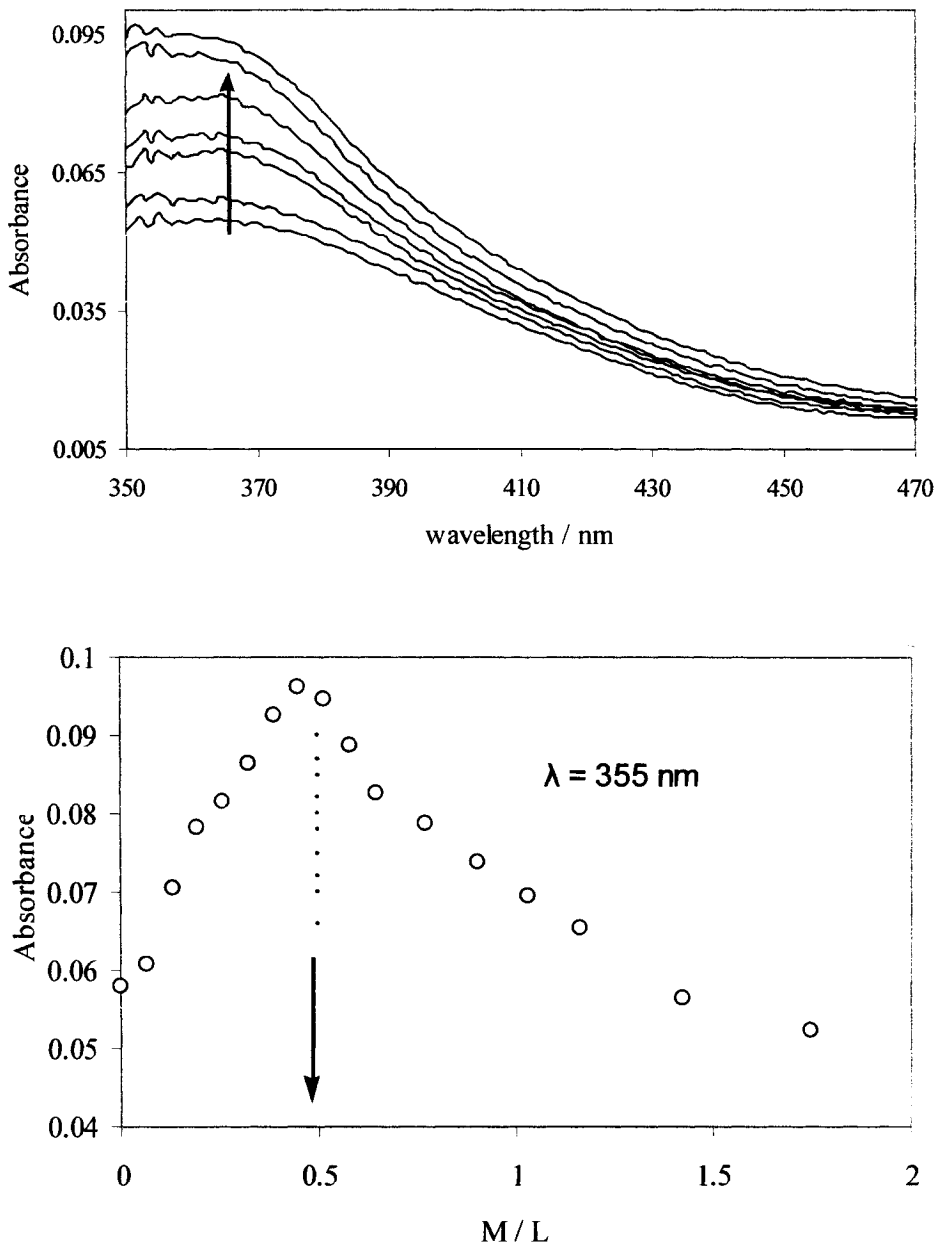


**Figure 4.17 (a)** Evolution of the UV spectrum of an aqueous solution of dimercaptobenzene upon addition of 0.53 mM Hg(II) at pH 5 and T= 25 °C. **(b)** Plot of the absorbance at 355 nm versus the molar ratio Hg(II)/dimercaptobenzene.

## 4.6 Speciation of Hg(II) in the presence of HS

Various complexes of Hg(II) can co-exist with in natural waters, the fraction of each complex being dependent on the concentrations of the competing ligands and their formation constants (K values), as well as the pH of the medium. Different Hg(II) species have different chemical properties. Speciation calculations were performed using Mathematica 4.2. This program calculates the distributional speciation of metal ion species in presence of competing ligands. Our calculations are based on the following parameters.

$K_1 = [HgHS]/ [Hg^{+2}] [HS] = 5.01 \times 10^{11}$ (4.6)[68]

$K_2 = [Hg(OH)_2]/ [Hg^{+2}] [OH]^2 = 5.13 \times 10^{21}$ (4.7)

$K_3 = [ Hg(OH)_3^-] / [ Hg(OH)_2] [ OH^-] = 0.2$ (4.8)

$K_4 = [HgCl_2]/ [ Hg^{+2}] [Cl^-]^2 = 3.23 \times 10^{12}$ (4.9)

$K_5 = [HgCl_3^-]/ [HgCl_2] [Cl^-] = 6.7$ (4.10)

$K_6 = [HgCl_4^{-2}]/ [HgCl_3^-] [Cl^-] = 13$ (4.11)

$K_7 = [HgClOH]/[Hg^{+2}][Cl^-] [OH^-] = 4.68 \times 10^3$ (4.12)

Equilibrium constants for equations 4.1-4.2 are from Martel and Smith.[69] These equations predict that in lake waters with low chloride concentrations most of Hg(II) at

neutral pH will exist as $Hg(OH)_2$. However, the dominant species in sea water is $HgCl_2$. In both cases, we assumed the absence of strong competing ligands like DOC and sulfide.

In the calculation of Hg distributional speciation, we assumed that the formation constant K for reaction of Hg with humic substances (HS) is independent of pH, even though there is evidence to show that K increases at higher pH. We used the low $K_1$ value for Hg-HS interactions, which is valid only in the case of high Hg/HS ratio. Under our experimental conditions where $[Hg^{+2}]$ is 10-100 μg/L, this approximation is valid. The speciation calculation shows that whith 10 mg/L fulvic acid and 1 μM chloride, 99% of the Hg(II) will be complexed to HS in the pH range 3-5. This fraction drops to 79% when chloride concentration increases to 0.4 mM. However, $Hg(OH)_2$ was the predominant species at pH ≥ 7 in both cases mentioned above.

It is important to note that for the high $K_1$ value for the Hg-HS complexation reaction, log K = 28.7, [70] the speciation calculation predicts that most of Hg(II) ( > 99.9%) will be complexed to HS even at high pH values. In natural waters where the Hg/HS ratio is very small, most of Hg(II) will be strongly associated with DOC.

### 4.7 Possible mechanisms of Hg(II) photoreduction

Irradiation of aqueous solutions of HS in the presence of dissolved oxygen leads to the formation of various reactive oxygen species (ROS). The enhanced efficiency of reduction of Hg(II) under an inert gas atmosphere( argon) shows that (ROS) do not play a significant role in this reaction. Absorption in the UV-VIS by organic compounds such as carboxylic and polyhdroxyl aromatics can lead to the formation of hydrated electrons.[71]

Such functional groups are important constituents of HS. Consequently, irradiation of HS could produce hydrated electrons that reduce Hg(II) under suitable conditions.

Under our experimental conditions, the dependence of the pseudo-first-order rate constants on the initial concentration of HS is consistent with the hypothesis that the hydrated electron is the reducing species. There is a linear relationship between the photoreduction rate of Hg(II) and the fulvic acid concentration up to 10 mg/L fulvic acid. Above 10 mg/L, the rates decline, implying that the hydrated electrons may be trapped by fulvic acid aggregates. However, the dependence on pH is not consistent with this hypothesi,s since the formation yield of hydrated electrons $e_{(aq)}^-$ showed little pH effect in the range of 4-8,[29] yet we observed higher reduction rates in the range pH 5 to 6. The reduction of Hg(II) should be enhanced significantly when the solution is argon-saturated, because oxygen molecule competes with Hg(II) for the hydrated electron. We observed only small increase in the reduction efficiency.

A third possible mechanism similar to that of the photodecomposition of the Fe(III) polyhydoxylate complexes, requires that Hg(II) be complexed to the HS before reduction takes place. The mechanism of such a process is shown in Scheme 4.1. In this mechanism, one electron transfer from ligand to metal produces Hg(I). This ion disproportionates to produce Hg(0). The other important point is that the decarboxylation process produces $CO_2$ and an organic radical which attacks either the Hg(I) or the uncomplexed Hg(II)in the solution. If this is the correct mechanism for the photoreduction of Hg(II) then at pH $\geq$ 7, the formation constant K for the Hg-HS complex must be high enough to compete with formation of $Hg(OH)_2$.

**Scheme 4.1** Mechanistic steps for complexation and photoreduction of Hg(II) ions.

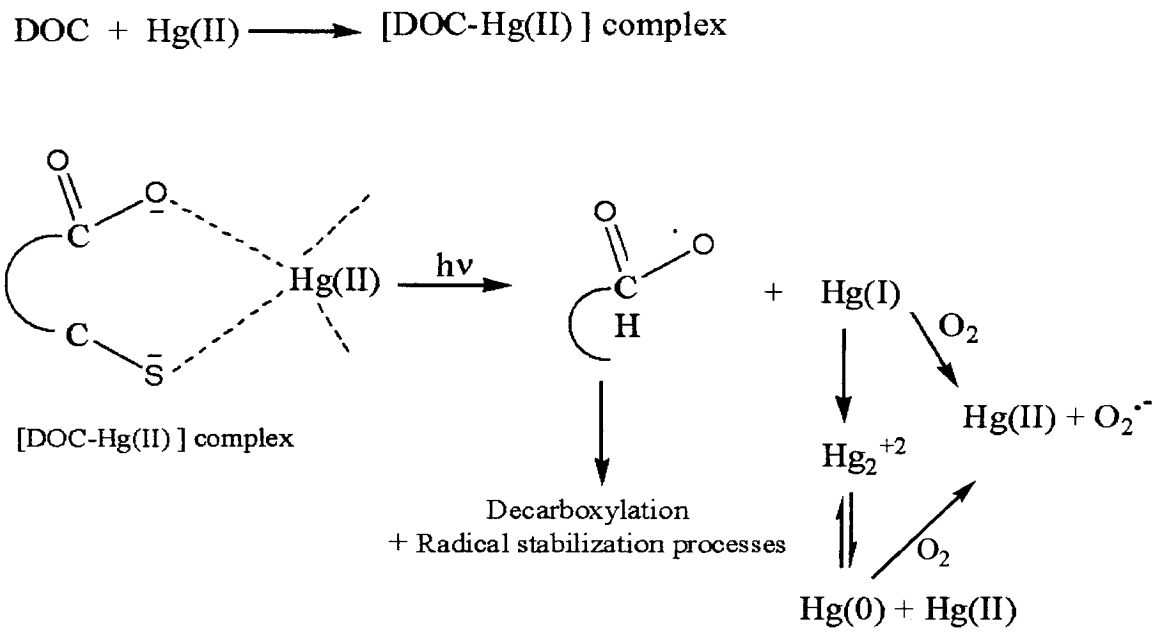


In the 3rd chapter, we showed that the $CO_2^{\bullet-}$ with its high reducing capability, ($E^\circ(CO_2/CO_2^{\bullet-})$ = -2.0 V), was able to reduce Hg(II). The UVA irradiation of HS leads to decarboxylation of the HS and release of $CO_2$. This is another route for the reduction of Hg(II).

## 4.10 Conclusions

Humic substances play an important role in the speciation of Hg(II) ions in the aquatic environment. They have the ability to reduce Hg(II) ions in the dark (thermally) with very slow reduction rates, if Hg(II) is present μMn levels. This level of Hg(II) concentration is expected only in heavily polluted water such as runoff from gold mine

tailings. However, the photoreduction of Hg(II) ions was found to be significant even at very low levels of Hg(II). The rate and efficiency of photoreduction are decreased in the presence of chloride. The optimum pH values for photoreduction were found to be in the range of 5 to 6, which is relevant to most aquatic environments. In this pH range, most of the Hg(II) will bind to DOC, and this may explain the enhanced photoreduction.

The complexity of HS and its ill-defined chemical structure make it difficult to assign a specific mechanism for the photoreduction, but our evidence supports the hypothesis that the Hg (II) ions must be complexed to HS before reduction.

**References**


(1) Aiken, G. R.; McKnight, D. M.; Wershaw, R. L.; MacCarthy, P. In Humic Substances in Soil, Sediment, and Water; Aiken, G.R., McKnight, D. M., Wershaw, R. L., MacCarthy. P., Eds.; Wiley: New York, 1985; pp. 1-9.

(2) Piccolo, A. *Soil Sci.* **2001**, *166*, 810- 832.

(3) Cabaniss, S. E.; Zhou, Q.; Maurice, P. A.; Chin, Y-P.; Aiken, G. R. *Environ. Sci. Technol.* **2000**, *34*, 1103-1109.

(4) Rostad, C. E.; Leenheer, J. A. *Anal. Chim. Acta* **2004**, *523*, 269-278.

(5) Reid, P. M.; Wilkinson, A. E.; Tipping, E.; Jones, M. N. *Geochim. Cosmochim. Acta* **1990**, *54*, 131-138.

(6) Aiken, G. R.; Malcolm, R. L. *Geochim. Cosmochim. Acta* **1987**, *51*, 2177-2184.

(7) Yamada, E.; Doi, K.; Okano, K.; Fuse, Y. *Anal. Sci.* **2000**, *16*, 125-129.

(8) Artinger, R.; Buckau, G.; Geyer, S.; Fritz, F.; Wolf, W.; Kim, J. I. *Appl.Geochem.* **1999**, *15*, 97-116.

(9) Robertson, A. I.; Bunn, S. E.; Boon, P. I.; Walker, K. F. *Mar. Freshwater Res.* **1999**, *50*, 813-829.

(10) Rocha, J. C.; de Sene, J. J.; dos Santos, A.; Toscano, I. A. S.; Zara, L. F. *J. Environ. Monit.* **2000**, *2*, 39-44.

(11) Xue, H. B.; Sigg, L. *Aquat. Geochem.* **1999**, *5*, 313-335.

(12) Otto, W. H.; Carper, W. R.; Larive, C. K. *Environ. Sci. Technol.* **2001**, *35*, 1463-1468.

(13) Day, K. E. *Environ. Sci. Technol.* **1991**, *10*, 91-101.

(14) Steinberg, C. E. W.; Sturm, A.; Kelbel, J.; Lee, S. K.; Hertkorn, N.; Freitag, D.; Kettrup, A. *Acta. Hydrochim. Hydrobiol.* **1992**, *20*, 326-332.

(15) Lovley, D. R.; Coates, J. D.; Blunt-Harris, E. L.; Phillips, E. J. P.; Woodward, J. C. *Nature* **1996**, *382*, 445-448.

(16) Sunda, W. G.; Huntsman, S. A. *Mar. Chem.* **1994**, *46*, 133-152.

(17) Lu, X.; Johnson, W. D.; Hook, J. *Environ. Sci. Technol.* **1998**, *32*, 2257-2263.

(18) Albert, J. J.; Schindler, J. E.; Miller, R. W. *Science* **1974**, *184*, 895-897.

(19) Allard, B.; Arsenie, I. *Water Air Soil Pollut.* **1991**, *56*, 457-464.

(20) Cooper, W. J. In Aquatic humic substances: influence on fate and treatment of pollutants, Advances in Chemistry Series No. 219. Suffit, I. H.; MacCarthy, P., Eds.; American Chemical Society: Washington D.C., 1989; pp. 133-140.

(21) Hoigne, J.; Faust, B. C.; Haag, W. R.; Scully, F. E. Jr.; Zepp, R. G. In Aquatic humic substances: influence on fate and treatment of pollutants, Advances in Chemistry Series No. 219. Suffit, I. H., MacCarthy, P., Eds.; American Chemical Society: Washington D.C., 1989; pp. 329-332.

(22) Faust, B. C.; Hoigné, J. *Environ. Sci. Technol.***1987**, *21*, 957-964.

(23) Scully, N. M. ; McQueen, D. J.; Lean, D. R. S.; Cooper, W. J. *Limnol. Oceanogr.* **1996**, *41*, 540-548.

(24) Lean, D. R. S.; Cooper, W. J. In Aquatic and surface photochemistry. Helz, G. R., Zepp, R. G., Eds.; Lewis Pub, 1994; pp. 207-214.

(25) Petasne, R. G.; Zika, R. G. *Nature* **1987**, *325*, 516-518.

(26) Zepp, R. G.; Wolf, N. L.; Baughman, G. L.; Hollis, R. C. *Nature* **1977**, *207*, 421-423.

(27) Haag, W. R.; Hoigné, J. *Environ. Sci. Technol.***1986**, *20*, 341-348.

(28) Mill, T.; Hendry, D. G.; Richardson, H. *Science* **1980**, 207, 886-888.

(29) Zepp, R. G.; Braun, A. M.; Hoigné, J.; Leenheer, J. A. *Environ. Sci. Technol.* **1987**, 21, 485-490.

(30) Miller, W. L. In Aquatic and surface photochemistry. Helz, G. R., Zepp, R.G., Eds.; Lewis Pub, 1994; pp. 111-128.

(31) Allard, B.; Borén, H.; Pettersson, C.; Zhang, G. *Environ. Intern.* **1994**, *20*, 79-101.

(32) Jones, R. D. *Deep Sea Res.* **1991**, *38*, 625-632

(33) Backlund, P. *Chemosphere* **1992**, *25*, 1869-1878.

(34) Tarr, M. A.; Wang, W.; Bianchi, T. S.; Engelhaupt, E. *Water Res.* **2001**, *35*, 3688-3696.

(35) Dahlén, J.; Bertilsson, S.; Petterson, C. *Environ. Intern.* **1996**, *22*, 501-506.

(36) Bertilsson, S.; Tranvik, L. J. *Limnol.Oceanogr.* **2000**, *45*, 753-762.

(37) Driscoll, C. T.; Blette, V.; Yan, C.; Schofield, C. L.; Munson, R.; Holsapple, J. *Water Air Soil Pollut.* **1995**, *80*, 499-508.

(38) Lindberg, S. E.; Harriss, R. C. *Environ. Sci. Technol.* **1975**, *8*, 459-462.

(39) Meili, M.; Iverfeldt, A.; Hakanson, L. *Water Air Soil Pollut.* **1991**, *56*, 439-453.

(40) Kolka, R. K., Grigal, D. F.; Verry, E. S.; Nater, E. A. *J. Environ. Qual.* **1999**, *28*, 766-775

(41) Watras, C. J.; Morrison, K. A.; Bloom, N. S. *Water Air Soil Pollut.* **1995**, *84*, 253-267

(42) Sellers, P.; Kelly, C. A.; Rudd, J. W. M; Machutchon, A. R. *Nature*, **1996**, *380*, 694-697.

(43) Leiva-Presa, À.; Capdevila, M.; Cols, N.; Atrian, S.; González-Duarte, P *Eur. J. Biochem.* **2004**, *271*, 1323-1328.

(44) Chen, J.; Pehkonen, S.O.; Lin, C. –J. *Water Res.* **2003**, *37*, 2496-2504

(45) Xiao, Z. F.; Stromberg, D.; Lindqvist, O. *Water Air Soil Pollut.* **1995**, *80*, 789-798.

(46) Amyot, M.; Mierle, G.; Lean, D. R. S.; McQueen, D. J. *Geochim. Cosmochim. Acta* **1997**, *61*, 975-988.

(47) Lin, C. –J.; Pehkonen, S. O. *J. Geophys. Res.* **1998**, *103*, 28093-28102.

(48) Clever, H. L.; Johnson, S. A.; Derrick, M. E. *J. Phys. Chem. Ref. Data* **1985**, *14*, 632-680.

(49) O'Driscoll, N. J.; Beauchamp, S.; Siciliano, S. D.; Rencz, A. N.; Lean, D. R. S. *Environ. Sci. Technol.* **2003**, *37*, 2226-2235.

(50) Lindberg, S. E.; Vette, A. F.; Miles, C.; Schaedlich, F. *Biogeochem.* **2000**, *48*, 237-259.

(51) Amyot, M.; Lean, D.; Mierle, G. *Environ. Toxicol. Chem.* **1997**, *16*, 2054-2063.

(52) Lalonde, J.; Amyot, M.; Kraepiel, A.; Morel, F. *Environ. Sci. Technol.* **2001**, *35*, 1367-1372.

(53) Watras, C. J.; Morrison, K. A.; Host, J. S. *Limnol.Oceanogr.***1995**, *40*, 556-565.

(54) O'Driscoll, N. J.; Lean, D. R. S.; Loseto, L. L.; Carignan, R.; Siciliano, S. D. *Environ. Sci. Technol.* **2004**, *38*, 2664 -2672.

(55) Langhals, H.; Abbt-Braun, G.; Frimmel, F. H. *Acta hydrochim. Hydrobiol.* **2000**, *28*, 329-332.

(56) Amon, R. M. W.; Benner, R. *Geochim. Cosmochim. Acta* **1996**, *60*, 1783-1792.

(57) Morris, D. P.; Hargreaves, B. R. *Limnol. Oceanogr.* **1997**, *42*, 239-249.

(58) Bertilsson, S.; Tranvik, L. J. *Limnol. Oceanogr.* **2000**, *45*, 753-762.

(59) Vähätalo, A.V.; Salkinoja-Salonen, M.; Taala, P.; Salonen, K. *Limnol. Oceanogr.* **2000**, *45*, 664-676.

(60) Dahelen, J.; Bertilsson, S.; Pettersson, C. *Environ. Intern.* **1996**, *22*, 501-506.

(61) Szllagyl, M. *Soil Sci.* **1973**, *115*, 434-441.

(62) Wilson, S. A.; Weber, J. H. *Chem. Geol.* **1979**, *26*, 345-351.

(63) Skogerboe, R. K.; Wilson, S. A. *Anal. Chem.* **1981**, *53*, 228-232.

(64) Xu, H.; Allard, B. *Water Air Soil Pollut.* **1991**, *56*, 709-717.

(65) Horváth, O.; Vogler, A. *Inorg. Chem.* **1993**, *32*, 5485-5489.

(66) Mills, G. L.; Schwind, D. *Environ. Toxicol. Chem.* **1990**, *9*, 569-574.

(67) Patel-Sorrentino, N.; Mounier, S.; Lucas, Y.; Benaim, J. Y. *Sci. Total Environ.* **2004**, *321*, 231-239.

(68) Haitzer, M.; Aiken, G. R.; Ryan, J. N. *Environ. Sci. Technol.* **2002**, *36*, 3564-3570.

(69) Martell, A. E.; Smith. R. M. In Critical stability constants. Plenum press: New York, 1974, v 5, P 394.

(70) Haitzer, M.; Aiken, G. R.; Ryan, J. N. *Environ. Sci. Technol.* **2003**, *37*, 2436-2441.

(71) Köhler, G.; Solar, S.; Getoff, N.; Holzwarth, A. R.; Schaffner, K. *J. Photochem.* **1985**, *28*, 383-391.

# Chapter 5

## Kinetic studies of the speciation of Hg(II) and $MeHg^+$ complexes with natural ligands in aquatic systems

### 5.1 Introduction

In natural waters, the chemical speciation of mercury is influenced by environmental factors such as pH, temperature, and the concentrations of organic and inorganic complexing ligands. In addition, the conditional stability constants for Hg(II) complexation play a significant role. DOC, sulfide ($S^{2-}$), hydroxide ($OH^-$) and chloride ($Cl^-$) are the most relevant competing ligands for complexation of $Hg^{2+}$ and $MeHg^+$ in aquatic environments.

As a soft Lewis acid, $Hg^{2+}$ tends to form strong complexes with sulfur donor ligands. For instance, in anoxic water, soluble mercury sulfide complexes such as $Hg(SH)_2$, $HgS_2^{2-}$, and Hg(SH)(OH) predominate.[1-3] The formation of insoluble HgS tends to occur at relatively high pH. The fraction of each complex depends on the sulfide concentration and the pH of the water. Organic compounds that contain reduced sulfur are unstable in oxic water since reduced sulfur atoms are oxidized when dissolved oxygen levels increase. However, their complexation with metal ions such as Cu(II) and Zn(II) leads to stabilization.[4-6]This stabilization effect may also be relevant to Hg(II) complexation.

In seawater, due to the complexation of DOC by abundant calcium ($Ca^{2+}$) and magnesium ($Mg^{2+}$) ions,[7] the high concentration of chloride ions (salinity 35%) along

with the low concentrations of DOC(ca 0.2 mg C/L),[8] the formation of various chloro-mercury complexes such as $HgCl_2$, $HgCl_3^-$, and $HgCl_4^{2-}$ is enhanced. In contrast, in freshwater systems, the speciation of Hg(II) is largely dominated by DOC,[9] at levels of 2-20 mg C/L. Many studies illustrate that a high percentage of Hg(II) present in natural water is complexed to organic ligands.[10-14]

Methylmercury ($CH_3Hg^+$) is one of the most toxic forms of mercury in the aquatic environment. It has been reported to be 20-30 % of the total Hg in freshwater systems.[15] However, recent data from our laboratory showed that it can range from 1-80% of total Hg. This form is bioaccumulated in the food web, and represents more than 90% of total Hg in fish.[16] The sources of $MeHg^+$ in surface water may include atmospheric deposition,[17] inputs from watershed,[18] leaching from wetland areas[19] and in situ production, including biotic[20,21] and abiotic[22-24] methylation of $Hg^{2+}$. Both processes are affected by temperature, pH, DOC concentration and alkalinity.[25] It is also reported that $MeHg^+$ is photo-[26] and biodegradable.[27] The speciation of $CH_3Hg^+$ is largely affected by DOC concentration.[24,28]

The presence of chemical functionality in DOC gives it the ability to bind various metal ions in natural waters.[29] Carboxylate and phenolate groups contribute to ~90% of the acidity of DOC, while thiols and other acidic functional groups are present in low concentrations. DOC is considered to be a polydentate ligand and can bind to metal ions through a variety of different binding sites. Reduced sulfur groups of DOC play a major role in binding of Hg(II),[30-32] $MeHg^+$ [33] and Cd(II).[34]

Complexation of DOC in freshwater plays a key role in the speciation of Hg(II), and this, in turn, affects the bioavailability and mobility of Hg species. On one hand, Hg-

DOC complexation leads to leaching of Hg from soil and sediments into lakes,[35,36] increasing the concentration of Hg(II) in water bodies. On the other hand, this complexation may reduce the bioavailability of Hg(II) to aquatic organisms.[37-39]

In order to describe the binding behavior of HS towards metal ions, a variety of models have been proposed.[40-42] Some assume that HS contains different classes of binding sites. Carboxylic and phenolic groups provide distribution affinity constants toward the same metal ion. Furthermore, at low concentrations of some metal ions, complexing sites with sulfur (S) and /or nitrogen (N) atoms plays a significant role in metal ion binding.[34,43] Other models propose that the interaction of metal ions with HS could lead to variation of the charge on the HS. As a result, the electric field around the HS particles changes, and this influences further ion binding. In one of the models, HS is described as a gel with the electrostatic potential distributed throughout the gel volume.[40] Another model[42] describes HS as a rigid sphere with multidentate binding sites positioned on its surface. HS is also described as a monodentate ligand which interacts with various metal ions in a 1:1 stoichiometric ratio.[40,41]

Hg-HS complexes and other metal complexes (M-HS) are generally considered to be macromolecular complexes which can be partially characterized by thermodynamic stability functions. Literature values for conditional stability constants, K, for Hg-HS complexes vary widely (Table 5.1). This variation is due to several factors: 1) different types and compositions of HS; 2) different methods used; 3) variable ratios of Hg/HS; and 4) the way in which the concentration of HS is expressed. If we assume that the complexation reaction has a 1:1 stoichiometry (equation 5.1), then the conditional stability constant is calculated from equation 5.2.

$$Hg + HS \overset{K}{\rightleftarrows} Hg\text{-}HS \qquad (5.1)$$

$$K = \frac{[Hg\text{-}HS]}{[Hg]\,[HS]} \qquad (5.2)$$

In these equations, charges have been omitted for simplicity. [Hg-HS] is the concentration of Hg complexed HS, and [HS] is the concentration of free HS. Different methods are used to express the concentration of HS (**a-d,** table 5.1). The same treatment is also applied to the complexation of $CH_3Hg^+$ by HS (Table 5.2).

**Table 5.1** Reported values for the conditional stability constant of the Hg-HS complex.

| Method used | HS-Source or type | pH | Ionic strength and other experimental conditions | log K* |
|---|---|---|---|---|
| EDLE [43] | Diverse aquatic | ~7 | 0.1 M $NaClO_4$<br>$[Hg^{+2}]$= 0.1µg / mg DOM | 28.7[a]<br>22.5-23.5[c] |
| EDLE [11] | Aquatic Florida Everglades | 7 | 0.1 M $NaClO_4$<br>low Hg/HS ratio<br>( ≤ 1µg Hg/ mg HS) | 28.5[a]<br>23.2[c] |
| | | 4.9-5.6 | 0.1 M $NaClO_4$<br>high Hg/ HS ratio<br>( ~ 10µg Hg/ mg of HS) | 10[b]<br>10.7[c] |
| CLE-SPE [44] | Waste water treatment plants | 6.6-7.4 | $[Hg^{+2}]$= 0.22-0.26 µg/ L<br>DOC= 10-14 mg/ L | > 30[a] |
| Potentiometric [45] | Soil fulvic acid | 3 | 0.1 M $NaNO_3$<br>$[Hg^{+2}]$: [DOC] = 1:1<br>$[Hg^{+2}] < 1.5 \times 10^{-5}$ M | 4.86[d] |
| | | 4 | | 5.08[d] |
| Competitive ligand and $D_{ow}$ [13] | Aquatic Florida Everglades, both low and high sulfidic contents sites | 6 | I= 0.06<br>0.04 M Phosphate buffer<br>$Cl^-$=0.01 M<br>$[Hg^{+2}]$= 6 nM<br>$[DOC]=10^{-5} - 10^{-9}$ M | 10.6-11.8[e]<br>22.4-23.8[a] |
| Reducible Hg fractions using different reducing agents ($BH_4^-$, Sn(II), $Cu^0$)[14] | Aquatic (rivers, lakes, bogs) | 7.5 | Phosphate buffer<br>0.025 M as Phosphorus<br>$[Hg^{+2}]$ up to 20 nM | 21-23.9[a] |
| Adsorption and desorption, using $KBr_{(aq)}$ as the strong competing ligand.[10] | Peat Soil | 2.98-3.4 | I=0.5 M,<br>Electrolytes:<br>KBr, $Al(NO_3)_3$, $KNO_3$<br>$[Hg^{+2}]$= 2-4 µmole/ kg(C). | 22.4-23.5[e]<br>31.6-32.2[a] |
| GFC [7] | Diverse;<br>Rivers, Lakes, peat | 8.0 | I=0.02<br>$[Hg^{+2}]$ not given. | 18.3-21.1[e] |

**Table 5.2** Reported values for the conditional stability constant of the MeHg-HS complex

| Method used | HS-Source or type | pH ± 0.2 | Ionic strength and other experimental conditions | log K* |
|---|---|---|---|---|
| CLE with various halides: $Cl^-$,$Br^-$ and $I^-$ [46] | Organic Soil | 3.5-3.6 | I= 0.01- 1 M KCl, KBr or KI.<br>SOC= 303-330 g/kg.<br>[MeHg] = 9.15-9.76 ng/ g soil. | 16.1-16.7[a] |
| Equilibrium Dialysis [47] | Aquatic (lakes) | 7 | I=0.1 M $KClO_4$.<br>[MeHg]= 0.5-100 ng/ L.<br>[HS]= 1 mg/L<br>(data fitted to 2-binding sites) | 12.15-13.07[c]<br>13.02-14.56[c] |
| CLE with different halides<br>$Br^-$ and $I^-$ [33] | Organic peat soil | 3<br>3.4-3.8<br>4.3<br>7 | I=0.01 M in KBr or KCl<br>[MeHg] ~ $10^{-12}$ M<br>MeHg / $Org.S_{reduced}$ ~ $10^{-7}$ | 16.3[a]<br>16.5[a]<br>16.7[a]<br>14.5[c] |
| Equilibrium Dialysis [48] | Diverse; River, Peat, and Soil | 5.2-9.2 | I= 1 mM<br>[MeHg] range ~ 0.1-1.2 nM<br>[HS]= 1 mg/L<br>Data fitted to 3-binding sites | 10.39-10.54<br>12.39-14.77<br>14.47-14.96 |

The following definitions apply to Tables 5.1 and 5.2

EDLE: Equilibrium dialysis ligand exchange, CLE-SPE: Competitive ligand exchange followed by solid phase extraction, GFC: Gel filtration chromatography, $D_{ow}$: Octanol-water partition-coefficients, SOC: soil organic carbon.

**a**: Molar concentration of fully deprotonated thiol sites; **b**: Molar concentration of carboxylates; **c**: Mass concentration of humic substances, i.e. K has $L.Kg^{-1}$ units; **d**: Mass concentration of humic substances as carbon; **e**: Molar concentration of humic substances using the number average molecular weight.

The chemical equilibria involved in the complexation of Hg by HS have been studied in great detail. Table 5.1 shows that when the Hg/HS ratio is low, the conditional stability constant is high, with a range for log K between 25 and 31.

In aquatic environments, metal complexes with humic substances (M-HS) are constituents of a complex and dynamic colloid system.[49] Both the thermodynamic and kinetic stability of M-HS complexes influence the accumulation and bioavailability of metal species. In a dynamic system like fresh water, kinetic speciation provides valuable details about the kinetic distribution of different M-HS species, and hence bioavailability.

In this work, we studied the kinetics of dissociation of Hg-HS and MeHg-HS complexes by means of a competitive ligand exchange method (CLEM), using Duolite GT-73 as the solid competing ligand. During the CLEM experiments, ICP-MS was used to follow changes in the Hg(II) concentration. Different isotopes of Hg were used to cover a wide range of its concentrations.

## 5.2 Theory

To characterize the kinetic speciation of mercury and methyl mercury bound to humic substances, we used a competitive ligand exchange method. This method depends on stripping the metal ions from the natural ligand complex system by forming a new complex with the competing ligand. The method was proposed by Olson and Shuman.[50] They presented a comprehensive approach to resolve the dissociation kinetics of heterogeneous metal-HS complexes. As a result, the concentrations of kinetically

different species with respect to dissociation rate constants can be determined. Various modifications and applications for this model have been published.[51-54]

The complexation of metal ions with HS is reported to occur on a time scale of minutes.[55,56] Nevertheless, our samples were equilibrated for 4-6 hours. The complexation reaction of Hg with HS is shown in equation 5.3, in which $k_a$ and $k_d$ are the association and dissociation rate constants, respectively. The charges have been omitted for simplicity.

$$\text{Hg-HS} \underset{k_a}{\overset{k_d}{\rightleftarrows}} \text{Hg} + \text{HS} \qquad (5.3)$$

Because different binding sites are available in HS, the complexed Hg can be represented by $\text{Hg-HS}_1$, $\text{Hg-HS}_2$... and $\text{Hg-HS}_i$ for *i* binding sites. For each complex, a different kinetic behavior is expected.

By swamping the sample solution that contains Hg(II) and HS (previously equilibrated) with an excess of a suitable resin, Duolite GT-73 in our study, the Hg(II) released by dissociation will be trapped by the resin according to the following equations:

$$\text{Hg}^{+2}_{(aq)} + \text{Resin} \rightarrow \text{Hg-Resin} \qquad (5.4)$$

$$\text{Hg-HS}_1 + \text{Resin} \underset{k_{-1}}{\overset{k_1}{\rightleftarrows}} \text{Hg-Resin} + \text{HS}_1 \qquad (5.5)$$

$$\text{Hg-HS}_2 + \text{Resin} \underset{k_{-2}}{\overset{k_2}{\rightleftarrows}} \text{Hg-Resin} + \text{HS}_2 \qquad (5.6)$$

$$\text{Hg-HS}_i + \text{Resin} \underset{k_{-i}}{\overset{k_i}{\rightleftarrows}} \text{Hg-Resin} + \text{HS}_i \qquad (5.7)$$

The rate of reaction of free $Hg^{2+}$, equation 5.4, is expected to be very fast since the resin (Duolite GT-73) is known to form a very strong complex with Hg(II) through thiol binding sites.[57] For other reactions represented in equations 5.5 to 5.7, in which the Hg(II) is complexed to HS, the rate will depend on the binding strength of each site toward Hg(II). Even though the reactions are shown as equilibria, the excess of resin added shifts the reactions to the right, so the overall reaction is irreversible, equation 5.8.

$$\text{Hg-HS}_i + \text{Resin (Excess)} \overset{k_i}{\rightarrow} \text{Hg-Resin} + \text{HS}_i \qquad (5.8)$$

When the [Resin] >> [Hg] and [Resin] >> [Hg-HS], and under the condition where Hg-Resin interaction is very strong, and dissociation of Hg from the resin is negligible, then the representative reaction 5.7 will be the rate determining step since it will be the slowest reaction. If the kinetics of the dissociation reactions of the Hg-HS complexes are considered as first-order or pseudo-first-order, then the amount $C_i(t)$ of the complex Hg-$HS_i$ at any time is given by equation 5.9.

$$C_i(t) = C_i(0)\, e^{-k_i t} \qquad (5.9)$$

If each complex dissociates simultaneously and independently, the total concentration of all complexes C, at any time *t*, is given by a summation (equation 5.10).

$$C(t) = \sum_{i=1}^{n} C_i(0)\, e^{-k_i t} \qquad (5.10)$$

where n is the number of different ligand sites. For a continuous range of dissociation constants, equation 5.10 may be converted to the integral form. In our work, sites which are kinetically similar considered as a single site. Therefore, our results represent the minimum number of discrete sites available.

## 5.3 Method Validation

The competitive ligand exchange method has many applications in the field of analytical chemistry, including kinetic speciation. In the literature, most of the applications for kinetic speciation were carried out for Ni(II), Cu(II), Cd(II), Co(II) and Zn(II) ions, either in natural waters or in model solutions with a variety of humic substances[51,52,54,58,59]. Because of the lack of the information regarding Hg-HS dissociation kinetics, it is important to validate the method with a well-known chelating ligand toward Hg(II) such as ethylenediaminetetraacetic acid, EDTA..

EDTA, represented as $H_4Y$, is a strong chelating agent known to form 1:1 complexes with $Hg^{2+}$ with high thermodynamic stability constants. The complexation reaction is shown in equation 5.11.

$$Hg^{2+}_{(aq)} + Y^{4-}_{(aq)} \overset{K}{\rightleftarrows} [HgY]^{2-} \qquad (5.11)$$

At 20 °C, the above reaction (5.11) has a log K value of 21.7 [60] for the completely ionized species $[Y]^{4-}$. This means that a high fraction of $Hg^{2+}$ will be complexed to EDTA at high pH in the absence of other strong competing ligands. Upon the addition of excess of Duolite GT-73 resin to a solution containing $[HgY]^{2-}$, the uptake of Hg can be explained by two pathways: disjunctive, in which the Duolite GT-73 resin traps the $Hg^{2+}$ released from the thermodynamic equilibrium of $[HgY]^{2-}$ complex and adjunctive, in which the resin reacts directly with [Hg-EDTA] complex. In general, both pathways will contribute to the observed rate constant. Hering *et al.*[61] found that the disjunctive pathway predominates at high loadings, which was the case in our application.

Under our experimental conditions, 5 nM Hg(II) was mixed with 50 nM EDTA at pH 5 and pH 9. Solutions were left to equilibrate for 24 hours, and then 2.5 g of Duolite GT-73 Resin was added to 250 ml of the Hg-EDTA solutions. The change in $Hg^{2+}$ concentration of the solutions was continuously monitored on real time by ICP-MS, in which the Hg isotopes $^{202}Hg$, $^{200}Hg$, $^{199}Hg$, $^{201}Hg$, $^{198}Hg$, and $^{204}Hg$ were simultaneously quantified. The results of the dissociation kinetics of [Hg-EDTA] at pH 9 are shown in Figure 5.1. In this figure, the isotopes $^{198}Hg$ and $^{201}Hg$ are not shown because they are

superimposed on $^{204}Hg$ and $^{199}Hg$, respectively. For other kinetic experiments, only the most abundant isotope $^{202}Hg$ is presented in the figure(s). The analytical results are expressed in terms of standard deviations to take into account contributions from other isotopes. A comparison of the dissociation kinetics of the [Hg-EDTA] complex at pH 5 and 9 is shown in Figure 5.2.

$[H_2Y]^{2-}$ and $[HY]^{3-}$ are the predominant species of EDTA at pH 5, while at pH 9 it is $[Y]^{4-}$. Consequently, it is expected that at pH 9, $Hg^{2+}$ would be more strongly complexed with EDTA.

The kinetic components and their rate constants were extracted using a biphasic fitting, equation 5.12.

$$Y = ae^{-k_1 x} + be^{-k_2 x} \qquad (5.12)$$

a and b are constants; $k_1$ and $k_2$ are the dissociation rate constants of different components.

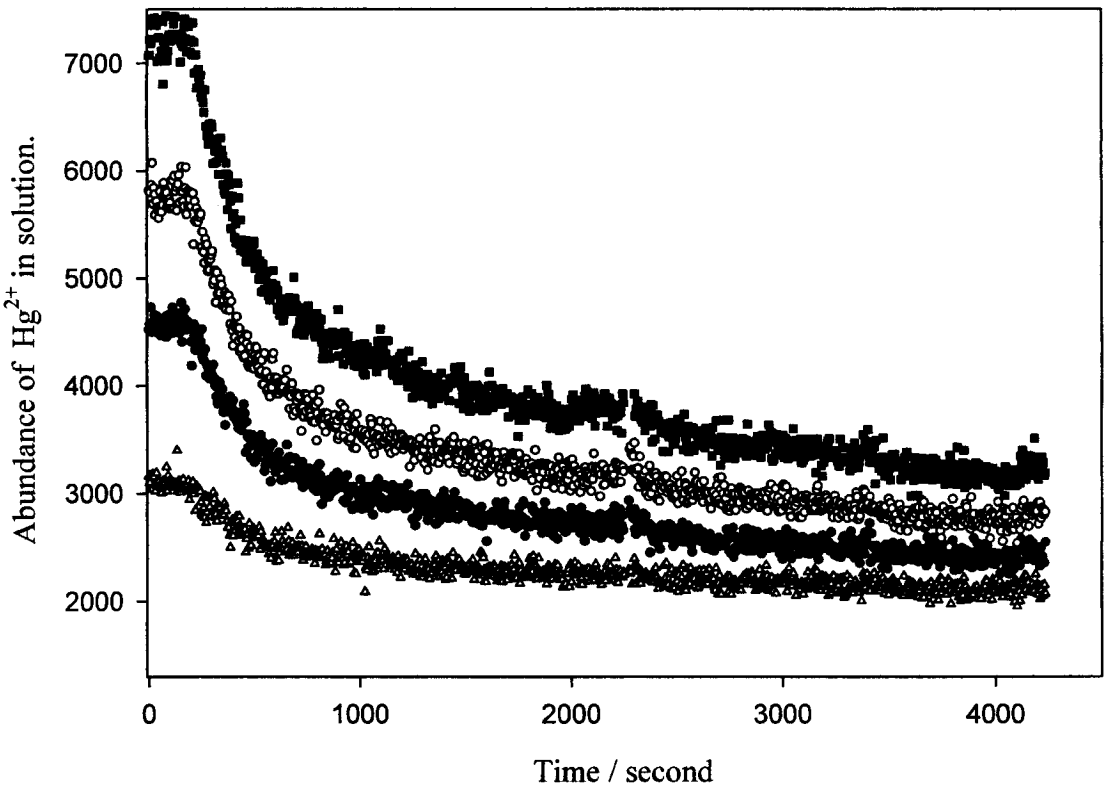


**Figure 5.1** Dissociation kinetics of Hg-EDTA complexes using Duolite GT-73 as the competing ligand and ICP-MS to measure the dissociation kinetics.

$[Hg^{2+}]$ =1 μg/L (~ 5 nM), [EDTA] = 50 nM, $[Cl^-]$ =10 nM, the solution at pH 9 and T=23°C. ■ $^{202}Hg$, ○ $^{200}Hg$, ● $^{199}Hg$, △ $^{204}Hg$

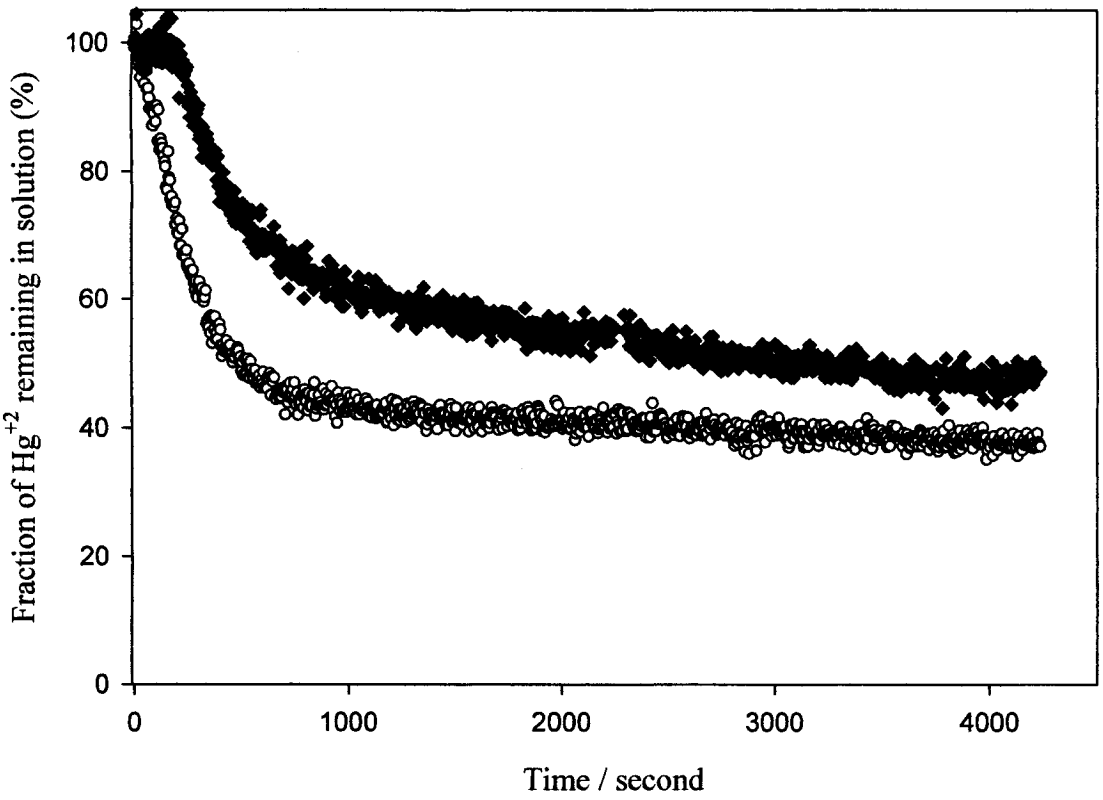


**Figure 5.2** Comparison of dissociation kinetics of Hg-EDTA complexes at two pH values using Duolite GT-73 as the competing ligand and ICP-MS of $^{202}Hg$ to measure the dissociation kinetics. $[Hg^{2+}]$ = 1 μg/L (~ 5 nM), T = 23°C, [EDTA] = 50 nM and ○ pH 5, ◆ pH 9.

Figure 5.2 shows that at both pH 5 and pH 9, there are two kinetically distinguishable components of Hg species: a labile component that is trapped by the resin within the first 900 s ($k_d \sim 3.5 \times 10^{-3}$ $s^{-1}$) and an inert component that starts to dissociate slowly after 900 s ($k_d \sim 4.5 \times 10^{-5}$ $s^{-1}$). The fraction of the inert component was higher at pH 9. This reflects the stronger complexation with [$Y^{4-}$], which is the predominant species of EDTA at this pH. These results (Table 5.3) confirm that the Duolite GT-73 resin is a good competing ligand for studying the kinetic dissociation of Hg-HS complexes.

**Table 5.3** Kinetic components of the Hg-EDTA complex at two different pH values and 23 °C, as measured by ICP-MS. $[Hg^{2+}]$ = 1 μg/L (~5 nM), $[Cl^-]$ = 10 nM, [EDTA] = 50 nM.

| pH | $C_1$ / % | $k_1$ / $10^3$ $s^{-1}$ | $C_2$ / % | $k_2$ / $10^5$ $s^{-1}$ |
|---|---|---|---|---|
| 5 | 54 ± 5 | 4.01 ± 0.06 | 45 ± 4 | 3.43 ± 0.24 |
| 9 | 35 ± 5 | 3.23 ± 0.09 | 66 ± 3 | 5.76 ± 0.35 |

$k_1$ and $k_2$ are the dissociation rate constants of the rapidly dissociating and the slowly dissociating components, respectively. $C_1$ and $C_2$ are the relative concentrations of the rapidly dissociating and the slowly dissociating components, respectively. The uncertainties are represented by the standard deviation of the results for the six isotopes of Hg used in this work.

## 5.4 Kinetic speciation of Hg-HS complexes

Compared to EDTA which forms strong complexes with Hg(II) with known stability constants, humic substances (both FA and HA) form [Hg-HS] complexes with conditional stability constants over wide ranges due to the reasons discussed previously in section 5.1. At concentration ratios of 0.02 – 1.0 μg Hg(II) per mg DOM and at pH 7, the complex formed between Hg and DOM has a high conditional stability constant (log K= 28.5).[11] In our work, we examined the kinetic species formed when a 1 μg of Hg as HgO solution was added to a 1 mg fulvic acid solution at pH 5. The results of the kinetic speciation are shown in Figure 5.3.

Analysis of the data by non-linear regression to equation 5.12 shows that the Hg-FA system has at least two kinetically distinguishable components. Prior to 900 seconds, the initial rapid decrease in Hg concentration implies a weak or labile Hg-FA complex. This component has $k_d$ of $2.5 \times 10^{-3}$ $s^{-1}$, and it contributes 74% of the initial Hg(II) concentration. Free Hg(II), found as the hexaaqua complex, can not contribute significantly to the labile component because it is trapped by the resin with a higher rate constant than that determined for the first component. Under our experimental conditions, the speciation calculation assumes complete Hg(II) complexation by humic substances(HS), excluding any $Hg(H_2O)_6^{2+}$ complex. The second component becomes predominant after 900 seconds. The slow dissociation refers to a less labile or more inert Hg-FA complex or complexes. It has a $k_d$ value of $5.34 \times 10^{-5}$ $s^{-1}$, and contributes only 25% of the initial Hg(II) concentration. These results are presented in Table 5.4.

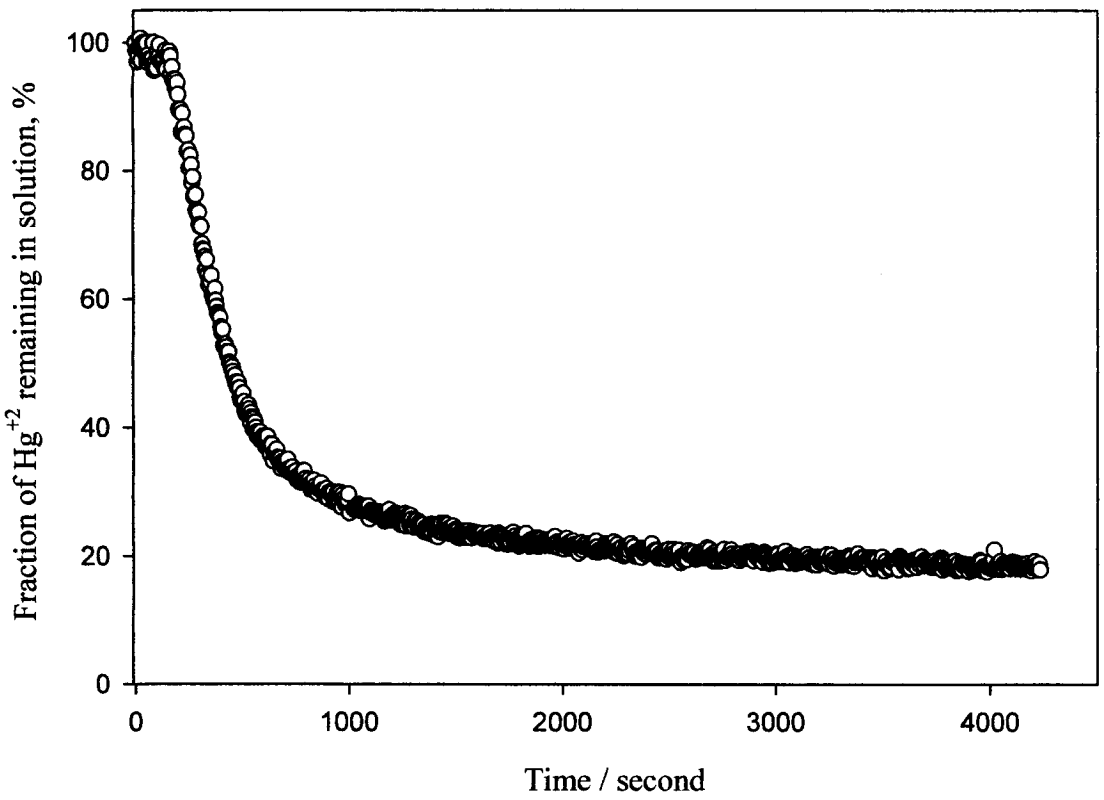


**Figure 5.3** Dissociation kinetics of Hg-FA complexes in model solutions of Suwannee River fulvic acid using Duolite GT-73 as the competing ligand and ICP-MS of $^{202}Hg$ to measure the dissociation kinetics. $[Hg^{2+}]$ = 1 μg/L ( ~ 5 nM) , FA = 1 mg/L, T = 23°C,and pH 5.

**Table 5.4** Kinetic components of the dissociation of the Hg-FA complex in model solutions of Suwannee River fulvic acid measured by ICP-MS at pH 5.0 and T = 23 °C. $[Hg^{2+}]$ = 1 μg/L, [FA] =1 mg/L.

| [Hg]/[FA] μg/mg | $C_1$ / % | $k_1$ / $10^{-3}$ $s^{-1}$ | $C_2$ / % | $k_2$ / $10^{-5}$ $s^{-1}$ |
|---|---|---|---|---|
| 1 | 74 ± 5 | 2.51 ± 0.07 | 25 ± 3 | 5.34 ± 1.0 |

$k_1$ and $k_2$ are the dissociation rate constants of the rapidly dissociating and the slowly dissociating components, respectively. $C_1$ and $C_2$ are the relative concentrations of the rapidly dissociating and the slowly dissociating components, respectively. The uncertainties are represented by the standard deviation of the results for six Hg isotopes used in this work.

*5.4.1 Effect of [Hg]/[FA] concentration ratio*

The effect of [Hg]/[FA] ratio was studied by keeping the Hg(II) concentrations constant at 1 μg/L (~ $5 \times 10^{-9}$ M) while varying the FA concentration from 1 to 20 mg/L. Figure 5.4 presents the effects of FA concentration on the dissociation kinetics of Hg-FA complexes at pH 5 and T = 23 °C. At least two kinetically distinguishable components are observed. The fraction of the slower (more inert) component increases with increasing FA concentration. The fit results are summarized in Table 5.3. The fraction of the kinetically slow component with $k_d = 4.5 \times 10^{-5}$ $s^{-1}$ increased from 25% to 46% when the fulvic acid concentration was increased from 1 to 10 mg/ L, while only a slight increase in this fraction was obtained when the fulvic concentration raised to 20 mg/L compared to 10 mg/L. The rate constants for the slow and fast components did not change significantly by varying the FA concentrations at the same pH. This indicates that we are probing the same binding sites of the fulvic acid.

From the information provided in Tables 2.1 and 2.3, the concentration of carboxylate groups in 1mg/L of the Suwannee River fulvic acid model solution was estimated to be 5.9 μM. Almost all of the carboxylate functional groups ($pK_{a1} = 3.8$) are expected to be ionized at pH 5. Under our experimental conditions, Hg(II) has a lower molar concentration by 3-fold than that of carboxylate, implying that Hg(II) should be complexed predominantly with this functional group in the absence of strong competing ligands. However, Hg(II) has a stronger affinity toward reduced S-donor ligands than for O-donor ligands. FA contains both S and O donor sites, and the concentration of O-sites is much greater than that of S-sites. For 1 mg/L FA used in this study, the total S content was calculated to be 125 nM. It has been reported that only 35% [62] or 48% [43] of the total

sulfur in Suwannee River FA is in the reduced form. As shown in Table 5.5, we found that 250 ng/L and 440 ng/L of Hg(II) complexes are kinetically more inert (slow) in the presence of 1 and 5 mg/L fulvic acid, respectively. If it is assumed that only one sulfur atom is complexed to each Hg atom (1:1 mole ratio), and the binding of Hg to S-donor sites is responsible for the kinetically inert fractions, then only 1.0% to 2.8% of the reduced sulfur atoms are involved in the Hg(II) complexation.

The low abundance of reduced S-sites compared to O-sites may result in the mixed bidentate complexation of $Hg^{2+}$. Xia *et al.*[31] provide evidence to support the hypothesis that $Hg^{2+}$ binds to soil humic acid in a two coordinate fashion. The proposed model which fits their EXAFS data is shown below.

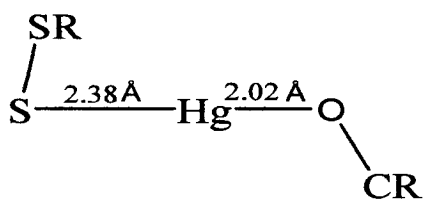


R represents various organic groups in HS. In this model, both sulfur and oxygen atoms are bound to Hg. However, Hesterberg *et al.*[32] reported that at high molar ratio of $S_{total}$/Hg(II) in soil humic acid, a high fraction of the Hg atoms were bonded to two S-atoms and a smaller fraction were bound to S and O atoms simultaneously.

When the FA concentration was raised from 10 to 20 mg/L, the fraction of Hg(II) bound to the strong sites (kinetically more inert) did not increase significantly. This can be explained by conformational changes in the HS. The changes could be driven by the high concentration of HS and by the ion binding, which in turn affects the size and shape of the humic substances. Metal ion binding shields the charges of the HS which causes

conformational changes in HS. [63] increasing the concentration of HS will not necessarily result in an increase in metal ion binding.[64]

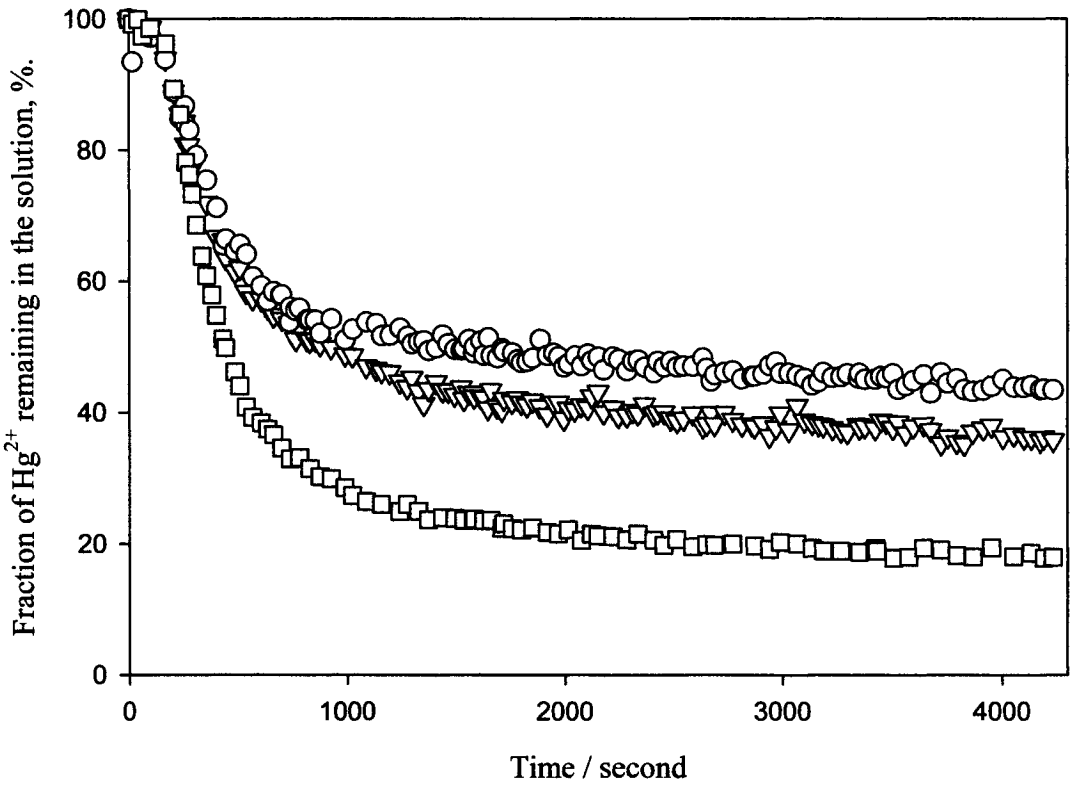


**Figure 5.4** Influence of the Hg(II) to FA ratio on the kinetic speciation of the model solution of Hg(II) and Suwannee River fulvic acid at pH 5.0 and T = 23 °C. Duolite GT-73 is used as competing ligand, $Hg^{2+}$ = 1 μg/L (~5 nM), ■ FA=1 mg/L, ▼ FA = 10 mg/L and ○ FA = 20 mg/L.

**Table 5.5** Effects of the $[Hg^{2+}]/[FA]$ ratio on the dissociation rate constants of Hg-FA complexes and their distributions in aqueous solution at pH 5 and T = 23 °C, $[Hg^{2+}]$ = 1 μg/L.

| [Hg]/[FA] μg/mg | $C_1$ / % | $k_1$ / $10^3$, $s^{-1}$ | $C_2$ / % | $k_2$ / $10^5$ $s^{-1}$ |
|---|---|---|---|---|
| 1 | 74 ± 5 | 2.51 ± 0.07 | 25 ± 3 | 5.34 ± 1.0 |
| 0.1 | 55 ± 7 | 2.56 ± 0.03 | 44 ± 5 | 4.24 ± 0.83 |
| 0.05 | 50 ± 3 | 2.41 ± 0.06 | 49 ± 4 | 4.02 ± 0.96 |

$k_1$ and $k_2$ are the dissociation rate constants of the rapidly dissociating and the slowly dissociating components, respectively. $C_1$ and $C_2$ are the relative concentrations of the rapidly dissociating and the slowly dissociating components, respectively. The uncertainties are represented by the standard deviation of the results for six Hg isotopes used in this work.

*5.4.2 Effects of pH*

The kinetic dissociation of Hg-HS components is greatly affected by the pH of the medium. Under acidic conditions, the proton ($H^+$) competes with Hg(II) for the complexing sites. Figure 5.5 shows a comparison of the kinetic dissociation of Hg-FA complexes at pH 5 and 9. The results show that the fraction of the kinetically more inert component increased with increases pH. It contributes 25% of the initial Hg(II) concentration at pH 5 and 65% at pH 9. This illustrates proton competition with Hg(II) for the strongly complexing sites.

As shown in Table 5.6, raising the concentration of FA from 1 to 10 and even to 20 mg/L under the same initial conditions (pH 9 and $[Hg^{2+}]$ = 1 μg/L) did not result in any increase of the fraction of the kinetically more inert component. This effect was also observed at pH 5 for a high initial concentration of FA. It should be noted that at pH 9 all of the phenol functional groups ($pK_a \leq 9$) should be deprotonated. This would result in a further increase of the O-site density compared to the S-sites and this may be another factor which limits the formation of the inert component.

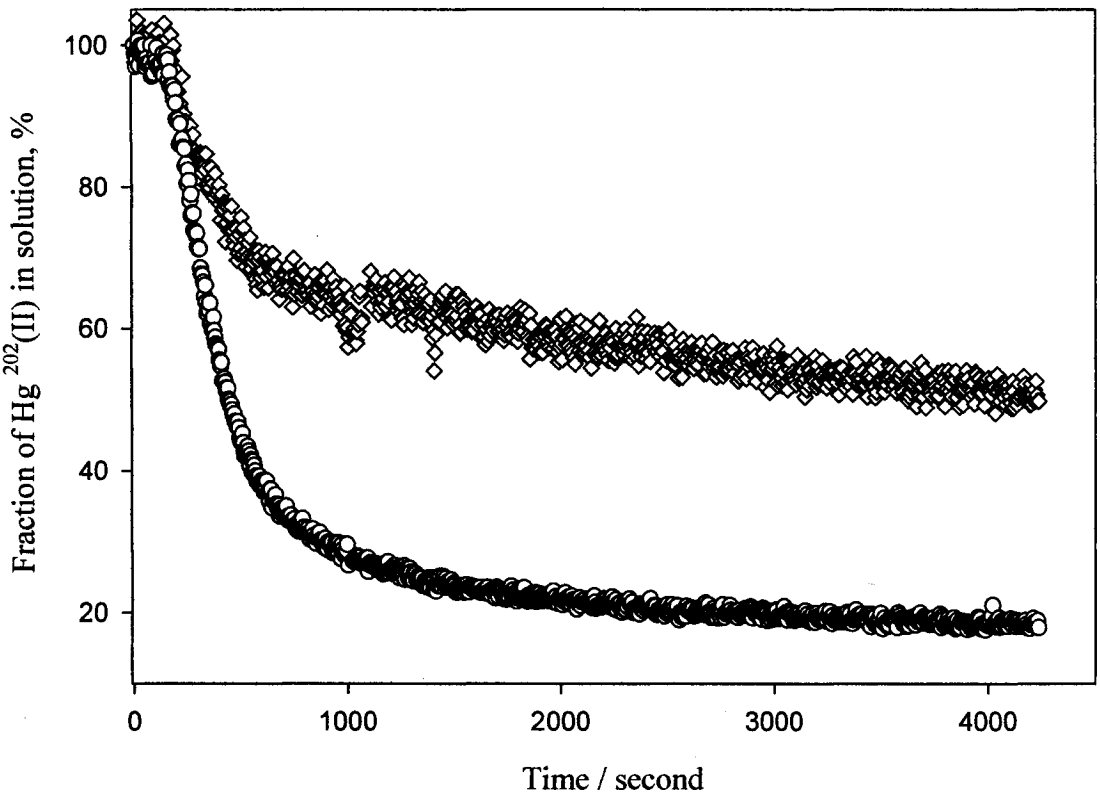


**Figure 5.5** Dissociation kinetics of Hg-FA complexes at two pH values using Duolite GT-73 as the competing ligand and ICP-MS to measure the dissociation kinetics. $[Hg^{2+}]$ = 1 μg/L (~ 5 × $10^{-9}$ M), [FA] = 1 mg/L, T = 23 °C, ○ pH 5 and ◊ pH 9.

**Table 5.6** Dissociation rate constants of Hg-FA complexes and their distributions in aqueous solution at pH 9, T = 23 °C, and at constant $[Hg^{2+}]$ = 1 μg/L.

| [Hg]/[FA] μg/mg | $C_1$ / % | $k_1$ / $10^3$ $s^{-1}$ | $C_2$ / % | $k_2$ / $10^5$ $s^{-1}$ |
|---|---|---|---|---|
| 1 | 36 ± 4 | 2.86 ± 0.09 | 65 ± 4 | 6.25 ± 0.33 |
| 0.1 | 37 ± 6 | 2.87 ± 0.06 | 63 ± 5 | 6.42 ± 0.46 |
| 0.05 | 40 ± 5 | 2.55 ± 0.04 | 59 ± 3 | 5.32 ± 0.46 |

$k_1$ and $k_2$ are the dissociation rate constants of the rapidly dissociating and the slowly dissociating components, respectively. $C_1$ and $C_2$ are the relative concentrations of the rapidly dissociating and the slowly dissociating components, respectively. The uncertainties are represented by the standard deviation of the results for six Hg isotopes used in this work.

*5.4.3 Comparison of kinetic speciation of Hg(II) complexation with FA and HA*

Both FA and HA are major fractions of DOC in freshwater. FA has a higher carboxylic and phenolic content. According to Tables 2.1 and 2.3, an aqueous solution of 1 mg/L FA used in this study contains 5.9 μM carboxylic groups, 1.5 μM phenolic group and 0.125 μM sulfur, while a solution of 1 mg/L HA used in this study contains 4.4 μM carboxylic, 1.36 μM phenolic groups, and 0.220 μM sulfur.

The sulfur content of HA is higher than that of FA. Thus, if we assume that the amount of reduced sulfur is correlated positively to total sulfur, then the kinetically more inert component (slow) which results from the Hg-S complexation in humic acid should contribute to a higher fraction of the initial Hg(II) compared to FA. However, if the Hg complexation by the carboxylate functional groups leads to the kinetically inert component, then the fraction of this component will be higher in FA compared to HA.

To test the previous hypothesis about the role of reduced sulfur in the formation of kinetically more inert (slow) components, solutions containing 1 μg/L $Hg^{2+}$ and 1 mg/L Leonardite humic acid were prepared at pH 5 and 9. After equilibration, the dissociation kinetics was measured (Figure 5.6).

At least two kinetically distinguishable components were observed in the system. This result is the same as for Hg-FA complexes, but the fraction of the slower (more inert) component is different. For the Hg-FA complex, contribution of the kinetically more inert component was 25% of initial Hg(II), whereas, it contributes 35% in the Hg-HA complex. This increase is attributed to the higher S-content of HA compared to FA. Both carboxylic and phenolic group contents of HA is less than that of FA, ruling out the possibility that the kinetically inert component could be formed from a chelating structure

of multiple oxygen donors. At pH 9, there is no kinetically significant difference between the components of the Hg(II) complexes with FA and HA. The results of the kinetic analysis of Hg-HA complexes are presented in Table 5.7.

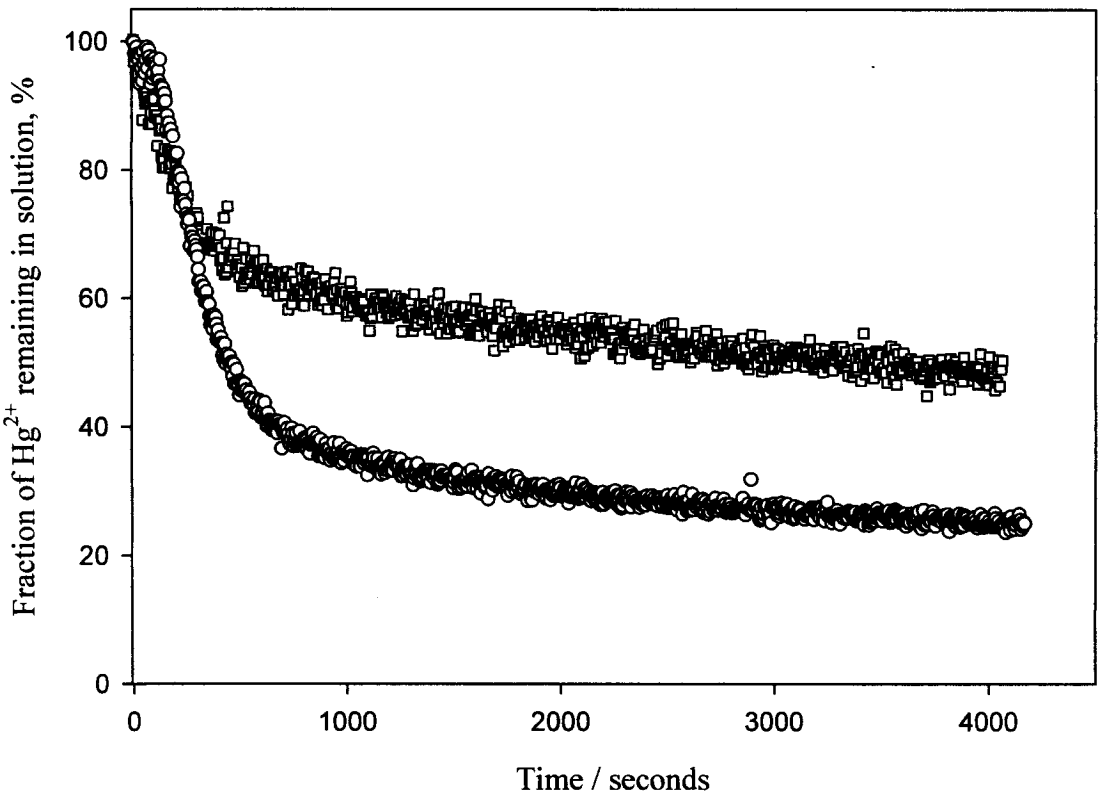


**Figure 5.6** Dissociation kinetics of Hg-HA complexes at two different pH values, using Duolite GT-73 as the competing ligand and ICP-MS to measure the dissociation kinetics. [HA] = 1 mg/ L, [$Hg^{2+}$] = 1 µg/L (~ 5 nM), T = 23 °C, ○ pH 5 and □ pH 9.

**Table 5.7** Comparison of the dissociation rate constants of Hg-HA complexes and their distributions in aqueous solution of pH 5 and pH 9 at T = 23 °C. [HA] = 1 mg/L (Leonardite humic acid), $[Hg^{2+}]$ = 1 μg/L.

| pH | $C_1$ / % | $k_1$ / $10^3$ $s^{-1}$ | $C_2$ / % | $k_2$ / $10^5$ $s^{-1}$ |
|---|---|---|---|---|
| 5 | 63 ± 5 | 3.07 ± 0.09 | 35 ± 3 | 7.33 ± 0.24 |
| 9 | 38 ± 5 | 4.3 ± 0.07 | 62 ± 3 | 6.76 ± 0.45 |

$k_1$ and $k_2$ are the dissociation rate constants of the rapidly dissociating and the slowly dissociating components, respectively. $C_1$ and $C_2$ are the relative concentrations of the rapidly dissociating and the slowly dissociating components, respectively. The uncertainties represent the standard deviation of the results for six Hg isotopes used in this work.

## 5.5 Kinetic speciation of MeHg-HS complexes

Both $Hg2^{+}$ and $MeHg^{+}$ are considered to be soft acids, and they have a high affinity for binding to reduced S-atoms. However the complexes formed between $MeHg^{+}$ and HS have lower conditional stability constants than that of $Hg^{2+}$. This is clearly shown in Tables 5.1 and 5.2. The electron donating group ($CH_3$) reduces the coordination possibilities of Hg toward S-atoms.

From a kinetic point of view, a solution of MeHg-FA at pH 5, we observed only one component with $k_d \sim 10^{-4}\ s^{-1}$. As shown in Figure 5.7, the dissociation rate constant of MeHg-FA was found to decrease as the FA concentration increases. This implies that this curve represents an average of several components. If the system has only one component, then increasing the FA concentration would not be expected to affect its dissociation rate constant. However if the system is a mixture of components, then the fraction of the components is changed as a result of FA addition. Because all of the components are observed as a single component, the average observed dissociation constant will change. The results for the kinetic dissociation of MeHg-HS complexes at different initial concentrations are presented in Table 5.8.

At pH 9 (Figure 5.8), we observed two kinetically distinguishable components. At this pH, the hydroxide ion competes efficiently for $MeHg^{+}$, so formation of the MeHg-OH is possible. In aqueous solution, methylmercury hydroxide found as $(CH_3Hg)_2OH^{+}$ may dissociate faster than the MeHg-HS complex. This explains the observed labile fraction ( $k_d$ of $10^{-3}\ s^{-1}$) which contributes 60% of the initial MeHg..

The fraction of $MeHg^+$ that bound to the reduced S atom in HS is assumed to be very low compared to our initial concentration of $MeHg^+$ and

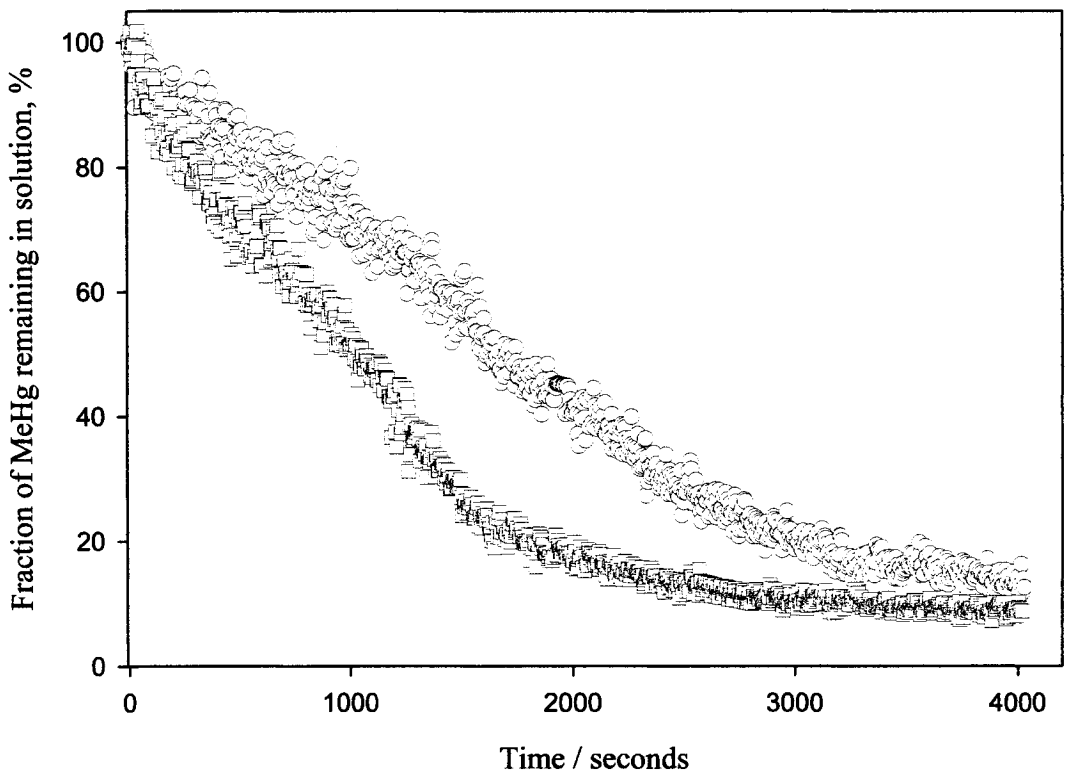


**Figure 5.7** Dissociation kinetics of MeHg-FA complexes in model solution of Suwannee River fulvic acid using Duolite GT-73 as the competing ligand and ICP-MS for $^{202}Hg$ to measure the dissociation kinetics. [MeHg]= 1.7μg/L (~ 8 nM), T=23 °C, and pH 5, ○ FA= 10 mg/L, □ FA= 5 mg/L.

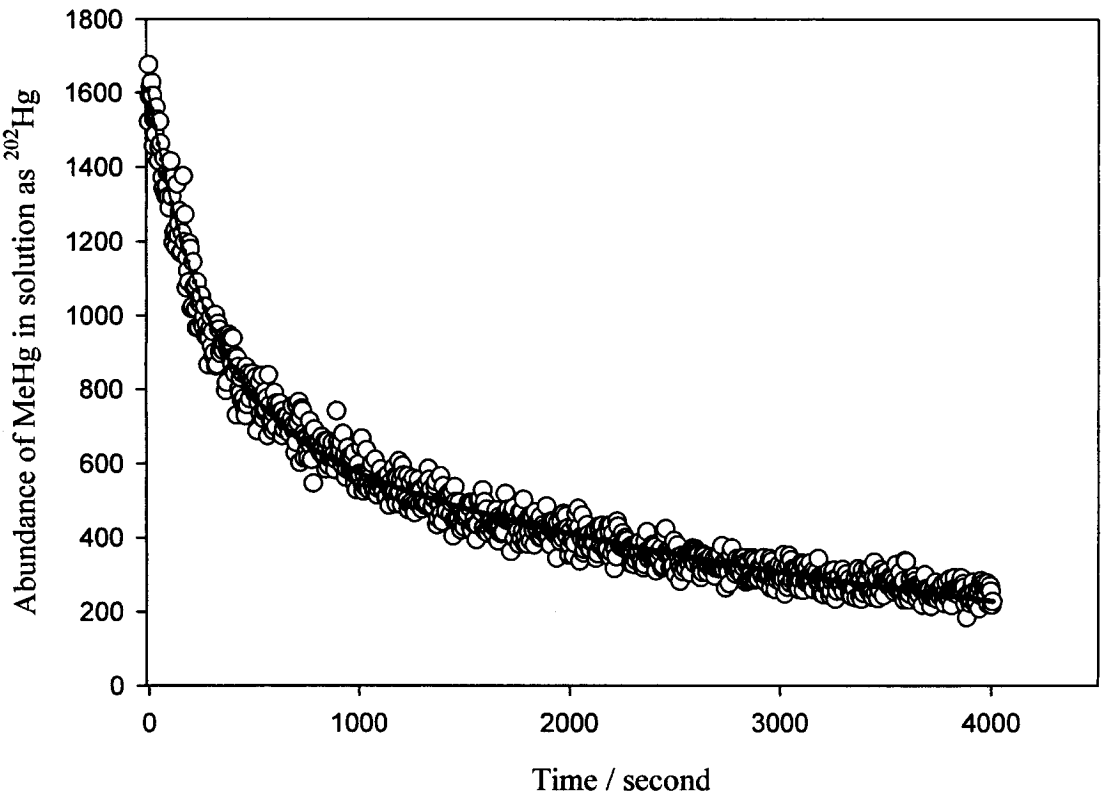


**Figure 5.8** Kinetic speciation of MeHg-HA complexes in model solution of Leonardite Humic acid using Duolite GT-73 Resin as the competing ligand and ICP-MS to measure the dissociation kinetics. HA= 5 mg/L, [MeHg]= 1.7μg/L (~ 8 nM), T=23 °C, and pH 9.

**Table 5.8** The dissociation rate coefficients "k" of MeHg-HS complexes in model solutions with different initial [MeHg] / [ HS] ratios and at two different pH values, T= 23 °C.

| [MeHg] µg/L | HS in | mg/L | pH ± 0.2 | $k_1 \times 10^3$, $s^{-1}$ | $k_2 \times 10^4$, $s^-$ |
|---|---|---|---|---|---|
| 1.7 | HA | 1 | 5 | -- | 9.4 ± 2.06 |
| 1.7 | HA | 5 | 9 | 3.53 ± 1.12 contributes to 60% | 2.91 ± 1.84 |
| 1.7 | FA | 10 | 5 | --- | 3.49 ± 1.29 |
| 1.7 | FA | 5 | 5 | --- | 8.19 ± 1.76 |
| 4.25 | FA | 10 | 5 | --- | 7.90 ± 1.57 |
| 4.25 | FA | 5 | 5 | ---- | 11.0 ± 2.14 |

$k_1$ is the dissociation rate coefficients of MeHg-HS component, HS represent the type of humic substance used; Suwannee fulvic acid (FA) or Leonardite humic acid (HA). The uncertainties represent the standard deviation of the results for six Hg isotopes used in this work

The fraction of $MeHg^+$ bound to the reduced S-atoms of HS is low. It has been illustrated that only thiol groups are involved in the complexation of $MeHg^+$ while other reduced S-groups were not involved even after the saturation of thiol groups.[65] However carboxylate groups of HS are involved in the $MeHg^+$ complexation at high MeHg/HS ratio.[47] This complexation is reported to be weak; log K = 3.36 was calculated for the acetate complexation of $MeHg^+$ with 1:1 stoichiometric ratio[66]

Two [47] and three [48] discrete sites with 1:1 stoichiometric ratio were used to describe and fitting the data for the complexation of MeHg to different HS. However it has been reported that $MeHg^+$ can form a 2:1 and 3:1 complexes with thioglycolate ($-SCH_2CO_2^{2-}$) in which 2 or 3 molecules of $MeHg^+$ are bonded to S-atom,[66] also it has been shown that $MeHg^+$ form a 1:1 complex with cysteinate($-SCH_2CH(NH_2)-COO^{2-}$) through S-atom, with Log K value of 16.6 and another molecule of $MeHg^+$ can be complexed through nitrogen atom resulting in 2:1 complex.[66]

## 5.6 Conclusions

From a kinetic point of view, the Hg-HS complexes can be described by at least two kinetically distinguishable components; the more inert (slow) with a dissociation rate constant in the order of $10^{-5}$ $s^{-1}$, and a labile component with a dissociation rate constant in the order of $10^{-3}$ $s^{-1}$. The fraction of each component is greatly affected by different parameters. Protons ($H^+$) compete with $Hg^{2+}$ for the strong binding sites with the competition being more pronounced at low pH values. The Hg/HS mole ratio also is an important parameter, when [$Hg^{2+}$] is high then it saturates the strong binding sites and the

excess binds to the weaker sites. The nature and the composition of HS affects the binding of $Hg^{2+}$, the more reduced sulfur content the higher fraction of kinetically inert component of Hg-HS, those parameters also affect the MeHg-HS complexes, while at pH 5 we noticed a one component system with a dissociation rate constant in the order of $10^{-4}$ $s^{-1}$, at pH 9 two kinetically distinguishable components were observed, and at higher HS concentration the dissociation of MeHgHS become slower.

For aqueous solutions containing 1 and 10 mg/L of Suwannee River fulvic acid at pH 5, the amount of Hg(II) involved in the kinetically inert components of Hg-HS complexes is found to be 240 and 440 ng/L, respectively. At higher pH this amount is increased. This shows that most of $Hg^{2+}$ in aquatic environment will be strongly complexed to HS in the absence of other strongly competing ligands.

Both of $Hg^{2+}$ and $MeHg^{+}$ show a tendency to complex with HS but it was very difficult to precisely quantify the amount of $MeHg^{+}$ involved in the formation of the kinetically inert MeHgHS components; this may be due to the presence of mixed components with similar rates of kinetic dissociation. This is further refined using an ultrafiltration technique, in which the dissociation kinetics of MeHg species in different size fractions was investigated (see next chapter).

**References**

(1) Jay, J. A.; Morel, F. M. M.; Hemond, H. F. *Environ. Sci. Technol.* **2000**, *34*, 2196-2200.

(2) Paquette, K. E.; Helz, G. R. *Environ. Sci. Technol.* **1997**, *31*, 2148-2153.

(3) Tossel, J. A. *J. Phys. Chem. A* **2001**, 105, 935-941.

(4) Al-Farawati, R.; Van De Berg, C. M. G. *Mar. Chem.* **1999**, *63*, 331-353.

(5) Sukola, K.; Wang, F.; Tessier, A. *Anal. Chim. Acta* **2005**, *528*, 183-195.

(6) Luther, G. W; Theberge, S. M.; Rickard, D. T. *Geochim. Cosmochim. Acta.* **1999**, *63*, 3159-3169.

(7) Mantoura, R. F. C.; Dickson, A.; Riley, J. P. *Estuar. Coast. Mar. Sci.* **1978**, *6*, 387-408.

(8) Danfer, E. V.; Wangersky, P. J. *J. Environ. Monit.* **2002**, *4*, 55-69.

(9) Coquery, M.; Cossa, D.; Sanjuan, J. *Mar. Chem.* **1997**, *58*, 213-227.

(10) Skyllberg, U.; Xia, K.; Bloom, P. R.; Nater, E. A.; Bleam, W. F. *J. Environ. Qual.* **2000**, *29*, 855-865

(11) Haitzer, M.; Aiken, G. R.; Ryan, J. N. *Environ. Sci. Technol.* **2002**, *36*, 3564-3570

(12) Wu, Q.; Apte, S. C.; Batley, G. E.; Bowles, K. C. *Anal. Chim. Acta* **1997**, *350*, 129-134.

(13) Benoit, J. M.; Mason, R. P.; Gilmour, C. C.; Aiken, G. R.. *Geochim. Cosmochim. Acta.* **2001**, *65*, 4445-4451.

(14) Lamborg, C. H.; Tseng, C-M.; Fitzgerald, W. F.; Balcom, P. H.; Hammerschmidt, C. R. *Environ. Sci. Technol.* **2003**, *37*, 3316-3322

(15) O' Driscoll, N. J. ; Evans, R. D. *Environ. Sci. Technol.* **2000**, *34*, 4039-4043.

(16) Krystek, P.; Ritsema, R. *Anal. Bioanal. Chem.* **2005**, *381*, 354-359.

(17) Mason, R. P.; Fitzgerald, W. F. *Nature* **1990**, *347*, 457-459.

(18) Balogh, S. J.; Nollet, Y. H.; Offerman, H. J. *Sci. Total Environ.* **2005**, *340*, 261-270.

(19) Balogh, S. J.; Nollet, Y. H.; Swain, E. B. *Environ. Sci. Technol.* **2004**, *38*, 4921-4927.

(20) Benoit, J. M.; Gilmour, C. C.; Mason, R. P. *Environ. Sci. Technol.* **2001**, *35*, 127-132.

(21) Siciliano, S. D.; Lean, D. R. S. *Environ. Toxicol. Chem.* **2002**, *22*, 1184-1190.

(22) Lean, D. R. S.; Siciliano, S. D. *J. Phys .IV* **2003**, *107*, 743-747.

(23) Beijer, K.; Jernelov, A. In The Biogeochemistry of mercury in aquatic environment. Nriagu, J. O., Eds.; Elsevier: North-Holland Biomedical press. 1979, pp 203-210.

(24) Siciliano, S. D.; O' Driscoll, N. J.; Tordon, R.; Hill, J.; Beauchamp, S.; Lean, D. R. S. *Environ. Sci. Technol.* **2005**, *39*, 1071-1077.

(25) Watras, C. J.; Back, R. C.; Halvorsen, S.; Hudson, R. J. M.; Morrison, K. A.; Wente, S. P. *Sci. Total Environ.* **1998**, *219*, 183-208.

(26) Sellers, P.; Kelley, C. A.; Rudd, J. W. M.; MacHutchon, A. R. *Nature* **1996**, *380*, 694-697.

(27) Marvin-Dipasquale, M.; Agee, J.; McGowan, C.; Oremland, R. S.; Thomas, M.; Krabbenhoft, D.; Gilmour, C. C. *Environ. Sci. Technol.* **2000**, *34*, 4908-4916.

(28) Skylberg, U.; Qian, J.; Frech, W.; Kang, X.; Bleam, W. F. *Biogeochem.* **2003**, *64*, 53-76.

(29) Stumm, W.; Morgan, J. J. Aquatic Chemistry; John Wiley and Sons: New York, 1996.

(30) Ravichandran, M. *Chemosphere* **2004**, *55*, 319-331.

(31) Xia, K.; Skyllberg, U. L.; Bleam, W. F.; Bloom, P. R.; Nater, E. A.; Helmke, P. A. *Environ. Sci. Technol.* **1999**, *33*, 257-261.

(32) Hesterberg, D. ; Chou, J. W.; Hutchison, K. J. ; Sayers, D. E. *Environ. Sci. Technol.* **2001**, *35*, 2741-2745.

(33) Qian, J.; Skylberg, U.; Frech, W.; Bleam, W. F.; Bloom, P. R.; Petit, P. E. *Geochim. Cosmochim. Acta* **2002**, *66*, 3873-3885.

(34) Karlsson, T.; Persson, P.; Skyllberg, U. *Environ. Sci. Technol.* **2005**, *39*, 3048-3055.

(35) Driscoll, C. T.; Blette, V.; Yan, C.; Schofield, C. L.; Munson, R.; Holsapple, J. *Water Air Soil Pollut.* **1995**, *80*, 499-508.

(36) Wallschlager, D. ; Desai, M. V. M.; Spengler, M.; Windmoller, C. C.; Wilken, R. D. *J. Environ. Qual.* **1998**, *27*, 1044-1054.

(37) Guo, L.; Hunt, B. J.; Santchi, P. H.; Ray, S. M. *Environ. Sci. Technol.* **2001**, *35*, 885-893

(38) Watras, C. J.; Back, R. C.; Halvorsen, S.; Hudson, R. J.; Morrison, K. A.; Wente, S. P. *Sci. Total Environ.* **1998**, *219*, 189-208.

(39) Sjoblom, A.; Meili, M.; Sundbom, M. *Sci. Total Environ.* **2000**, *261*, 115-124.

(40) Perdue, E.M. In Aquatic Humic Substances: Ecology and Biochemistry. Hessen, D. O., Tranvik, L. J., Eds.; Springer: Germany, 1998; pp. 41-61.

(41) Milne, C. J.; Kinnigurgh, D. G.; Tipping, E. *Environ. Sci. Technol.* **2001**, *35*, 2049-2059.

(42) Tipping, E. *Aquat. Geochem.* **1998**, *4*, 3-48.

(43) Haitzer, M.; Aiken, G. R.; Ryan, J. N. *Environ. Sci. Technol.* **2003**, *37*, 2436-2441.

(44) Hsu, H.; Sedlak, D. L. *Environ. Sci. Technol.* **2003**, *37*, 2743-2749.

(45) Cheam, V.; Gamble, D. S. *Can. J. Soil Sci.* **1974**, *54*, 413-417.

(46) Karlsson, T.; Skylberg, U. *Environ. Sci. Technol.* **2003**, *37*, 4912-4918.

(47) Hintelmann, H.; Welbourn, P. M.; Evans, R. D. *Environ. Sci. Technol.* **1997**, *31*, 489-495.

(48) Amirbahman, A.; Reid, A. L.; Haines, T. A.; Kahl, J. S.; Aronold, A. *Environ. Sci. Technol.* **2002**, *36*, 690-695.

(49) Buffle, J.; Leppard, G. G. *Environ. Sci. Technol.* **1995**, *29*, 2169-2175.

(50) Olson, D. L.; Shuman, M. S. *Geochim. Cosmochim. Acta* **1985**, *49*, 1371-1375.

(51) Mandal, R.; Hassan, N. M.; Murimboh, J.; Chakrabarti, C. L.; Back, M. H.; Rahayu, U.; Lean, D. R. S. *Environ. Sci. Technol.* **2002**, *36*, 1477-1484.

(52) Langford, C. H.; Cook, R. L. *Analyst* **1995**, *120*, 591-596.

(53) Morel, F. M.; Hering, J. G. Principles and Applications of Aquatic Chemistry; John Wiley and Sons: New York, 1993; pp 380-388.

(54) Fasfous, I. I.; Yapici, T.; Murimbuh, J.; Hassan, N. M.; Chakrabarti, C. L.; Back, M. H.; Lean, D. R. S.; Grégoire, D. C. *Environ. Sci. Technol.* **2004**, *38*, 4979-4986

(55) Lin, C. F.; Houng, L. M.; Lo, K. S.; Lee, D. Y. *Toxicol. Environ. Chem.***1994**, *43*, 1-12.

(56) Wu, F.; Cai, Y.; Evans, D.; Dillon, P. *Biogeochem.* **2004**, *71*, 339-351

(57) Pohl, P.; Prusisz, B. *Anal. Sci.* **2004**, *20*, 1367-1370.

(58) Rocha, J. C.; Rosa, A. H. ; Bergh, J. V. ; Burba, P. *J. Environ. Monit.* **2002**, *4*, 799-802.

(59) Sekaly, A. L. R.; Mandal, R.; Hassan, N. M.; Murimbuh, J.; Chakrabarti, C. L.; Back, M. H.; Grégoire, D. C.; Schroeder, W. H. *Anal. Chim. Act.* **1999**, *402*, 211-221.

(60) Martell, A. E.; Smith. R. M. In Critical stability constants. V1, Plenum press: New York, 1974, p. 208.

(61) Hering, J, G.; Morel, F. M. M. *Environ. Sci. Technol.* **1988**, *22*, 1469-1478

(62) Xia, K.; Weesner, F.; Bleam, W. F.; Bloom, P. R.; Skyllberg, U. L.; Helmke, P. A. *Soil. Sci. Soc. Am. J.* **1998**, *62*, 1240-1246.

(63) Nifant'eva, T. I.; Shkinev, V. M.; Spivakov, B. Ya.; Burba, P. *Talanta* **1999**, *48*, 257 - 267.

(64) Li, J.; Perdue, E. M.; Gelbaum, L. T. *Environ. Sci. Technol.* **1998**, *32*, 483-487.

(65) Yoon, S. –J.; Diener, L. M.; Bloom, P. R.; Nater, E. A.; Bleam, W. F. *Geochim. Cosmochim. Acta.* **2005**, *69*, 1111-1121.

(66) Alderighi, L.; Gans, P.; Midollini, S.; Vacca, A. *Inorg. Chim. Acta* **2003**, *356*, 8-18.

# Chapter 6

## Size fractionation and kinetic studies of Hg(II) and $MeHg^+$ complexes with natural ligands in aquatic systems

### 6.1 Introduction

The size distribution of HS is an important aspect of metal ion speciation. In natural waters, the size fraction of organic complexes can range from small molecules to particles.[1] The metals associated with each size class can have different motilities and bioavailabilities. For example, the residence time of colloidal metal species in the water column is less than that of truly dissolved metal ions, because of the coagulation and sedimentation of colloidal metal-humic complexes (M-HS). Aggregation of colloids represents the principle method of separating metals and HS from water by ultrafiltration techniques.[2]

Various methods have been used for the isolation and separation of DOC into molecular weight (MW) size fractions. There are many ultrafiltration techniques (UF). Their performance can be influenced by pH, ionic strength, concentration of HS, and the type of membrane used. A common problem is membrane fouling, caused by the accumulation of macromolecules (i.e., adsorption) on the surface of the membrane. Membrane fouling is affected by ionic strength, $Ca^{2+}$ concentration, HS contents, pH and the type of membrane material. In tangential flow ultrafiltration (TFUF), the solution moves along the filtration medium surface, while a small fraction of the solution

permeates the membrane, minimizing membrane fouling. Its ease of use, ability to handle large sample volumes and applicability to a wide variety of different types of water samples are distinct advantages of TFUF. Size separation is achieved by using membranes with different molecular weight cutoffs (WCO). WCO is defined as the critical MW of the solute that will be > 90% rejected by the membrane. In practice, the size of the molecules, rather than their MW, determines the rejection. Hence, the shape and the conformations of some molecules affect their separations regardless of their MW.

The TFUF technique has been widely-used in size speciation of M-HS complexes and in DOC fractionation.[3,4] In a review based on more than 30 published papers, Town *et al.*[5] showed that in different river waters, the size distribution of DOC is 30-33% greater than 100 kiloDalton (kD) and 66-71% < 100 kD. It has also been reported that 54-69% of freshwater DOC is < 5 kD and 30-43% is in the range of >5 kD to 0.1 μm.[6,7] It has been shown that the high molecular weight (HMW) fractions of DOC with size > 10 kD are more bioavailable and they are utilized by bacteria more rapidly than the low molecular weight fractions (LMW).[8] Carbohydrate moieties and aliphatic groups are predominant in HMW fraction,[9] while the LMW fractions of (1-10 kD) contain more carboxylic functional groups.[10]

The number average ($M_n$) and weight average ($M_w$) molecular weight are commonly used to describe the size distribution of HS. Both terms are defined in equations 6.1 and 6.2. The ratio of the two termed as the polydispersity (P) of HS and defined in equation 6.3.

$$M_n = \frac{\sum_{i=1}^{n} M_i \times F_i}{\sum_{i=1}^{n} F_i} \qquad (6.1)$$

$$M_w = \frac{\sum_{i=1}^{n} (M_i)^2 \times F_i}{\sum_{i=1}^{n} M_i \times F_i} \qquad (6.2)$$

$$P = \frac{M_n}{M_w} \qquad (6.3)$$

$M_i$ is the molecular mass of the $i$th component, and $F_i$ is the frequency of the component with mass $M_i$, which is represented by the peak intensity in the mass spectrum or the peak area in the size exclusion chromatograph.

Various methods have been used to determine these parameters. For Suwannee River fulvic acid, based on size exclusion chromatography, the values $M_n$ = 1260 and $M_w$ = 2170 (g/mole) were reported.[11] Another study found values of 1360 and 2310 for $M_n$ and $M_w$, respectively.[12] It has also been calculated that 32.5% of Suwannee River fulvic acid has a molecular weight distribution of > 3000 Da and 61.9% of < 1360 Da.[13] Electrospray ionization-mass spectrometric (ESI-MS) techniques have reported lower trends in the molecular weight values of Suwannee River fulvic acid: $M_n$ = 591-617 and $M_w$ = 914-936.[14]

In aquatic systems, the presence of metal ions bound to HS causes changes in the size distribution of HS. It has been reported that loading of copper, even at low concentration (3% of HS capacity), led to an increase in the macromolecular fraction of > 50 kD.[15]

In this chapter, the distributional speciation of Hg-HS and MeHg-HS complexes in different MW size fractions was characterized using the TFUF technique. The effects of pH and concentration ratio on the size distribution as well as the dissociation kinetics for different size fractions are studied.

## 6.2 Distributional speciation of Hg-HS complexes in model HS solutions

Our results for the distributional speciation of Hg-HS complexes with different MW size fractions are shown in Table 6.1. For the system which contains 10 μg/L Hg(II) and 1 mg/L fulvic acid at pH 5, the percent Hg-HS in the size fraction > 30 kD was 73%, while 10% was < 5 kD. Upon increasing HS to 10 mg/L under the same conditions, the fraction of Hg-HS complexes with sizes > 30 kD decreased to 54%, while those < 5 kD increased to 25%. For the system containing 2.2 μg/L Hg(II) and 5 mg/L fulvic acid at pH 5, the fraction of Hg-HS in the size fraction < 5 kD was 35%. This result suggests that when the Hg/HS ratio is low, the amount of Hg-HS in the lower size fraction increases.

**Table 6.1** Distributional speciation of [Hg-HS] complexes by size fractionation with different initial [Hg] / [HS] concentration ratios at pH 5 and 9; T= 23 °C.

| Initial $[Hg^{2+}]$ µg/L | HS, mg/L | | pH ± 0.2 | $[Hg^{2+}]$ µg/L in filtrate | | | | |
|---|---|---|---|---|---|---|---|---|
| | | | | < 500 kD | < 300 kD | < 30 kD | < 5 kD | < 1 kD |
| 10.82 ± 0.13 | FA | 1 | 5 | 8.16 ± 0.13 | 4.29 ± 0.16 | 2.94 ± 0.31 | 1.08 ±0.18 | 0.31 ± 0.10 |
| 10.05 ± 0.11 | FA | 10 | 5 | 8.48 ± 0.07 | 6.06 ± 0.13 | 4.63 ± 0.21 | 2.51 ± 0.27 | 0.89 ± 0.07 |
| 2.259 ± 0.12 | FA | 5 | 5 | 1.56 ± 0.08 | 1.12 ± 0.04 | 0.83 ± 0.07 | 0.79 ± 0.06 | 0.43 ± 0.06 |
| 2.032 ± 0.08 | HA | 5 | 5 | - | 0.39 ± 0.03 | 0.26 ± 0.04 | 0.11 ± 0.04 | ≤ 0.06* |
| 2.02 ± 0.054 | HA | 5 | 9 | - | 0.66 ± 0.05 | 0.38 ± 0.04 | 0.28 ± 0.031 | 0.15 ± 0.05 |
| 2.00 ± 0.063 | HA | 1 | 9 | - | 0.41 ± 0.03 | 0.29 ± 0.05 | 0.19±0.023 | 0.096± 0.04 |

*: Limit of detection (LOD) ~ 0.05 µg/L

For systems which contain humic acid, the fraction of Hg-HS complexes in the small size fractions (< 5 kD) is lower than in the fulvic acid system, Table 6.1.

When solutions of 2.2 μg/L Hg(II) and 5 mg/L humic acid at pH 5 were fractionated, the percent Hg-HS in the size fraction < 5 kD was less than 6%. This component increased to ~ 14% when pH value was raised from 5 to 9 under the same initial conditions. The difference in Hg-HS distribution between fulvic and humic acids can be explained by the higher MW of humic acid and its higher carbohydrate content[16] found in the HMW fractions. These groups bind metal ions.

The effect of pH on the distribution of Hg-HS complexes can be explained by the conformational changes in the HS. Humic substances have been modeled as spheres that form colloids at either high concentrations or low pH values, and with linear shapes at high pH or low concentrations.[17] It also has been reported that the proton ($H^+$), divalent ($M^{2+}$) and trivalent ($M^{3+}$) metal ions can lead to aggregation of HS resulting in formation of HMW colloids.[18] The mechanism of coagulation (aggregation) can be explained by cation shielding of the HS charges, in which the negative charge of HS is compensated by the bound metal ion, leading to decrease the HS solubility in aqueous solutions. Another possible mechanism is the bridging of two or more HS molecules by metal cations.[19]

Table 6.1 shows that a relatively high percentage (50-70%) of Hg-HS was found in the size fraction > 30 kD. It is noteworthy that some evidence has been provided to suggest enrichment of Hg in the colloidal phase > 10 kD.[20] This is in agreement with our results, but we also show that Hg/HS ratio plays an important role in the distribution of Hg-HS complexes. Recently, it has been suggested that metal ions with high binding strength toward DOC are distributed more in the larger MW size fraction.[21] Mercury is

known to have high tendency to form strong complexes with DOC,[22-24] suggesting that most Hg-HS complexes will be distributed in the higher MW size fraction.

### 6.3 Kinetic speciation of the Hg-HS ultrafiltrate

Different size fractions of Hg-HS complexes separated by TFUF were studied kinetically using the CLEM technique. Figures 6.1 and 6.2 show the dissociation kinetics for different size fractions for two different concentrations of FA at pH 5. Both have the same initial Hg(II) concentration, 10 μg/L, but different HS concentrations, 1 and 10 mg/L. The results of the kinetic analysis for both systems are presented in Table 6.2. Two kinetically distinguishable components are observed in both systems. A labile component with a dissociation rate constant of $k_d \sim 2$ to $3 \times 10^{-3}$ $s^{-1}$ is predominant in the high MW fractions (> 30 kD), while the kinetically inert component with a dissociation rate constant of $k_d \sim 2$ to $4 \times 10^{-5}$ $s^{-1}$ is predominant in the low MW fractions of < 5 kD. For the system containing 1 mg/L fulvic acid, 75 ng and 173 ng Hg(II) in the 1-5 kD and < 1 kD size fractions, respectively, are kinetically inert. For the containing 10 mg/L fulvic acid, the amount of kinetically inert Hg(II) was higher, with the following distribution: 140 ng Hg(II) in the 1-5 kD size fraction and 312 ng Hg(II) in the < 1 kD size fraction. In both systems, the kinetically inert species of Hg-HS is found totally in the < 5 kD size fraction, with 70% below the 1 kD.

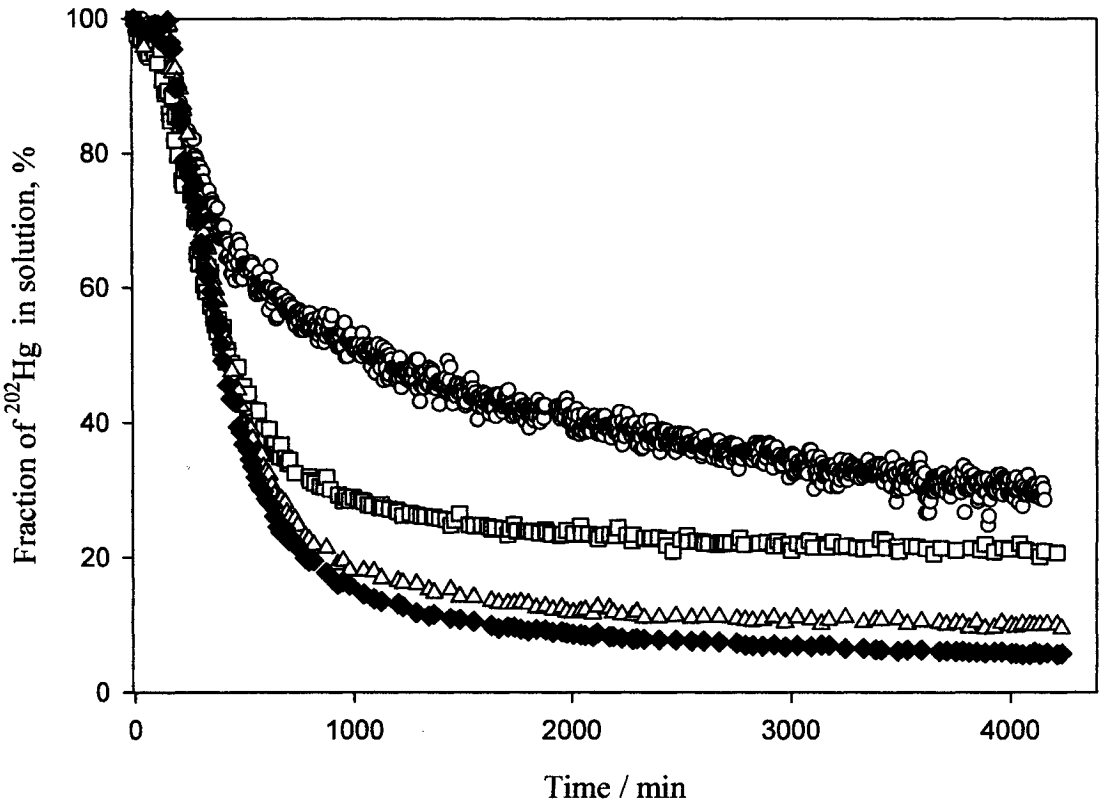


**Figure 6.1** Dissociation kinetics for different size fractions of Hg-FA complexes at pH 5, using Duolite GT-73 as the competing ligand and ICP-MS of $^{202}$Hg to measure the dissociation kinetics. [$Hg^{2+}$] = 10μg/L (~ 50 nM); [FA] = 1 mg/L; T = 23 °C.

○ 1 kD, □ 5 kD, △ 30 kD, ◆ 300 kD.

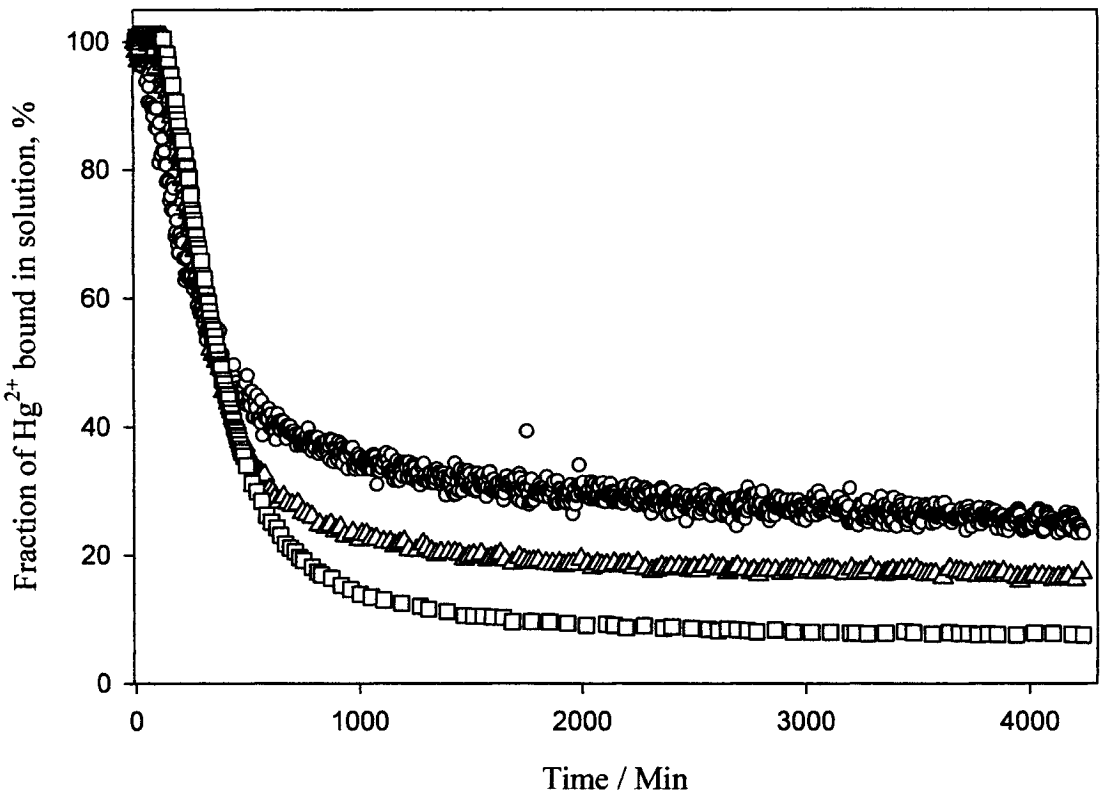


**Figure 6.2** Dissociation kinetics for different size fractions of Hg-FA complexes at pH 5, using Duolite GT-73 as the competing ligand and ICP-MS of $^{202}Hg$ to measure the dissociation kinetics. $[Hg^{2+}]$ = 10 μg/L (~ 50 nM); [FA] = 10 mg/L; T = 23 °C.

○ 1 kD, △ 5 kD, □ 30 kD.

**Table 6.2** Dissociation rate constants and distributions of the size fractions of [Hg-HS] and [MeHg-HS] complexes in aqueous solution at pH 5 and T = 23 °C.

**A-** $[Hg^{2+}]$ = 10 µg/L; [FA] = 1 mg/L.

| Fraction | $C_1$ , % | $k_1 \times 10^3$ $s^{-1}$ | $C_2$ , % | $k_2 \times 10^5$ $s^{-1}$ |
|---|---|---|---|---|
| Spiked unfiltered | ≥ 96 | 2.43 ± 0.02 | < 5 | --- |
| < 300 kD | ≥ 92 | 2.46 ± 0.04 | < 7 | --- |
| < 30 kD | ≥ 90 | 2.38 ± 0.06 | < 12 | --- |
| < 5 kD | 75 ± 5 | 2.62 ± 0.032 | 23 ± 3 | 2.29 ± 0.53 |
| < 1 kD | 45 ± 4 | 2.42 ± 0.08 | 56 ± 3 | 1.87 ± 0.23 |

**B-** $[Hg^{2+}]$ = 10 µg/L; [FA] = 10 mg/L.

| Fraction | $C_1$, % | $k_1 \times 10^3$ $s^{-1}$ | $C_2$, % | $k_2 \times 10^5$ $s^{-1}$ |
|---|---|---|---|---|
| < 5 kD | 82 ± 3 | 3.02 ± 0.04 | 18 ± 4 | 1.99 ± 0.63 |
| < 1 kD | 66 ± 4 | 3.22 ± 0.08 | 35 ± 3 | 4.03 ± 0.23 |

## 6.4 Distributional speciation and kinetic dissociation of MeHg-HS complexes in HS model solutions

The size distribution of MeHg-HS complexes under various conditions is shown in Table 6.3. Similar to the Hg-HS system, a high percentage of MeHg-HS components is found in the HMW fractions. For initial concentrations of MeHg of 5 μg/L and HA of 5 mg/L at pH 5, more than 75% of the MeHg-HS components was located in the size fractions >30 kD while only 15% was present in the size fraction < 5 kD. However, when the pH was raised from 5 to 9 under the same initial conditions, the percentage of MeHg-HS species in the size fraction > 30 kD dropped to 42%, while the amount increased to 44% in the size fraction < 5 kD. This may indicate that the hydroxide ion concentration plays an important role in the speciation of MeHg in aquatic the environment. In basic medium, formation of the hydroxide complex MeHgOH is significant. To test this hypothesis, we studied the dissociation kinetics of these size fractions of MeHg-HS complexes at pH 5 and pH 9, Figures 6.3 and 6.4. At both pH values, there are at least 2 components in the HMW (>30 kD) size fractions. The dynamic (labile) component has a dissociation rate constant of $k_d$= 1-2 × $10^{-3}$ $s^{-1}$, and another one with k= 7-9 × $10^{-4}$ $s^{-1}$. Below 30 kD, the dissociation rate constant decreased to 4-5 × $10^{-4}$ $s^{-1}$. In the size fractions < 5kD, two kinetically distinguishable components were observed: a labile one with $k_d$ = 2-3 × $10^{-3}$ $s^{-1}$ and an inert component with $k_d$ 4-5 × $10^{-5}$ $s^{-1}$. At pH 9, the labile component contributes ~77% of the MeHg complexes in the < 1 kD fraction and ~24% of the total $MeHg^+$ in the system. Since theoretical calculations show that the free $CH_3Hg^+$ can be found only in gas phase but not in water,[25] this may imply that the labile component is a

hydroxide species such as $CH_3HgOH_2^+$, $CH_3HgOH_{(aq)}$ or $(CH_3Hg)_2OH^+$. The latter is the predominant form of methyl mercury hydroxide in the pH 4-5 range.[26] For both systems at pH 5 and 9, the inert component in the size fraction < 5 kD represents ~ 300 ng/L $MeHg^+$. The results of the kinetic analysis are presented in Table 6.4.

The dissociation kinetics of MeHgHS are generally more complex than those of HgHS. In the HgHS system, two kinetically distinguishable components were observed that were easily identified in the different size fractions. In MeHgHS, two kinetically distinguished components were only observed in the < 1 kD size fraction. They were attributed to the hydroxide form ($k = 1\text{-}2 \times 10^{-3}\ s^{-1}$) and an inert complexed one ($k = 4\text{-}5 \times 10^{-5}\ s^{-1}$). In the HMW fraction (> 30 kD), a third MeHgHS component was observed with $k = 5\text{-}6 \times 10^{-4}\ s^{-1}$. The possibility that this component resulted from a mixture of the previous components is reasonable, since some fitting results (Table 6.4 with **b** sign) can separate those components.

**Table 6.3** Distributional speciation of [MeHg-HS] complexes by size fractionation at a constant [HS] concentration of 5 mg/L, at pH 5 and pH 9. T= 23 °C.

| Initial[MeHg] µg/L | HS | pH ± 0.2 | [ MeHg] µg/L in filtrate | | | | |
|---|---|---|---|---|---|---|---|
| | | | < 500 kD | < 300 kD | < 30 kD | < 5 kD | < 1 kD |
| 5.02 ± 0.12 | HA | 5 | 3.07 ± 0.13 | 1.56 ± 0.06 | 1.07 ± 0.08 | 0.76 ± 0.05 | 0.42 ± 0.07 |
| 4.85 ± 0.13 | HA | 9 | 4.11± 0.10 | 3.54 ± 0.11 | 2.8 ± 0.07 | 2.17± 0.09 | 1.53 ± 0.08 |
| 5.08 ± 0.20 | FA | 5 | 3.37 ± 0.09 | 3.2 ± 0.11 | 1.95 ± 0.09 | 1.19 ± 0.07 | 0.71 ± 0.10 |

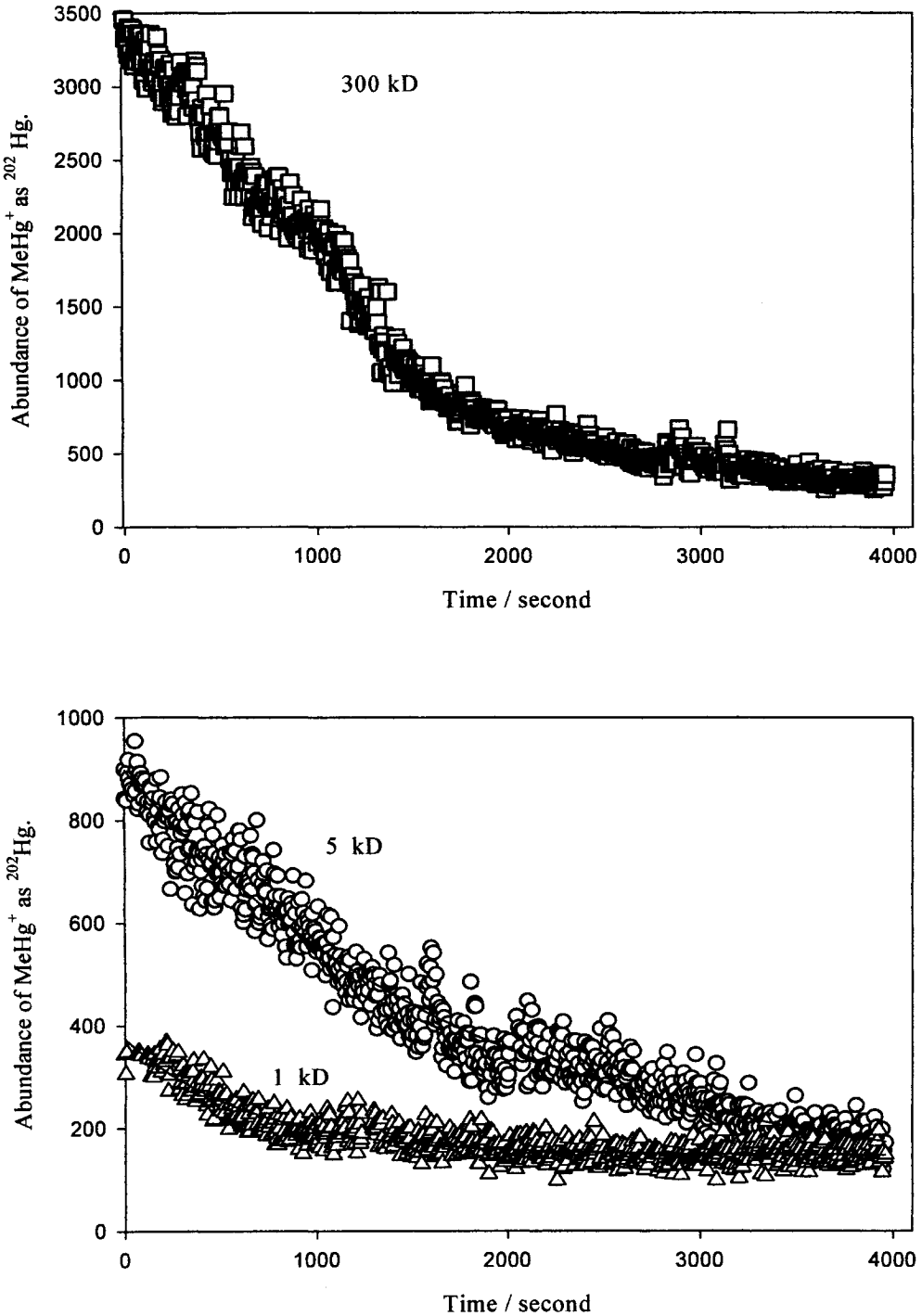


**Figure 6.3** Dissociation kinetics for different size fractions of MeHg-FA complexes at pH 5, using Duolite GT-73 Resin as the competing ligand and ICP-MS of $^{202}Hg$ to measure the dissociation kinetics. [MeHg]= 5 μg/L, [FA] = 5mg/L, T= 23 °C.

△ 1 kD, ○ 5 kD, □ 30 kD.

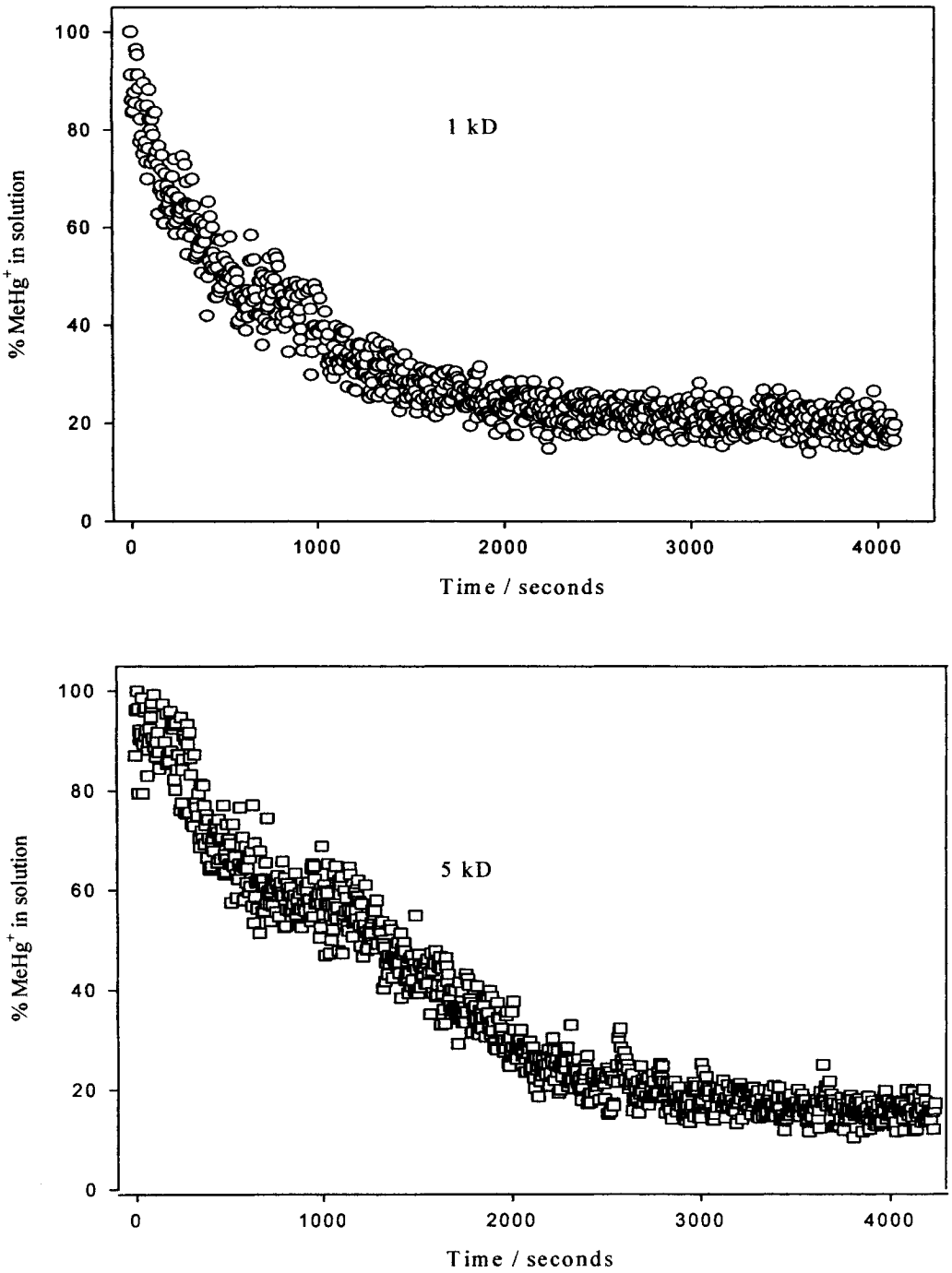


**Figure 6.4** Dissociation kinetics for different size fractions of MeHg-FA complexes at pH 9, using Duolite GT-73 Resin as the competing ligand and ICP-MS of $^{202}Hg$ to measure the dissociation kinetics. [MeHg]= 5 μg/L, [HA] =5mg/L, T=23 °C.

○ 1 kD, □ 5 kD.

**Table 6.4** The dissociation rate constants and their distributions of the different size fractions of [MeHg-HS] complexes in different aqueous solution at T = 23 °C.

| Size fraction in KD | $C_1$, % | $k_1 \times 10^3$, $s^{-1}$ | $C_2$, % | $k_2 \times 10^4$, $s^{-1}$ | $C_3$, % | $k_2 \times 10^5$, $s^{-1}$ |
|---|---|---|---|---|---|---|
| **A-** [MeHg] = 5µg/L, FA = 5mg/L and pH 5 | | | | | | |
| 300[a] | --- | --- | >90[c] | 7.12 ± 2.06 | --- | --- |
| 30[a] | --- | --- | > 90[c] | 9.24± 1.49 | --- | --- |
| 30[b] | 73± 7 | 1.07 ± 0.56 | 23 ± 6 | 1.32 ± 0.58 | | |
| 5[a] | --- | --- | >90[c] | 4.2 ± 0.83 | --- | --- |
| 5[b] | --- | --- | 82 ± 7 | 5.92 ± 1.86 | 17 ± 5 | 8.12 ± 1.32 |
| 1[b] | 59± 4 | 2.93 ± 0.872 | --- | --- | 40± 3 | 5.1 ± 0.13 |
| **B-** [MeHg] = 5µg/L, HA = 5mg/L and pH 9. | | | | | | |
| 300[a] | >92[c] | 1.08 ± 0.06 | --- | --- | | |
| 30[a] | --- | --- | >88[c] | 7.92 ± 0.56 | | |
| 5[a] | --- | --- | >90[c] | 6.27 ± 0.40 | | |
| 1[b] | 77 ± 3 | 1.97 ± 0.36 | --- | --- | 22 ± 4 | 4.6 ± 0.28 |

**a**: fitted to one component system, **b**: fitted to two component system **c**: percentage estimated from plateau in the curve fit.

## 6. 5 Application to Ottawa River water samples

Water samples from the Ottawa River at Aylmer were collected in August and September 2004. The physical and chemical properties of the samples are presented in Table 6.5. Because of the very low mercury concentrations in the Ottawa River water samples, which is below the detection limit of the ICP-MS, we artificially spiked the samples with either 2 μg/L $Hg^{2+}$ or 4 μg/L $MeHg^{+}$.

### *6.5.1 Distributional speciation of Hg(II) and $MeHg^{+}$ in the Ottawa River*

The results of the size fractionation of the spiked water samples from the Ottawa River are presented in Table 6.6. As in the model solutions, a relatively high percentage of Hg-DOC complexes were found in the high MW fractions > 30 kD. Approximately 62% of the Hg-DOC was found in the size fraction > 30 kD while 20% was found in the < 5 kD fraction. For MeHg complexes, 48% was found in the size fraction > 30 kD and 31% below 5 kD. The relatively high percentage of MeHg in the LMW (< 5 kD) is believed to be due to the formation of MeHg hydroxide complexes.

**Table 6.5** Physical and chemical properties of Ottawa River water samples.

| Parameter | Value |
|---|---|
| pH | 7.5 |
| T / °C | 18.7-19.1 |
| Color | Pale-Yellow |
| DOC (mg/L) | 6.2 |
| $Ca^{2+}$ ( mg/L) | 8.3 |
| $SO_4^{2-}$(mg/L) | 7.4 |
| $Cl^-$ (mg/L) | 2.8 |

**Table 6.6** Distributional speciation of Hg(II) and $MeHg^+$ for different size fractions as a result of spiking samples of the 0.45 μm filtrate of Ottawa River water with Hg(II) or $MeHg^+$, T = 23 °C.

| Spiked species / concentration (μg/L) | Concentration( μg/L ) in filtrate | | | | |
|---|---|---|---|---|---|
| | < 500 kD | < 300 kD | < 30 kD | < 5 kD | < 1 kD |
| Hg(II) / 2.08 ± 0.04 | 1.30 ± 0.05 | 1.13 ± 0.03 | 0.78 ± 0.04 | 0.41 ± 0.03 | 0.22 ± 0.05 |
| $MeHg^+$ / 4.08 ± 0.094 | 2.68 ± 0.05 | 2.51 ± 0.07 | 2.1 ± 0.08 | 1.28 ± 0.04 | 0.97 ± 0.06 |

6.5.2 *Kinetic speciation of Hg(II) and MeHg(I) in Ottawa River water filtrate*

The dissociation kinetics for different size fractions from Hg(II)-spiked Ottawa River water samples are shown in Figure 6.5. As with the model solutions, two kinetically distinguishable components were observed (Table 6.7). The labile component had a dissociation rate constant $k_d$ of ~ $2 \times 10^{-3}$ $s^{-1}$ to $3 \times 10^{-3}$ $s^{-1}$, similar to that of the model solutions. However, the more inert component had a higher dissociation rate constant, $k_d$ ~ 1.0-2.0 $\times$ $10^{-4}$ $s^{-1}$. The presence of other metal ions and cations, or the type and composition of DOC, may have caused this deviation. It has been reported that in the presence of 2.5 mM $Ca^{2+}$ and pH 7 - 8, the humic substances coagulate.[27] This leads to a decrease in the complexation ability of DOC toward metals, due to precipitation or sedimentation.

The amount of reduced sulfur in DOC is probably the most important factor that affecting the lability of Hg-HS complexes. It may explain differences in kinetic dissociation between the model solutions and Ottawa River water samples.

The results in Table 6.7 show that Ottawa River water samples have the ability to strongly complexe 187 ng Hg(II)/L (93 nM kinetically more inert), of which 53% was found in the 1-5 kD size fraction, 42% in the < 1 kD size fraction and ~ 5% in the 5-30 kD size fraction.

The dissociation kinetics of the MeHg-DOC complex in Ottawa River water are shown in Figure 6.6. For the system containing 2 μg/L of MeHg, two kinetically distinguishable components were observed. The first has $k_d = 2.36 \times 10^{-3}$ $s^{-1}$ and constitutes 46% of the total MeHg. The second component constitutes 54%, with a slower dissociation rate constant of $k_d = 4.7 \times 10^{-4}$ $s^{-1}$.

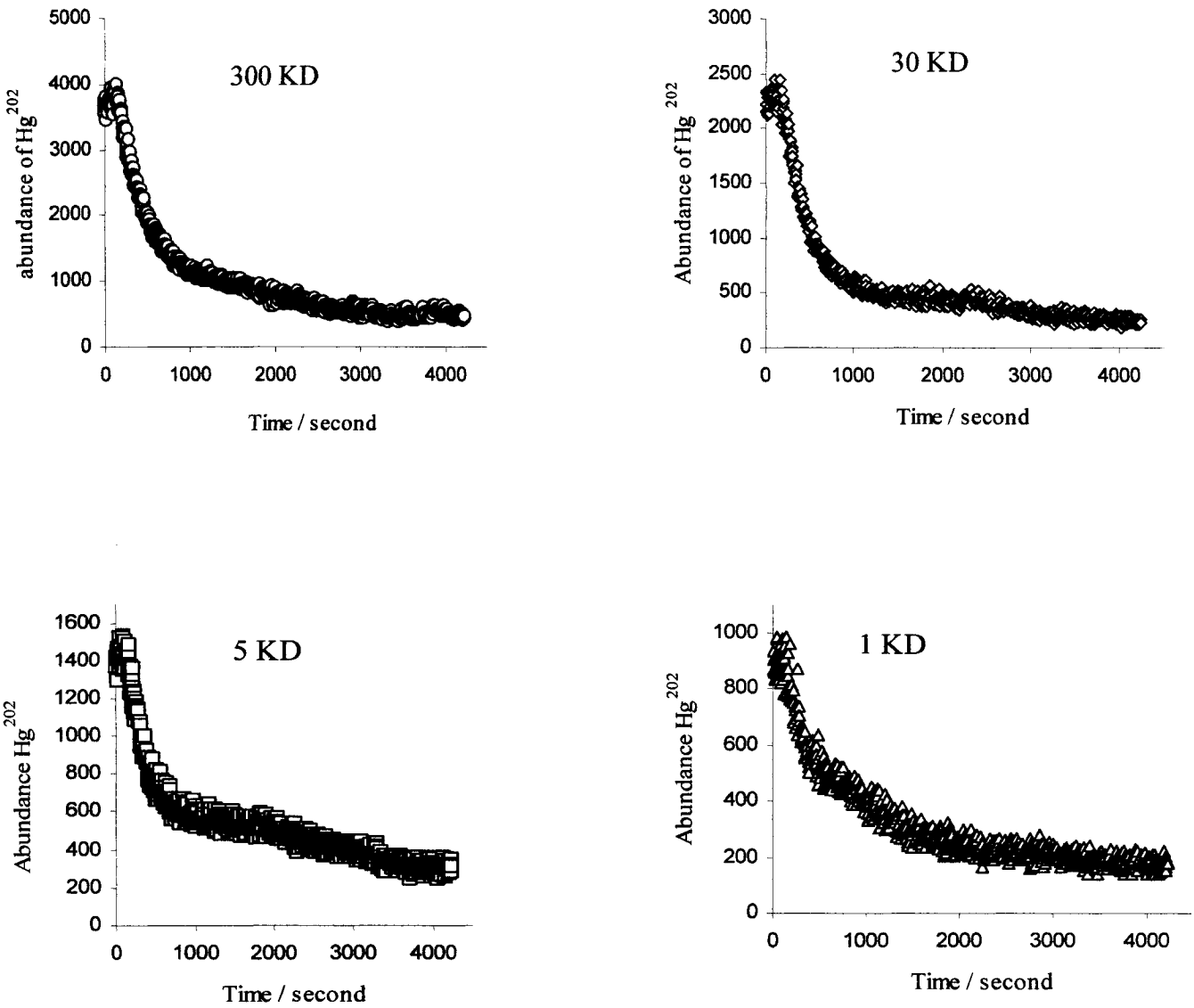


**Figure 6.5** Dissociation kinetics for different size fractions of Hg-DOC complexes in mercury spiked water samples from the Ottawa River, using Duolite GT-73 as the competing ligand and ICP-MS of $^{202}Hg$ to measure the dissociation kinetics.

**Table 6.7** Dissociation rate constants for different size fractions of [Hg-DOC] complexes in Ottawa River water samples, as a result of spiking the 0.45 μm filtrate with 2.08 ± 0.04 μg/L $Hg^{2+}$ as HgO.

| Fraction | $C_1$ / % | $k_1$ / $10^3$ $s^{-1}$ | $C_2$ / % | $k_2$ / $10^5$ $s^{-1}$ |
|---|---|---|---|---|
| Spiked of 0.45 um filtrate | ≥ 90 | 1.37 ± 0.06 | < 10 | - |
| < 500 KD | ≥ 83 | 1.08 ± 0.05 | < 15 | - |
| < 30 KD | 75 ± 3 | 2.37 ± 0.07 | 24 ± 4 | 20.5 ± 3.4 |
| < 5 KD | 55 ± 3 | 3.27 ± 0.07 | 43 ± 5 | 14.4 ± 2.0 |
| < 1 KD | 65 ± 3 | 1.74 ± 0.08 | 35 ± 2 | 10.5 ± 3.0 |

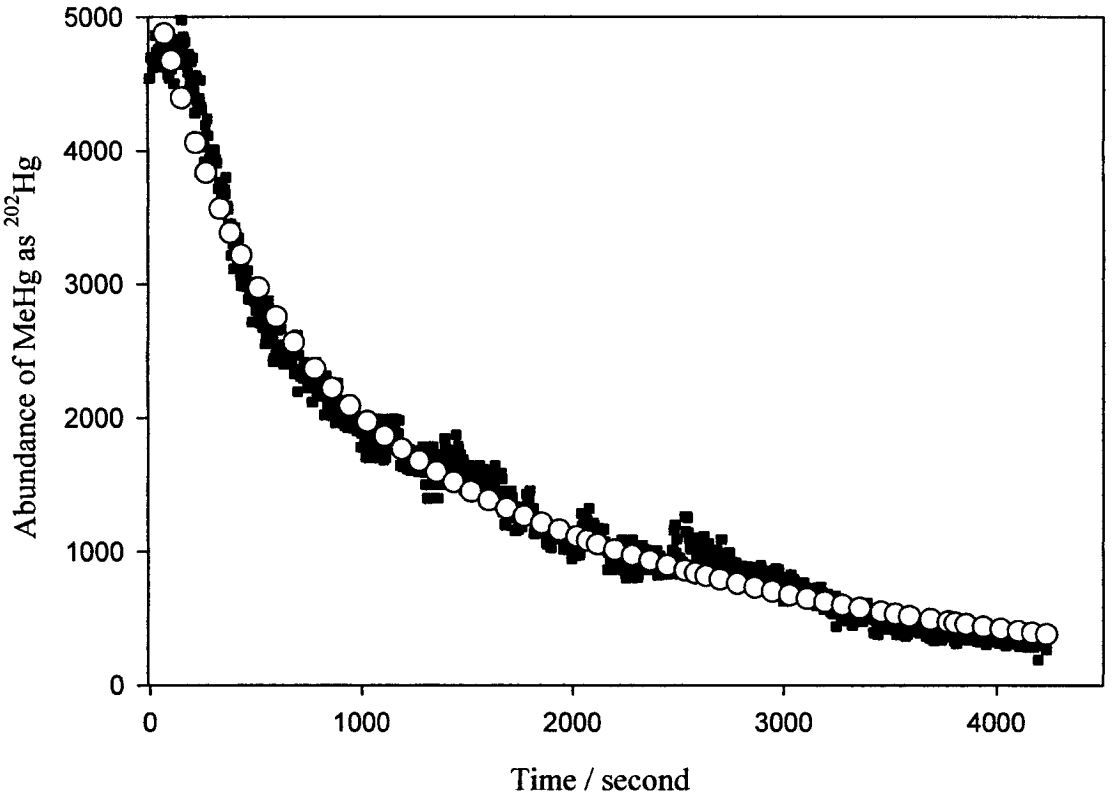


**Figure 6.6** Dissociation kinetics for MeHg-DOC complexes in spiked water sample from Ottawa River, using Duolite GT-73 as the competing ligand and ICP-MS of $^{202}$Hg to measure the dissociation kinetics. (■ experimental, ○ calculated)

The 0.45 μm filtrate of Ottawa River water samples was spiked with (2.14 ± 0.14) μg/L $MeHg^+$.

The second slow component ($k_d$= 4.7 × $10^{-4}$ $s^{-1}$) may associate with another slower component(s). Analysis of the 5 kD fraction (Figure 6.7), which contains 1.28 μg/L MeHg, shows that a slower component with $k_d$= 8.5 × $10^{-5}$ $s^{-1}$ contributes 26% of this fraction, while 64% of this fraction dissociates faster, with $k_d$= 2.19 × $10^{-3}$ $s^{-1}$.

We conclude that, in Ottawa River water samples, MeHg is complexed 50-75% to DOC; only 8-15 % belongs to the kinetically inert component with $k_d$ ~ $10^{-5}$ $s^{-1}$. The latter represents 300-350 ng/L of MeHg, most was found in the 1-5 kD size fraction. A significant percentage (> 80 %) of the 1 kD size fraction contains the labile component, with kd~ $10^{-3}$ $s^{-1}$. This represents more than 20% of total MeHg. The high initial concentration of MeHg used in these experiments (2-4 μg/L) may result in this high percentage of uncomplexed MeHg; at the low concentrations relevant to natural waters, a high percentage of MeHg may be strongly complexed to DOC.

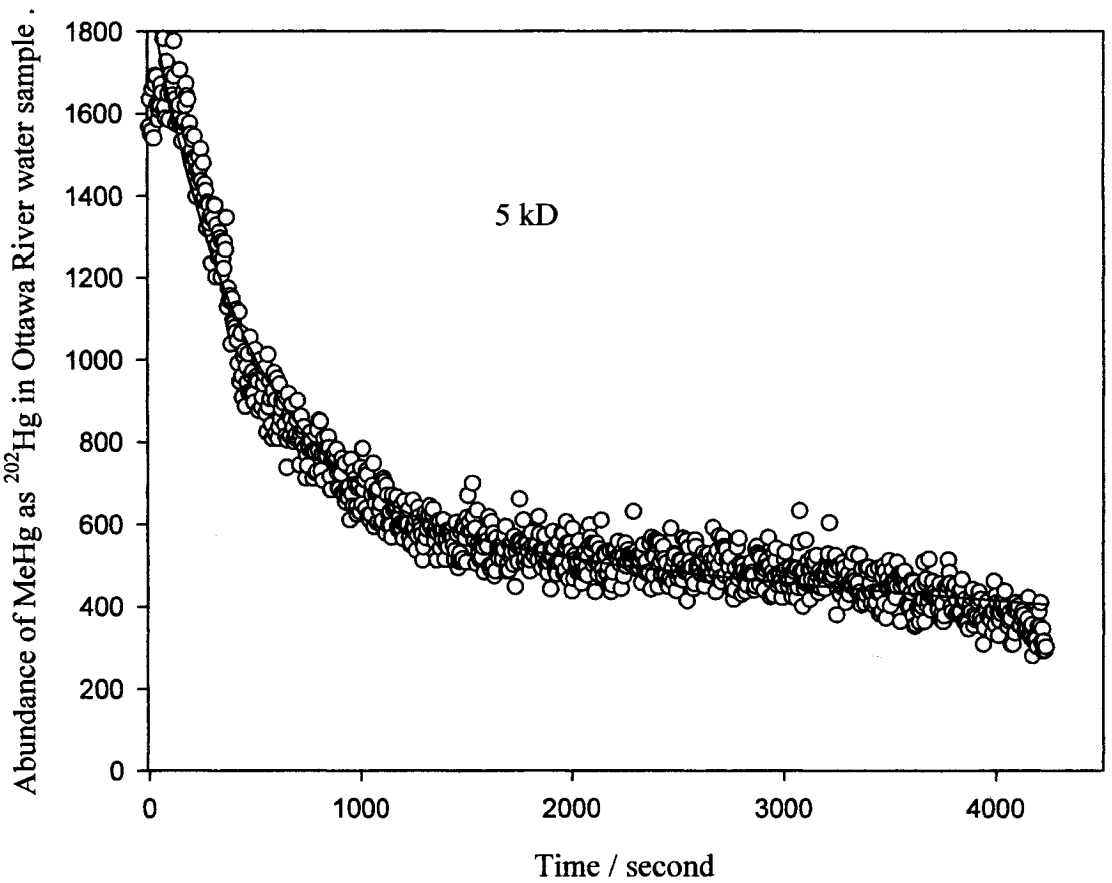


**Figure 6.7** Dissociation kinetics for the size fraction < 5 kD of MeHg-DOC in spiked water samples from Ottawa River, using Duolite GT-73 as the competing ligand and ICP-MS of $^{202}$Hg to measure the dissociation kinetics.

### 6.5.3 *Comparison between Hg(II) and other heavy metal ions in Ottawa River water*

To study the effects of trace metal ions on the dissociation kinetics of Hg-DOC complexes in Ottawa River water, samples were spiked with Pb(II) and Cd(II). Both copper and zinc were detected at high concentrations without spiking.

The distributional speciation of these metal ions in Ottawa River water samples is presented in Table 6.8. This table shows that 75, 40, and 35 % of DOC complexes of Pb(II), Cd(II) and Zn(II), respectively, were found in the size fractions > 30 kD, while 7, 35, and 49% were found in the size fraction < 5 kD.

It has been shown that the carbohydrate moiety in DOC occurs in the molecular weight fraction > 10 kD.[9,28,29] Polysaccharides and carbohydrates associate efficiently with metal ions[28] and this may explain the high proportion of dissolved metal ions in high MW fractions. Various studies have shown that the majority of trace metal ions like Cu, Zn, and Cd are associated with the colloidal material in natural waters.[30-32] However, it has been reported that the aliphatic character of DOC increases as the MW increases, while the low MW fraction (< 10 kD) contains more aromatics and carboxylic groups.[10] This implies that the low MW fraction of DOC has the highest affinity toward metal ions. According to a recent review,[5] the majority of trace metal ions like Cu, Zn, Cd, and Ni in freshwater systems are found in the size fraction < 1kD. The origin of this apparent contradiction in the literature may be the difference in the ratio of metal ion to DOC concentration, the nature of DOC or the presence of other cations such as $Ca^{2+}$ and $Mg^{2+}$ and the pH.

**Table 6.8** Distributional speciation of some metal ions by size fraction, metal ions are naturally occurring in Ottawa River water samples or artificially spiked

| Metal ions | Concentration of metal ions in different size fractions (filtrates), µg/L. | | | | | |
|---|---|---|---|---|---|---|
| | 0.45 µm filtrate | < 500 kD | < 300 kD | < 30 kD | < 5 kD | < 1 kD |
| Cu found | 3.21 ± 0.05 | -- | -- | -- | -- | -- |
| Pb(II) spiked | 2.01± 0.006 | 1.07 ± 0.02 | 0.504 ± 0.001 | 0.18 ± 0.001 | 0.15 ± 0.003 | 0.13 ± 0.002 |
| Cd(II) spiked | 1.04 ± 0.001 | 1.01 ± 0.01 | 0.72 ± 0.003 | 0.63 ± 0.001 | 0.36 ± 0.003 | 0.064±0.001 |
| Zn found | 6.02 ± 0.41 | 5.6 ± 0.29 | 4.58 ± 0.18 | 3.90 ± 0.33 | 2.94 ± 0.25 | 1.94 ± 0.19 |

In order to study the kinetic dissociation of these trace metal ion complexes with DOC, we replaced the Duolite GT-73 by Chelex-100. The latter is a resin based on iminodiacetic acid. It has been used in different studies of metal speciation in water.[33-35] The carboxylate group is a suitable choice for complexing the metal ions in this study. Figure 6.8 shows the kinetics of dissociation of various metal complexes in the Ottawa River water samples. It is clear that Hg(II), Cu(II), and Pb(II) tend to be complexed to a greater extent than Cd(II) and Zn(II). This is in good agreement with their affinities to organic ligands.

Analysis of the kinetic data by non-linear regression to equations 5.10 or 5.12 shows that for Hg(II), Cu(II) and Pb(II), there is a major component which dissociates very slowly. For Cd(II) and Zn(II), two kinetically distinguishable components are observed for both metal ions. The results of the analysis are presented in Table 6.9.

If the kinetic stability of a metal ion complexe is directly related to its conditional stability constants, the affinity of these ions toward DOC is:

$$Hg(II) > Cu(II) > Pb(II) > Cd(II) \geq Zn(II).$$

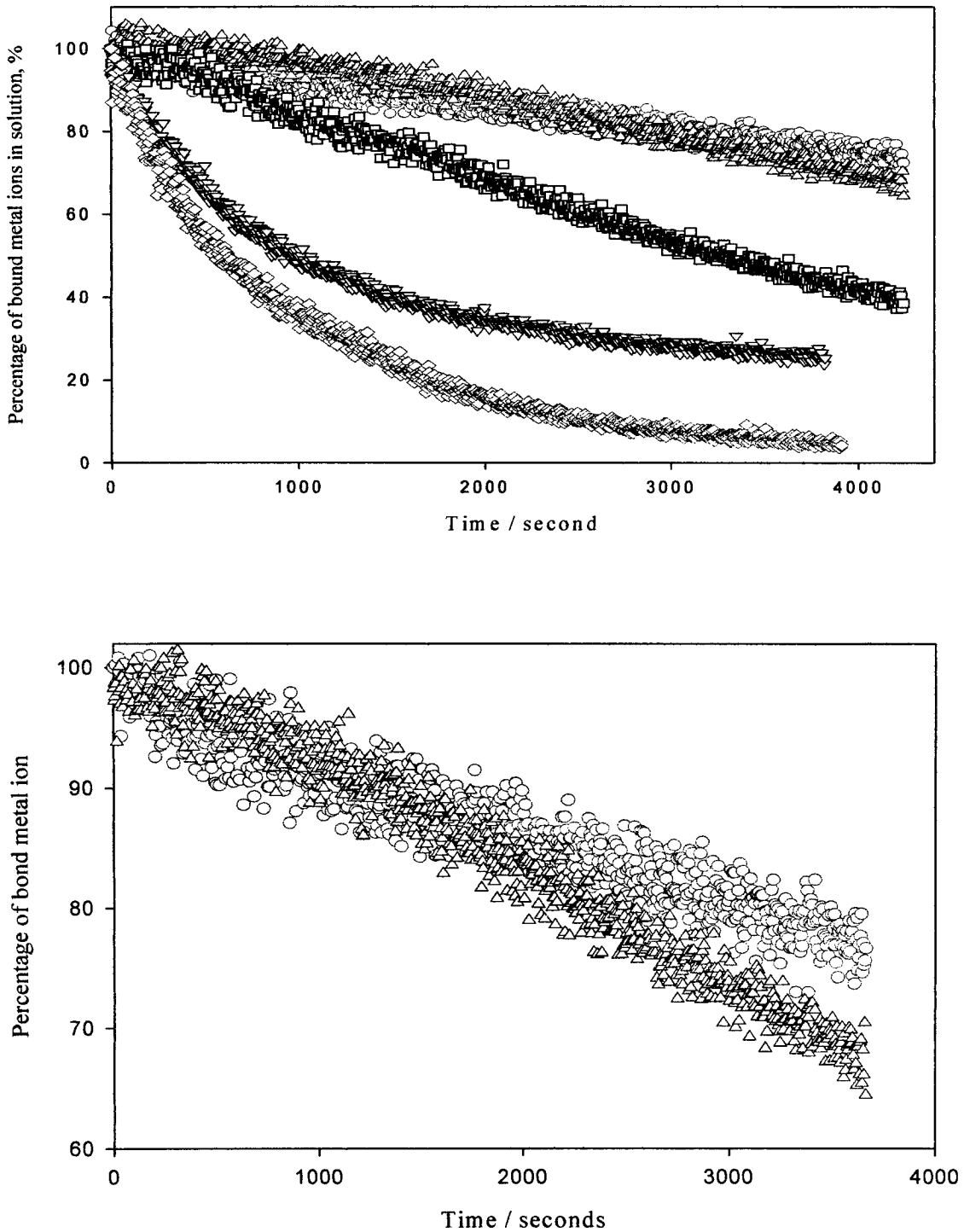


**Figure 6.8** Kinetic speciation of trace metals in a freshwater sample collected from the Ottawa River using Chelex-100 as the competing ligand and ICP-MS to measure the dissociation kinetics. ○Hg, △ Cu, □ Pb, ▽ Cd, ◊ Zn (upper graph for all data, lower graph: data for $Hg^{2+}$& $Cu^{2+}$ expanded)

**Table 6.9** Dissociation rate constants and distributions of metal complexes in Ottawa River water samples, using Chelex-100 as the competing ligand.

| Metal | $C_1$ / % | $k_1$ / $10^3$ $s^{-1}$ | $C_2$ / % | $k_2$ / $10^5$ $s^{-1}$ |
|---|---|---|---|---|
| Hg(II) | < 3 | - | ≥ 98 | 9.1 ± 1.5 |
| Cu(II) | < 3 | - | ≥ 98 | 9.8 ± 2.3 |
| Pb(II) | < 4 | - | ≥ 95 | 18.4 ± 1.4 |
| Cd(II) | 51 ± 3 | 1.55 ± 0.28 | 48 ± 4 | 25.5 ± 7.1 |
| Zn(II) | 71 ± 4 | 2.88 ± 0.19 | 28 ± 5 | 65.7 ± 10.0 |

The two components of Hg-HS reported many times in this work appeared as one slow component when the GT-73 resin was replaced by Chelex-100. This provides good evidence that the labile component (fast) observed with GT-73, is mainly formed by (Hg-O) interactions. This implies that a carboxylate and /or a phenolate complexation of Hg(II) are dominant. Such strong complexes are relatively weaker than Hg-S complexes, so GT-73 with its dithiolate functionality can easily trap and replace Hg-O by Hg-S complexes. This allows the determination of the labile component. The kinetically inert component is attributed to strong Hg-S complexation in HS. GT-73 may compete with such ligands depending on their concentration.

Chelex-100 has carboxylate functional groups. The labile Hg(II)-HS component with Hg-O interactions (carboxylate and phenolate) competes with Chelex-100 for Hg(II). As a result, the two components of Hg(II) appeared as a single slow component when Chelex-100 is used.

Our work shows that copper has only one kinetically inert component, with a dissociation constant of ~$9.8 \times 10^{-5}$ $s^{-1}$. This component represents more than 98% of the total dissolved copper and is in good agreement with recent studies[36,37] showing that the DOC of freshwaters (lakes and rivers) has a high complexing capacity toward Cu, with conditional stability constants in the range (log K =7.52 –10.3).

The dissociation kinetics of various metal ion complexes (M-DOC) in the size fraction < 1 kD show that these complexes are kinetically more inert (slower) compared to the HMW fractions. The dissociation rate constant for Pb(II) complexes in the 1 kD fraction (Figure 6.9), $k_d$= 2-5 $\times 10^{-5}$ $s^{-1}$ is slower than in the HMW fractions ($k_d$= 18.4 $\times$ $10^{-5}$ $s^{-1}$). Analysis of the dissociation kinetics of Cd(II) in the <1 kD fraction (Figure

6.10) yields $k_d = 2.4 \times 10^{-4}$ $s^{-1}$. Even though this fraction is totally inert but it represents only 13% of the total inert components of Cd(II)-HS complex. The rest (87%) may be represented in other fractions. The kinetically inert species of Cd(II) may be a result of Cd-S interactions. Recently,[38] it has been reported that at very low Cd(II) concentrations, and in the presence of HS, Cd(II) can form 4 and 6 coordinate complexes. In the 4-coordinate complexes, two reduced sulfur atoms were involved. However, $^{113}Cd$ NMR shows that Cd(II) predominantly form complexes with O-donor ligands in humic substances.[39]

The inert component for Zn(II) is totally recovered (found) in the 1 kD fraction (Figure 6.11), with $k_d = 2.5 \times 10^{-4}$ $s^{-1}$. This result again illustrates the importance of this size fraction (< 1 kD) in the metal ion complexation.

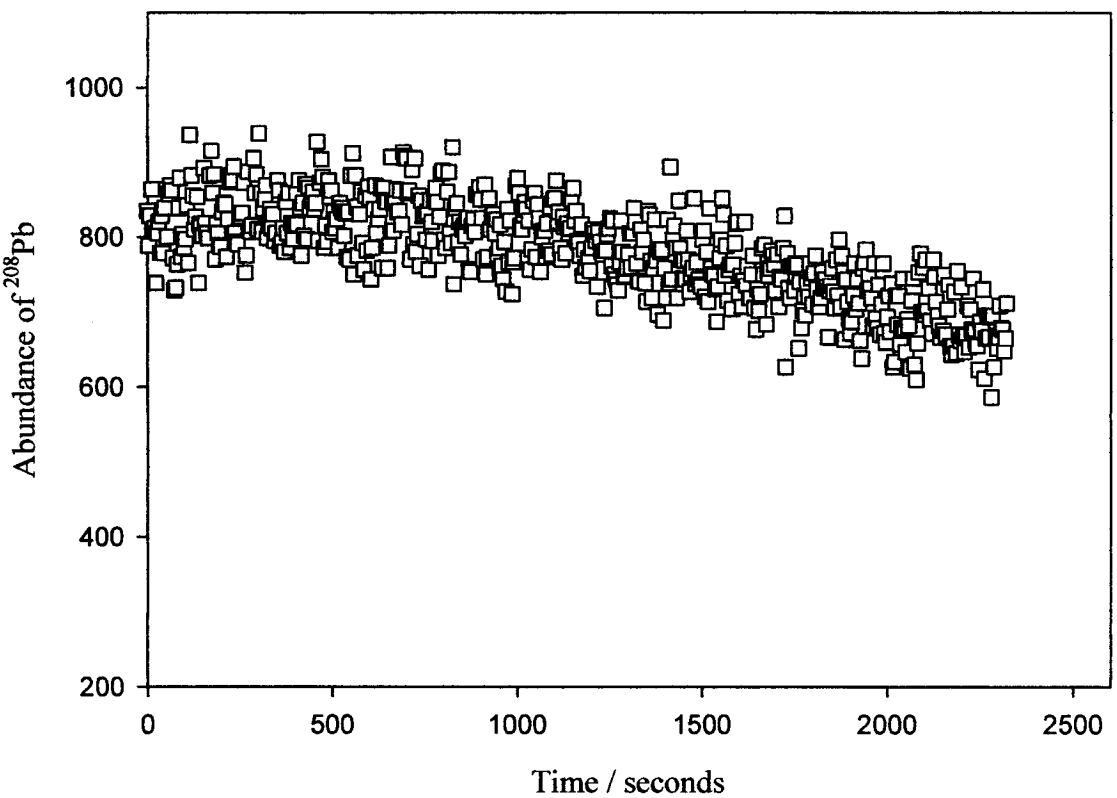


**Figure 6.9** Dissociation kinetics for Pb(II) in the <1 kD size fraction of Ottawa River water, using Chelex-100 as the competing ligand and ICP-MS to measure $^{208}$Pb in solution.

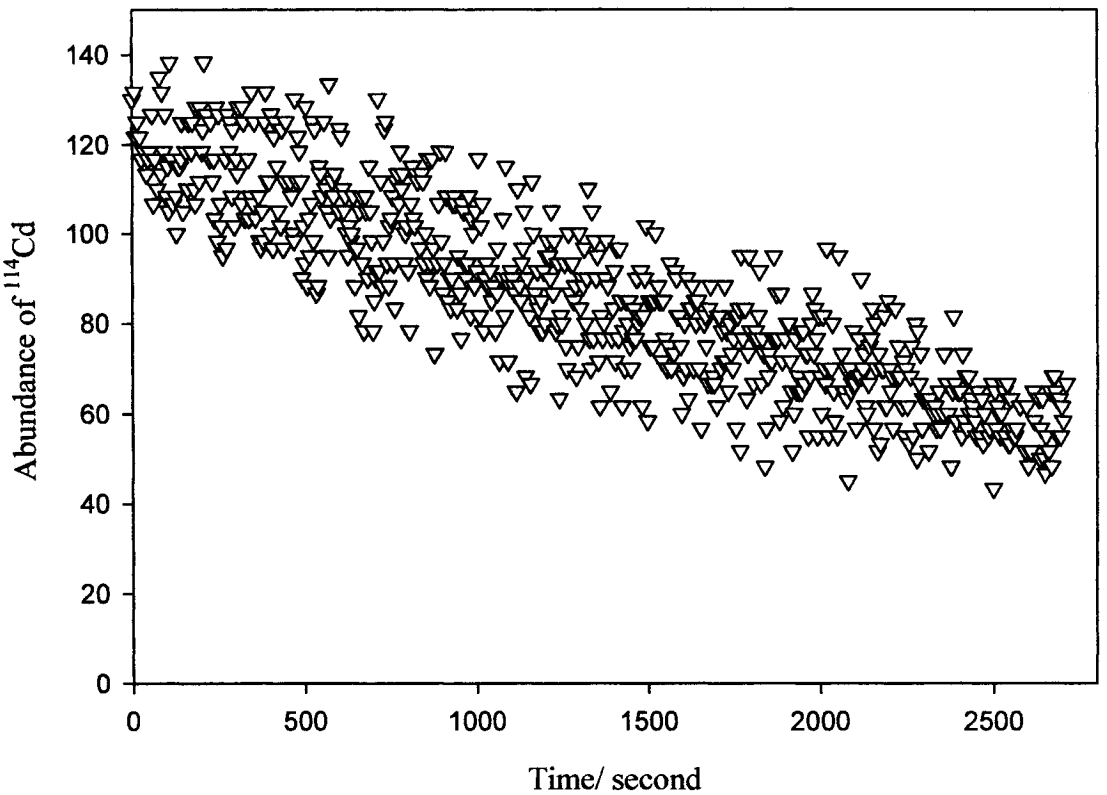


**Figure 6.10** Dissociation kinetics for Cd(II) in the <1 kD size fraction of Ottawa River water, using Chelex-100 as the competing ligand and ICP-MS to measure $^{114}$Cd in solution.

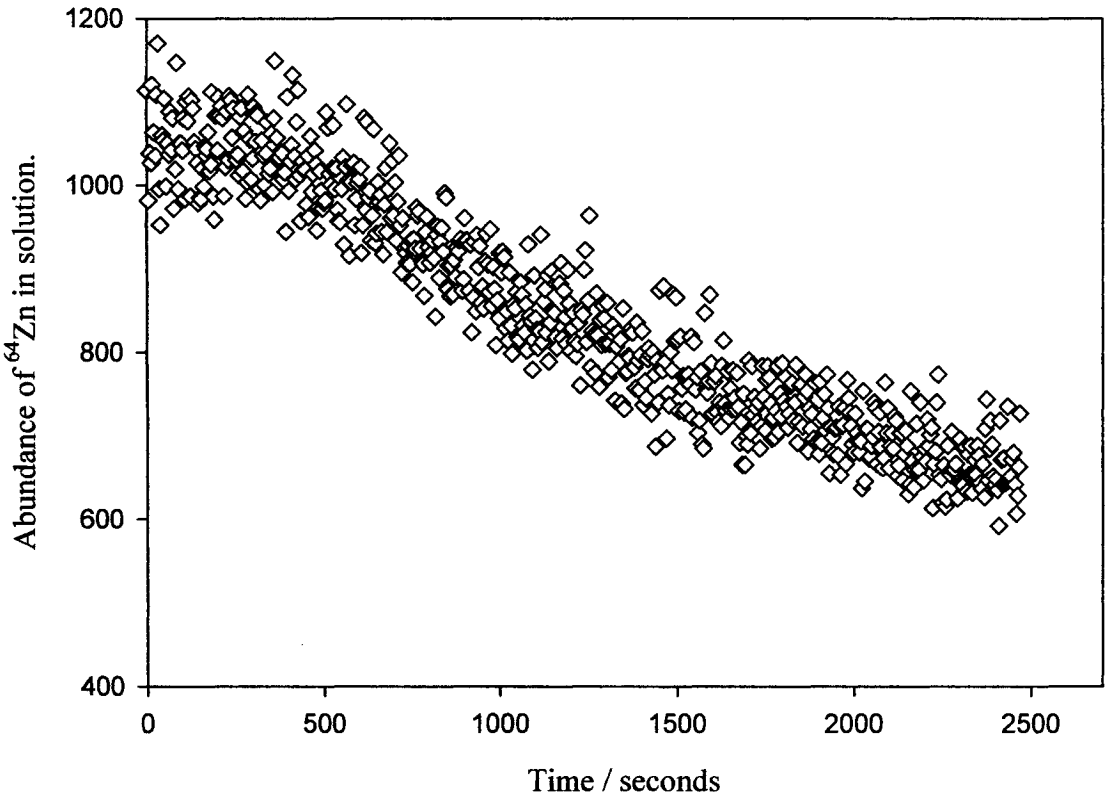


**Figure 6.11** Dissociation kinetics for Zn(II) in the <1 kD size fraction of Ottawa River water, using Chelex-100 as the competing ligand and ICP-MS to measure $^{64}$Zn in solution.

## 6.6 Conclusions

The size distributional speciation of Hg-HS and MeHg-HS shows that an appreciable fraction of these complexes is found in the colloidal phase of > 30 kD. For solutions of 10 mg/L Suwannee River fulvic acid and 10 μg/L Hg(II) at pH 5, the distribution of Hg-FA shows 54% in size fraction >30 kD and 25% in size fraction < 5 kD. This distribution is affected by the Hg/HS ratio. When this ratio is low, more Hg-HS is found in the lower size fractions < 5 kD. The pH of the solution also affects this distribution by changing the conformational structure of HS. At high pH, more Hg-HS and MeHg-HS are found in the low size fractions. The formation of MeHg hydroxide complexes is enhanced at high pH values. For artificially spiked freshwater (Ottawa River), both $MeHg^+$ and Hg(II) complexes of DOC were found at ≥ 50% in the colloidal phase, >30 kD.

From a kinetic point of view, the Hg-HS complexes can be described by two kinetically distinguishable components. The labile component, with a dissociation rate constant on the order of $10^{-3}$ $s^{-1}$ is predominant in the HMW size fractions. The inert component, with a dissociation rate constant on the order of $10^{-5}$ $s^{-1}$ is predominant in the LMW size fractions < 5 kD, with 70 % below 1 kD. This kinetic distribution of Hg-DOC is also observed in spiked Ottawa River water samples.

In the system MeHg-HS, the kinetically inert component was observed in the fraction < 5kD, but unlike Hg-HS, in the size fraction < 1 kD MeHg-HS is 75% labile. This may be due to the formation of MeHgOH. In artificially spiked Ottawa River water samples ~ 23 % of $MeHg^+$ is very weakly bound or not complexed at all. Between 300-

350 ng/L is strongly complexed to DOC and found in the 1-5 kD size fraction, with $k_d$ in the order of $10^{-5}s^{-1}$.

In Ottawa River water samples containing various metal ions, we find that Hg(II), Cu(II), and Pb(II) tend to be complexed to a greater extent than Cd(II) or Zn(II). This is in good agreement with their affinities for organic ligands. The LMW size fractions < 5 kD are very important for complexing metal ions. The kinetically inert component ($k_d$= $10^{-4}s^{-1}$) of Zn(II) complexes was totally recovered in the <1 kD fraction. Cd(II) and Pb(II) complexes are also inert in this size fraction , but the inert fractions are also distributed in other LMW size fractions.

**References**


(1) Eyrolle, F.; Benedetti, M. F.; Benaim, J. Y.; Février, D. *Geochim. Cosmochim. Acta* **1996**, *60*, 3643-3656.

(2) Alpatova, A.; Verbych, S.; Bryk, M.; Nigmatullin, R.; Hilal. N. *Sep. Pur. Technol.* **2004**, *40*, 155-162.

(3) Hoffmann, S. R.; Shafer, M. M.; Babiarz, C. L.; Armstrong, D. E. *Environ. Sci. Technol.* **2000**, *34,* 3402-3427.

(4) Guo, L.; Wen, L-S.; Tang, D.; Santschi, P. H. *Mar. Chem.* **2000**, *69*, 75-90.

(5) Town, R. M.; Filella, M. *Rev. Environ. Sci. Bio.Technol.* **2002**, *1,* 277-297.

(6) Wu, F.; Tanoue, E.; *Org. Geochem.* **2001**, *32*, 11-20.

(7) Hill, J. R. M.Sc thesis: Ottawa University, Ottawa-Canada. **2005**.

(8) Amon, R. M. W.; Benner, R. *Limnol. Oceanogr.* **1996**, *41*, 41-51.

(9) Engelhaupt, E.; Bianchi, T. S. *Limnol. Oceanogr.* **2001**, *46*, 917-926.

(10) Shin, H-S.; Monsallier, J. M.; Choppin, G. R. *Talanta* **1999**, *50*, 641-647.

(11) Maurice, P.; Pullin, M. J.; Cabaniss, S. E.; Zhou, K.; Dejanovic, K. N.; Aiken, G. R. *Water Res.* **2002**, *36*, 2357-2371.

(12) Chin, Y-P.; Aiken, G. R.; O' Loughlin, E. *Environ. Sci. Technol.* **1994**, *29*, 1853- 1858.

(13) Cabaniss, S. E.; Zhou, Q.; Maurice, P. A.; Chin, Y-P.; Aiken, G. R. *Environ. Sci. Technol.* **2000**, *34*, 1103-1109.

(14) Rostad, C. E.; Leenheer, J. A. *Anal. Chim. Acta* **2004**, *523*, 269-278.

(15) Ater, B.; Burba, P.; Broekaert, J. A. C. *Fresenius J. Anal. Chem.* **1996**, *354*, 722- 728.

(16) Jahnel, J. B.; Frimmel, F. H. *Acta Hydrochim. Hydrobio.* **1995**, *23*, 31-35.

(17) Ghosh, K.; Schnitzer, M. *Soil Sci.* **1980**, *129*, 266-276.

(18) Myneni, S. C. B.; Brown, J. T.; Martinez, G. A.; Meyer, I. W. *Science* **1999**, *286*, 1335-1337.

(19) Tipping, E. Cation binding by humic substances; Cambridge University Press: UK, 2002.

(20) Babiarz, C. L.; Hurley, J. P.; Krabbenhoft, D. P.; Gilmourt, C.; Branfireum, B. A. *Sci. Tot. Environ.* **2003**, *304*, 295-303.

(21) Wu, F.; Evans, D.; Dillon, P.; Schiff, S. *J. Anal. At. Spectrom.* **2004**, *19*, 979-983.

(22) Haitzer, M.; Aiken, G. R.; Ryan, J. N. *Environ. Sci. Technol.* **2003**, 37, 2436-2441.

(23) Benoit, J. M.; Mason, R. P.; Gilmour, C. C.; Aiken, G. R. *Geochim. Cosmochim. Acta.* **2001**, *65*, 4445-4451.

(24) Lamborg, C. H.; Tseng, C-M.; Fitzgerald, W. F.; Balcom, P. H.; Hammerschmidt, C. R. *Environ. Sci. Technol.* **2003**, *37*, 3316-3322.

(25) Tossel, J. A. *J. Phys. Chem. A.* **1998**, *102*, 3587-3591.

(26) Libich, S.; Rabenstein, D. L. *Anal. Chem.* **1973**, *45*, 118-124.

(27) Aoustin, E.; Schafer, A. I.; Fane, A. G.; Waite, T. D. *Sep. Pur. Technol.* **2001**, *22-23*, 63-78.

(28) Quigly, M. S.; Santschi, P. H.; Hung, C. C.; Guo, L.; Honeyman, B. D. *Limnol. Oceanogr.* **2002**, *47*, 367-377.

(29) Haiber, S.; Herzog, H.; Burba, B.; Gosciniak, B.; Labert, J. *Fres. J. Anal. Chem.* **2001**, *371*, 457-460.

(30) Hart, B. T.; Sdrauling, S.; Jones, M. J. *Aust. J. Mar. Freshwater Res.* **1992**, *43*, 457-489.

(31) Burba, P.; Vanden Bergh, J.; Klockow, D. *Fres. J. Anal. Chem.* **2001**, *371*, 660-669.

(32) Orlandini, K. A.; Penrose, W. R.; Harvey, B. R.; Lovett, M. B.; Findlay, M. W. *Environ. Sci. Technol.* **1990**, *24*, 706-712.

(33) Lin, T. –S.; Nriagu, J. O. *Anal. Chim. Acta* **1999**, *395*, 301-307.

(34) Downard, A. J.; Panther, J.; Kim, Y-C.; Powell, K. J. *Anal. Chim. Acta* **2003**, *499*, 17-28.

(35) Mandal, R.; Hassan, N. M.; Murimboh, J.; Chakrabarti, C. L.; Back, M. H.; Rahayu, U.; Lean, D. R. S. *Environ. Sci. Technol.* **2002**, *36*, 1477-1484.

(36) Bazzi, A. ; Lehman, J. T.; Nriagu, J. O.; Hollandsworth, D.; Irish, N.; Nosher, T. *J.Great Lakes Res.* **2002**, *28*, 466-478.

(37) Mansilla-Rivera, I. ; Nriagu, J. O. *J. Great Lakes Res.* **2003**, *29*, 105-115.

(38) Karlsson, T.; Persson, P.; Skyllberg, U. *Environ. Sci. Technol.* **2005**, *39*, 3048-3055

(39) Otto, W. H.; Carper, W. R.; Larive, C. K. *Environ. Sci. Technol.* **2001**, *35*, 1463-1468.